DISSERTATION | DOCTORAL THESIS

Titel | Title

The Hedonic Experience: From Neural Emergence to Modulation by Ketamine

verfasst von | submitted by

Maximilian Kathofer BSc. MSc

angestrebter akademischer Grad | in partial fulfilment of the requirements for the degree of

Doktor der Naturwissenschaften (Dr.rer.nat.)

Wien | Vienna, 2026

Studienkennzahl lt. Studienblatt | Degree programme code as it appears on the student record sheet:	UA 796 605 298
Dissertationsgebiet lt. Studienblatt | Field of study as it appears on the student record sheet:	Psychologie
Betreut von | Supervisor:	Mag. Dr. Julia Sophia Crone

Acknowledgement

Für meine Mama, die immer an mich glaubte.
Für meine Mama, die mir immer gesagt hat, dass ich alles erreichen kann, was ich will.
Für meine Mama, die von Anfang an mein größter Fan war.
Danke, dass du so bist, wie du bist.

Für meine Familie, die immer für mich da ist. Im Besonderen für meine Oma, die immer Wärme und Liebe ausstrahlt. Und natürlich für Heinz, den besten Stiefpapa, den man sich vorstellen kann. Für meinen Opa, meinen Papa und meine Papaoma.

Pursuing a PhD is a long, interesting journey that is heavily shaped by all the people you meet along the way. I want to thank Julia for being an amazing supervisor. For investing so much time and energy, discussing so many weird ideas, and helping me to find my own way. I also want to thank Kirren and Margot, who made the office life fun and enjoyable and always made me smile. Furthermore, I want to thank Pedro for welcoming me to his lab and for his supervision. Also, a heartfelt thank you to Hanna, Fred, Alberto, George, Daniel, and Alex, who made my stay at Imperial unforgettable. Lastly, I want to thank the OeAD-GmbH and BMFWF for awarding me the Marietta-Blau fellowship.

Table of Contents

Abstract in English

Effective reward processing is vital for all living organisms, ensuring that basic needs are met and providing the foundation for motivation, learning, and goal-directed behavior. Despite decades of extensive interdisciplinary efforts, critical gaps remain in our understanding of the neural mechanisms that govern reward and how they can be effectively modulated. This thesis focuses on the hedonic experience, the consummatory component of reward, and seeks to meaningfully contribute to an advanced understanding of its neural emergence, its encoding in the brain, the multivariate information dynamics underlying peak hedonic states, and its modulation by the prohedonic agent ketamine.

Recognizing that hedonic experience is multifaceted, spanning dimensions beyond valence such as experiences of beauty and being emotionally moved, this thesis integrates traditional reward paradigms with neuroaesthetic methods to provide a richer account of the consummatory phase of reward processing. Thereby, the four studies presented within this thesis deploy a diverse set of hedonic stimuli, including paintings, music, money, and faces, across visual, auditory, and imagery conditions and leverage complementary multivariate analytic approaches to illuminate the neural dynamics underlying hedonic experience and their modulation by ketamine. Fundamentally, the empirical work addresses four key questions: 1) does hedonic experience necessitate direct sensory input; 2) how is the hedonic experience encoded across stimulation modalities; 3) what multivariate neural information dynamics underlie hedonic states; and 4) how are these processes, behaviorally and neurally, modulated by ketamine to facilitate its prohedonic effects? Together, the findings provide a crucial stepping stone for future research on the mechanisms of reward, shed light on ketamine's elusive mechanism of action, and contribute to a more comprehensive understanding of the neural basis of hedonic experience.

Abstract in German

Belohnungsverarbeitung ist für alle Lebewesen von zentraler Bedeutung, da sie die Grundlage für Motivation, Lernen und zielgerichtetes Verhalten bildet. Trotz jahrzehntelanger intensiver interdisziplinärer Forschung bestehen weiterhin kritische Wissenslücken hinsichtlich der neuronalen Mechanismen, die Belohnung steuern, und ihrer wirksamen Modulierbarkeit. Ziel dieser Dissertation ist es, die hedonische Erfahrung umfassend zu beleuchten: ihren neuronalen Ursprung, die Muster ihrer neuronalen Kodierung, sowie die multivariaten Informationsdynamiken, die ihr zugrunde liegen. Darüber hinaus werden die neuromodulatorischen Effekte charakterisiert, die den prohedonischen Wirkungen des Medikaments Ketamin zugrunde liegen könnten.

Da die hedonische Erfahrung ein multidimensionales Konstrukt ist, das über Valenz hinaus Dimensionen wie Schönheit und emotionales Bewegtsein umfasst, integriert diese Arbeit traditionelle Belohnungsparadigmen mit neuroästhetischen Methoden, um ein ganzheitlicheres Verständnis der hedonischen Erfahrung zu ermöglichen. Die vier in dieser Dissertation präsentierten Studien setzen hierzu ein breites Spektrum hedonischer Stimuli, darunter Gemälde, Musik, Geld und Fotos von Gesichtern, über visuelle, auditive und imaginäre Bedingungen hinweg ein und nutzen multivariate Analyseansätze, um die neuronalen Dynamiken des hedonischen Erlebens und deren Modulation durch Ketamin zu beleuchten. Dabei liefert diese Dissertation wichtige Einblicke in folgende Schlüsselfragen: 1) Erfordert das hedonische Erleben einen direkten sensorischen Input? 2) Wie wird die hedonische Erfahrung über verschiedene Stimulationsmodalitäten hinweg kodiert? 3) Welche multivariaten neuronalen Informationsdynamiken liegen hedonischen Erfahrungen zugrunde? 4) Wie werden diese Prozesse, behavioral und neuronal, durch Ketamin moduliert? Zusammengenommen liefern die Befunde einen entscheidenden Ausgangspunkt für zukünftige Forschung zu den Mechanismen der Belohnungsverarbeitung, geben Aufschluss über den schwer fassbaren Wirkmechanismus von Ketamin und tragen zu einem umfassenderen Verständnis der neuronalen Grundlagen des hedonischen Erlebens bei.

Introduction

The evolutionary significance of reward processing lies in ensuring that organisms fulfill their most basic needs, including foraging, reproduction, and seeking shelter (Berridge & Kringelbach, 2008). More generally, reward processing guides goal-directed behavior (Grace et al., 2007) and forms the foundation for motivation, learning, and decision-making (Dayan & Balleine, 2002; Rushworth et al., 2011). While lay intuition often treats reward processing as a single coherent process, reward processing is in fact commonly divided into three distinct phases (Berridge et al., 2009; Pool et al., 2016): 1) an anticipatory phase, reflecting wanting or motivation when a potential reward is signaled; 2) a consummatory phase, reflecting liking or the hedonic experience when the reward is received; and 3) a learning or evaluation phase, in which outcomes generate prediction errors that adjust future expectations and behavior. Likewise, hedonic experience is often reduced to pure valence, the liking or disliking of a stimulus, yet it is a multifaceted construct that encompasses complementary affective experiences as well, such as experiences of beauty or feeling emotionally moved (Becker et al., 2019; Pelowski et al., 2017). As the core building block of reward processing, the hedonic experience is a central focus across numerous disciplines, spanning a wide range of scales and perspectives, from flies seeking food (Barron et al., 2010) to humans deriving joy from music (Vuust et al., 2022). Similarly, understanding the basis of altered or aberrant reward processing is also of considerable interest, as it is closely associated with dysfunctional behavior. Focusing on humans, the diminished experience of pleasure, clinically referred to as anhedonia, is not only one of the two hallmark symptoms of depression (American Psychiatric Association, 2013) but also significantly affected in a broad spectrum of psychiatric disorders (Destoop et al., 2019; Rømer Thomsen et al., 2015; Trøstheim et al., 2020). Moreover, with rates of depressive and anhedonic symptoms surging in the general population, this phenomenon presents a significant challenge to mental health and poses an increasing economic burden (Abbott, 2021). Thus, considerable interdisciplinary effort is being devoted to understanding how hedonic experiences are elicited, how they emerge within neural circuits, and how they can be effectively modulated to advance clinical interventions and improve treatment outcomes.

The origin of the hedonic experience

From the very beginning, philosophers and scientists alike have pondered the origins of the hedonic experience, questioning what truly elicits it (Peacocke, 2024). Are things inherently rewarding by themselves, independent of any mental modulation, or does the hedonic experience emerge as an interplay between external stimulation and internal mental processes? Rather than being a simple either-or scenario, evidence suggests a continuum, where hedonic experiences can range from being almost entirely tied to the external properties of a stimulus (Kelleher & Gollub, 1962), requiring little to no cognitive

involvement, to being heavily shaped by complex internal mental processes (Leder et al., 2004).

On one end of the spectrum lie so-called primary reinforcers, as studied in the field of conditioning research, such as food or water (Dayan & Balleine, 2002). These are inherently rewarding because they are directly tied to the biological needs of an organism and are thought to require no significant higher-order mental activity to elicit a hedonic response. For instance, when an organism is on the verge of starvation, food always evokes a potent reward response, irrespective of food preference, social norms, or moral considerations (MacClancy et al., 2007). While these reinforcers are potent and can effectively guide learning behavior, their effectiveness is not absolute and also context dependent, as repeated exposure, i.e., eating the same food over and over again, leads to habituation, reducing the ability of these stimuli to motivate organisms (Murphy et al., 2003).

In contrast to these most elementary stimuli, secondary reinforcers, such as money, are not intrinsically rewarding but acquire their value through associations, making them more dependent on internal processes, including learning and memory (Kelleher & Gollub, 1962). Even further along this spectrum are the arts, including visual art and music. While hedonic responses to art are influenced by the properties of the artworks themselves, such as color (Palmer et al., 2013; Schloss & Palmer, 2011) and form (Sun & Firestone, 2022), they are not merely the product of these external features. Research has shown that evoked hedonic experiences are also profoundly shaped by cognitive factors, including perceived meaningfulness (Trupp et al., 2023) and ongoing thought processes (Brielmann & Pelli, 2017). Furthermore, contextual factors such as knowledge about the artist, their life, and the cultural or historical significance of the work quite significantly influence hedonic experiences (Darda & Chatterjee, 2023; Redies, 2015; Szubielska et al., 2021). Together, these findings highlight that higher-order mental processes can substantially shape hedonic experiences. This, in turn, raises the question: if some hedonic experiences depend almost entirely on the properties of the external stimulation, can some also arise solely from internal thought processes? Though, whether rewarding experiences always necessitate external stimulation or whether they can be elicited purely by internal mental processes remains an open question that has yet to be confirmed.

Measuring the hedonic experience

Over the past decades, a plethora of studies have examined reward processing across a wide range of stimuli, including food (Kringelbach, 2015), social approval (He et al., 2019), visual art (Ishizu & Zeki, n.d.; Tiihonen et al., 2017), music (Alí Diez et al., 2024; Ishizu & Zeki, 2011), and even poetry (Margulis et al., 2017). However, monetary rewards are among the most used and extensively studied stimuli, especially in economics (e.g.

see Gabay et al., 2014; Heinrich & Marschke, 2010; Sigmund et al., 2001), largely because they are universally valued and easily delivered.

In this context, the monetary incentive delay (MID) task has become a standard paradigm in neuroimaging for dissecting the phases of reward processing. Although many variations of the MID task exist (Hanewald et al., 2023; Vel Tromp et al., 2025), they all share the same core structure as in the original implementation (Knutson et al., 2000). First, cues indicate whether money can be won or lost, enabling the measurement of anticipatory reward processing. Next, participants need to quickly respond to a target, and if they succeed, feedback indicates whether the reward is received or the punishment is avoided, capturing the consummatory component of reward. In this way, the MID examines hedonic responses to positive outcomes while also illuminating neural responses to punishment and negative valence. Since its introduction, the MID has been used to probe the neural correlates of anticipatory and consummatory reward processing of both healthy and diseased populations (Oldham et al., 2018; Wilson et al., 2018) and has thereby revealed stage-specific alterations in activation profiles across various clinical populations (Balodis & Potenza, 2015; Eshel & Roiser, 2010; Lutz & Widmer, 2014; Zeng et al., 2022).

Although proven useful for differentiating stages in reward processing (Lutz & Widmer, 2014), it is questionable whether winning small amounts of money truly induces intense hedonic experiences. Consistent with this, sex, nature, and the arts – not money – are commonly considered the domains of highest pleasure (Maslow, 1971; Privette, 1983). In this regard, listening to music is not only a common tool for everyday emotion regulation but also reliably evokes intense pleasurable experiences (Vuust et al., 2022), sometimes even triggering physiological markers of peak hedonic responses such as piloerection (chills) (Vuust & Kringelbach, 2010). How such strong reward responses arise from music and art more generally, and whether they engage the same neural circuits as basic rewards, such as food, is a focus within the field of neuroaesthetics. Expanding beyond traditional reward components like wanting and liking, neuroaesthetics also investigates closely related emotions, commonly referred to as aesthetic experiences, such as judgments of beauty (Brielmann et al., 2017, 2017), experiences of awe (Arcangeli et al., 2020), and the feeling of being moved (Menninghaus et al., 2015). While these constructs are not pure reward measures (valence), their theoretical and neural dependence on common reward processes is substantial (Pelowski et al., 2017). Thus, by incorporating these aesthetic constructs and leveraging self-selected, personally meaningful stimuli, i.e., a person's favorite song, neuroaesthetics offers a more nuanced framework for mapping the full range of the hedonic experience, from its absence to peak pleasure.

The neural basis of the hedonic experience

The hedonic experience is not attributable to any one specific brain region alone but emerges from the coordinated interplay of various cortical and subcortical structures.

This so-called reward network classically includes the ventral tegmental area (VTA), the nucleus accumbens (NAc), and the medial prefrontal cortex (mPFC), yet also receives additional contributions from the orbitofrontal cortex (OFC), anterior cingulate cortex, amygdala, and hippocampus, among others (Höflich et al., 2019). Within this mesocorticolimbic network, nodes show relative, though not exclusive, tuning to distinct stages of reward processing: the OFC is thought to mainly support anticipatory processing (Kahnt et al., 2010; Kringelbach, 2005); distinct subnuclei of the NAc are engaged during reward anticipation and consumption (Castro et al., 2015; G. Chen et al., 2023), and the amygdala, generally associated with emotion and salience (Frank et al., 2014), contributes to valuation by encoding expected stimulus value and integrating anticipated effort costs (Johnson & Grabenhorst, 2025; Wassum, 2022).

Canonically, the dopaminergic system is associated with reward processing, a historical emphasis likely driven by the observed dense dopaminergic pathways connecting core nodes of the mesocorticolimbic circuit (Berridge & Kringelbach, 2008). Although converging evidence across animals (Ferenczi et al., 2016; Schultz, 2024) and humans (Ashok et al., 2017) indicates that intact dopaminergic signaling is essential for reward processing and that disruptions are associated with anhedonic behavior (Belujon & Grace, 2017; Cousins et al., 2009; Dunlop & Nemeroff, 2007; Lambert et al., 2000), the view of dopamine as the sole mediator of reward has shifted. More specifically, the notion that dopamine encodes pleasure, the consummatory aspect of reward, has long been challenged, as dopaminergic activity more reliably tracks predictive and motivational processes rather than the liking of a stimulus per se (Schultz, 2002). Thus, in recent decades, a more nuanced picture has emerged in which multiple neurotransmitter systems contribute to reward processing, with dopamine primarily subserving anticipation and motivation, opioidergic and serotonergic circuits supporting consummatory pleasure and affective valuation, and glutamatergic and GABAergic inputs further shaping complex neural reward dynamics (Russo & Nestler, 2013; Sesack & Grace, 2010). Importantly, these functions are not exclusive but overlap across neurotransmitter systems, as biological systems are rarely that simple.

Especially in humans, functional magnetic resonance imaging (fMRI) has been widely used to non-invasively assess which macroscopic neural structures are involved in reward processing and at which stages (Luijten et al., 2017; Sescousse et al., 2013; Wilson et al., 2018). Traditionally, fMRI studies rely on mass-univariate analyses that test whether a voxel, a 3D recording unit of brain activity, shows greater activation in a manipulation condition than in a baseline. This approach treats voxels independently and is powerful for detecting mean amplitude differences. However, mass-univariate methods are less sensitive when information is distributed across several voxels, for instance, when some voxels within a region of interest encode reward magnitude while others encode preference, producing distinct patterns rather than uniform changes (Davis et al., 2014). To capture such multidimensional distributed representations, multivoxel pattern analysis (MVPA) aggregates information across voxels to decode

conditions or psychological dimensions from collective spatial patterns of activity (Haxby et al., 2001). Fundamentally, MVPA enables the decoding of neural information that is heterogeneously distributed across voxels and participants (Haxby, 2012), and it has substantially reshaped our understanding of the neural substrates of reward. Since its inception, MVPA has not only corroborated the involvement of canonical reward hubs identified by univariate analyses but also revealed that the same neural populations can express distinct activation patterns depending on the presented stimulus and processing stage (Kahnt, 2018). Furthermore, unlike univariate analyses, MVPA showed that reinforcement signals related to task outcomes can be decoded from almost the entire brain, not just from the few regions associated with the reward network, vastly expanding our view of reward processing in the brain (Ramayya et al., 2015; Vickery et al., 2011).

While MVPA is a powerful tool for examining whether information about cognitive processes can be decoded from brain activity, representational similarity analysis (RSA), in contrast, enables the straightforward testing of theory-derived encoding models and identification of the specific stimulus' properties represented within a given region (Popal et al., 2019). By comparing the geometry of the dissimilarity patterns associated with evoked neural responses across stimulus feature dimensions, RSA provides a more fine-grained understanding of how neural communities encode high-dimensional feature spaces (Diedrichsen & Kriegeskorte, 2017; Kriegeskorte & Douglas, 2019). In this regard, a recent study by Yan and colleagues (2016) tested various models of anticipatory and consummatory reward processing in the OFC, showing that the OFC encodes stimulus value during anticipation and reward magnitude during consumption, while ruling out encoding of outcome favorability in the OFC. This highlights RSA's potential to systematically test theory-derived models synthesized from the extensive reward literature, thereby advancing our fundamental understanding of how particular regions facilitate reward processing.

Yet, hedonic experiences do not arise from a static instantaneous process but rather emerge from the dynamic multivariate integration of neural information over time, as all cognitive processes do. Characterizing these multivariate information dynamics is, however, extremely challenging, made possible only by recent advancements in information theory (Barrett & Seth, 2011; Mediano et al., 2022; Rosas et al., 2019; Timme et al., 2014; Williams & Beer, 2010). Synergy and redundancy, two complementary forms of integration, provide valuable insights into these higher-order dynamics. Whereas synergistic information emerges exclusively from the joint interaction of multiple brain regions, redundancy refers to information being present simultaneously across multiple regions. As a result, synergy is fragile, disrupting even a single node can degrade it, while redundancy provides robustness to perturbation, albeit at the computational cost of having to represent the same information across multiple nodes of a system. Nonetheless, both forms of information dynamics have

been shown to be crucial for cognition and behavior (Koçillari et al., 2023a; Varley, Sporns, et al., 2023a).

A useful global measure of the balance between these two information dynamics is O-information (Rosas et al., 2019). Although it does not explicitly separate synergy and redundancy, it captures their net balance and reveals the dominant mode of multivariate interdependence, indicating whether a system relies primarily on synergistic emergent information processing or on robust collaborative redundant information sharing. In contrast, the evolution of such dynamics across time is often quantified using whole-minus-sum integrated information (WMS) (Barrett & Seth, 2011). Fundamentally, WMS assesses whether temporally synergistic processes and pure information transfer across regions outweigh the persistence of shared redundant information over time (Mediano et al., 2021). In addition, integrated information decomposition now even makes it possible to isolate these distinct multivariate information dynamics, i.e., pure synergistic, transfer, or redundant processes, providing an unprecedented view into a system's most elementary integration dynamics (Mediano et al., 2021; Williams & Beer, 2010). Since hedonic experiences depend on integrating information about external stimulus features with internal cognitive processes across widespread neural networks, multivariate information-theoretic tools are especially well suited to characterize such dynamics. Collectively, these novel higher-order information measures provide a unique opportunity to systematically examine, for the first time, the neural information-integration dynamics underlying reward processing and to illuminate the intricate multivariate processes that give rise to the hedonic experience.

Modulating the hedonic experience

Effectively modulating dysfunctional reward processing is particularly important in the clinical context, as anhedonia is a prevalent symptom across various psychiatric disorders (Destoop et al., 2019; Rømer Thomsen et al., 2015; Trøstheim et al., 2020). Anhedonia has been consistently linked to poorer treatment outcomes, prompting increased interest in recent years in targeting specifically anhedonic symptoms in clinical populations as a means to enhance prognosis (Crits-Christoph et al., 2018; Garfield et al., 2013; Luca et al., 2024; Vrieze et al., 2014; Wong et al., 2024). Despite this growing focus, alleviating anhedonia has proven challenging as many commonly prescribed antidepressants, including serotonin reuptake inhibitors and tricyclic antidepressants, often fail to effectively address anhedonic symptoms and, in some cases, even exacerbate them (Cao et al., 2019; Craske et al., 2016; Price et al., 2009).

Consequently, the discovery of ketamine's rapid-acting antidepressant and especially antianhedonic (prohedonic) properties has garnered considerable attention as it represents a potential breakthrough in the treatment of this debilitating condition (Krystal et al., 2019). Originally developed as an anesthetic, ketamine, most notably known for its N-methyl-D-aspartate receptor antagonism, induces an altered state of

consciousness when administered at subanesthetic dose. Remarkably, even patients with former treatment-resistant depression report rapid mood improvements following ketamine administration at this dose (Bahji et al., 2021). Thus, unlike traditional antidepressants, which often require weeks to exert their therapeutic effects (Boku et al., 2018), ketamine not only effectively alleviates both depressive and anhedonic symptoms but does so within hours (Lally et al., 2014).

While an ever-growing body of research underscores ketamine's effectiveness in ameliorating anhedonic symptoms (Nikolin et al., 2023), its precise mechanism of action remains elusive. Several molecular pathways have been proposed to underlie its prohedonic effects, with most theories converging on the general idea that ketamine's therapeutic benefits are tied to its neuroplastic properties (for a review see Zanos & Gould, 2018). In essence, neuroplasticity enables the brain to adapt dynamically to changing demands caused by new experiences or trauma, either by rerouting impaired neural signaling through alternative pathways (functional neuroplasticity) or by physically forming new synapses (structural neuroplasticity) to accommodate shifting demands. Recent seminal work in mice has, for the first time, causally linked ketamine's therapeutic effects to its neuroplastic properties (Moda-Sava et al., 2019). The study demonstrated that chronic stress leads to the loss of dendritic spines, impairing functional connectivity, which is accompanied by overt depressive behavior. Following ketamine treatment, neural signaling is restored to healthy, pre-disease levels, indicating a reactivation of impaired functional pathways. This phase of functional neuroplasticity is followed by synaptogenesis, during which ketamine facilitates the formation of new dendritic spines to sustain the long-term effects initiated by the functional improvements. This process effectively prolongs the therapeutic effects, extending their impact well beyond the drug's metabolism. Crucially, when these newly formed dendrites are destroyed, the animals revert to depressive behaviors, providing causal evidence that ketamine's therapeutic effects are intrinsically linked to its neuroplastic properties. Together, their data suggests that ketamine exerts its therapeutic effects by first inducing widespread functional neuroplasticity, which serves as a critical initial step. This functional reorganization then drives the induction of structural plasticity, ensuring the brain can adapt and sustain the new demands arising from these functional changes.

Yet, ketamine is not a miracle drug. Firstly, not all patients benefit from ketamine to the same extent, with responses varying from complete remission to only modest transient improvements (Alnefeesi et al., 2022; Becker et al., 2019; Nikolin et al., 2023). This considerable heterogeneity has motivated research into interindividual predictors of treatment response, including variations in the phenomenological experience evoked during ketamine administration. While it remains debated whether ketamine's psychomimetic effects are necessary for its therapeutic benefit (Ballard & Zarate, 2020; Grabski et al., 2020), emerging evidence indicates that more positive acute experiences, such as awe (Aepfelbacher et al., 2024) and happiness (M.-H. Chen et al., 2020), are

associated with better treatment outcomes. Conversely, ketamine can also induce acute anxiety, nausea, and dizziness (Ceban et al., 2021). These adverse effects not only increase discontinuation rates, but the intensity of induced anxious states in particular has been strongly associated with blunted treatment responses (Aust et al., 2019). Thus, to advance personalized care and optimize treatment outcomes, more basic research is required to determine whether specific neural predispositions, such as the morphology of specific brain areas, might predict vulnerability to ketamine-induced anxiety. Successfully identifying such pre-treatment factors could inform more targeted interventions in the long run, avoiding the exposure of vulnerable patients to suboptimal or potentially contraindicated treatments.

Secondly, ketamine's therapeutic effects are typically short-lived, subsiding after roughly 7 days (Lapidus et al., 2014; Zarate et al., 2006). As a result, significant effort is being dedicated to exploring ways to extend ketamine's therapeutic benefits, including repeated administration (Kryst et al., 2020), combining it with psychotherapy (Drozdz et al., 2022), and more experimental approaches currently limited to animal models (Ma et al., 2025). However, to successfully prolong or even emulate ketamine's therapeutic effects, a more thorough understanding of its functional neuroplastic properties, which underlie its rapid-acting prohedonic effects, is necessary. While studies have investigated the acute effects of ketamine and its impact 1–10 days post-administration on neural dynamics (Kotoula et al., 2021; Medeiros et al., 2023), no functional neuroimaging studies have specifically focused on the subacute effects. This represents an important knowledge gap, particularly given the prominent conjecture that functional changes in neural dynamics not only facilitate the rapid-acting prohedonic effects but also play a causal role in triggering the structural changes that underpin ketamine's long-term therapeutic effects. Therefore, to better understand ketamine's therapeutic properties and develop urgently needed improved interventions, it is critical to examine changes in neural dynamics in this subacute stage, roughly four hours after administration, when psychomimetic effects have already subsided, and therapeutic effects begin to emerge (Zarate et al., 2006).

In summary, advancing ketamine-based prohedonic treatments requires the identification of potential predispositions that contribute to response heterogeneity and delineating ketamine's neuromodulatory effects during the critical subacute phase, when psychomimetic effects have already waned and the strong mood improvements emerge. Crucially, first characterizing these changes in healthy participants would most likely reveal neural correlates that are free of common clinical confounds, such as comorbidities and prior pharmacotherapy, providing a vital stepping stone for future clinical studies in anhedonic patients.

Open questions and contributions

While prior work in neuroaesthetics clearly demonstrates that hedonic experiences, including experiences of beauty, pleasure, and awe, are not solely shaped by the external properties of the stimulation itself and are also significantly modulated by internal mental processes (Brielmann & Pelli, 2017; Darda & Chatterjee, 2023; Redies, 2015), a key gap remains: Do hedonic experiences fundamentally necessitate direct sensory input, or can they similarly arise purely from mental processes in the absence of any external stimulation? Addressing this question, Study 1 (Kathofer, Lamm, et al., 2025) systematically compares hedonic experiences elicited by biological and culturally significant stimuli, faces and paintings respectively, across two modalities, visual perception and visual mental imagery, assessing whether imagery can evoke hedonic responses of comparable intensity to perception. Beyond testing the necessity of sensory input, the study leverages RSA to examine how evoked hedonic responses are neurally represented across stimulus types and modalities, elucidating how the reward network and its constituent regions encode these experiences.

Shifting the focus to how reward processing can be more effectively modulated, Studies 2-4 examine ketamine's prohedonic and neuromodulatory effects in healthy participants across the acute and subacute phase. As aforementioned, emerging evidence suggests that ketamine's acute psychomimetic effects are associated with its therapeutic efficacy (Aepfelbacher et al., 2024; Aust et al., 2019; M.-H. Chen et al., 2020). However, responses to ketamine dosing are highly heterogeneous, raising the question of whether biological predispositions, such as structural brain features, are predictive of these differences in phenomenological experience. Since induced anxiety during ketamine administration can considerably reduce its beneficial effects (Aust et al., 2019), Study 2 (Graf et al., 2024) examined whether morphological markers, specifically amygdala and hypothalamus volumes, predict heightened anxiety during dosing. Transitioning to the subacute phase, when psychotomimetic effects have typically waned and prohedonic effects begin to emerge (Zarate et al., 2006), there is a notable lack of data characterizing ketamine's neuromodulatory effects in this critical window. Therefore, Study 3 (Briem et al., 2025) employs the well-established MID task to determine whether ketamine modulates both anticipatory and consummatory neural signatures of reward processing, or more selectively influences just one, thereby advancing our understanding of its mechanisms of action during this vital phase. To further deepen insight into ketamine's therapeutic properties, Study 4 (Kathofer, Mediano, et al., 2025) employs a self-devised hedonic music task using participant-selected music to elicit a range of hedonic responses, from none to peak pleasure. Leveraging recent advances in information theory, the study uses both global (O-Information) and local (WMS) metrics of multivariate information dynamics to characterize how neural information integration changes with the intensity of hedonic phenomenology. Similarly focusing on the subacute window, the study specifically tests whether peak hedonic experiences depend more on synergistic interactions across

brain regions or on redundant information processes. By modulating individual reward responses using ketamine's rapid-acting prohedonic properties, the study further examines how ketamine reshapes neural information dynamics to facilitate its beneficial health effects. Thus, Study 4 (Kathofer, Mediano, et al., 2025) offers an unprecedented glimpse into the multivariate neural information dynamics that underpin both ketamine's prohedonic mechanism of action and the hedonic experience.

Empirical Work

Hedonic Experiences in Response to Visual Imagery

Study 1: **Kathofer, M.**, Lamm, C., Leder, H., & Crone, J. S. (2025). Aesthetic experiences across visual perception and mental imagery: Behaviorally indistinguishable, neurally distinct. iScience, 28(6). DOI: 10.1016/j.isci.2025.112588

My contribution

As the first author of this publication, I was heavily involved in all stages of this project. I personally collected the fMRI data, preprocessed it, proposed the usage of Bayesian statistics to show that evoked experiences are indistinguishable across visual perception and strong visual imagery, and devised the analytical approach to deploy RSA to investigate the extent to which neural signals encode reward information versus stimulus modality across different levels of resolution within the brain. Finally, I drafted the manuscript.

iScience

CellPress
OPEN ACCESS

Article

Aesthetic experiences across visual perception and mental imagery: Behaviorally indistinguishable, neurally distinct

Maximilian Kathofer,[1,5,*] Claus Lamm,[1,2] Helmut Leder,[1,3,4] and Julia Sophia Crone[1,4]
[1]Vienna Cognitive Science Hub, University of Vienna, Vienna, Austria
[2]Social, Cognitive, and Affective Neuroscience Unit, Department of Cognition, Emotion, and Methods in Psychology, Faculty of Psychology, University of Vienna, Vienna, Austria
[3]EVA-Labs, Department of Cognition, Emotion, and Methods in Psychology, Faculty of Psychology, University of Vienna, Vienna, Austria
[4]These authors contributed equally
[5]Lead contact
*Correspondence: maximilian.kathofer@univie.ac.at
https://doi.org/10.1016/j.isci.2025.112588

SUMMARY

Studies suggest that vivid mental imagery can blur the boundaries between reality and imagination in simple detection tasks by eliciting similar neural patterns. The question arises as to whether aesthetic experiences can similarly emerge through imagery or whether these complex experiences necessitate direct input into the sensory system. Alternating between visually perceiving and reimagining encountered stimuli, 34 participants rated faces and artworks across aesthetic dimensions. While slightly less potent, imagery is equally sufficient in evoking aesthetic experiences, and for highly vivid imaginations, evoked experiences even become behaviorally indistinguishable across conditions. Yet, representational similarity analysis reveals distinct neural patterns across conditions as the brain mainly encodes stimulus modality, even in areas canonically associated with aesthetic processing. Thus, although evoked experiences might be behaviorally identical across modalities during highly vivid trials, neural patterns differ substantially due to differences in modality, as evoked experiences are only marginally encoded.

INTRODUCTION

The aesthetic experience is a fundamental human trait that shows considerable cultural variability.[1] Deeply rooted within our sense of pleasure,[2] neuroaesthetics employs the aesthetic experience as an umbrella-term for a wide range of cognitive concepts, emotional states, and their brain responses, encompassing nuanced facets, such as beauty, the sublime,[3] and the state of being moved.[4] Yet, despite its crucial role in shaping human experiences, finding a universal definition of the aesthetic experience has continuously challenged philosophers, psychologists, and neuroscientists alike.[5] At the core of this debate is whether aesthetic experiences are a quality of the perceived object itself or whether they emerge from an internal state reflecting the complex interplay between the inducing sensory properties of an object and ongoing internal cognitive processes.[5–9] While there is prevailing consensus that aesthetic experiences stem from first-hand encounters, it is also well established that aesthetic experiences are more than just the mere product of the directly perceived stimulus properties, and thus, are affected by factors beyond characteristics of the external sensory stimulation. For instance, peak aesthetic moments, experiences of awe or chills, are profoundly influenced by cognitive factors such as meaningfulness[10–12] and ongoing thought processes.[2]

More direct evidence against the notion that the aesthetic experience is merely the result of the properties of an external stimulation comes from a study investigating the complexity of the brain network response to music.[13] The more rewarding the music was, that is, the higher the aesthetic experience, the less did the complexity of brain network dynamics match the complexity of the music. This strongly indicates that the processes underlying the emergence of an aesthetic experience involve more than just the original stimulation properties. In consequence, the question arises whether the emergence of an aesthetic experience even necessitates the immediate external perception of an object, such as viewing an artwork, or if direct physical input to the sensory system is merely one of several effective means to evoke such an experience, with internally generated representations being equally sufficient. While it may seem intuitive, given the essential role attributed to subjectivity and cognitive processes in aesthetic experiences, the significance of the external stimulus perception for aesthetic processing has surprisingly never been evaluated in empirical research. Answering the question whether the external perception is necessary and how much it contributes to an experience, however, has broader implications for understanding how experiences emerge in general from the interaction between the external world and the internal processes of each individual.

iScience 28, 112588, June 20, 2025

If indeed external stimulation merely acts as a trigger initiating internal, subjective processes which are responsible for the aesthetic experience or, for that matter, any experience at all, then mental imagery (the ability to voluntarily represent objects in the mind in the absence of immediate external stimulation of the sensory system) should also lead to an aesthetic experience of similar quality. Neuroimaging studies indicate that visual mental imagery largely recruits brain regions commonly engaged in visual perception.[14] More specifically, there is a significant overlap of neural activation particularly within the ventral visual stream between visual mental imagery and visual perception, with more pronounced similarity of activation patterns for higher visual areas, yet, nuanced differences for earlier visual regions.[15] This is unsurprising as activation in these lower-level areas is significantly affected by the level of detail of the imagined object as well as the vividness of the mental image itself.[16–19] Vividness is defined as the degree of clarity of the mental image[20] and individuals significantly differ in their ability to represent objects in their mind with some lacking the ability to perform visual mental imagery completely.[21,22] Depending on the imagined content, mental imagery can evoke both positive and negative affective responses comparable to those triggered by visual perception,[23–25] by similarly recruiting key emotional and reward-related regions, such as the amygdala and the nucleus accumbens.[26–28] Involuntary imagery even contributes to psychopathological symptoms, most notably in post-traumatic stress disorder, in which intrusive flashbacks elicit intense emotional distress and serve as a hallmark of the disorder itself.[29] Additionally, adverse imagery contributes to various other clinical conditions,[30,31] driving cravings,[32,33] and maladaptive behavior.[34] Thus, due to its profound impact on affective processing, clinicians leverage techniques such as imagery rescripting[35] and neurofeedback[36] to fundamentally reshape emotional responses to distressing mental images and modulate subjective emotional processing long-term.[37,38] Taken together, external sensory stimulation and mental imagery are deeply intertwined, engaging overlapping brain regions and often producing remarkably similar phenomenological experiences.

In light of these qualitative and neural similarities, a long-standing question has centered on the precise mechanism enabling the brain to reliably distinguish visual perception from mental imagery. Recently, differences in neural signal strength emerged as a potential mechanism facilitating this distinction.[39] These findings suggest that if the strength of neural representations is high enough, vivid mental images might even be perceived as real. Acknowledging the potency of mental imagery in shaping our perception, it seems highly plausible that mental images themselves should also be able to evoke more complex second-order effects such as aesthetic experiences. Thus, if an aesthetic experience does not necessitate external sensory stimulation and if there was no unique contribution of the external sensory stimulation to shaping the aesthetic experience, the quality of the aesthetic experience itself should not substantially differ whether they are sparked by external stimulation or by mental imagery of the same aesthetic stimulus. In this case, both stimulation modalities (external visual perception and internal visual mental imagery)—if controlled for vividness—should result in phenomenologically very similar subjective aesthetic experiences.

Lastly, since neural activity in the reward network and more precisely the nucleus accumbens and the caudate nucleus are closely associated with aesthetic processing,[40–43] activity in these highly specialized areas should primarily reflect the nature of the aesthetic experience itself. In contrast, in areas such as the visual cortex, neural patterns are significantly shaped by modality, even though the neural response to external visual perception and mental imagery becomes more similar as the vividness of the mental image increases.[17] Thus, if mental imagery can evoke subjective experiences phenomenologically similar to those triggered by external stimulation, we expect that these similarities would be encoded in the neural activity of these highly specialized areas rather than the differences between modalities in which the stimulus was originally perceived.

The present study aimed to provide empirical evidence for the question of whether the emergence of an aesthetic experience truly necessitates external sensory stimulation or whether it can equally arise in its absence, solely triggered through internally generated images. First, we created an aesthetic task utilizing a diverse range of both cultural and biological pre-rated stimuli—artworks and faces—presented across visual perception and mental imagery conditions, to examine whether aesthetic experiences can similarly arise in response to mental imagery (hypothesis 1 (H1)). Crucially, to capture a broad range of aesthetic responses, participants rated evoked experiences across three dimensions; pleasure (which reflects the extent to which the experience was liked), beauty (a measure closely linked to pleasure but reliant on cognitive assessment of the stimulus and its properties[2]), and being moved (a strong affective response that can even trigger physiological reactions, such as chills[44]). In line with our hypothesis, we indeed find that imagery can elicit the full range of aesthetic experiences similarly to visual perception, albeit to a lesser extent. Next, we investigated whether naturally occurring trial-by-trial variability of an individual's proficiency to vividly imagine a stimulus[17] might influence evoked responses (H2). We not only show that aesthetic experiences become more similar across modalities dependent on the clarity of the mental image but also that aesthetic experiences become virtually indistinguishable across modalities for highly vivid trials. Lastly, given the suspected similarity of aesthetic experiences across modalities, we reasoned that the neural signal underlying these experiences should be similar as well (H3). More specifically, we expected that the dominant stimulus feature encoded in the neural signal, i.e., modality, type, or experience, would vary depending on the level of resolution, that is, whole-brain, reward network, or highly specialized regions within the reward network, such as the nucleus accumbens and caudate nucleus. Whereas global neural patterns were expected to differ significantly across modalities—despite similarities in the evoked experience—due to the inclusion of primary visual areas, the ventral and dorsal pathways, neural patterns in highly specialized regions were predicted to be highly similar, reflecting shared behavioral responses despite differences in stimulation modality. Testing several theory-driven models using representational similarity analysis (RSA), we found that at the global level, neural patterns exclusively encoded modality differences.

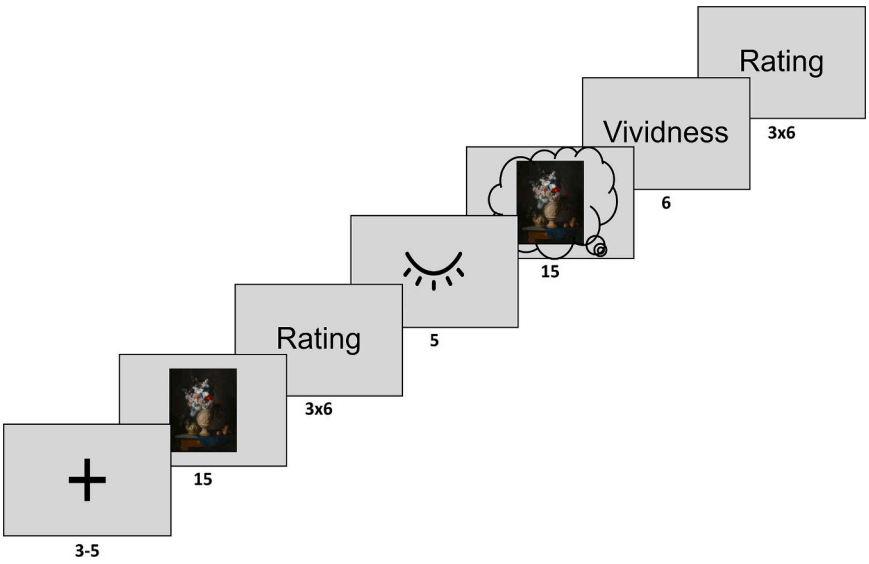

Figure 1. Aesthetic task

Participants were randomly presented with 40 pictures of representational artworks and faces. First, participants directly viewed the stimulus for 15 s and rated the evoked aesthetic experience across three scales: pleasure, moving, and beauty. Next, participants closed their eyes and imagined the previously encountered stimulus for 15 s. Lastly, the vividness of the mental image was assessed as well as the evoked experience in response to the mental image. Durations are in seconds.

However, as we zoomed into the reward network and its constituents, the neural signal increasingly reflected evoked experiences and stimulus type. Nevertheless, modality differences remained the dominant factor, contributing twice as much to the neural signal. Ultimately, this shows that the neural signal still largely differs across conditions, and despite a highly similar behavioral experience, does not need to be identical.

RESULTS

Highly vivid imagery elicits indistinguishable aesthetic experiences from visual perception

To determine whether external sensory perception is necessary for the emergence of an aesthetic experience (see H1), participants (N = 34) performed an aesthetic task in which they rated their subjective aesthetic experience in response to images of faces and artworks across a visual perception and a mental imagery condition (see Figure 1). To assess whether visual perception is necessary or mental imagery is equally sufficient in eliciting profound aesthetic experiences, we compared the ratings of evoked experiences across different stimulation modalities (visual perception and visual mental imagery) for each stimulus type (faces and artworks). Crucially, to capture a plurality of aesthetic dimensions, participants rated evoked experiences across three key facets: pleasure, which reflects the extent to which a stimulus evokes hedonic experiences; beauty, a measure closely linked to pleasure but reliant on cognitive assessment of the stimulus and its properties[2]; and being moved, a strong affective response that can even trigger physiological reactions, such as chills.[44]

In line with our initial hypothesis that mental imagery is equally capable of eliciting aesthetic experiences, Bayesian ordinal regressions highlight that visual mental imagery elicits aesthetic experiences comparable to those evoked by visual perception, albeit to a lesser extent: moving (β_{stand} = −0.29 [CI_{95}: −0.37–0.21] (see Table S1); beauty (β_{stand} = −0.28 [CI_{95}: −0.37–0.20]) (see Table S2); pleasure (β_{stand} = −0.22 [CI_{95}: −0.31–0.14] [see Table S3]). Suspecting that naturally occurring trial-by-trial fluctuations in participants' vividness abilities might drive these small differences across stimulation modalities (see H2), we calculated an absolute similarity score between aesthetic responses across modalities. This was done by subtracting each individual rating in the imagery condition from its visual counterpart, squaring it, and then adding them together for each stimulus per subject. This resulted in a vector ranging from 0 (perfect similarity) to 48 (highest observed dissimilarity). Using a Bayesian linear model, we find a clear negative association between the vividness of mental images and the dissimilarity of responses (β_{stand} = −0.27 [CI_{95}: −0.40–0.14] [see Tables S4.1 and S4.2]), indicating that differences in evoked experiences across modalities became larger when mental images were less precisely imagined.

Thus, to substantiate the claim that both stimulation modalities—when controlled for vividness—evoke phenomenologically equivalent subjective aesthetic experiences, we conducted a subgroup analysis using only trials with the highest vividness ratings (6 and 7) for each participant. Across all 3 facets, the observed differences across stimulation conditions became exceedingly small, and most importantly, all effect size estimates now included 0 as a probable value for the effect size estimates: moving (β_{stand} = −0.14 [CI_{95}: −0.29 0.01] [see Table S5]); beauty (β_{stand} = −0.14 [CI_{95}: −0.29 0.01] [see Table S6]); pleasure (β_{stand} = −0.07 [CI_{95}: −0.22 0.07] [see Table S7]). Further harnessing the advantages of the Bayesian framework, we then calculated a Bayes Factor for each of these parameters to assess whether their posterior distribution shifted away or toward a region of effect sizes typically deemed as negligible. This region traditionally ranges from −0.1 to 0.1,[45,46] as effects of this size are generally deemed insignificant. For all three aesthetic facets, we find moderate to strong evidence[47] that observed effects fall into this range of negligible effect sizes ($BF_{01\text{-moving}}$ = 4.6; $BF_{01\text{-beauty}}$ = 4.7; $BF_{01\text{-pleasure}}$ = 22.7) (see Figure 2). Given that the detected effect sizes are exceedingly small and would be typically considered as negligible within the field of psychology, we conclude that there is no compelling evidence that visual mental imagery results in meaningfully different aesthetic experiences compared to visual perception during highly vivid trials. Thus, when controlled for vividness,

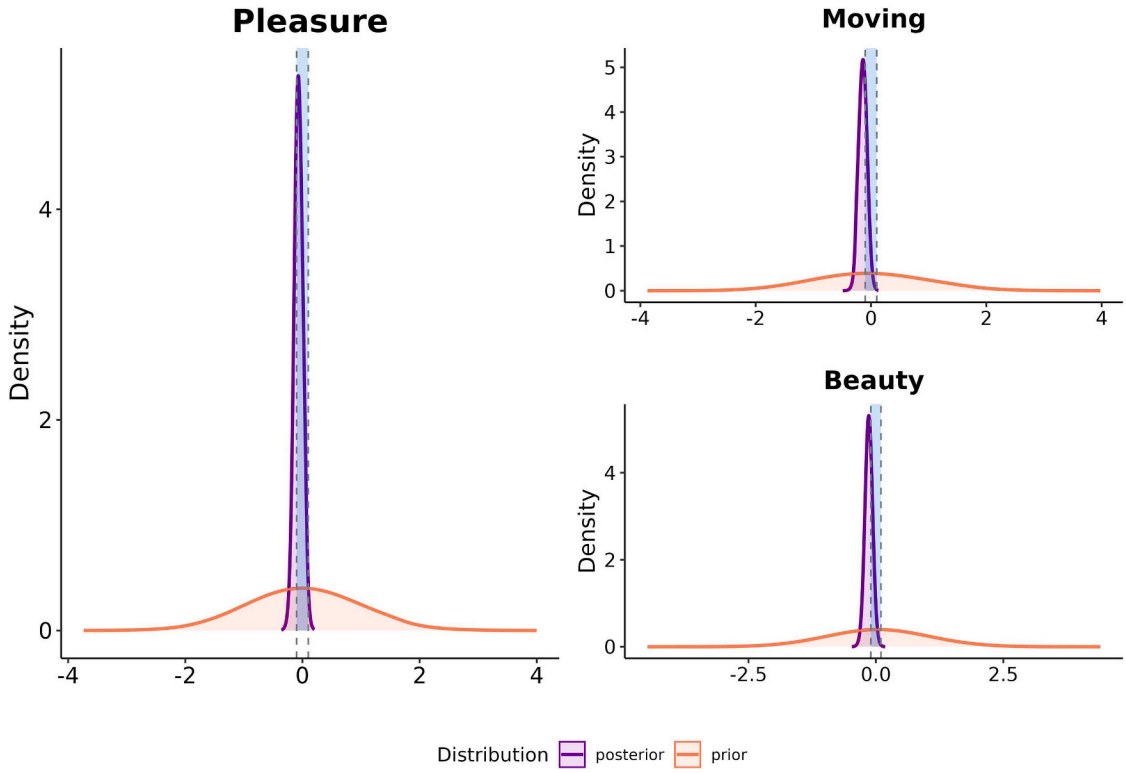

Figure 2. Bayes Factor analysis for parameter estimates of highly vivid trials

Each plot shows parameter estimates of the ordinal regression. Plots show prior distributions (green) and posterior distributions of the parameter estimate (red) across all 3 aesthetical facets as well as the range of effect sizes generally considered not meaningful (gray).

evoked aesthetic experiences across stimulation modalities are largely indistinguishable from each other.

In addition, we used two different types of stimuli to induce an aesthetic experience; biological stimuli, that is, faces and cultural stimuli, that is, artworks. The results clearly indicate that faces elicited weaker experiences than representational artworks across all three facets of aesthetic experience (moving [$\beta_{stand} = -0.56$ [CI_{95}: −0.77–0.35]) (see Table S1); beauty ($\beta_{stand} = -0.43$ [CI_{95}: −0.71–0.13]) (see Table S2); pleasure ($\beta_{stand} = -0.82$ [CI_{95}: −1.06–0.58]) (see Table S3), even though we used a pre-rated set of stimuli for both.

Neural similarity patterns, even in regions within the reward network, are mainly driven by stimulation modality

To confirm that the neural patterns encoding the aesthetic experience are locally restricted within areas specialized in aesthetic processing while differences in modality are encoded more strongly across the entire brain, we performed a RSA across three levels of resolution; the whole brain; the reward system as defined by a meta-analytical mask using Neurosynth[48]; and two specific regions of interest (ROIs) within the striatum, that is, nucleus accumbens and caudate nucleus. The latter two ROIs were specifically chosen due to the consistent evidence in the literature that they are robustly involved in the anticipation as well as processing of aesthetic experiences.[40–42] Ultimately, this approach enabled us to examine a common, implicit assumption; the effect of the external stimulation on the neural response is strongest at the whole brain level, while the subtler effects of the aesthetic experience are mainly encoded in highly specialized areas. Thus, at the whole brain level, we expected neural patterns to primarily reflect differences in stimulation modality since neural patterns would largely involve signals from primary visual areas and regions of the dorsal and ventral visual stream. However, when narrowing the focus to the reward network and even further to its constituents, we expected a shift in the neural signal to now largely reflect differences in the evoked aesthetic experience and only to a lesser extent other stimulus properties. Thus, depending on the level of interest, we hypothesized that the neural signal would be dominated by different aspects of the stimulation: at the whole brain, it would be dominated by differences in stimulation modality whereas at the more fine-grained level within the reward network, it would be dominated by differences in the evoked experiences. To investigate this assumption we used RSA, which assesses the dissimilarity of neural response patterns between conditions by creating neural representational dissimilarity matrices (RDMs) and comparing their similarity structure to theory-derived predictions about the geometry of evoked responses.[49] To disentangle the influence of different aspects of the stimulation, such as modality of perception, stimulus type, and evoked aesthetic experience (high and low) on the recorded neural patterns, we tested 9

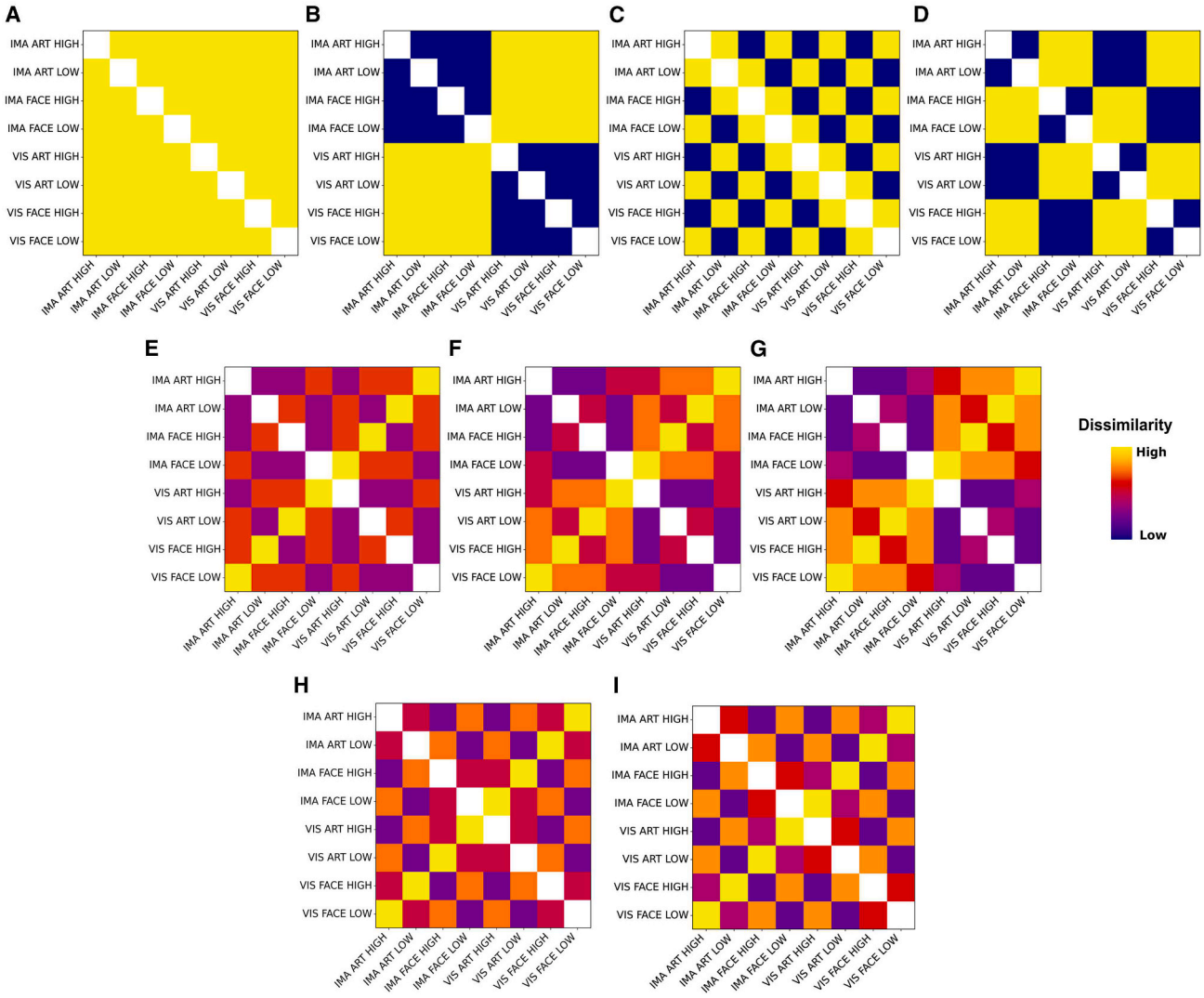

Figure 3. Candidate models

(A) Independent model: predicts that all conditions are maximally dissimilar to each other.
(B) Modality model: predicts that conditions across modalities are maximally dissimilar.
(C) Experience model: predicts that conditions across elicited aesthetic experiences are maximally dissimilar.
(D) Type model: predicts that conditions across stimulus types are maximally dissimilar.
(E) Mod|Exp|Type model: combines equally the dissimilarity structure of modality, experience, and stimulus type.
(F) Mod|(Exp|Type)/2 model: combines modality, experience, and stimulus type but downweighs experience and type by a factor of 2.
(G) Mod|(Exp|Type)/3: combines modality, experience, and stimulus type but downweighs experience and type by a factor of 3.
(H) Exp|(Mod|Type)/2: combines modality, experience, and stimulus type but downweighs modality and type by a factor of 2.
(I) Exp|(Mod|Type)/3: combines modality, experience, and stimulus type but downweighs modality and type by a factor of 3.

candidate models (see Figure 3). These models tested mainly five assumptions: (1) The neural patterns are completely independent of the stimulus properties (independent model). (2) Evoked neural patterns are solely driven by specific properties of the stimulus, that is, either by the modality of the stimulus, the experience the stimulus evoked, or the type of the stimulus (modality model; experience model; type model). (3) Evoked neural patterns are equally driven by stimulus properties (Mod|Exp|Type model). (4) Modality has a stronger influence on the neural signal compared to other stimulus properties. Models captured this assumption by downweighing the influence of evoked experience and type by a factor of 2 or 3 (Mod|(Exp|Type)/2 model; Mod|(Exp|Type)/3 model). (5) Experience has a stronger influence on the neural signal compared to other stimulus properties. Models captured this assumption by downweighing the influence of modality and type by a factor of 2 or 3 (Exp|(Mod|Type)/2 model; Exp|(Mod|Type)/3 model). Note that the latter two model types (4 and 5) were particularly designed to test H3, examining whether the contribution of stimulus properties to the neural

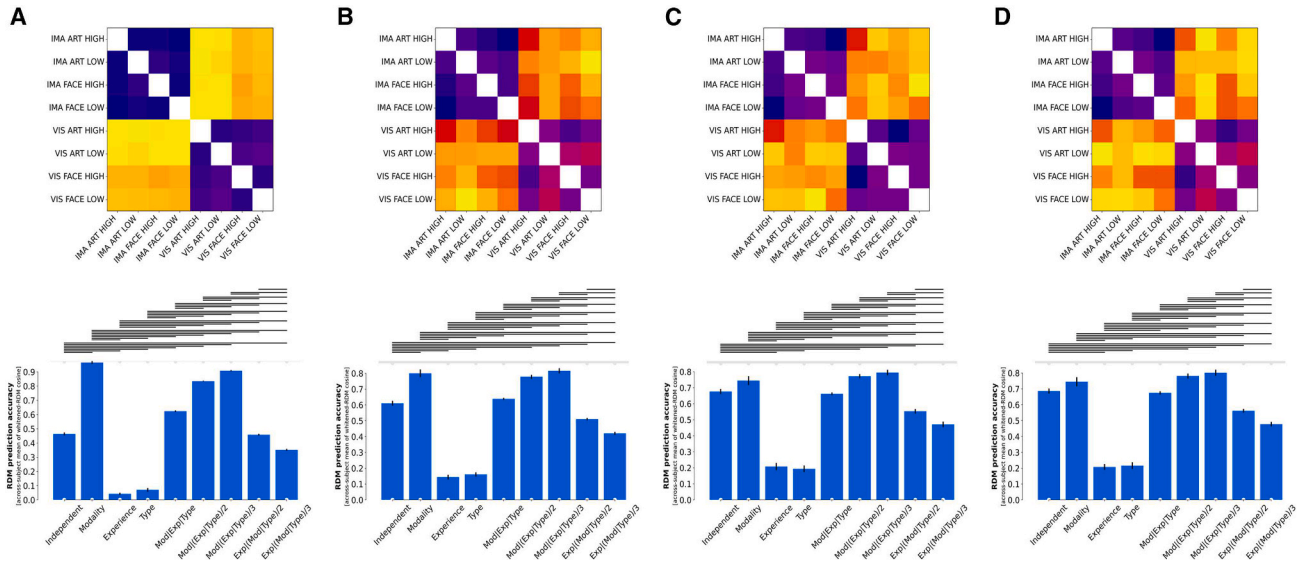

Figure 4. Performance of candidate models across brain regions for all participants (n = 30)

(A) Model comparison for whole brain data.

(B) Model comparison for reward network data.

(C) Model comparison for nucleus accumbens data.

(D) Model comparison for caudate nucleus data. Upper panels show across subject averaged neural RDMs. Lower panels show performance of candidate models across brain regions. Bars show means of whitened cosine similarity between candidate models and neural reference RDMs. Error bars indicate standard error of the mean (95% CI over 2000 bootstrap samples). Horizontal lines indicate significant differences in model performances (FDR $q < 0.01$). Gray dots on top depict significant differences from the noise ceiling (Bonferroni-corrected for 9 models). White dots at the bottom depict significant differences from 0. See also Table S9.

signal varies across levels of resolution. Specifically, we expected model type 4 to perform better at the whole-brain level, while at the level of the reward network and its individual regions, we expected the evoked experience to play a more dominant role, as captured by model 5. Model performances were compared against the noise ceiling, which can be intuitively thought of as the performance that the true underlying data-generating model would achieve given the noise in the data. Thus, models that are indistinguishable from the noise ceiling can be viewed as adequately specified as they reach optimal performance. Additionally, at each level of resolution, we compared performances across models to examine whether certain models predict observed similarity patterns better than others. Notably, upon reviewer's request, we additionally created a partial model solely combining aesthetic experience and stimulus type [Exp|Type] to investigate their combined influence on neural patterns; results are shown in the Supplemental Material (see Figure S1; Table S8).

As expected, at the whole brain level, the Modality model—predicting that observed (dis)similarities are solely driven by differences in stimulation modality (perception vs. imagery)—outperformed all other candidate models while also reaching the noise ceiling, indicating that observed (dis)similarity patterns were best described by purely taking differences in modality into account (accuracy: 0.965 [+/− 0.010]) (see Figure 4). While this result aligns with our initial hypothesis that neural signals at the whole brain level would primarily encode differences in modality, the strength of this association is still surprising (for model performances see Table S9). Notably, even models that predicted just minor contributions from other stimulus properties, e.g., Mod|(Exp|Type)/3 model, performed significantly worse, underscoring the overwhelming influence of the difference in modality (perception vs. imagined) on the neural signal at this level.

Within the reward network, both the Modality model (accuracy: 0.801 [+/− 0.024]) and the Mod|(Exp|Type)/3 model (accuracy: 0.816 [+/− 0.016]) reached the noise ceiling, indicating that observed (dis)similarity patterns were still predominantly driven by differences in modality. Subsequent model comparisons did not result in a significant difference between the two models. Thus, despite anticipating a shift in the relative contribution of stimulus properties to the neural signal in favor of the evoked aesthetic experience (high vs. low), the signal within the reward network remains predominantly driven by modality. Even more striking is that only one of the winning models predicts that type and aesthetic experience are driving similarity patterns at this level. This indicates that within the reward network—a network of areas canonically associated with reward processing—the neural signal continues to be dominated by differences in modality, while the subjective aesthetic experience contributes at most 20 percent to the signal.

Focusing more closely on the constituents of the reward network, that is, zooming even further into the nucleus accumbens and the caudate nucleus, the Mod|(Exp|Type)/3 model not only reached the noise ceiling but also outperformed all other models (nucleus accumbens [accuracy: 0.794 [+/− 0.018]]; caudate nucleus [accuracy: 0.801 [+/− 0.019]). This suggests that as the level of resolution becomes more fine-grained within the reward network, neural patterns increasingly reflect the evoked aesthetic

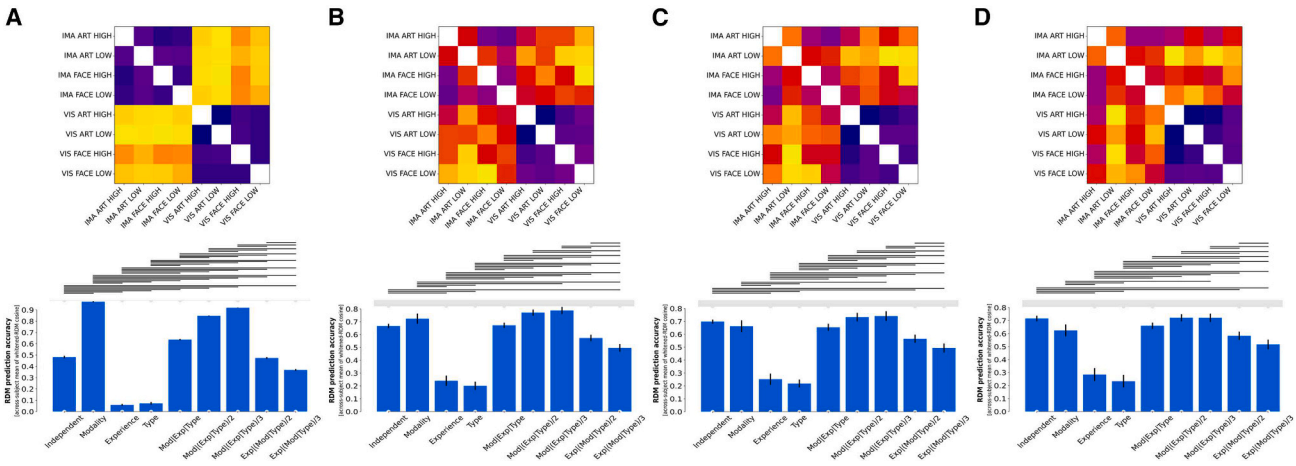

Figure 5. Subgroup analysis including only highly vivid trials for each participant (n = 11)

(A) Whole brain results exclusively using highly vivid trials.

(B) Reward network results exclusively using highly vivid trials.

(C) Nucleus accumbens results exclusively using highly vivid trials.

(D) Caudate nucleus results exclusively using highly vivid trials. Upper panels show across subject averaged neural RDMs. Lower panels show performance of candidate models across brain regions. Bars show means of whitened cosine similarity between candidate models and neural reference RDMs. Error bars indicate standard error of the mean (95% CI over 2000 bootstrap samples). Horizontal lines indicate significant differences in model performances (FDR q < 0.01). Gray dots indicate significant differences from the noise ceiling (Bonferroni-corrected for 9 models). White dots at the bottom depict significant differences from 0. See also Table S10.

experience. Yet, contrary to our assumption, modality—not subjective aesthetic experience—remains the primary driving factor in nucleus accumbens and the caudate nucleus.

Taken together, these results showcase that even within highly specialized areas canonically associated with aesthetic processing neural (dis)similarities are still mainly driven by differences in modality and only to a much lesser extent by the evoked experience itself.

To ensure that modality itself, rather than differences in vividness of the mental image, is driving observed similarity patterns, we conducted a subgroup analysis using only trials with the highest vividness ratings (6 and 7). Despite the reduction in sample size, the results remain largely comparable across the three levels of resolution (see Figure 5). The modality model continued to outperform all other models at the whole brain level (accuracy: 0.972 [+/− 0.005]) (see Table S10). Likewise, models that predicted stimulus type and experience had a small but significant impact on observed (dis)similarity patterns besides stimulus modality, i.e., Mod|(Exp|Type)/2 model and Mod|(Exp|Type)/3 model, performed exceptionally well within the reward network and its constituents (Mod|(Exp|Type)/2 model: reward network [accuracy: 0.771 [+/− 0.025]); nucleus accumbens (accuracy: 0.732 [+/− 0.035]); caudate nucleus (accuracy: 0.721 [+/− 0.028]); Mod|(Exp|Type)/3 model: reward network (accuracy: 0.787 [+/− 0.029]); nucleus accumbens (accuracy: 0.740 [+/− 0.039]); caudate nucleus (accuracy: 0.721 [+/− 0.034]). While the lower power from using exclusively highly vivid trials affected variance estimates and in turn model comparisons, the overall findings remain largely consistent with the main analysis. Thus, in light of these similar findings across the two analyses, it becomes apparent that aesthetic experiences generally are only marginally encoded in the neural patterns even within the reward network while the modality, in which the stimulus is originally perceived in, is dominantly driving neural dissimilarities across all levels of resolution.

DISCUSSION

This study tested the implicit assumption, prevalent within the field of neuroaesthetics, whether the aesthetic experience necessitates direct input into the sensory system by examining whether this complex and profound state could equally arise through purely internally generated representations. By presenting a diverse range of pre-rated aesthetic stimuli—artworks and faces—across sensory perception and mental imagery conditions, our study provides first conclusive, experimental-based evidence that the emergence of an aesthetic experience does not necessitate external sensory stimulation. The behavioral data clearly demonstrates that visual mental imagery is sufficient to elicit very similar aesthetic experiences to those evoked by visual perception when controlled for vividness. Interestingly, despite these overwhelming behavioral similarities, the neural signal in highly specialized areas canonically associated with aesthetic processing is only minimally driven by the subjective experience but rather dominated by differences in stimulation modality.

Across all tested facets of the aesthetic experience, visual perception evoked stronger aesthetic experiences than mental imagery. Yet, given that vividness plays a crucial role in shaping mental representations and naturally varies between trials,[17] we suspected that these observed differences are driven by the variations in vividness of the mental images rather than the modality of presentation. When examining these trial-to-trial changes in vividness, the data clearly shows that the similarity in aesthetic ratings—that is, the similarity in subjective experiences—across

visual perception and mental imagery is significantly affected by the vividness of the mental image. Thus, as mental representations more closely mirror those created by external perception, the resulting aesthetic experiences also become more similar. Notably, this effect is even present in participants specifically recruited for their average to high vividness abilities, suggesting that vividness might play a much stronger role in shaping the aesthetic experience in the general population. However, harnessing the advantages of the Bayesian framework, our results also evidently showed that for trials in which participants were able to clearly picture the presented stimulus, the two stimulation modalities elicited identical aesthetic experiences. This is in line with work by Dijkstra and colleagues who demonstrate that if the vividness of a mental image crosses a certain threshold, the induced experience becomes almost indistinguishable from the one induced by real-world events.[39] In that respect, our findings reveal that mental imagery is not only potent enough to evoke complex second-order effects, such as aesthetic experiences but that these experiences—provided that mental images are vivid enough—become virtually indistinguishable from those elicited by visual perception.

Furthermore, using a diverse pool of aesthetic stimuli, the present study reveals that aesthetic experiences can reliably be evoked by a variety of stimulation types, man-made, culturally significant objects (artworks), and biological stimuli (faces), both during immediate sensory perception and visual mental imagery. However, it appears that man-made objects lead to a stronger aesthetic experience. This would indeed make sense given the notion that man-made, culturally significant stimuli are rich of contextual complexity, which can also particularly appeal to the specific cultural characteristics, expertise, and learned expectations of the respective viewer.[9,50] Previous studies have continuously indicated that the more context and complex information provided for a stimulus, the higher was the aesthetic response.[51–59] In addition, prior research has demonstrated that both shared and individual (idiosyncratic) taste play a crucial role in shaping an aesthetic experience. However, individual taste has a greater potential to elicit strong aesthetic moments such as awe and being moved. Since aesthetic judgments of artworks, compared to faces, are significantly more affected by idiosyncratic taste,[60] it is to be expected that artworks consistently elicited more profound experiences than faces. Nonetheless, the aesthetic experience can reliably emerge—independently of direct external sensory perception—across a diverse range of visual stimuli, as our behavioral data unambiguously demonstrates, even though the type of stimulation has a significant influence on the strength of the evoked experience.

Two key implications arise from the results of the RSAs. First, stimulus modality is clearly driving observed (dis)similarities across conditions. Among all three levels of resolution, the modality model, which exclusively assumes modality is driving observed dissimilarity patterns, performed exceptionally well compared to other candidate models even reaching the noise ceiling at the whole brain and reward network level. The noise ceiling indicates that observed differences were explained just as accurately by purely considering the conceptual (dis)similarities across direct external sensory perception and visual mental imagery as they could have been by the underlying true (albeit unknown) data-generating model. Even though, we hypothesized that the neural signal would primarily encode differences in modality at the whole brain level, this basic model outperformed even models which were taking only minor contributions of stimulus type and the aesthetic experience into account. The fact that this association was also evident in the subgroup analysis, using exclusively highly vivid trials, suggests that the difference between visual perception and visual imagery dominates the neural signal (despite studies showing that similarity of neural patterns increases with vividness[17,61]). Even though the whole brain mask included also a variety of regions typically linked to stimulus recognition (e.g., the ventral visual stream[62]) and aesthetic processing (e.g., the reward network[40–42]), neither stimulus type nor the evoked aesthetic experience significantly influenced the neural signal at this broad level of analysis. But more surprisingly is the fact that the dominance of modality persists even when zooming into highly specialized areas for reward processing such as the reward network and the nucleus accumbens and caudate nucleus. This is contrary to our hypothesis (H3) predicting that the neural signal at the whole brain level would be dominated by modality but that this pattern would reverse within areas highly specialized in reward processing. In contrast to this common notion, however, our study revealed that the neural signal predominantly reflects whether a stimulus was externally or internally generated—even in areas highly specialized in aesthetic processing. Taken together, neural patterns across all levels of resolution did quite substantially encode differences in stimulation modality rather than evoked experience, despite the finding that behaviorally aesthetic experiences were indistinguishable across modalities for highly vivid trials.

Second, nonetheless, the more the regions were restrained to areas associated with aesthetic experiences, the more were neural (dis)similarity patterns encoding differences in evoked experiences and stimulus type besides changes in stimulus modality. In other words, within areas closely associated with aesthetic experiences such as the caudate nucleus and the nucleus accumbens, the Mod|(Exp|Type)/3 model, which was taking the experience and type of stimulus into account (albeit three times less significant as modality), not only outperformed all other models but also reached the noise ceiling indicating that this model perfectly described the recorded patterns. Focusing on the relative contribution of the subjective experience to the neural signal of about 20 percent, it is remarkable that despite its name, neural patterns within the reward network only encode evoked experiences to a quite small extent. The same pattern emerged when further zooming into the reward network, that is, the nucleus accumbens and the caudate nucleus—two areas reliably and continuously associated with aesthetic processing. Hence, although visual mental imagery is capable of generating complex and profound aesthetic experiences almost indistinguishable from those induced by visual perception, the neural signal underlying these very similar experiences differs substantially between the two modalities.

In conclusion, the present study provides first experimental-based proof that aesthetic experiences can arise solely through visual mental imagery without the need of immediate external sensory perception. Even though vividness predicts the similarity between evoked experiences across modalities, highly vivid and precise internally generated representations elicit indistinguishable

experiences from visual perception. Finally, contrary to our initial hypothesis, peak aesthetic experiences are not dominantly encoded in regions primarily associated with aesthetic processing. Rather, neural patterns are primarily driven by stimulation modality and only to a marginal extent by stimulus type and aesthetic experience. Thus, despite the fact that the subjective quality of the aesthetic experience does not appear to be affected, the stimulation modality provides a unique contribution to its underlying neural pattern. Taken together, this provides a new perspective on how the external world and an individual's internal processes shape the emergence of experiences, particularly aesthetic ones. While the modality of stimulation plays a significant role in how the brain processes information at all levels, the resulting aesthetic experiences can be remarkably similar, making them largely independent of the origin of the experience-inducing stimulus.

Limitations of the study

Despite efforts of the current study to recover unbiased similarity estimates by distantly spacing stimulus presentations, not all sources of bias could be fully eliminated. In general, it is advised to use crossnobis dissimilarity estimates if more than one run is recorded as they recover similarity structures more accurately.[63] Unfortunately, the subjective nature of the aesthetic task resulted in a majority of participants having a condition (e.g., a high aesthetic experience in response to an imagined facial stimulus) only being present in one run, rendering cross-validated similarity measures futile. Thus, if peak subjective experiences are of scientific interest, future research needs to balance methodological constraints with stimulus novelty and feasibility. Nonetheless, given the high similarity between the results of the complete dataset and the subset including only trials that had a high vividness rating, we are confident that the winning theory-derived candidate models adequately describe the recorded patterns. Furthermore, we acknowledge that it might have been possible that participants retained previously seen visual stimuli in their visual working memory rather than reimagining them. We deem this rather unlikely as the two modality conditions were spaced roughly 23 s apart in which several questions regarding the evoked aesthetic experience have been assessed. Lastly, a potential limitation of the current design is the possibility that ratings of the aesthetic experience persisted from the visual perception to the mental imagery condition. However, given the variability in ratings—sometimes leading to extremely different behavioral experiences across modalities—we consider this as unlikely as well. Nonetheless, future studies might aim to better separate the rating phases between the two modalities. Achieving this, would likely require training participants to memorize stimuli and recall them when cued, making it difficult to examine a large set of complex, novel, and naturalistic stimuli, as has been implemented in the present study.

RESOURCE AVAILABILITY

Lead contact

Requests for further information and resources should be directed to and will be fulfilled by the lead contact, Maximilian Kathofer (maximilian.kathofer@univie.ac.at).

Materials availability

This study did not generate new materials.

Data and code availability

- All behavioral data and beta estimates have been deposited at OSF: https://osf.io/apjud/?view_only=13f6a8e9adbb485385306b7204c31456 and are publicly available as of the date of publication.
- All original code has been deposited at OSF: https://osf.io/apjud/?view_only=13f6a8e9adbb485385306b7204c31456 and is publicly available as of the date of publication.
- All stimulus materials can be freely downloaded for scientific use.
- Chicago Face database: https://www.chicagofaces.org/.
- Face Research Lab London Set: https://figshare.com/articles/dataset/Face_Research_Lab_London_Set/5047666.
- Vienna Art Picture System: https://osf.io/a7xcr/.

ACKNOWLEDGMENTS

This research was funded in whole or in part by the Austrian Science Fund (FWF) 10.55776/CM11. M.K. is funded by BMBWF and OeAD-GmbH MMC-2023-06988. We want to thank Marc Esmeyer and Marius Schaffer for their fundamental work in helping to create stimulus material, in data acquisition, and in implementing the pilot study. The smiling person icon in the graphical abstract was created by iconcheese from the Noun Project.

AUTHOR CONTRIBUTIONS

Conceptualization, H.L. and J.S.C.; data collection, M.K. and J.S.C.; formal analysis, M.K. and J.S.C.; writing – original draft, M.K. and J.S.C.; writing – review and editing, H.L., C.L., J.S.C., and M.K.; resources, H.L., J.S.C., and C.L.; supervision, J.S.C.; visualization, M.K.

DECLARATION OF INTERESTS

The authors declare no competing interests.

DECLARATION OF GENERATIVE AI AND AI-ASSISTED TECHNOLOGIES

During the preparation of this work the author(s) used ChatGPT and Grammarly in order to check spelling, grammar, and phrasing. After using this tool/service, the author(s) reviewed and edited the content as needed and take(s) full responsibility for the content of the publication.

STAR★METHODS

Detailed methods are provided in the online version of this paper and include the following:

- KEY RESOURCES TABLE
- EXPERIMENTAL MODEL AND STUDY PARTICIPANT DETAILS
- METHOD DETAILS
  - Procedure
  - Sample size calculation
  - Stimulus selection
  - Aesthetic task
  - MRI data acquisition
  - MRI data preprocessing
  - Excessive motion
  - Regions of interest
- QUANTIFICATION AND STATISTICAL ANALYSIS
  - Missing data
  - Hierarchical Bayesian ordinal regression to compare experiences across conditions
  - Hierarchical Bayesian linear regression to probe vividness
  - Region of practical equivalence testing using Bayes Factors
  - Beta estimates

- Representational similarity analysis

SUPPLEMENTAL INFORMATION

Supplemental information can be found online at https://doi.org/10.1016/j.isci.2025.112529.

Received: November 28, 2024
Revised: February 20, 2025
Accepted: April 30, 2025
Published: May 5, 2025

REFERENCES

1. Dissanayake, E. (2008). The arts after Darwin: Does art have an origin and adaptive function. In World Art Studies: Exploring Concepts and Approaches, K. Zijlmans and W. van Damme, eds. (Valiz), pp. 241–263.
2. Brielmann, A.A., and Pelli, D.G. (2017). Beauty Requires Thought. Curr. Biol. *27*, 1506–1513.e3. https://doi.org/10.1016/j.cub.2017.04.018.
3. Pelowski, M., Hur, Y.-J., Cotter, K.N., Ishizu, T., Christensen, A.P., Leder, H., and McManus, I.C. (2021). Quantifying the if, the when, and the what of the sublime: A survey and latent class analysis of incidence, emotions, and distinct varieties of personal sublime experiences. Psychol. Aesthet. Creat. Arts *15*, 216–240. https://doi.org/10.1037/aca0000273.
4. Vessel, E.A., Ishizu, T., and Bignardi, G. (2022). Neural correlates of visual aesthetic appeal. In The Routledge International Handbook of Neuroaesthetics, M. Skov and M. Nadal, eds. (Routledge), pp. 103–133.
5. (2022). Empirical Aesthetics: An Overview. In The Oxford Handbook of Empirical Aesthetics, M. Nadal and O. Vartanian, eds. (Oxford University Press), pp. 3–38.
6. Kant, I. (2003). In Kritik der praktischen Vernunft, H.D. Brandt and H.F. Klemme, eds. (Felix Meiner Verlag), pp. 145–198.
7. T.H. Green and T.H. Grose, eds. (1974). The Philosophical Works of David Hume (Longman), pp. 371–471.
8. Porter, J.I. (2010). Plato and the Platonic Tradition: The Image beyond the Image (University of Toronto Press), pp. 75–103.
9. Leder, H., Belke, B., Oeberst, A., and Augustin, D. (2004). A model of aesthetic appreciation and aesthetic judgments. Br. J. Psychol. *95*, 489–508. https://doi.org/10.1348/0007126042369811.
10. Chatterjee, A., and Vartanian, O. (2016). Neuroscience of aesthetics. Ann. N. Y. Acad. Sci. *1369*, 172–194. https://doi.org/10.1111/nyas.13035.
11. Pelowski, M., Gerger, G., Chetouani, Y., Markey, P.S., and Leder, H. (2017). But Is It really Art? The Classification of Images as "Art"/"Not Art" and Correlation with Appraisal and Viewer Interpersonal Differences. Front. Psychol. *8*, 1729. https://doi.org/10.3389/fpsyg.2017.01729.
12. Trupp, M.D., Bignardi, G., Specker, E., Vessel, E.A., and Pelowski, M. (2023). Who benefits from online art viewing, and how: The role of pleasure, meaningfulness, and trait aesthetic responsiveness in computer-based art interventions for well-being. Comput. Hum. Behav. *145*, 107764. https://doi.org/10.1016/j.chb.2023.107764.
13. Carpentier, S.M., McCulloch, A.R., Brown, T.M., Faber, S.E.M., Ritter, P., Wang, Z., Salimpoor, V., Shen, K., and McIntosh, A.R. (2020). Complexity Matching: Brain Signals Mirror Environment Information Patterns during Music Listening and Reward. J. Cogn. Neurosci. *32*, 734–745. https://doi.org/10.1162/jocn_a_01508.
14. Winlove, C.I.P., Milton, F., Ranson, J., Fulford, J., MacKisack, M., Macpherson, F., and Zeman, A. (2018). The neural correlates of visual imagery: A co-ordinate-based meta-analysis. Cortex *105*, 4–25. https://doi.org/10.1016/j.cortex.2017.12.014.
15. Pearson, J. (2019). The human imagination: the cognitive neuroscience of visual mental imagery. Nat. Rev. Neurosci. *20*, 624–634. https://doi.org/10.1038/s41583-019-0202-9.
16. Bergmann, J., Genç, E., Kohler, A., Singer, W., and Pearson, J. (2016). Smaller Primary Visual Cortex Is Associated with Stronger, but Less Precise Mental Imagery. Cereb. Cortex *26*, 3838–3850. https://doi.org/10.1093/cercor/bhv186.
17. Dijkstra, N., Bosch, S.E., and van Gerven, M.A.J. (2017). Vividness of Visual Imagery Depends on the Neural Overlap with Perception in Visual Areas. J. Neurosci. *37*, 1367–1373. https://doi.org/10.1523/JNEUROSCI.3022-16.2016.
18. Keogh, R., Bergmann, J., and Pearson, J. (2020). Cortical excitability controls the strength of mental imagery. Elife *9*, e50232. https://doi.org/10.7554/eLife.50232.
19. Lee, S.-H., Kravitz, D.J., and Baker, C.I. (2012). Disentangling visual imagery and perception of real-world objects. Neuroimage *59*, 4064–4073. https://doi.org/10.1016/j.neuroimage.2011.10.055.
20. Marks, D.F. (1973). Visual Imagery Differences in the Recall of Pictures. Br. J. Psychol. *64*, 17–24. https://doi.org/10.1111/j.2044-8295.1973.tb01322.x.
21. Galton, F. (1880). os-V, Statistics of mental imagery (Mind os-V), pp. 301–318. https://doi.org/10.1093/mind/os-V.19.301.
22. Zeman, A. (2024). Aphantasia and hyperphantasia: exploring imagery vividness extremes. Trends Cogn. Sci. *28*, 467–480. https://doi.org/10.1016/j.tics.2024.02.007.
23. Wicken, M., Keogh, R., and Pearson, J. (2021). The critical role of mental imagery in human emotion: insights from fear-based imagery and aphantasia. Proc. Biol. Sci. *288*, 20210267. https://doi.org/10.1098/rspb.2021.0267.
24. Holmes, E.A., and Mathews, A. (2010). Mental imagery in emotion and emotional disorders. Clin. Psychol. Rev. *30*, 349–362. https://doi.org/10.1016/j.cpr.2010.01.001.
25. Suess, F., and Abdel Rahman, R. (2015). Mental imagery of emotions: Electrophysiological evidence. Neuroimage *114*, 147–157. https://doi.org/10.1016/j.neuroimage.2015.03.063.
26. Bray, S., Shimojo, S., and O'Doherty, J.P. (2010). Human Medial Orbitofrontal Cortex Is Recruited During Experience of Imagined and Real Rewards. J. Neurophysiol. *103*, 2506–2512. https://doi.org/10.1152/jn.01030.2009.
27. Greer, S.M., Trujillo, A.J., Glover, G.H., and Knutson, B. (2014). Control of nucleus accumbens activity with neurofeedback. Neuroimage *96*, 237–244. https://doi.org/10.1016/j.neuroimage.2014.03.073.
28. Kirschner, M., Sladky, R., Haugg, A., Stämpfli, P., Jehli, E., Hodel, M., Engeli, E., Hösli, S., Baumgartner, M.R., Sulzer, J., et al. (2018). Self-regulation of the dopaminergic reward circuit in cocaine users with mental imagery and neurofeedback. EBioMedicine *37*, 489–498. https://doi.org/10.1016/j.ebiom.2018.10.052.
29. American Psychiatric Association (2013). Diagnostic and Statistical Manual of Mental Disorders (DSM-5®) (American Psychiatric Publishing), p. 271.
30. Pearson, D.G., Deeprose, C., Wallace-Hadrill, S.M.A., Burnett Heyes, S., and Holmes, E.A. (2013). Assessing mental imagery in clinical psychology: A review of imagery measures and a guiding framework. Clin. Psychol. Rev. *33*, 1–23. https://doi.org/10.1016/j.cpr.2012.09.001.
31. Ji, J.L., Kavanagh, D.J., Holmes, E.A., MacLeod, C., and Di Simplicio, M. (2019). Mental imagery in psychiatry: conceptual & clinical implications. CNS Spectr. *24*, 114–126. https://doi.org/10.1017/S1092852918001487.
32. May, J., Kavanagh, D.J., and Andrade, J. (2015). The Elaborated Intrusion Theory of desire: A 10-year retrospective and implications for addiction treatments. Addict. Behav. *44*, 29–34. https://doi.org/10.1016/j.addbeh.2014.09.016.
33. Zorjan, S., and Schienle, A. (2023). Temporal dynamics of mental imagery, craving and consumption of craved foods: an experience sampling study. Psychol. Health *38*, 1443–1459. https://doi.org/10.1080/08870446.2022.2033239.

34. Lawrence, H.R., Balkind, E.G., Ji, J.L., Burke, T.A., and Liu, R.T. (2023). Mental imagery of suicide and non-suicidal self-injury: A meta-analysis and systematic review. Clin. Psychol. Rev. *103*, 102302. https://doi.org/10.1016/j.cpr.2023.102302.

35. Holmes, E.A., Arntz, A., and Smucker, M.R. (2007). Imagery rescripting in cognitive behaviour therapy: Images, treatment techniques and outcomes. J. Behav. Ther. Exp. Psychiatry *38*, 297–305. https://doi.org/10.1016/j.jbtep.2007.10.007.

36. Linhartová, P., Látalová, A., Kóša, B., Kašpárek, T., Schmahl, C., and Paret, C. (2019). fMRI neurofeedback in emotion regulation: A literature review. Neuroimage *193*, 75–92. https://doi.org/10.1016/j.neuroimage.2019.03.011.

37. Linke, J., and Wessa, M. (2017). Mental Imagery Training Increases Wanting of Rewards and Reward Sensitivity and Reduces Depressive Symptoms. Behav. Ther. *48*, 695–706. https://doi.org/10.1016/j.beth.2017.04.002.

38. Lowry, N., Marsden, J., Clydesdale, B., Eastwood, B., Havelka, E.M., and Goetz, C. (2021). Acute impact of self-guided mental imagery on craving in cocaine use disorder: a mixed-methods analysis of a randomized controlled trial. Addiction *116*, 2418–2430. https://doi.org/10.1111/add.15405.

39. Dijkstra, N., and Fleming, S.M. (2023). Subjective signal strength distinguishes reality from imagination. Nat. Commun. *14*, 1627. https://doi.org/10.1038/s41467-023-37322-1.

40. Vessel, E.A., Starr, G.G., and Rubin, N. (2012). The brain on art: intense aesthetic experience activates the default mode network. Front. Hum. Neurosci. *6*, 66.

41. Belfi, A.M., Vessel, E.A., Brielmann, A., Isik, A.I., Chatterjee, A., Leder, H., Pelli, D.G., and Starr, G.G. (2019). Dynamics of aesthetic experience are reflected in the default-mode network. Neuroimage *188*, 584–597. https://doi.org/10.1016/j.neuroimage.2018.12.017.

42. Salimpoor, V.N., Benovoy, M., Larcher, K., Dagher, A., and Zatorre, R.J. (2011). Anatomically distinct dopamine release during anticipation and experience of peak emotion to music. Nat. Neurosci. *14*, 257–262. https://doi.org/10.1038/nn.2726.

43. Ishizu, T. (2022). Functional Neuroimaging in Empirical Aesthetics and Neuroaesthetics. In The Oxford Handbook of Empirical Aesthetics, M. Nadal and O. Vartanian, eds. (Oxford University Press), pp. 308–338. https://doi.org/10.1093/oxfordhb/9780198824350.013.14.

44. Menninghaus, W., Wagner, V., Wassiliwizky, E., Schindler, I., Hanich, J., Jacobsen, T., and Koelsch, S. (2019). What are aesthetic emotions? Psychol. Rev. *126*, 171–195. https://doi.org/10.1037/rev0000135.

45. Cohen, J. (1988). Statistical Power Analysis for the Behavioral Sciences, 2nd ed. (Routledge), pp. 273–474. https://doi.org/10.4324/9780203771587.

46. Funder, D.C., and Ozer, D.J. (2019). Evaluating Effect Size in Psychological Research: Sense and Nonsense. Adv. Methods Pract. Psychol. Sci. *2*, 156–168. https://doi.org/10.1177/2515245919847202.

47. Wetzels, R., Matzke, D., Lee, M.D., Rouder, J.N., Iverson, G.J., and Wagenmakers, E.-J. (2011). Statistical Evidence in Experimental Psychology: An Empirical Comparison Using 855 t Tests. Perspect. Psychol. Sci. *6*, 291–298. https://doi.org/10.1177/1745691611406923.

48. Yarkoni, T., Poldrack, R.A., Nichols, T.E., Van Essen, D.C., and Wager, T.D. (2011). Large-scale automated synthesis of human functional neuroimaging data. Nat. Methods *8*, 665–670. https://doi.org/10.1038/nmeth.1635.

49. Popal, H., Wang, Y., and Olson, I.R. (2019). A Guide to Representational Similarity Analysis for Social Neuroscience. Soc. Cogn. Affect. Neurosci. *14*, 1243–1253. https://doi.org/10.1093/scan/nsz099.

50. Commare, L., Rosenberg, R., and Leder, H. (2018). More than the sum of its parts: Perceiving complexity in painting. Psychol. Aesthet. Creat. Arts *12*, 380–391. https://doi.org/10.1037/aca0000186.

51. Brieber, D., Nadal, M., and Leder, H. (2015). In the white cube: Museum context enhances the valuation and memory of art. Acta Psychol. *154*, 36–42. https://doi.org/10.1016/j.actpsy.2014.11.004.

52. Brieber, D., Nadal, M., Leder, H., and Rosenberg, R. (2014). Art in Time and Space: Context Modulates the Relation between Art Experience and Viewing Time. PLoS One *9*, e99019. https://doi.org/10.1371/journal.pone.0099019.

53. Gerger, G., and Leder, H. (2015). Titles change the esthetic appreciations of paintings. Front. Hum. Neurosci. *9*, 464. https://doi.org/10.3389/fnhum.2015.00464.

54. Grüner, S., Specker, E., and Leder, H. (2019). Effects of Context and Genuineness in the Experience of Art. Empir. Stud. Arts *37*, 138–152. https://doi.org/10.1177/0276237418822896.

55. Huang, M., Bridge, H., Kemp, M.J., and Parker, A.J. (2011). Human Cortical Activity Evoked by the Assignment of Authenticity when Viewing Works of Art. Front. Hum. Neurosci. *5*, 134. https://doi.org/10.3389/fnhum.2011.00134.

56. Kirk, U., Skov, M., Hulme, O., Christensen, M.S., and Zeki, S. (2009). Modulation of aesthetic value by semantic context: An fMRI study. Neuroimage *44*, 1125–1132. https://doi.org/10.1016/j.neuroimage.2008.10.009.

57. Millis, K. (2001). Making meaning brings pleasure: The influence of titles on aesthetic experiences. Emotion *1*, 320–329. https://doi.org/10.1037/1528-3542.1.3.320.

58. Specker, E., Tinio, P.P.L., and van Elk, M. (2017). Do you see what I see? An investigation of the aesthetic experience in the laboratory and museum. Psychol. Aesthet. Creat. Arts *11*, 265–275. https://doi.org/10.1037/aca0000107.

59. Szubielska, M., Imbir, K., and Szymańska, A. (2021). The influence of the physical context and knowledge of artworks on the aesthetic experience of interactive installations. Curr. Psychol. *40*, 3702–3715. https://doi.org/10.1007/s12144-019-00322-w.

60. Leder, H., Goller, J., Rigotti, T., and Forster, M. (2016). Private and Shared Taste in Art and Face Appreciation. Front. Hum. Neurosci. *10*, 155.

61. Cui, X., Jeter, C.B., Yang, D., Montague, P.R., and Eagleman, D.M. (2007). Vividness of mental imagery: Individual variability can be measured objectively. Vision Res. *47*, 474–478. https://doi.org/10.1016/j.visres.2006.11.013.

62. Cloutman, L.L. (2013). Interaction between dorsal and ventral processing streams: Where, when and how? Brain Lang. *127*, 251–263. https://doi.org/10.1016/j.bandl.2012.08.003.

63. Diedrichsen, J., and Kriegeskorte, N. (2017). Representational models: A common framework for understanding encoding, pattern-component, and representational-similarity analysis. PLoS Comput. Biol. *13*, e1005508. https://doi.org/10.1371/journal.pcbi.1005508.

64. Gorgolewski, K., Burns, C.D., Madison, C., Clark, D., Halchenko, Y.O., Waskom, M.L., and Ghosh, S.S. (2011). Nipype: A Flexible, Lightweight and Extensible Neuroimaging Data Processing Framework in Python. Front. Neuroinform. *5*, 13. https://doi.org/10.3389/fninf.2011.00013.

65. Jenkinson, M., Beckmann, C.F., Behrens, T.E.J., Woolrich, M.W., and Smith, S.M. (2012). FSL. Neuroimage *62*, 782–790. https://doi.org/10.1016/j.neuroimage.2011.09.015.

66. RSAtoolbox Development Group Representational Similarity Analysis 3.0. https://github.com/rsagroup/rsatoolbox.

67. Hoopes, A., Mora, J.S., Dalca, A.V., Fischl, B., and Hoffmann, M. (2022). SynthStrip: skull-stripping for any brain image. Neuroimage *260*, 119474. https://doi.org/10.1016/j.neuroimage.2022.119474.

68. Pruim, R.H.R., Mennes, M., van Rooij, D., Llera, A., Buitelaar, J.K., and Beckmann, C.F. (2015). ICA-AROMA: A robust ICA-based strategy for removing motion artifacts from fMRI data. Neuroimage *112*, 267–277. https://doi.org/10.1016/j.neuroimage.2015.02.064.

69. Peirce, J., Gray, J.R., Simpson, S., MacAskill, M., Höchenberger, R., Sogo, H., Kastman, E., and Lindeløv, J.K. (2019). PsychoPy2: Experiments in behavior made easy. Behav. Res. Methods *51*, 195–203. https://doi.org/10.3758/s13428-018-01193-y.

70. Faul, F., Erdfelder, E., Buchner, A., and Lang, A.-G. (2009). Statistical power analyses using G*Power 3.1: Tests for correlation and regression analyses. Behav. Res. Methods *41*, 1149–1160. https://doi.org/10.3758/BRM.41.4.1149.

71. Burton, L.J., and Fogarty, G.J. (2003). The factor structure of visual imagery and spatial abilities. Intelligence *31*, 289–318. https://doi.org/10.1016/S0160-2896(02)00139-3.

72. Campos, A., and Pérez-Fabello, M.J. (2009). Psychometric quality of a revised version Vividness of Visual Imagery Questionnaire. Percept. Mot. Skills *108*, 798–802. https://doi.org/10.2466/PMS.108.3.798-802.

73. Takahashi, J., Saito, G., Omura, K., Yasunaga, D., Sugimura, S., Sakamoto, S., Horikawa, T., and Gyoba, J. (2023). Diversity of aphantasia revealed by multiple assessments of visual imagery, multisensory imagery, and cognitive style. Front. Psychol. *14*, 1174873. https://doi.org/10.3389/fpsyg.2023.1174873.

74. Silvia, P.J., and Nusbaum, E.C. (2011). On personality and piloerection: Individual differences in aesthetic chills and other unusual aesthetic experiences. Psychol. Aesthet. Creat. Arts *5*, 208–214. https://doi.org/10.1037/a0021914.

75. Köchel, A., Plichta, M.M., Schäfer, A., Leutgeb, V., Scharmüller, W., Fallgatter, A.J., and Schienle, A. (2011). Affective perception and imagery: A NIRS study. Int. J. Psychophysiol. *80*, 192–197. https://doi.org/10.1016/j.ijpsycho.2011.03.006.

76. Kawabata, H., and Zeki, S. (2004). Neural Correlates of Beauty. J. Neurophysiol. *91*, 1699–1705. https://doi.org/10.1152/jn.00696.2003.

77. Hönekopp, J. (2006). Once more: Is beauty in the eye of the beholder? Relative contributions of private and shared taste to judgments of facial attractiveness. J. Exp. Psychol. Hum. Percept. Perform. *32*, 199–209. https://doi.org/10.1037/0096-1523.32.2.199.

78. O'Doherty, J., Winston, J., Critchley, H., Perrett, D., Burt, D.M., and Dolan, R.J. (2003). Beauty in a smile: the role of medial orbitofrontal cortex in facial attractiveness. Neuropsychologia *41*, 147–155. https://doi.org/10.1016/S0028-3932(02)00145-8.

79. Valuch, C., Pelowski, M., Peltoketo, V.-T., Hakala, J., and Leder, H. (2023). Let's put a smile on that face—A positive facial expression improves aesthetics of portrait photographs. R. Soc. Open Sci. *10*, 230413. https://doi.org/10.1098/rsos.230413.

80. Ma, D.S., Correll, J., and Wittenbrink, B. (2015). The Chicago face database: A free stimulus set of faces and norming data. Behav. Res. *47*, 1122–1135. https://doi.org/10.3758/s13428-014-0532-5.

81. DeBruine, L., and Benedict, J. (2017). Face Research Lab London Set. figshare. Dataset. https://doi.org/10.6084/m9.figshare.5047666.v5.

82. Schacht, A., Werheid, K., and Sommer, W. (2008). The appraisal of facial beauty is rapid but not mandatory. Cogn. Affect. Behav. Neurosci. *8*, 132–142. https://doi.org/10.3758/CABN.8.2.132.

83. Fekete, A., Pelowski, M., Specker, E., Brieber, D., Rosenberg, R., and Leder, H. (2023). The Vienna Art Picture System (VAPS): A data set of 999 paintings and subjective ratings for art and aesthetics research. Psychol. Aesthet. Creat. Arts *17*, 660–671. https://doi.org/10.1037/aca0000460.

84. Tustison, N.J., Avants, B.B., Cook, P.A., Zheng, Y., Egan, A., Yushkevich, P.A., and Gee, J.C. (2010). N4ITK: improved N3 bias correction. IEEE Trans. Med. Imaging *29*, 1310–1320. https://doi.org/10.1109/TMI.2010.2046908.

85. The MathWorks Inc. MATLAB Version: 9.13.0 (R2022b). The MathWorks Inc.

86. Greve, D.N., and Fischl, B. (2009). Accurate and Robust Brain Image Alignment using Boundary-based Registration. Neuroimage *48*, 63–72. https://doi.org/10.1016/j.neuroimage.2009.06.060.

87. Klein, A., Andersson, J., Ardekani, B.A., Ashburner, J., Avants, B., Chiang, M.-C., Christensen, G.E., Collins, D.L., Gee, J., Hellier, P., et al. (2009). Evaluation of 14 nonlinear deformation algorithms applied to human brain MRI registration. Neuroimage *46*, 786–802. https://doi.org/10.1016/j.neuroimage.2008.12.037.

88. Tustison, N.J., Cook, P.A., Holbrook, A.J., Johnson, H.J., Muschelli, J., Devenyi, G.A., Duda, J.T., Das, S.R., Cullen, N.C., Gillen, D.L., et al. (2021). The ANTsX ecosystem for quantitative biological and medical imaging. Sci. Rep. *11*, 9068. https://doi.org/10.1038/s41598-021-87564-6.

89. Parkes, L., Fulcher, B., Yücel, M., and Fornito, A. (2018). An evaluation of the efficacy, reliability, and sensitivity of motion correction strategies for resting-state functional MRI. Neuroimage *171*, 415–436. https://doi.org/10.1016/j.neuroimage.2017.12.073.

90. Buuren, S.v., and Groothuis-Oudshoorn, K. (2011). mice: Multivariate Imputation by Chained Equations in R. J. Stat. Softw. *45*, 1–67. https://doi.org/10.18637/jss.v045.i03.

91. Papageorgiou, G., Grant, S.W., Takkenberg, J.J.M., and Mokhles, M.M. (2018). Statistical primer: how to deal with missing data in scientific research? Interact. Cardiovasc. Thorac. Surg. *27*, 153–158. https://doi.org/10.1093/icvts/ivy102.

92. Lee, K.J., Tilling, K.M., Cornish, R.P., Little, R.J.A., Bell, M.L., Goetghebeur, E., Hogan, J.W., and Carpenter, J.R.; STRATOS initiative (2021). Framework for the treatment and reporting of missing data in observational studies: The Treatment And Reporting of Missing data in Observational Studies framework. J. Clin. Epidemiol. *134*, 79–88. https://doi.org/10.1016/j.jclinepi.2021.01.008.

93. Bürkner, P.-C. (2017). brms: An R Package for Bayesian Multilevel Models Using Stan. J. Stat. Software *80*, 1–28. https://doi.org/10.18637/jss.v080.i01.

94. Liddell, T.M., and Kruschke, J.K. (2018). Analyzing ordinal data with metric models: What could possibly go wrong? J. Exp. Soc. Psychol. *79*, 328–348. https://doi.org/10.1016/j.jesp.2018.08.009.

95. Bürkner, P.-C., and Vuorre, M. (2019). Ordinal Regression Models in Psychology: A Tutorial. Adv. Methods Pract. Psychol. Sci. *2*, 77–101. https://doi.org/10.1177/2515245918823199.

96. Gelman, A. Prior Choice Recommendations. GitHub. https://github.com/stan-dev/stan/wiki/prior-choice-recommendations.

97. Lüdecke, D., Ben-Shachar, M., Patil, I., and Makowski, D. (2020). Extracting, Computing and Exploring the Parameters of Statistical Models using R. J. Open Source Softw. *5*, 2445. https://doi.org/10.21105/joss.02445.

98. Makowski, D., Ben-Shachar, M., and Lüdecke, D. (2019). bayestestR: Describing Effects and their Uncertainty, Existence and Significance within the Bayesian Framework. J. Open Source Softw. *4*, 1541. https://doi.org/10.21105/joss.01541.

99. Kriegeskorte, N., Mur, M., and Bandettini, P. (2008). Representational similarity analysis - connecting the branches of systems neuroscience. Front. Syst. Neurosci. *2*, 4.

100. Walther, A., Nili, H., Ejaz, N., Alink, A., Kriegeskorte, N., and Diedrichsen, J. (2016). Reliability of dissimilarity measures for multi-voxel pattern analysis. Neuroimage *137*, 188–200. https://doi.org/10.1016/j.neuroimage.2015.12.012.

101. Diedrichsen, J., Berlot, E., Mur, M., Schütt, H.H., Shahbazi, M., and Kriegeskorte, N. (2021). Comparing representational geometries using whitened unbiased-distance-matrix similarity. Preprint at arXiv. https://doi.org/10.48550/arXiv.2007.02789.

102. Nili, H., Wingfield, C., Walther, A., Su, L., Marslen-Wilson, W., and Kriegeskorte, N. (2014). A Toolbox for Representational Similarity Analysis. PLoS Comput. Biol. *10*, e1003553. https://doi.org/10.1371/journal.pcbi.1003553.

STAR★METHODS

KEY RESOURCES TABLE

REAGENT or RESOURCE	SOURCE	IDENTIFIER
Deposited data		
All code, stimuli, beta maps and behavioral data	Center for Open Science https://www.cos.io/	https://osf.io/apjud/?view_only=13f6a8e9adbb485385306b7204c31456
Software and algorithms		
R 4.4.0	The R Project for Statistical Computing	https://www.r-project.org/
MATLAB 2019a	Mathworks, Inc, MA, USA	https://www.mathworks.com/products/matlab.html
Nipype	Gorgolewski et al.[64]	https://github.com/nipy/nipype
ANTs	Advanced Normalization Tools	https://github.com/ANTsX/ANTs
FSL	Jenkinson et al.[65]	https://fsl.fmrib.ox.ac.uk/fsldownloads_registration/
rsatoolbox	RSAtoolbox Development Group[66]	https://rsatoolbox.readthedocs.io/en/stable/
synthstrip	Hoopes et al.[67]	https://surfer.nmr.mgh.harvard.edu/docs/synthstrip/
ICA-AROMA	Pruim et al.[68]	https://github.com/maartenmennes/ICA-AROMA
NeuroSynth	Yarkoni et al.[48]	https://neurosynth.org/
PsychoPy	Pierce et al.[69]	https://www.psychopy.org/
G*Power	Faul et al.[70]	https://www.psychologie.hhu.de/arbeitsgruppen/allgemeine-psychologie-und-arbeitspsychologie/gpower

EXPERIMENTAL MODEL AND STUDY PARTICIPANT DETAILS

Participants were recruited at the campus of the University of Vienna and the central Viennese metropolitan area using flyers. To control for the effects of vividness on the aesthetic experience, participants were preselected using the Vividness of Visual Imagery Questionnaire (VVIQ)[20] to exclude all with low visual imagery abilities. The original VVIQ (see Data S1) is a 16-item self-report questionnaire assessing the ability to create clear mental images, yet, for screening efficiency and given its unidimensional structure[71] in conjunction with its extremely high internal consistency,[72] we only used 8 of its items. Typically, a 32-point cut-off is applied to identify individuals with extremely low imagery ability, a condition known as aphantasia.[73] For our shortened version, we implemented a more conservative proportional threshold of 25 instead of 16 points to ensure that participants did not exhibit very low imagery abilities. The translation of items into German was implemented by an English teacher and verified by a bilingual researcher. Items were adapted to fulfill the University's gender policy and to improve comprehensibility (see Data S2). To additionally ensure that participants experience at least average emotional and physiological responses to aesthetic stimuli, we used a slightly adapted version of the Aesthetic Experience Scale (AES)[74] (see Data S3), which measures the frequency and strength of aesthetic experiences. Translation to German and then back to English was implemented by three native speakers in each language respectively. Slight modifications were made to tailor questions to entail favorite art domains and frequency of exposure to these domains (see Data S4). Participants needed a minimum sum score of 35 on the AES and 25 on the VVIQ to qualify for the study, ensuring the exclusion of individuals with low aesthetic and imagery capabilities. Since this study was not interested in investigating the effect of vividness across the whole population, these cut-offs ensured that imagery was vivid and comparisons between modalities were safeguarded against potential biases stemming from participants' inability to mentally imagine stimuli, and thus, low ability to have aesthetic experiences in the first place. Additionally, participants had to meet the following inclusion criteria: at least 18 years of age, fluency in German, right-handedness, MRI compatibility, and normal or corrected to normal vision. Exclusion criteria included history of psychiatric and psychological disorders, medication affecting mood, (possible) pregnancy, and claustrophobia.

One participant was excluded during the study because of previously not declared mood-affecting medication and one other because of a technical issue terminating the scan session during recording. The final sample consisted of 34 participants (21 females, 1 diverse, 12 males), with a mean age of 23.48 years (SD = 4.01), all of whom provided informed consent. Thirty-two were native German speakers and the other two participants reported high proficiency in German. The study was approved by the ethics committee of the University of Vienna (Reference Number: 00636).

METHOD DETAILS

Procedure

To assess the neural representation of hedonic experiences in response to perception and imagery, participants had to complete an aesthetic task while functional magnetic resonance imaging (fMRI) data were collected. Commonly in aesthetic research, definitions of assessed concepts, such as being moved, are not adequately provided as they are assumed to be universally known. This is not only unwarranted, but an in-house pre-study (data not shown) demonstrated that laypeople differ quite considerably in their definitions of these concepts, which is why we provided clear instructions and definitions of the rating dimensions prior to the aesthetic task. To further mitigate any semantic misconceptions, participants had to pass comprehension questions assessing their understanding of the individual concepts (see Data S5).

Sample size calculation

A-priori sample-size calculations were based on a study with similar design[75] for a within-subject main effect of at least Cohen's d = 0.25 using G*Power[70] (alpha: 0.05; power: 0.80).

Stimulus selection

The stimulus set contained both representational artworks[40,41,60,76] and faces[77–79] as they are the most prevalent stimulation types used in aesthetic research. Additionally, using these two very distinct types of stimulation enabled us to examine whether our findings generalize across different types of stimuli, that is, either biologically or culturally significant (man-made).

A pre-study was conducted to maximize the likelihood of face stimuli eliciting strong aesthetic experiences. Seventeen participants (female: 7; *M*: 29.7; *SD* = 11.3) rated a predefined set of 56 faces extracted from the Chicago Face Database,[80] the Face Research London Set,[81] and the database of Schacht.[82] Using Adobe Photoshop, unnatural color gradings were edited and picture backgrounds were standardized. Faces were rated along the dimensions: beauty, arousal, valence, aesthetically moving, interest, and liking. The final set of 20 stimuli (12 male & 8 female faces) was chosen in such a way that half of the set elicited neutral and the other half maximal aesthetic experiences. We believe that the unbalanced distribution of gender does not affect our research question since we are not interested in investigating whether faces across gender induce a distinct brain response but rather use these stimuli to induce an aesthetic experience. The selected stimuli were rated the highest independent of gender and sexuality.

Using the pre-rated "Viennese Art Picture System" database (VAPS),[83] which contains 999 artworks of various styles, we extracted 20 highly beautiful and neutral representational paintings. Half of the selected stimuli elicited high mean beauty ratings – usually above 90 out of 100 points – with low variance while the other half was characterized by ratings below 50. Importantly, even though this study primarily focuses on the strong aesthetic experience of being moved, artworks were not extracted depending on their moving ratings from the database since participants initially rating these artworks were not given a sufficient definition of this rather complex concept *a priori*, and we suspected high interrater variance due to semantical misconception.

Aesthetic task

The final stimulus set consisted of 20 faces and 20 representational artworks, which were split randomly across 4 runs. PsychoPy was used for stimulus presentation.[69] Following a jittered fixation cross (3–5 s), a stimulus was presented for 15 s. Presentation length was chosen based on results from Belfi and colleagues,[41] showing that areas important for reward processing (nucleus accumbens and caudate nucleus) only respond to aesthetic processing during longer trial durations (5–15 s). Thereafter, participants rated the evoked experience along the dimensions 1) beauty ("How beautiful was the image"), 2) aesthetically moving ("How aesthetically moving was the image"), and 3) valence ("How pleasurable was the image") on a 7-point Likert scale. Given that pleasure and beauty are commonly assessed aesthetic dimensions, despite a lack of precise definitions in previous studies, we included them to explore whether induced effects differ across these aesthetic dimensions as well, even though the main focus of this study was the profound state of being moved. The order of questions was randomized across trials, and participants had 6 s to answer each question. Subsequently, participants were shown a symbol for 5 s which prompted the participants to close their eyes and prepare for the visual imagery trial, in which they had 15 s to imagine the previously encountered stimulus as vividly as possible. The beginning and end of this time interval were marked by a sinus tone (1 s), so participants knew when to start imagining and when to open their eyes again. Participants rated the mental image alongside the dimensions described above as well as its vividness ("How vivid was your mental image"). Each run lasted approximately 13–14 min.

Due to a technical issue, participants 3–11 were only presented 36 of the 40 stimuli, which alternated randomly between participants. Furthermore, compared to all other subjects, the task for subjects 1 and 2 was not split in 4 equal runs but 1 and 2 runs, respectively. Due to the subjective nature of the experiment, elicited subjective experiences generally resulted in some of the 8 conditions being only present in one of the runs, rendering crossnobis similarity estimates futile. Thus, we opted for a priori-defined across-runs averaged beta estimates and consequently could also use the data of subject 1 and 2 without biasing the estimates.

MRI data acquisition

Each block was recorded in a separate fMRI run. Functional data were acquired on a Siemens MAGNETOM Skyra 3T scanner with a sequentially increasing multiband 4 sequence (voxel size: 2.2^3 mm; TR: 0.915 s; TE: 34 ms; FA: 55°, FoV: 210 mm, FoV phase: 100%)

and a 32-channel head coil. To aid magnetic inhomogeneity correction, field maps were recorded at the end of each session. T1-weighted structural scans (MPRAGE; voxel size: 0.94^3; TR: 2.3 s; TE: 2.29 ms; TI: 900 ms; FA: 8°; FoV: 240 mm, FoV phase: 100%) were acquired for each participant.

MRI data preprocessing

Structural

Using nipype,[64] T1 scans were bias field corrected using the well-known N4ITK bias field correction algorithm due to its superior performance compared to its predecessor[84] and its subjective better performance than FSL FAST. Then, the images were brain extracted using Synthstrip as it outperforms other commonly used algorithms once with the –no-csf flag and once with the flags –no-csf and -b 2 (since those parameter settings usually yielded the best extractions).[67] Results were visually inspected and the best extractions were chosen for further analysis.

Field maps

Using custom MATLAB[85] scripts, magnitude images were reoriented, bias field corrected (N4ITK), brain extracted (Synthstrip), and eroded, so images only contained brain voxels following FSL recommendations. Phase images were prepared for their use within the FEAT pipeline using fsl_prepare_fieldmaps.

Functional

Using the FSL FEAT[65] pipeline, images were B0-unwarped (FUGUE), realigned to the middle volume (McFLIRT), coregistered to the structural scan using Boundary Based Registration (BBR) as it is more accurate than other commonly used methods (that is, correlation and mutual information)[86] and spatially smoothed using a 6mm FWHM (SUSAN). A 6 mm kernel was chosen since ICA-AROMA[68] is validated with the same settings. Images were registered to MNI 2mm standard space using the default settings of antsRegistrationSyN.sh as it outperforms other commonly used nonlinear algorithms.[87,88] To further mitigate potential bias introduced by artifacts, we used ICA-AROMA in its default settings (non-aggressive) since it is superior to other pipelines in balancing efficiency with data loss.[89] High-pass filtering was performed using fslmaths' -bptf flag with a sigma of 44.08 (82 s), which corresponds to one full trial cycle.

Excessive motion

Since the efficiency of ICA-AROMA decreases for high-motion data, we additionally excluded whole datasets based on the recommendations of Parkes et al.[89] exceeding a threshold of 0.2 mean framewise displacement (FD), having more than 20% outliers, or a maximal FD of 5 mm. Based on these criteria, one participant was excluded.

Regions of interest

To confirm that the neural patterns encoding the aesthetic experience are locally restricted within areas specialized in aesthetic processing in contrast to differences in modality which are encoded in the neural patterns across the entire brain, we have chosen three levels of resolution: (1) the whole brain; (2) the whole reward system as defined by a meta-analytical mask using the term 'reward' in Neurosynth[48] (https://www.neurosynth.org/analyses/terms/reward/, association test map thresholded at FDR <0.01); (3) two specific ROIs within the striatum, that is, nucleus accumbens and caudate nucleus. These two ROIs were chosen as they are consistently implicated in the anticipation as well as the processing of aesthetic experiences.[40–42]

QUANTIFICATION AND STATISTICAL ANALYSIS

Missing data

Except for the 4 missing stimuli for participants 3–11, which alternated randomly between partitions of the whole stimulus set for each subject, missingness only occurred in dependent variables, i.e., judgments of each evoked experience. Overall, less than 2.6% of recorded responses were missing (see Figure S2). In general, statistical tests can only detect whether data are missing completely at random (MCAR), thus not biasing the statistical analysis, or missing at random (MAR), that is, missingness depends on unobserved variables and consequently might substantially bias estimates. Using the R package mice[90] and its mcar function, we found no conclusive evidence that the data might be MAR as our data were not multivariate normally distributed (Anderson-Darling: median $T = 8.10$; median $p = 0.25$), and thus, the Hawkin's test could not be interpreted. As statistical assessment of MAR is often regarded suboptimal,[91] we reasoned that missingness might most probably be due to the restricted 6-s time window to answer each question. Judging from the almost uniform distribution of missing values across response dimensions and no clear patterns emerging between participants, we did not suspect hidden variables to cause missingness. In summary, we conclude that the missing values were truly MCAR. In line with the fact that the proportion of missing data remained below the commonly cited 5% threshold,[92] we opted for a complete case analysis, which in this case ensures unbiased estimates.

Hierarchical Bayesian ordinal regression to compare experiences across conditions

To assess whether aesthetic experiences can occur without external sensory stimulation and whether this affects the quality of the experience (H1), we tested whether ratings of aesthetic experiences differ between stimulation modalities (visual perception & visual imagery) and stimulation type (face & artwork). We opted for a hierarchical Bayesian ordinal regression using the brms package[93]

since it takes both the nestedness and the nonnormal distribution of responses into account. In such cases, it is beneficial to model Likert-scale data as truly ordinal as studies have shown that modeling Likert-scale responses instead as metric increases both Type 1 and 2 errors and potentially leads to inverted effect sizes.[94] Prior to modeling, we assessed which link function [probit, logit, cloglog, and cauchit] and threshold [flexible and equidistant] fitted our data best by creating null models with a series of possible configurations using the resulting log likelihood of each model as benchmark for model fit. Following the recommendations of Bürkner & Vuorre,[95] we used leave-one-out cross-validation to systematically compare potential models containing various combinations of category-specific effects, included regressors and hierarchical effects. As initially expected, the winning cumulative model with a probit link function contained regressors for stimulus type (face & artwork) and modality (visual perception & mental imagery), and random intercepts for both participants (ID) and each stimulus (stimulus_ID) (see Table S11). Weakly informative priors were used for stimulus type and modality [normal: 0,1][96] and default brms priors for all other parameters [student t: 3,0,2.5]. All reported models converged and posterior predictive checks assessed adequate data description.

Hierarchical Bayesian linear regression to probe vividness

To assess whether evoked experiences become more similar between stimulation modalities depending on the vividness of the mental image (H2), we calculated an absolute similarity score between responses across modalities by subtracting each individual rating in the imagery condition from its visual counterpart, squaring it and then adding them together for each individual stimulus. This resulted in a vector ranging from 0 (perfect similarity) to 48 (highest observed dissimilarity). The Bayesian linear model used a student distribution and contained a regressor for vividness and a random intercept for each participant to account for the hierarchical structure of the data. Parameter estimates were standardized using the parameters package.[97]

Region of practical equivalence testing using Bayes Factors

To examine whether evoked aesthetic experiences across stimulation modalities result in equal subjective experiences (H1) - if controlled for vividness - we performed a region of practical equivalence test using the bayestestR package[98] and assessed significance using the Bayes Factor. The resulting Bayes Factor indicates whether the posterior distribution of a parameter estimate has shifted away or toward a region of effect sizes [-0.1–0.1] typically considered as negligible.[45,46] For this analysis, we only used trials with the highest vividness ratings (6 and 7), performed hierarchical ordinal Bayesian regressions using the brms package and then calculated the Bayes Factor for the modality regressor using the bf_rope function of bayestestR. The models included main regressors for stimulus modality and type and random intercepts for each participant and stimulus.

Beta estimates

Here, we focus on the profound emotional state of being moved as the main concept of interest as it describes a deep emotional response to aesthetic stimuli. To compare high and low aesthetic experiences across the range of different stimulation modalities and types, we excluded trials with average ratings (4) and then split moving responses into high and low experiences.

First, a standard GLM in FSL was constructed convolving stimulus onsets and durations with a gamma response function to obtain beta estimates for all task regressors of interest. The GLM contained separate regressors for each unique combination of the three conditions, that is, experience (high and low), modality (perception and imagery), and type (art and face): high perception art (HPA), low perception art (LPA), high perception face (HPF), low perception face (LPF), high imagery art (HIA), low imagery art (LIA), high imagery face (HIF), and low imagery face (LIF). Furthermore, to account for residual variance of the task regressors temporal derivatives were added to the model. Additionally, a separate regressor modeling question blocks and trials with missing values was added to the GLM. The fMRI time series was pre-whitened within FSL FEAT to account for temporal autocorrelation using an AR (1) model. Due to the subjective nature of evoked experiences resulting in the absence of certain conditions within specific runs for a given participant, empty regressors were included in such cases to maintain consistent degrees of freedom across runs. The resulting run-wise beta maps were averaged for each participant using a fixed-effects model.

Representational similarity analysis

Representational similarity analysis (RSA) enables the investigation of the neural representational structure of a stimulus across multiple dimensions.[99] More specifically, RSA can be used to investigate how and if different aspects of a stimulus such as modality of perception, stimulus type, and experience are represented within a given neural pattern. To do so, RSA measures how dissimilar neural response patterns between conditions are by creating neural representational dissimilarity matrices (RDMs) and comparing them to theory-derived predictions about the geometry of evoked responses.[49] Here, we probe 9 candidate models: 1.) Independent model: conditions are maximal dissimilar to each other, meaning the neural patterns are completely independent from the stimulus properties; 2.) Modality model: neural similarity patterns are solely driven by differences in modality, meaning that observed patterns are similar within the same and dissimilar across stimulus modalities regardless of stimulus type and evoked experience (external sensory perception vs. mental imagery); 3.) Experience model: neural similarity patterns are solely driven by differences in experience, meaning that observed patterns are similar within the same and dissimilar across evoked experiences regardless of stimulus modality and type (low vs. high); 4.) Type model: neural similarity patterns are solely driven by differences in stimulus type, meaning that observed patterns are similar within the same and dissimilar across stimulus type regardless of stimulus modality and evoked experience (faces vs. artworks); 5.) Mod|Exp|Type: this model is a combination of the three previous models and takes the similarity

within experience, modality, and type into account, meaning neural patterns are equally driven by modality, experience, and type of stimulus; 6.) Mod|(Exp|Type)/2 model: This model predicts that the brain primarily encodes the initial modality of a stimulus, as it needs to track where a stimulus originated from – it still combines modality, type, and experience but reduces the influence of experience and type on the similarity of neural patterns by half, meaning differences in modality have 2 times more influence on neural patterns than experience or type; 7.) Mod|(Exp|Type)/3 model: similar to model 6, this model combines the similarity structure of stimulus modality, type, and experience, however, downweighs the latter two contributions by a factor of 3, meaning differences in modality have 3 times more influence on neural patterns than differences in experience or type; 8.) Exp|(Mod|Type)/2 model: this model predicts that the brain primarily encodes the strength of the experience induced by a stimulus – it still combines modality, type, and experience but reduces the influence of modality and type on the similarity of neural patterns by half, meaning differences in experience have 2 times more influence on neural patterns than modality or type; 9.) Exp|(Mod|Type)/3 model): similar to model 8, this model combines the similarity structure of stimulus modality, type, and experience, however, downweighs the former two contributions by a factor of 3, meaning differences in experience have 3 times more influence on neural patterns than modality or type.

Three participants were excluded from further analysis because they did not have responses in all conditions across the recorded runs.

The RSA analysis was performed using the Python Representational Similarity Analysis toolbox.[66] First, we z-scored the across-runs averaged beta estimates and created neural RDMs using squared Euclidian distances for each participant.[100] Neural RDMs were constrained to the aforementioned ROIs to examine whether the representational structure changes across different processing regions and levels of resolution. Next, we calculated the whitened cosine similarity between neural RDMs and the 9 candidate models.[101] Within each ROI, the 9 candidate models were compared against 0 and the lower bound of the noise ceiling. Intuitively, the noise ceiling is a measurement of how good the true data generating model would perform if stimulus responses were fixed and would only differ in noise. Thus, comparing candidate models to the noise ceiling indicates whether they are appropriately specified (no significant difference) or lack specification (significant difference).[102] Additionally, candidate models were compared against each other across all ROIs using two-tailed t-tests with FDR, $q < 0.01$. To calculate stable uncertainty estimates and compare model performances, we randomly sampled subjects 2000 times, which is twice the recommended sampling rate.[66]

iScience, Volume *28*

Supplemental information

Aesthetic experiences across visual perception and mental imagery: Behaviorally indistinguishable, neurally distinct

Maximilian Kathofer, Claus Lamm, Helmut Leder, and Julia Sophia Crone

Representational Similarity Analysis: partial model

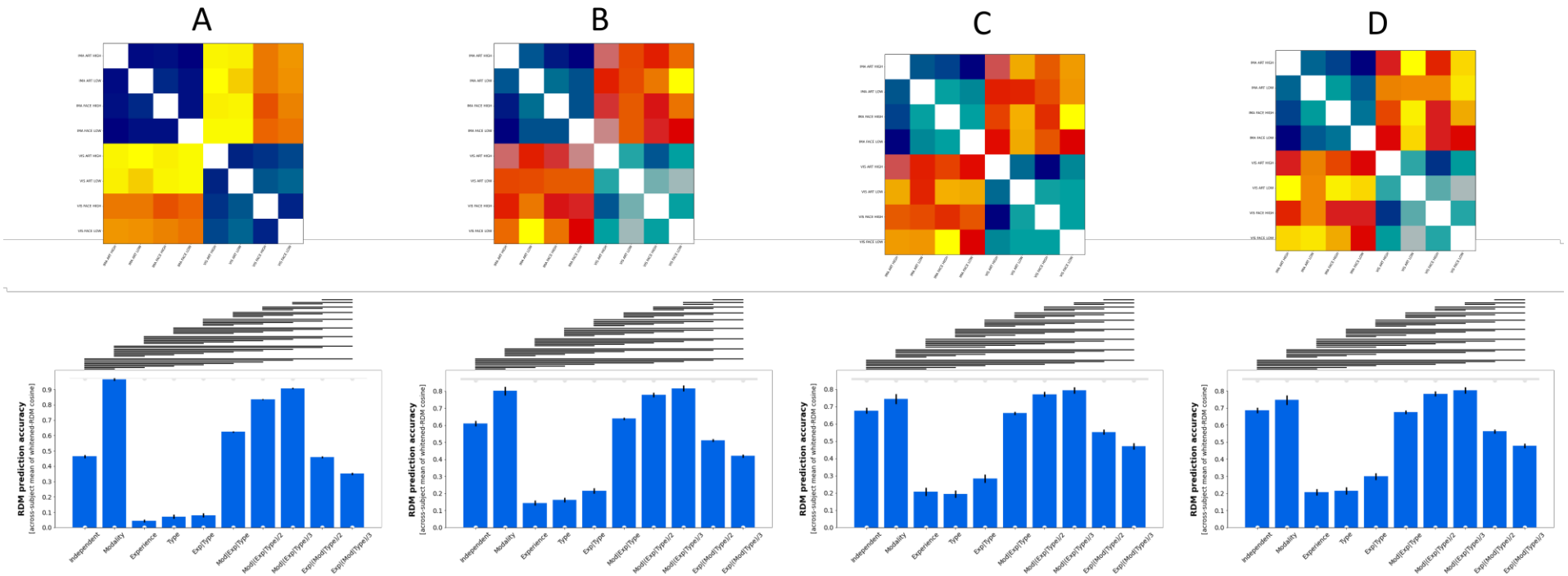

Figure S1. Performance of candidate models across brain regions for all participants (n = 30). (A) Model comparison for whole brain data. (B) Model comparison for reward network data. (C) Model comparison for nucleus accumbens data. (D) Model comparison for caudate nucleus data. Upper panels show across subject averaged neural RDMs. Lower panels show performance of candidate models across brain regions. Bars show means of whitened cosine similarity between candidate models and neural reference RDMs. Error bars indicate standard error of the mean (95% CI over 2000 bootstrap samples). Horizontal lines indicate significant differences in model performances (FDR q < 0.01). Grey dots on top depict significant differences from the noise ceiling (Bonferroni-corrected for 10 models). White dots at the bottom depict significant differences from 0.

Missing data

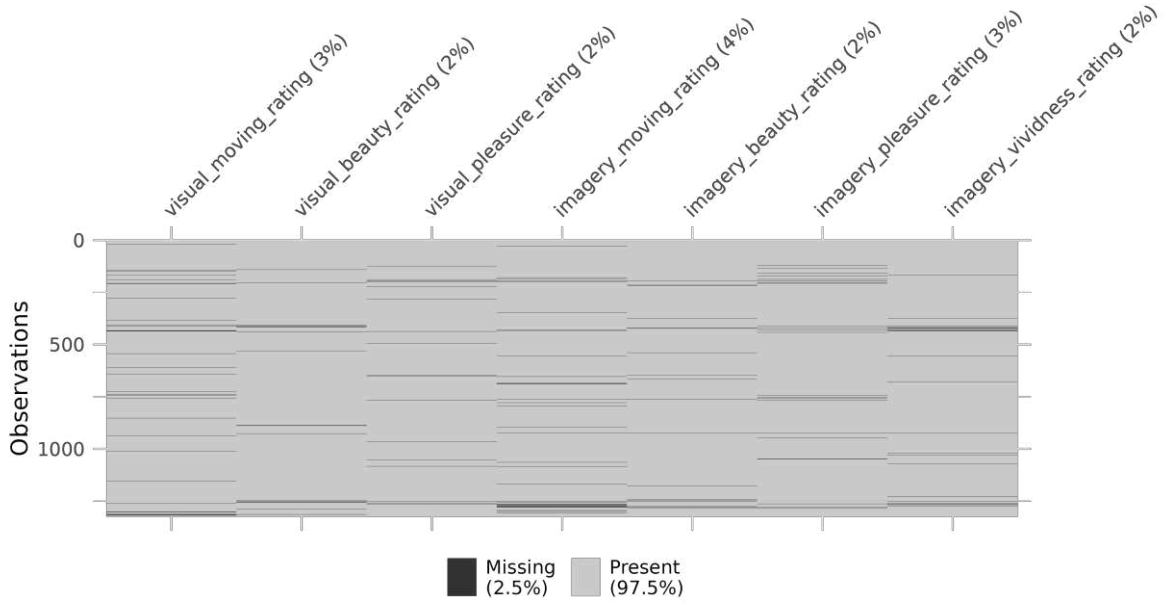

Figure S2. Missing data of response variables aggregated across participants. Data was plotted using the naniar package [S1].

Hierarchical ordinal Bayesian analyses of aesthetic facets for all trials

Moving:

Predictors	Estimate	Est.Error	l-95% CI	u-95% CI	Rhat	Bulk_ESS	Tail_ESS
Intercept[1]	-2.27	0.14	-2.55	-2.01	1.00	1678	3073
Intercept[2]	-1.34	0.13	-1.60	-1.08	1.00	1626	2807
Intercept[3]	-0.61	0.13	-0.87	-0.35	1.00	1611	2853
Intercept[4]	-0.15	0.13	-0.41	0.11	1.00	1602	2741
Intercept[5]	0.74	0.13	0.48	0.99	1.00	1627	2746
Intercept[6]	1.78	0.14	1.51	2.05	1.00	1787	3420
Modality: Imagery	-0.29	0.04	-0.37	-0.21	1.00	13091	7149
Type: Face	-0.56	0.11	-0.77	-0.35	1.00	2905	4787
Random effects							
ID	0.60	0.08	0.47	0.79	1.00	2064	3786
Image_ID	0.31	0.04	0.23	0.40	1.00	2833	3830

Table S1. Results of the hierarchical ordinal regression for moving ratings using all trials. Readers are reminded that estimates shown are standardized as they represent beta estimates on the latent standardized normal scale. Intercepts denote partitions of the latent scale to derive cumulative probabilities [S2]. Est.Error = estimation error. CI = Credible Interval. ESS = effective sample size. ID = random intercept for each participant (n=34). Image_ID = random intercept for each stimulus (n=40). Observations = 2553.

Beauty:

Predictors	Estimate	Est.Error	l-95% CI	u-95% CI	Rhat	Bulk_ESS	Tail_ESS
Intercept[1]	-2.48	0.14	-2.76	-2.21	1.00	1387	2596
Intercept[2]	-1.58	0.13	-1.84	-1.32	1.00	1296	2381
Intercept[3]	-0.95	0.13	-1.21	-0.69	1.00	1293	2374
Intercept[4]	-0.45	0.13	-0.71	-0.19	1.00	1273	2281
Intercept[5]	0.46	0.13	0.19	0.71	1.00	1262	2247
Intercept[6]	1.44	0.14	1.17	1,70	1.00	1367	2189
Modality: Imagery	-0.28	0.04	-0.37	-0.20	1.00	11821	6478
Type: Face	-0.43	0.15	-0.71	-0.13	1.00	1588	2736
Random effects							
ID	0.46	0.07	0.35	0.61	1.00	1927	3499
Image_ID	0.44	0.06	0.34	0.56	1.00	1869	3318

Table S2. Results of the hierarchical ordinal regression for beauty ratings using all trials. Readers are reminded that estimates shown are standardized as they represent beta estimates on the latent standardized normal scale. Intercepts denote partitions of the latent scale to derive cumulative probabilities [S2]. Est.Error = estimation error. CI = Credible Interval. ESS = effective sample size. ID = random intercept for each participant (n=34). Image_ID = random intercept for each stimulus (n=40). Observations = 2603.

Pleasure:

Predictors	Estimate	Est.Error	l-95% CI	u-95% CI	Rhat	Bulk_ESS	Tail_ESS
Intercept[1]	-2.37	0.14	-2.65	-2.09	1.00	1579	2752
Intercept[2]	-1.47	0.14	-1.74	-1.20	1.00	1510	2720
Intercept[3]	-0.74	0.14	-1.01	-0.48	1.00	1498	2844
Intercept[4]	-0.28	0.13	-0.54	-0.01	1.00	1491	2727
Intercept[5]	0.57	0.14	0.31	0.84	1.00	1502	2835
Intercept[6]	1.47	0.14	1.20	1.75	1.00	1585	3256
Modality: Imagery	-0.22	0.04	-0.31	-0.14	1.00	14675	7021
Type: Face	-0.82	0.12	-1.06	-0.58	1.00	2312	3569

Random effects							
ID	0.60	0.08	0.47	0.79	1.00	1936	3375
Image_ID	0.35	0.05	0.27	0.46	1.00	2989	3983

Table S3. Results of the hierarchical ordinal regression for pleasure ratings using all trials. Readers are reminded that estimates shown are standardized as they represent beta estimates on the latent standardized normal scale. Intercepts denote partitions of the latent scale to derive cumulative probabilities [S2]. Est.Error = estimation error. CI = Credible Interval. ESS = effective sample size. ID = random intercept for each participant (n=34). Image_ID = random intercept for each stimulus (n=40). Observations = 2588.

Correlation between vividness and similarity of evoked experiences across modalities

Predictors	**Estimate**	**Est.Error**	**l-95% CI**	**u-95% CI**	**Rhat**	**Bulk_ESS**	**Tail_ESS**
Intercept	-2.89	0.28	2.33	3.45	1.00	2774	4860
Vividness	-0.19	0.04	-0.28	-0.10	1.00	10211	7792
Random effects							
ID	0.97	0.17	0.67	1.35	1.00	1690	3294

Table S4.1. Correlation between the similarity of subjective experiences across stimulation modalities and vividness of the mental image. Unstandardized parameter estimates are shown. Est.Error = estimation error. CI = Credible Interval. ESS = effective sample size. ID = random intercept for each participant (n=34). Observations = 1130.

Parameter	**Std. Median**	**95% CI**
Intercept	2.00	[1.66, 2.38]
Vividness	-0.27	[-0.40, -0.14]

Table S4.2. Standardized parameter estimates for the correlation between the similarity of subjective experiences across stimulation modalities and vividness of the mental image. Parameters were standardized using the effectsize package [S3].

Hierarchical ordinal Bayesian analyses of aesthetic facets for highly vivid trials

Moving:

Predictors	**Estimate**	**Est.Error**	**l-95% CI**	**u-95% CI**	**Rhat**	**Bulk_ESS**	**Tail_ESS**
Intercept[1]	-2.47	0.16	-2.81	-2.16	1.00	1918	2940
Intercept[2]	-1.64	0.14	-1.92	-1.36	1.00	1847	2871
Intercept[3]	-0.99	0.14	-1.27	-0.72	1.00	1824	3067
Intercept[4]	-0.50	0.14	-0.78	-0.24	1.00	1791	2834
Intercept[5]	0.38	0.13	0.11	0.64	1.00	1786	2750
Intercept[6]	1.42	0.15	1.14	1.71	1.00	2100	2926

Modality: Imagery	-0.14	0.08	-0.29	0.01	1.00	6221	3558
Type: Face	-0.62	0.14	-0.89	-0.35	1.00	1858	2692
Random effects							
ID	0.48	0.09	0.33	0.68	1.00	1213	2123
Image_ID	0.33	0.07	0.21	0.47	1.00	1750	2425

Table S5. Results of the hierarchical ordinal regression for moving ratings using only highly vivid trials. Readers are reminded that estimates shown are standardized as they represent beta estimates on the latent standardized normal scale. Intercepts denote partitions of the latent scale to derive cumulative probabilities [S2]. Est.Error = estimation error. CI = Credible Interval. ESS = effective sample size. ID = random intercept for each participant (n=34). Image_ID = random intercept for each stimulus (n=40). Observations = 772.

Beauty:

Predictors	Estimate	Est.Error	l-95% CI	u-95% CI	Rhat	Bulk_ESS	Tail_ESS
Intercept[1]	-2.71	0.18	-3.07	-2.36	1.00	2928	3024
Intercept[2]	-1.80	0.15	-2.11	-1.51	1.00	2917	3430
Intercept[3]	-1.29	0.15	-1.59	-1.01	1.00	2769	3548
Intercept[4]	-0.89	0.14	-1.17	-0.62	1.00	2734	3485
Intercept[5]	0.08	0.14	-0.20	0.36	1.00	2719	3227
Intercept[6]	1.18	0.15	0.89	1.47	1.00	2801	3433
Modality: Imagery	-0.14	0.08	-0.29	0.01	1.00	7722	3348
Type: Face	-0.46	0.16	-0.80	-0.15	1.00	2281	2546
Random effects							
ID	0.40	0.08	0.27	0.58	1.00	1625	2593
Image_ID	0.43	0.07	0.30	0.58	1.00	1821	2930

Table S6. Results of the hierarchical ordinal regression for beauty ratings using only highly vivid trials. Readers are reminded that estimates shown are standardized as they represent beta estimates on the latent standardized normal scale. Intercepts denote partitions of the latent scale to derive cumulative probabilities [S2]. Est.Error = estimation error. CI = Credible Interval. ESS = effective sample size. ID = random intercept for each participant (n=34). Image_ID = random intercept for each stimulus (n=40). Observations = 783.

Pleasure:

Predictors	Estimate	Est.Error	l-95% CI	u-95% CI	Rhat	Bulk_ESS	Tail_ESS
Intercept[1]	-2.46	0.18	-2.80	-2.12	1.00	1535	2306
Intercept[2]	-1.78	0.16	-2.10	-1.46	1.00	1442	2174
Intercept[3]	-1.19	0.16	-1.51	-0.89	1.00	1367	2058
Intercept[4]	-0.74	0.16	-1.04	-0.43	1.00	1369	2162
Intercept[5]	0.20	0.15	-0.10	0.50	1.00	1392	2229
Intercept[6]	1.05	0.16	0.75	1.35	1.00	1481	2584
Modality: Imagery	-0.07	0.07	-0.22	0.07	1.00	5810	3712
Type: Face	-0.92	0.15	-1.21	-0.62	1.00	1857	2770
Random effects							
ID	0.56	0.10	0.40	0.78	1.00	1558	2416
Image_ID	0.39	0.07	0.27	0.54	1.00	1574	2266

Table S7. Results of the hierarchical ordinal regression for pleasure ratings using only highly vivid trials. Readers are reminded that estimates shown are standardized as they represent beta estimates on the latent standardized normal scale. Intercepts denote partitions of the latent scale to derive cumulative probabilities [S2]. Est.Error = estimation error. CI = Credible Interval. ESS = effective sample size. ID = random intercept for each participant (n=34). Image_ID = random intercept for each stimulus (n=40). Observations = 783.

Representational Similarity Analysis: partial model

Whole brain

Model	Eval ± SEM	p (against 0)	p (against NC)
Independent	0.464 ± 0.010	< 0.001	< 0.001
Modality	0.965 ± 0.010	< 0.001	0.484
Experience	0.044 ± 0.008	< 0.001	< 0.001
Type	0.071 ± 0.013	< 0.001	< 0.001
Exp|Type	0.081 ± 0.013	< 0.001	< 0.001
Mod|Exp|Type	0.624 ± 0.006	< 0.001	< 0.001
Mod|(Exp|Type)/2	0.835 ± 0.003	< 0.001	< 0.001
Mod|(Exp|Type)/3	0.908 ± 0.005	< 0.001	< 0.001
Exp|(Mod|Type)/2	0.459 ± 0.007	< 0.001	< 0.001
Exp|(Mod|Type)/3	0.352 ± 0.007	< 0.001	< 0.001

Reward network

Model	Eval ± SEM	p (against 0)	p (against NC)
Independent	0.610 ± 0.016	< 0.001	< 0.001
Modality	0.800 ± 0.025	< 0.001	0.015
Experience	0.144 ± 0.014	< 0.001	< 0.001
Type	0.161 ± 0.014	< 0.001	< 0.001
Exp|Type	0.216 ± 0.016	< 0.001	< 0.001
Mod|Exp|Type	0.638 ± 0.007	< 0.001	< 0.001
Mod|(Exp|Type)/2	0.778 ± 0.013	< 0.001	< 0.001
Mod|(Exp|Type)/3	0.816 ± 0.016	< 0.001	0.007
Exp|(Mod|Type)/2	0.510 ± 0.008	< 0.001	< 0.001
Exp|(Mod|Type)/3	0.420 ± 0.010	< 0.001	< 0.001

Caudate nucleus

Model	Eval ± SEM	p (against 0)	p (against NC)
Independent	0.686 ± 0.016	< 0.001	< 0.001
Modality	0.746 ± 0.028	< 0.001	< 0.001
Experience	0.208 ± 0.019	< 0.001	< 0.001
Type	0.215 ± 0.021	< 0.001	< 0.001
Exp|Type	0.299 ± 0.021	< 0.001	< 0.001
Mod|Exp|Type	0.675 ± 0.010	< 0.001	< 0.001
Mod|(Exp|Type)/2	0.782 ± 0.015	< 0.001	< 0.001
Mod|(Exp|Type)/3	0.802 ± 0.019	< 0.001	0.004
Exp|(Mod|Type)/2	0.562 ± 0.013	< 0.001	< 0.001
Exp|(Mod|Type)/3	0.478 ± 0.014	< 0.001	< 0.001

Nucleus accumbens

Model	Eval ± SEM	p (against 0)	p (against NC)
Independent	0.677 ± 0.016	< 0.001	< 0.001
Modality	0.745 ± 0.027	< 0.001	< 0.001
Experience	0.208 ± 0.022	< 0.001	< 0.001
Type	0.194 ± 0.020	< 0.001	< 0.001
Exp|Type	0.285 ± 0.022	< 0.001	< 0.001
Mod|Exp|Type	0.662 ± 0.009	< 0.001	< 0.001
Mod|(Exp|Type)/2	0.772 ± 0.013	< 0.001	< 0.001
Mod|(Exp|Type)/3	0.795 ± 0.017	< 0.001	0.002
Exp|(Mod|Type)/2	0.553 ± 0.014	< 0.001	< 0.001
Exp|(Mod|Type)/3	0.472 ± 0.017	< 0.001	< 0.001

Table S8. Candidate model performance across regions of interest using the whole dataset. p-values are based on uncorrected t-tests. NC = noise ceiling; SEM = standard error of the mean.

Representational Similarity Analysis: whole dataset

Whole brain

Model	Eval ± SEM	p (against 0)	p (against NC)
Independent	0.465 ± 0.010	< 0.001	< 0.001
Modality	0.965 ± 0.010	< 0.001	0.492
Experience	0.044 ± 0.008	< 0.001	< 0.001
Type	0.072 ± 0.013	< 0.001	< 0.001
Mod|Exp|Type	0.624 ± 0.006	< 0.001	< 0.001
Mod|(Exp|Type)/2	0.835 ± 0.003	< 0.001	< 0.001
Mod|(Exp|Type)/3	0.908 ± 0.004	< 0.001	< 0.001
Exp|(Mod|Type)/2	0.459 ± 0.007	< 0.001	< 0.001
Exp|(Mod|Type)/3	0.352 ± 0.007	< 0.001	< 0.001

Reward network

Model	Eval ± SEM	p (against 0)	p (against NC)
Independent	0.610 ± 0.015	< 0.001	< 0.001
Modality	0.801 ± 0.024	< 0.001	0.012
Experience	0.144 ± 0.014	< 0.001	< 0.001
Type	0.161 ± 0.013	< 0.001	< 0.001
Mod|Exp|Type	0.638 ± 0.007	< 0.001	< 0.001
Mod|(Exp|Type)/2	0.778 ± 0.012	< 0.001	< 0.001
Mod|(Exp|Type)/3	0.816 ± 0.016	< 0.001	0.005
Exp|(Mod|Type)/2	0.510 ± 0.008	< 0.001	< 0.001
Exp|(Mod|Type)/3	0.420 ± 0.010	< 0.001	< 0.001

Caudate nucleus

Model	Eval ± SEM	p (against 0)	p (against NC)
Independent	0.687 ± 0.016	< 0.001	< 0.001
Modality	0.745 ± 0.028	< 0.001	< 0.001
Experience	0.208 ± 0.019	< 0.001	< 0.001
Type	0.216 ± 0.021	< 0.001	< 0.001
Mod|Exp|Type	0.675 ± 0.010	< 0.001	< 0.001
Mod|(Exp|Type)/2	0.781 ± 0.015	< 0.001	< 0.001

Mod|(Exp|Type)/3	0.801 ± 0.019	< 0.001	0.004
Exp|(Mod|Type)/2	0.562 ± 0.013	< 0.001	< 0.001
Exp|(Mod|Type)/3	0.478 ± 0.014	< 0.001	< 0.001

Nucleus accumbens

Model	Eval ± SEM	p (against 0)	p (against NC)
Independent	0.677 ± 0.016	< 0.001	< 0.001
Modality	0.744 ± 0.028	< 0.001	< 0.001
Experience	0.208 ± 0.023	< 0.001	< 0.001
Type	0.194 ± 0.021	< 0.001	< 0.001
Mod|Exp|Type	0.662 ± 0.009	< 0.001	< 0.001
Mod|(Exp|Type)/2	0.772 ± 0.013	< 0.001	< 0.001
Mod|(Exp|Type)/3	0.794 ± 0.018	< 0.001	0.003
Exp|(Mod|Type)/2	0.554 ± 0.015	< 0.001	< 0.001
Exp|(Mod|Type)/3	0.472 ± 0.018	< 0.001	< 0.001

Table S9. Candidate model performance across regions of interest using the whole dataset. p-values are based on uncorrected t-tests. NC = noise ceiling; SEM = standard error of the mean

Representational Similarity Analysis: highly vivid trials

Whole brain

Model	Eval ± SEM	p (against 0)	p (against NC)
Independent	0.483 ± 0.012	< 0.001	< 0.001
Modality	0.972 ± 0.005	< 0.001	0.099
Experience	0.059 ± 0.009	< 0.001	< 0.001
Type	0.073 ± 0.013	< 0.001	< 0.001
Mod|Exp|Type	0.637 ± 0.007	< 0.001	< 0.001
Mod|(Exp|Type)/2	0.847 ± 0.003	< 0.001	< 0.001
Mod|(Exp|Type)/3	0.919 ± 0.002	< 0.001	< 0.001
Exp|(Mod|Type)/2	0.475 ± 0.008	< 0.001	< 0.001
Exp|(Mod|Type)/3	0.368 ± 0.009	< 0.001	< 0.001

Reward network

Model	Eval ± SEM	p (against 0)	p (against NC)
Independent	0.667 ± 0.017	< 0.001	< 0.001
Modality	0.723 ± 0.041	< 0.001	0.041
Experience	0.241 ± 0.042	< 0.001	< 0.001
Type	0.202 ± 0.032	< 0.001	< 0.001
Mod|Exp|Type	0.673 ± 0.021	< 0.001	< 0.001
Mod|(Exp|Type)/2	0.771 ± 0.025	< 0.001	0.076
Mod|(Exp|Type)/3	0.787 ± 0.029	< 0.001	0.296
Exp|(Mod|Type)/2	0.565 ± 0.025	< 0.001	< 0.001
Exp|(Mod|Type)/3	0.493 ± 0.030	< 0.001	< 0.001

Caudate nucleus

Model	Eval ± SEM	p (against 0)	p (against NC)
Independent	0.716 ± 0.022	< 0.001	0.002
Modality	0.626 ± 0.047	< 0.001	0.003
Experience	0.281 ± 0.050	< 0.001	< 0.001
Type	0.235 ± 0.047	< 0.001	< 0.001
Mod|Exp|Type	0.659 ± 0.024	< 0.001	< 0.001
Mod|(Exp|Type)/2	0.721 ± 0.028	< 0.001	0.014
Mod|(Exp|Type)/3	0.721 ± 0.034	< 0.001	0.031
Exp|(Mod|Type)/2	0.581 ± 0.030	< 0.001	< 0.001
Exp|(Mod|Type)/3	0.514 ± 0.035	< 0.001	< 0.001

Nucleus accumbens

Model	Eval ± SEM	p (against 0)	p (against NC)
Independent	0.698 ± 0.016	< 0.001	< 0.001
Modality	0.662 ± 0.048	< 0.001	0.010
Experience	0.252 ± 0.044	< 0.001	< 0.001
Type	0.218 ± 0.032	< 0.001	< 0.001
Mod|Exp|Type	0.653 ± 0.028	< 0.001	< 0.001
Mod|(Exp|Type)/2	0.732 ± 0.035	< 0.001	0.042

Mod|(Exp|Type)/3	0.740 ± 0.039	< 0.001	0.091
Exp|(Mod|Type)/2	0.565 ± 0.032	< 0.001	< 0.001
Exp|(Mod|Type)/3	0.493 ± 0.035	< 0.001	< 0.001

Table S10. Candidate model performance across regions of interest using only highly vivid trials. p-values are based on uncorrected t-tests. NC = noise ceiling; SEM = standard error of the mean

Model evaluation

Model name	ELPD difference	SE difference
Model_mod_type_rand	0.0	0.0
Model_type_rand_acat_cs(mod)	-2.3	3.8
Model_mod_type_rand_acat	-2.6	2.2
Model_rand_acat_cs(mod)_cs(type)	-6.3	3.9
Model_mod_type	-17.6	6.4
Model_mod	-43.9	10.4
Model_null	-44.0	10.6

Table S11. Assessment of model performance using leave-one-out cross-validation [S2]. The best-performing model is plotted first. Lower expected log predictive density (ELPD) [S4] compared to the winning model highlights worse performance overall. Model names denote which regressors were included. Null: none; Mod: Modality (perception vs imagery); Type: Type (face vs artwork); Rand; random intercept for each participant and each stimulus; acat_cs(): category-specific effect.

Data S1: Vividness of Visual Mental Imagery Questionnaire

Taken from the original publication by Marks in 1973 [S5].

For items 1-4, think of some relative or friend whom you frequently see (but who is not with you at present) and consider carefully the picture that comes before your mind's eye.

Item
1. The exact contour of face, head, shoulders and body.
2. Characteristic poses of head, attitudes of body, etc.
3. The precise carriage, length of step, etc., in walking.
4. The different colours worn in some familiar clothes.

Visualize a rising sun. Consider carefully the picture that comes before your mind's eye.

Item
5. The sun is rising above the horizon into a hazy sky.
6. The sky clears and surrounds the sun with blueness.
7. Clouds. A storm blows up, with flashes of lightning.
8. A rainbow appears.

Think of the front of a shop which you often go to. Consider the picture that comes before your mind's eye.

Item
9. The overall appearance of the shop from the opposite side of the road.
10. A window display including colours, shapes and details of individual items for sale.
11. You are near the entrance. The colour, shape and details of the door.

12. You enter the shop and go to the counter. The counter assistant serves you.
Money changes hands.

Finally, think of a country scene which involves trees, mountains and a lake. Consider the picture that comes before your mind's eye.
Item
13. The contours of the landscape.
14. The colour and shape of the trees.
15. The colour and shape of the lake.
16. A strong wind blows on the trees and on the lake causing waves.

Data S2: Adapted and translated version of the Vividness of Visual Mental Imagery Questionnaire

Schließen Sie die Augen. Denken Sie an eine mit Ihnen verwandte oder befreundete Person, die Sie häufig sehen (aber die im Moment nicht bei Ihnen ist), und betrachten Sie sorgfältig das Bild, das Sie vor Ihrem geistigen Auge sehen. Bewerten Sie anschließend die folgenden Aspekte danach, wie anschaulich Sie diese vor Ihrem geistigen Auge gesehen haben:

Die genaue Kontur von Gesicht, Kopf, Schultern und Körper.
überhaupt nicht anschaulich 1 2 3 4 5 äußerst anschaulich

Charakteristische Kopfhaltung, Körperhaltungen, etc.
überhaupt nicht anschaulich 1 2 3 4 5 äußerst anschaulich

Die genaue Haltung, Schrittlänge etc. beim Gehen.
überhaupt nicht anschaulich 1 2 3 4 5 äußerst anschaulich

Die verschiedenen Farben der Kleidung, die die Person häufig trägt.
überhaupt nicht anschaulich 1 2 3 4 5 äußerst anschaulich

Denken Sie daran, dass Sie vor einem Laden stehen. Betrachten Sie sorgfältig das Bild, das Sie vor Ihrem geistigen Auge sehen. Bewerten Sie anschließend die folgenden Punkte.

Das Gesamtbild des Ladens von der gegenüberliegenden Straßenseite aus.
überhaupt nicht anschaulich 1 2 3 4 5 äußerst anschaulich

Eine Schaufensterdekoration mit Farben, Formen und Details von einzelnen Verkaufsartikeln.
überhaupt nicht anschaulich 1 2 3 4 5 äußerst anschaulich

Sie sind in der Nähe des Eingangs. Die Farbe, Form und Details der Tür.
überhaupt nicht anschaulich 1 2 3 4 5 äußerst anschaulich

Sie betreten den Shop und gehen zur Theke. Die Thekenkraft bedient Sie. Geld wechselt den Besitzer.
überhaupt nicht anschaulich 1 2 3 4 5 äußerst anschaulich

Data S3: Original version of the Aesthetic Experience Scale

Taken from the original publication by Silvia and Nusbaum [S6].

Please write down areas of the arts you encounter most often in your daily life:

How often do you . . . (1: never or rarely - 7: nearly always)

_____ feel absorbed and immersed
_____ completely lose track of time
_____ feel chills down your spine
_____ get goose bumps
_____ feel like you're somewhere else
_____ feel like your hair is standing on end
_____ feel like crying
_____ feel touched
_____ feel detached from your surroundings
_____ feel a sense of awe and wonder

Data S4: Adapted and translated version of the Aesthetic Experience Scale

Bitte wählen Sie die Kunstdomäne aus, die bei Ihnen die stärksten Emotionen bzw. das stärkste ästhetische Empfinden auslöst:

- Musik hören
- Videos schauen (Fernsehen, Kino, Youtube, etc)
- Bildende Kunst (Gemälde, Malerei, Kunstfotografie, etc.)
- Literatur
- Tanzaufführungen
- Theater
- Eigenes kreatives Schaffen
- Andere

Wie häufig sind Sie der von Ihnen angegebenen Kunstdomäne in etwa ausgesetzt?

- täglich
- mehrmals die Woche
- einmal die Woche
- ein- bis zweimal im Monat
- alle paar Monate
- ein- bis zweimal im Jahr

noch seltener

Bitte beantworten Sie die folgenden Fragen in Bezug auf die oben von Ihnen ausgewählte Kunstdomäne. Dabei sollen Sie beurteilen, wie oft die folgenden emotionalen und physischen Zustände bei Ihnen ausgelöst werden, wenn Sie dieser Kunstdomäne ausgesetzt sind: (1: niemals oder kaum, 7: fast immer)

Labels (1-7):
1: *niemals oder kaum*, 7: *fast immer*

Wie oft fühlen Sie sich vollkommen eingenommen von und versunken in ihr Erleben?
niemals oder kaum 1 2 3 4 5 6 7 fast immer

Wie oft verlieren Sie vollkommen das Zeitgefühl?
niemals oder kaum 1 2 3 4 5 6 7 fast immer

Wie oft fühlen Sie einen Schauer über Ihren Rücken laufen?
niemals oder kaum 1 2 3 4 5 6 7 fast immer

Wie oft bekommen Sie eine Gänsehaut?
niemals oder kaum 1 2 3 4 5 6 7 fast immer

Wie oft haben Sie das Gefühl ganz woanders zu sein?
niemals oder kaum 1 2 3 4 5 6 7 fast immer

Wie oft haben Sie das Gefühl, dass Ihnen die Haare zu Berge stehen?
niemals oder kaum 1 2 3 4 5 6 7 fast immer

Wie oft haben Sie das Gefühl, weinen zu müssen?
niemals oder kaum 1 2 3 4 5 6 7 fast immer

Wie oft fühlen Sie sich tief berührt?
niemals oder kaum 1 2 3 4 5 6 7 fast immer

Wie oft fühlen Sie sich von Ihrer Umgebung losgelöst?
niemals oder kaum 1 2 3 4 5 6 7 fast immer

Wie oft fühlen Sie sich von Ehrfurcht und Staunen ergriffen?
niemals oder kaum 1 2 3 4 5 6 7 fast immer

Data S5: Comprehension Questions

When should you not move?

Explain the scale from 1-7 of the question “How beautiful was the image?”.

What is aesthetically moving?

What is pleasure?

What do you need to do when you hear the tone?

What does the question ”How vivid was your imagery?” assess?

Supplemental references

S1. Tierney, N., and Cook, D. (2020). Expanding tidy data principles to facilitate missing data exploration, visualization and assessment of imputations. Preprint at arXiv.

S2. Bürkner, P.-C., and Vuorre, M. (2019). Ordinal Regression Models in Psychology: A Tutorial. Advances in Methods and Practices in Psychological Science *2*, 77–101. https://doi.org/10.1177/2515245918823199.

S3. Ben-Shachar, M.S., Lüdecke, D., and Makowski, D. (2020). effectsize: Estimation of Effect Size Indices and Standardized Parameters. Journal of Open Source Software *5*, 2815. https://doi.org/10.21105/joss.02815.

S4. Vehtari, A., Gelman, A., and Gabry, J. (2017). Practical Bayesian model evaluation using leave-one-out cross-validation and WAIC. Stat Comput *27*, 1413–1432. https://doi.org/10.1007/s11222-016-9696-4.

S5. Marks, D.F. (1973). Visual Imagery Differences in the Recall of Pictures. British Journal of Psychology *64*, 17–24. https://doi.org/10.1111/j.2044-8295.1973.tb01322.x.

S6. Silvia, P.J., and Nusbaum, E.C. (2011). On personality and piloerection: Individual differences in aesthetic chills and other unusual aesthetic experiences. Psychology of Aesthetics, Creativity, and the Arts *5*, 208–214. https://doi.org/10.1037/a0021914.

Acute Negative Effects of Ketamine and Morphology

Study 2: Graf, S., Dörl, G., Milz, C., **Kathofer, M.**, Stöhrmann, P., Gomola, D., Briem, E., Schlosser, G., Mayerweg, A., Semmelweis-Tomits, J., Hoti, A., Eggerstorfer, B., Schmidt, C., Crone, J.S., Rujescu, D., Spies, M., Lanzenberger, R., Spurny-Dworak, B. (2024). Morphological correlates of anxiety-related experiences during a ketamine infusion. The World Journal of Biological Psychiatry, 25(9), 537–546. https://doi.org/10.1080/15622975.2024.2402261

My contribution

This study formed part of a larger clinical ketamine trial that I helped organize during my PhD. Given the project's collaborative nature, I contributed across multiple stages, including study design and protocol development, participant recruitment, data collection, methods refinement, and manuscript writing.

THE WORLD JOURNAL OF BIOLOGICAL PSYCHIATRY
2024, VOL. 25, NO. 9, 537–546
https://doi.org/10.1080/15622975.2024.2402261

ORIGINAL INVESTIGATION

OPEN ACCESS Check for updates

Morphological correlates of anxiety-related experiences during a ketamine infusion

S. Graf[a,b], G. Dörl[a,b], C. Milz[a,b], M. Kathofer[c], P. Stöhrmann[a,b], D. Gomola[a,b], E. Briem[a,b], G. Schlosser[a,b], A. Mayerweg[a,b], J. Semmelweis-Tomits[a,b], A. Hoti[a,b], B. Eggerstorfer[a,b], C. Schmidt[a,b], J. Crone[c,d,e], D. Rujescu[a,b], M. Spies[a,b], R. Lanzenberger[a,b] and B. Spurny-Dworak[a,b]

[a]Department of Psychiatry and Psychotherapy, Medical University of Vienna, Vienna, Austria; [b]Comprehensive Center for Clinical Neurosciences and Mental Health (C3NMH), Medical University of Vienna, Vienna, Austria; [c]Vienna Cognitive Science Hub, University of Vienna, Vienna, Austria; [d]Department of Psychology, University of California, Los Angeles, Los Angeles, CA, USA; [e]Faculty of Psychology, University of Vienna, Vienna, Austria

ABSTRACT

Objectives: Ketamine exerts rapid antidepressant effects by enhancing neuroplasticity, particularly in the amygdala and hippocampus—regions involved in fear processing and learning. While the role of ketamine's dissociative effects in its antidepressant response is debated, anxiety experienced during infusion has been negatively correlated with treatment outcomes. **Methods:** In this single-blind, placebo-controlled study, a subset of 17 healthy volunteers (6 males, 23.12 ± 1.9 years) received intravenously a placebo in the first and 0.5 mg/kg racemic ketamine in the second session. Anxiety-related experiences were assessed by the 5D-ASC score obtained post-infusion, structural magnetic resonance imaging scans were acquired 4 h post-infusion. An anxiety-score was obtained from the 5D-ASC. Relation between post-placebo amygdala volume, hippocampal volume, and its subfields with the anxiety-score were assessed using linear regression models. **Results:** Results showed a statistically significant negative relation between hippocampal head volume and the anxiety score ($\beta = -0.733$, $p = 0.006$), with trending negative association for each subfield's head and the score. **Conclusion:** These findings suggest that anxiety-related experiences during ketamine infusion may be mediated by the hippocampus, with smaller hippocampal volumes leading to more anxiety-related experiences. Thus, hippocampal subfield volumes may be used as a predictor for anxiety-related events during ketamine use and might predict treatment outcome in future approaches.

ARTICLE HISTORY
Received 24 July 2024
Revised 5 September 2024
Accepted 5 September 2024

KEYWORDS
Ketamine; anxiety; hippocampus; amygdala; morphology

Introduction

The N-methyl-D-aspartate (NMDA) antagonist ketamine has been proven as an effective and rapid antidepressant in unipolar and bipolar depressive disorder (Zarate et al. 2006; Kraus et al. 2017), exerting its effects by enhancing neuroplasticity (Zanos and Gould 2018). Previous studies indicate an inhibition of NMDA receptors mainly located on GABAergic interneurons, leading to an increased glutamatergic activity of postsynaptic cells (Duman et al. 2016). Adaptions in neurotransmitter content were reported with elevated glutamatergic levels in the medial prefrontal cortex (Abdallah et al. 2018) and decreased GABA levels in the hippocampus (Silberbauer et al. 2020). However, its exact mechanism of action remains elusive and is still subject of extensive research.

So far, ketamine is the only approved antidepressant emerging its antidepressant effects already hours after application (Zarate et al. 2006), with a rapid decrease of suicidal ideations (Witt et al. 2020). Recently, its clinical use in other neuropsychiatric disorders, such as anxiety spectrum disorders and substance use disorders, has been investigated with promising results (Johnston et al. 2024) However, its clinical use is limited due to its dissociative and psychomimetic side effects (Naughton et al. 2014).

Mostly, psychoactive effects induced by ketamine are described as a ´high´ accompanied by changed perception and a feeling of happiness (Griffiths et al. 2021).

CONTACT Rupert Lanzenberger rupert.lanzenberger@meduniwien.ac.at Department of Psychiatry and Psychotherapy, Medical University of Vienna, Waehringer Guertel 18-20, Vienna, 1090, Austria
Supplemental data for this article is available online at https://doi.org/10.1080/15622975.2024.2402261

However, some patients encounter negative experiences, such as anxiety (Ceban et al. 2021), agitation, intense out of body experiences and symptoms (Moore and Measham 2008) mimicking schizophrenia (Höflich et al. 2015). Its use in a clinical setting and for scientific use is considered safe (Wolff and Winstock 2006), but due to these potential adverse effects, observation by medical staff is required (Kraus et al. 2017).

The extent to which ketamine's psychoactive effects contribute to its antidepressant properties remains a topic of ongoing debate (Ballard et al. 2020; Grabski et al. 2020). Nonetheless, a recent study reported a negative correlation of anxiety-related experiences during a ketamine infusion and antidepressant response (Aust et al. 2019). Thus, experiences of anxiety during ketamine application are categorised as adverse events and have been reported as a reason for discontinuation of treatment (Feifel et al. 2020).

In general, the hippocampus and amygdala are key hubs of anxiety. Early studies have already linked the amygdala to fear response with evidence coming from functional magnetic resonance tomography (fMRI) as well as positron emission tomography (PET), which showed amygdalar activation in response to fearful stimuli (Phan et al. 2002; Ressler 2010) and early findings from lesion studies (Adolphs et al. 1995). This association is also supported by evidence from morphological studies, as a smaller amygdalar volume has also been associated with the trait anxiety and subclinical anxiety in healthy subjects (Blackmon et al. 2011; Hu et al. 2020).

Moreover, the amygdala is not only involved in induction of fear, but also plays a substantial role in communicating fear signals and processing fear unconsciously, and in contextualising fear (Garfinkel and Critchley 2014). In contrast to this well-document part of the amygdala, the role of the hippocampus is less understood, but studies suggest its involvement in fear conditioning (Pohlack et al. 2012), fear memory (Chaaya et al. 2018; Zaki et al. 2022) and fear memory extinction (Lacagnina et al. 2019). However, evidence has been provided, that not the entire hippocampus, but rather anterior parts, are implicated in fear (Strange et al. 2014).

An MRI study confirmed an immediate hippocampal volume increase in healthy human subjects following a single ketamine infusion, putting emphasis on the hippocampus as a key area of ketamine's action (Höflich et al. 2021). Moreover, a ketamine-induced decrease in functional connectivity of the hippocampus with nodes of the default mode network (DMN) and the dorsal attention network was reported in remitted depressed patients (Zhang et al. 2023). These alterations could mediate antidepressant effects, as the hippocampus is implied in pathophysiological alterations in major depressive disorder (MDD) (Campbell and MacQueen 2004; Harrisberger et al. 2015). Especially, hippocampal volume reduction is one of the most replicated neuroimaging findings in MDD, with more pronounced volumetric loss in the left CA1 subfield (Roddy et al. 2019), but also hyperconnectivity with other DMN nodes has been described (Kaiser et al. 2015). Additionally, the amygdala, a region that is predominantly overactivated in MDD (Klug et al. 2024), belongs to the main targets of ketamine's action. In contrast to the hippocampus, volumetric alterations of the amygdala in MDD are rather inconsistent, with reports of both decreased and increased amygdalar volumes (Hamilton et al. 2008; van Eijndhoven et al. 2009; Schmaal et al. 2016). However, findings indicate heightened amygdala reactivity to negative emotion processing (Klug et al. 2024) and increased resting-state functional connectivity with the right hippocampus (Tang et al. 2018). Moreover, ketamine seems to reduce this neural activity in the bilateral amagydalo-hippocampal complex when exposed to emotional stimuli (Scheidegger et al. 2016).

Hence, comprehending the morphological correlates of anxiety-related experiences therefore seem especially important and may allow the prediction the treatment outcome of ketamine.

Given that hippocampus and amygdala are key targets of ketamine's mechanism of action and are implicated in anxiety, they might be the main neural correlates of anxiety-related experiences in the context of ketamine application. Therefore, we investigated a possible correlation between the amygdalar and hippocampal volumes and their respective subregions with anxiety-related experiences.

Methods

Study design and subjects

This study was approved by the ethical committee of the Medical University of Vienna, Austria (EK 1572/2021) and performed in accordance with the declaration of Helsinki.

Overall, 36 healthy subjects (17 males, mean age: 23.9 ± 3.7) were enrolled in this single-blind, randomised, placebo-controlled cross-over study. Participants' physical health was evaluated through medical examinations including an electrocardiogram, blood, and urine tests, encompassing pregnancy and drug screening. Mental health was assessed *via* the Structured Clinical Interview for DSM-IV (Lobbestael et al. 2011). Exclusion criteria were any current medical

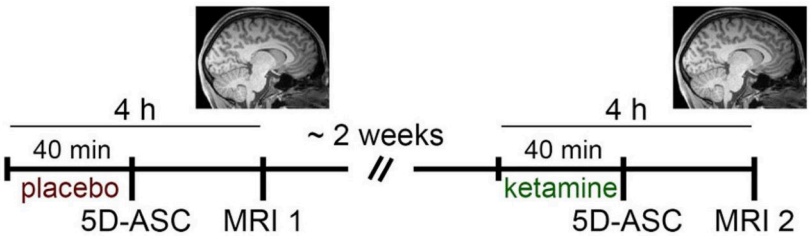

Figure 1. Study design of participants included in this subanalysis: At Session 1 participants were administered a placebo infusion (0.9% saline solution) and the 5 Dimension altered state of consciousness (5D-ASC) score was taken after infusion. Four hours later, structural magnetic resonance imaging (MRI) scans were acquired.

illness requiring pharmacological treatment including psychiatric disorders, a history of neurological or psychiatric disorders, pregnancy or breastfeeding, current or former substance abuse as well as any contraindications for MRI scans.

Each subject underwent two MRI scanning sessions. Participants received a continuous infusion over the course of 40 min of a placebo, consisting of 0.9% saline solution in one session, and 0.5 mg/kg of racemic ketamine diluted in 0.9% NaCl in the other session, with an aimed interval between the sessions of two weeks (see Figure 1). Study medication was provided by the hospital pharmacy of the University Hospital Vienna (AKH), preparation and administration were performed by a trained study doctor. The order of treatment during each study session, receiving ketamine or placebo infusion, respectively, was randomised at study inclusion. Only participants receiving placebo treatment in the first scanning session were included in our analyses on the relationship of morphological correlates and anxiety-related experiences during ketamine infusion, to ensure proper baseline data. Therefore, only 16 participants were included in our analyses.

Randomisation to one of the two study arms was carried out by using the software randomiser (https://www.meduniwien.ac.at/web/mitarbeiterinnen/it-hilfe-support/it4science/plattformen/randomiser/) and block randomisation. Both study drugs were administered by a continuous infusion intravenously over 40 min. The 5-Dimension Altered State of Consciousness Rating Scale (5D-ASC) was obtained within 15 min after the end of the infusion. MRI scans were conducted 4 h after the application of the study drug (see Figure 1).

As a possible association between baseline volumes of the hippocampus and the amygdala with anxiety-related experiences was assessed, only subjects receiving the placebo infusion in the first session ($n = 16$) were in included in the current analyses. Statistical considerations are discussed in the section of statistical analysis.

Psychometric measures

At each study visit, psychoactive effects of the infusion were assessed by the Visual Analog Scales (VAS) and the 5-Dimension Altered State of Consciousness Rating Scale (5D-ASC). The German version of the 5D-ASC is a 94-item self-report questionnaire, using a horizontal visual analogue scale with the endpoints 'No, not more than usually' and 'Yes, much more than usually' to describe experiences. It comprises five dimensions, namely oceanic boundlessness, anxious-ego disintegration, visionary restructuralization, acoustic alterations, and altered vigilance (Dittrich 1998). Studerus et al. enhanced the score by introducing new subscales, one of them called 'Anxiety', comprising the following items: 19 ('I was afraid that the state I was in would last forever'), 29 ('I was afraid without being able to say exactly why'), 30 ('I experienced everything terrifying distorted'), 32 ('I experienced my surroundings as strange and weird'), 38 ('I felt threatened'), and 63 ('I had the feeling something horrible would happen') (Studerus et al. 2010). Item 6 was added as an additional item, as the German Version differs from the English Version. While the English Version is 'I feel connected to superior powers', the German Version translates to English as 'I feel at the mercy of dark forces', which is interpreted as an anxious state. Therefore, a total of 7 items were used to calculate a score, which will be referred to as 'Anxiety score' in the following.

Magnetic resonance imaging and analysis

MRI scanning was performed on a 3 Tesla MR Scanner (MAGNETOM Prisma, Siemens Medical, Erlangen, Germany) at the Department of Biomedical Imaging and Image-guided Therapy, Medical University of Vienna. Structural T1-weighted MRI scans were acquired with a multi-echo MPRAGE sequence (TR = 2400 ms, TE = 2.22 ms, voxel size 0.8 × 0.8 × 0.8 mm, anterior-posterior face encoding, field of view read: 256 mm, slice oversampling 23.1%).

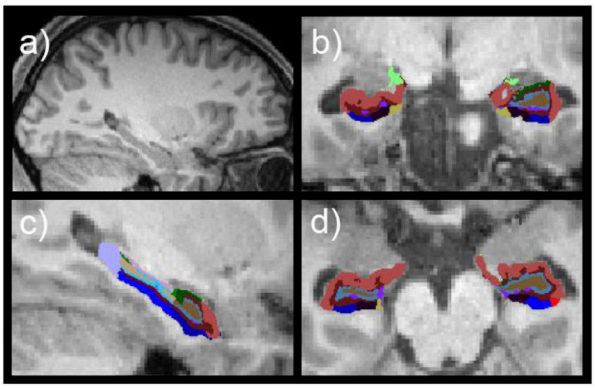

Figure 2. Illustration of the automated hippocampus segmentation from structural T1-weighted magnetic resonance images (a), in coronal (b), sagittal (c), and axial (d) view. Segmentations were visually checked by an experienced neuroscientist.

Whole-Brain segmentation and parcellation of subcortical regions was carried out automatically by FreeSurfer 7.1 (Harvard Medical School, Boston, MA, USA; http://surfer.nmr.mgh.harvard.edu/) with subsequent segmentation of hippocampus and amygdala subfields (freesurfer-linux-centos6_x86_64-7.1.0-20200511-813297b) (Iglesias et al. 2015; Saygin et al. 2017), as illustrated in Figure 2.

Statistical analysis

SPSS Statistics (v 29.0.2.0, 2023, SPSS, Inc., an IBM Company, Chicago, IL, USA) was used for statistical analyses. Subjects whose between-measurement interval exceeded 90 days between the two MRI scans were excluded from the analyses due to possible seasonal changes in the subcortical volumes (Book et al. 2021).

The difference in the anxiety score during the placebo infusion and during the ketamine infusion was calculated to attenuate the risk of confounding by inter-subject anxiety level differences in the test setting. This difference score was used for all statistical analyses.

To preclude effects of other variates than the hippocampal and amygdalar volume on the anxiety difference score, a regression model, using the score as the dependent variable, and the session (i.e. whether the placebo or ketamine was administered), the order of the administered study drug (i.e. whether placebo or ketamine was administered first), gender, and age as independent variables, was conducted for all subjects ($n = 36$). While the overall model revealed a significant effect ($R^2 = 0.496$, $p = 0.002$), only the session variable showed a significant result ($p < 0.001$). Therefore, we assumed that neither gender, age nor the order of the applied study medication had a significant impact on the occurrence of anxiety-related experiences. This finding supports the validity of the design for the following statistical analyses of only participants receiving the placebo in the first session, ensuring that the results are not confounded by the order in which the study medication was administered and infer that considering only a single study arm will not introduce bias related to a session effect.

Moreover, an independent samples *t*-test was performed to preclude gender-specific effects on the anxiety difference score.

Separate regression models were conducted for the whole hippocampus (head + body), the hippocampal body, the hippocampal head, and the amygdala. The obtained residuals of the volumes and the anxiety difference scores were assessed for normal distribution by Shapiro-Wilk tests.

As the regression model of the hippocampal head volume yielded a significant result, subsequent regression models were performed for each subfield individually. These analyses comprised the fimbria, fissure, hippocampus-Amygdala-transition-area (HATA), parasubiculum, tail, and the head and the body of each of the following subfields: CA1, CA3, CA4, granule cell layer of the dentate gyrus (GC-ML-DG), molecular layer, presubiculum and subiculum. The Benjamini-Hochberg false discovery rate correction was used to adjust the alpha-level for multiple comparison.

Results

Demographics and psychometric data

In total, 16 participants (6 males, mean age 23.31 ± *SD* 1.8), received the placebo treatment in the first and ketamine in the second scanning session and were included in the analyses. The mean ± interval between the measurements was 27.4 ± 13.6 days.

Mean ± *SD* 5D-ASC Score was 102.65 ± 145.29 with a mean ± *SD* anxiety score of 109.06 ± 147.54. The 5D-ASC Score did not differ significantly between males and females [$t(15) = 0.368$, $p = 0.718$].

Relationship of the hippocampus, the amygdala, and anxiety-related experiences

The volumes of the total hippocampus, hippocampal tail, and amygdala did not show any significant relationship with the anxiety score. However, the regression model indicated a significant effect of the hippocampal head volume on the anxiety score [$\beta - 0.745$, SE = 0.101, $p = 0.009$ (FDR q value = 0.0125)] and the model explained 56% of the variance in the anxiety score ($R^2 = 0.560$). This relationship is visualised in Figure 3.

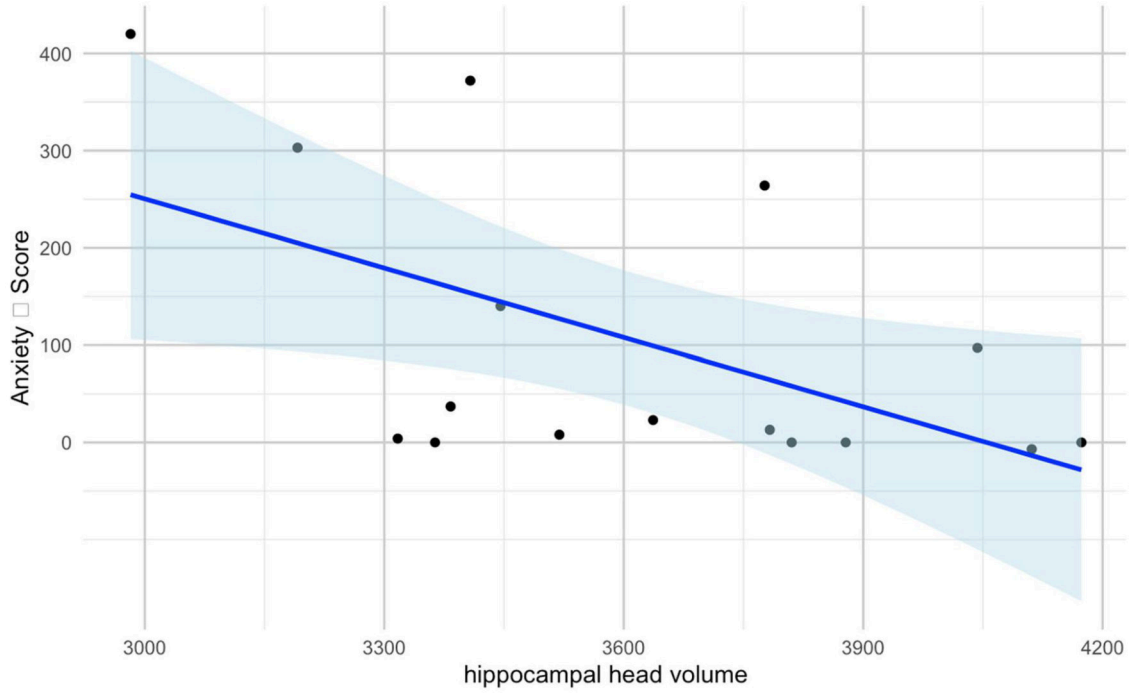

Figure 3. Scatter plot of the relationship of the bilateral hippocampal head volume after the placebo infusion and the anxiety score difference at the second session. The anxiety score difference was obtained by subtraction of the measures derived at each scanning session.

Subsequent linear regression models of the subfields showed a trend-wise negative correlation of the anxiety score with the CA1 head (β coefficient = −0.606, p = 0.039), CA3 head (β coefficient = −0.811, p = 0.008), CA4 head (β coefficient = −0.778, p = 0.010), GC-ML-DG head (β coefficient = −0.737, p = 0.019), fimbria (β coefficient = −0.874, p = 0.005), molecular layer head (β coefficient = −0.725, p = 0.013), presubiculum head (β coefficient = −0.610, p = 0.023), subiculum head (β coefficient = −0.565, p = 0.038). However, no subfield result met the criteria required by the Benjamini-Hochberg correction for multiple comparison. Individual results are shown in Table 1. Exemplary regression plots of the relationship of hippocampal subfield volumes and anxiety scores are depicted in Supplemental Figure 1.

Table 1. Results of all regression models.

	β coefficient	Standard error	p-Value	FDR q value
Hippocampus (head + body)	−0.486	0.081	0.124	0.0375
Hippocampal head	**−0.745**	**0.101**	**0.009**	**0.0125**
Hippocampal body	−0.152	0.324	0.672	0.05
Amygdala (whole)	−0.597	0.121	0.075	0.025
CA1 body	0.546	1.90	0.214	0.029
CA1 head	**−0.606**	**0.319**	**0.039***	**0.018**
CA3 body	−0.530	3.221	0.357	0.032
CA3 head	**−0.811**	**1.209**	**0.008***	**0.003**
CA4 body	0.223	3.347	0.610	0.042
CA4 head	**−0.778**	**1.461**	**0.010***	**0.005**
Fimbria	**−0.874**	**1.123**	**0.005***	**0.011**
Hippocampal fissure	0.077	0.819	0.788	0.047
GC-ML-DG body	0.218	2.774	0.573	0.039
GC-ML-DG head	**−0.737**	**1.279**	**0.019***	
HATA	−0.524	2.181	0.069	0.024
Hippocampal tail	0.146	0.360	0.618	0.045
Molecular layer body	−0.026	1.613	0.952	0.050
Molecular layer head	**−0.725**	**0.536**	**0.013***	**0.008**
Parasubiculum	−0.262	2.553	0.363	0.034
Presubiculum body	−0.341	0.970	0.224	0.026
Presubiculum head	**−0.610**	**1.031**	**0.023***	**0.016**
Subiculum body	0.177	0.931	0.533	0.037
Subiculum head	**−0.565**	**0.763**	**0.038***	**0.018**

FDR q value represents the adjusted α level according to the Benjamini-Hochberg correction for multiple testing.
*Represents significant effects on the anxiety difference score (uncorrected for multiple comparison).
**Represents a significant effect on the anxiety difference score.
p-Value: 0.009**.
Bold values represent significant effects uncorrected for multiple comparison.

Discussion

Our results yielded a significant negative correlation between the hippocampal head volume and anxiety-related experiences in a group of healthy volunteers. Moreover, a trend towards negative correlation of the head volume of each hippocampal subfield as well as of the fimbria with the anxiety score were found. Neither significant correlation between the amygdala nor any other subfield with the anxiety score was observed.

These findings are in line with previous literature, which reported a negative correlation between the hippocampal volume and anxiety disorders (Mueller

et al. 2013) and related symptoms (Lipschutz et al. 2024). Interestingly, the state of anxiety, which, in contrast to the trait of anxiety, is defined as a transient response to threatening events, has been related to the anterior hippocampus rather than the posterior hippocampus (Satpute et al. 2012). Correspondingly, in this study, only the hippocampal head volume was associated with anxiety during the ketamine infusion.

In general, the hippocampus is not only organised into distinct subfields, but also along a longitudinal axis. The posterior hippocampus is more involved in spatial processing, whereas the anterior hippocampus has rather been associated with emotion processing, such as unconditioned fear behaviour (Strange et al. 2014). Also, more frontal, and anterior temporal brain regions, which are involved in social behaviour, are more functionally connected to the anterior hippocampus (Vogel et al. 2020). This organisation of the hippocampus along the anterior-posterior axis might explain, why we observed a significant effect of the hippocampal head volume and a trend wise effect of all head areas of the hippocampal subfields, but not in a single hippocampal subfield. Furthermore, gene expression patterns differ along the longitudinal axis as well. The NR2F2 gene has been shown to be distinctively higher expressed in the ventral hippocampus (Vogel et al. 2020; Yang et al. 2023) and is associated with enhanced expression of somatostatin (SST) in GABAergic interneurons (Vogel et al. 2020). While it has been reported that ketamine disinhibits SST interneurons (Gerhard et al. 2020), exerting not only its antidepressant but also anxiolytic effect (Fuchs et al. 2017), deficits of these GABAergic interneurons have been shown to increase anxiety-like behaviour in mice. A smaller volume could be associated with a fewer number of GABAergic interneurons, leading to more anxiety-related experiences. However, no studies have investigated this possible association, and an analysis of receptor occupancy is required to give a valid explanation.

Furthermore, a positive correlation between the antidepressant effect of ketamine and the baseline volume of the left hippocampus was shown (Nogovitsyn et al. 2020). These findings were replicated in another study, additionally showing grey matter volume increases in the hippocampus after ketamine administration (Dutton et al. 2024). However, these studies did not report details on altered states of consciousness during ketamine application. Nevertheless, a higher baseline volume could be associated with less anxiety during ketamine administration and could therefore mediate the better treatment outcome observed in their study. Here, we did not find a relationship of the amygdalar volume with anxiety-related experiences after ketamine infusion. Since the amygdala and the hippocampus are implicated in different anxiety and fear related processes, morphological correlates may differ within these areas (Chaaya et al. 2018). While to our knowledge no studies on the different kinds of anxiety-related experiences during ketamine application have been conducted in humans, a study in rats has reported enhanced fear memory retrieval following a ketamine infusion (Radford et al. 2018). Especially contextual fear conditioning (Liu et al. 2012; Khaled et al. 2019) and contextual fear memory retrieval (Chaaya et al. 2018) strongly rely on the hippocampus, which could relate to enhanced fear processing mechanism during ketamine infusion.

In the previous decade, multiple studies investigated the relationship between psychoactive effects of ketamine and treatment outcome in MDD. Nevertheless, results have been mixed so far (Grabski et al. 2020). Most of these studies have focused on an overall altered state of consciousness rather than on specific levels. While one study has reported a positive association of experience of unity, insight, and spirituality with treatment outcome (Sumner et al. 2021), another study has reported a negative correlation with anxiety-related experiences, emphasising the differentiating the state of altered consciousness (Aust et al. 2019). In line with our findings, we would recommend using subscales of the 5D-ASC rather than the overall score for investigating psychoactive effects of ketamine.

Although ketamine is a very potent antidepressant, anxiety related experiences during or after ketamine treatment are considered as adverse events and lead to discontinuation of treatment (Ceban et al. 2021). Therefore, potential markers to predict possible anxiety related events are of high interest for clinical routine practice. Here, we provide data on the relationship of morphological correlates of the hippocampus and fearful experiences during ketamine infusion. Hence, our results may help to understand the role of the hippocampus in the antidepressant effect of ketamine and path the way to use hippocampal (subfield) volumes as predictors for anxiety related experiences during ketamine treatment in future studies. However, future studies are required to replicate our results in depressed patients and potentially use hippocampal volumes as predictors for treatment outcome. While this could be a step towards improving precision medicine in psychiatry, the cost- and time-consuming aspects of MRI scans have to be considered.

Nevertheless, several limitations of this study need to be considered. Our study population comprise

only young, healthy participants with mainly students. Thus, conclusions with regard to patient populations need to be drawn with caution. Therefore, future studies should be conducted in depressed patients as well. In general, other risk factors for depression, such as childhood trauma have been related to a smaller hippocampal volume (Teicher et al. 2012) and should therefore be considered as a covariate or grouping variable in future studies. Moreover, the experience of childhood-trauma may influence the occurrence of negative side-effects of ketamine use and should be further explored in future approaches.

Also, the 5D-ASC is not considered as a classic anxiety score, and further studies including other scores focusing specifically on anxiety are required. For the purpose of our analyses, we could only rely on subjects receiving the placebo treatment in the first study session, due to possible ketamine effects and missing baseline data of the other study participants. Although our voxel size of 0.8 mm isotropic is sufficient for the valid quantification of all subfields, a combination of both T1 and T2-weighted images for the quantification of hippocampal and amygdala subfields should be favoured in future investigations (Seiger et al. 2021). Last, we used racemic ketamine in this study. Therefore, it is unclear if effects emerge from the racemic composition or can be associated with either S- or R-ketamine. As only S-ketamine has been approved by the European Medicines Agency (EMA) for the treatment of MDD (European Commission 2024), further studies with esketamine are needed to clarify this issue, especially if the hippocampal head volume is considered as a predictor. In conclusion, our results indicate an association of the experience of anxiety during administration of ketamine with the hippocampal head. The analysis of the hippocampal subfields suggests a trend-wise negative correlation with the anxiety-score. Our findings highlight the role of the hippocampus in ketamine's mechanism of action. Moreover, we propose a method to predict anxiety related experiences using hippocampal subfields volume analyses, which could subsequently aid in predicting the outcome of ketamine treatment.

Acknowledgements

The authors thank the employees including medical doctors and technical colleagues, and diploma students of the Advanced Neuroimaging Labs (aNIL, head: R. Lanzenberger), Department for Psychiatry and Psychotherapy (chair: D. Rujescu). They also express their gratitude to their collaboration partners at the Vienna Science Hub of the University of Vienna, especially to Prof. H. Leder.

Statement of interest

R. Lanzenberger received investigator-initiated research funding from Siemens Healthcare regarding clinical research using PET/MR and travel grants and/or conference speaker honoraria from Janssen-Cilag Pharma GmbH in 2023, and Bruker BioSpin, Shire, AstraZeneca, Lundbeck A/S, Dr. Willmar Schwabe GmbH, Orphan Pharmaceuticals AG, Janssen-Cilag Pharma GmbH, Heel and Roche Austria GmbH., and Janssen-Cilag Pharma GmbH in the years before 2020. He is a shareholder of the start-up company BM Health GmbH, Austria since 2019.

D. Rujescu served as consultant for Janssen, received honoraria from Boehringer-Ingelheim, Gerot Lannacher, Janssen, and Pharmagenetix, received travel support from Angelini, Janssen, and Schwabe, and served on advisory boards of AC Immune, Boehringer-Ingelheim, Roche and Rovi.

M. Spies has received travel grants from AOP Oprhan Pharamceuticals, Janssen and Austroplant, speaker honoraria from Janssen and Austroplant, and workshop participation from Eli Lilly.

C. Schmidt has received a travel grant from Eli Lilly to attend a scientific exchange meeting.

All other authors declare no potential conflicts of interest with respect to the research, authorship, and/or publication of this article.

Funding

This study was partly funded by the Research Cluster 'Unraveling the aesthetic mind in anhedonia: Insights from pharmacological imaging of the human brain' between the Medical University of Vienna and the University of Vienna [Grant number: SO68900012]. G. Dörl, MSc, is a recipient of a DOC Fellowship of the Austrian Academy of Sciences at the Department of Psychiatry and Psychotherapy, Medical University of Vienna. E. Briem, A. Mayerweg, and G. Schlosser are supported by the MD, PhD Excellence Program of the Medical University of Vienna.

ORCID

G. Dörl http://orcid.org/0000-0001-5389-9804
C. Milz http://orcid.org/0000-0002-1347-0744
M. Kathofer http://orcid.org/0000-0002-8249-3237
P. Stöhrmann http://orcid.org/0000-0002-7324-0414
D. Gomola http://orcid.org/0009-0002-2059-6481
E. Briem http://orcid.org/0009-0007-4311-4031
B. Eggerstorfer http://orcid.org/0000-0002-3400-2181
J. Crone http://orcid.org/0000-0002-0787-7003
D. Rujescu http://orcid.org/0000-0002-1432-313X
M. Spies http://orcid.org/0000-0002-9963-9044
R. Lanzenberger http://orcid.org/0000-0003-4641-9539
B. Spurny-Dworak http://orcid.org/0000-0003-0230-1918

Data availability statement

Clinical datasets of participants presented in this article are not readily available due to ethical reasons. Please contact rupert.lanzenberger@meduniwien.ac.at for questions.

References

Abdallah CG, De Feyter HM, Averill LA, Jiang L, Averill CL, Chowdhury GMI, Purohit P, de Graaf RA, Esterlis I, Juchem C, et al. 2018. The effects of ketamine on prefrontal glutamate neurotransmission in healthy and depressed subjects. Neuropsychopharmacology. 43(10):2154–2160. doi: 10.1038/s41386-018-0136-3.

Adolphs R, Tranel D, Damasio H, Damasio AR. 1995. Fear and the human amygdala. J Neurosci. 15(9):5879–5891. doi: 10.1523/JNEUROSCI.15-09-05879.1995.

Aust S, Gärtner M, Basso L, Otte C, Wingenfeld K, Chae WR, Heuser-Collier I, Regen F, Cosma NC, van Hall F, et al. 2019. Anxiety during ketamine infusions is associated with negative treatment responses in major depressive disorder. Eur Neuropsychopharmacol. 29(4):529–538. doi: 10.1016/j.euroneuro.2019.02.005.

Ballard ED, Zarate J, Carlos A. 2020. The role of dissociation in ketamine's antidepressant effects. Nat Commun. 11(1):6431. doi: 10.1038/s41467-020-20190-4.

Blackmon K, Barr WB, Carlson C, Devinsky O, DuBois J, Pogash D, Quinn BT, Kuzniecky R, Halgren E, Thesen T. 2011. Structural evidence for involvement of a left amygdala-orbitofrontal network in subclinical anxiety. Psychiatry Res. 194(3):296–303. doi: 10.1016/j.pscychresns.2011.05.007.

Book GA, Meda SA, Janssen R, Dager AD, Poppe A, Stevens MC, Assaf M, Glahn D, Pearlson GD. 2021. Effects of weather and season on human brain volume. PLOS One. 16(3):e0236303. doi: 10.1371/journal.pone.0236303.

Campbell S, MacQueen G. 2004. The role of the hippocampus in the pathophysiology of major depression. J Psychiatry Neurosci. 29(6):417–426.

Ceban F, Rosenblat JD, Kratiuk K, Lee Y, Rodrigues NB, Gill H, Subramaniapillai M, Nasri F, Lui LMW, Lipsitz O, et al. 2021. Prevention and management of common adverse effects of ketamine and esketamine in patients with mood disorders. CNS Drugs. 35(9):925–934. doi: 10.1007/s40263-021-00846-5.

Chaaya N, Battle AR, Johnson LR. 2018. An update on contextual fear memory mechanisms: transition between amygdala and hippocampus. Neurosci Biobehav Rev. 92:43–54. doi: 10.1016/j.neubiorev.2018.05.013.

Dittrich A. 1998. The standardized psychometric assessment of altered states of consciousness (ASCs) in humans. Pharmacopsychiatry. 31 Suppl 2(2):80–84. doi: 10.1055/s-2007-979351.

Duman RS, Aghajanian GK, Sanacora G, Krystal JH. 2016. Synaptic plasticity and depression: new insights from stress and rapid-acting antidepressants. Nat Med. 22(3):238–249. doi: 10.1038/nm.4050.

Dutton M, Boyes A, Can AT, Mohamed AZ, Hajishafiee M, Shan ZY, Lagopoulos J, Hermens DF. 2024. Hippocampal subfield volumes predict treatment response to oral ketamine in people with suicidality. J Psychiatr Res. 169:192–200. doi: 10.1016/j.jpsychires.2023.11.040.

Feifel D, Dadiomov D, Lee KC. 2020. Safety of repeated administration of parenteral ketamine for depression. Pharmaceuticals. 13(7):151. doi: 10.3390/ph13070151.

Fuchs T, Jefferson SJ, Hooper A, Yee P, Maguire J, Luscher B. 2017. Disinhibition of somatostatin-positive GABAergic interneurons results in an anxiolytic and antidepressant-like brain state. Mol Psychiatry. 22(6):920–930. doi: 10.1038/mp.2016.188.

Garfinkel SN, Critchley HD. 2014. Neural correlates of fear: insights from neuroimaging. Neurosci Neuroecon. 3:111–125. doi: 10.2147/NAN.S35915.

Gerhard DM, Pothula S, Liu R, Wu M, Li X, Girgenti MJ, Taylor SR, Duman CH, Delpire E, Picciotto M, et al. 2020. GABA interneurons are the cellular trigger for ketamine's rapid antidepressant actions. J Clin Invest. 130(3):1336–1349. doi: 10.1172/JCI130808.

Grabski M, Borissova A, Marsh B, Morgan CJA, Curran HV. 2020. Ketamine as a mental health treatment: are acute psychoactive effects associated with outcomes? A systematic review. Behav Brain Res. 392:112629. doi: 10.1016/j.bbr.2020.112629.

Griffiths C, Walker K, Reid I, da Silva KM, O'Neill-Kerr A. 2021. A qualitative study of patients' experience of ketamine treatment for depression: the 'ketamine and me' project. Journal of Affective Disorders Reports. 4:100079. doi: 10.1016/j.jadr.2021.100079.

Hamilton JP, Siemer M, Gotlib IH. 2008. Amygdala volume in major depressive disorder: a meta-analysis of magnetic resonance imaging studies. Mol Psychiatry. 13(11):993–1000. doi: 10.1038/mp.2008.57.

Harrisberger F, Smieskova R, Schmidt A, Lenz C, Walter A, Wittfeld K, Grabe HJ, Lang UE, Fusar-Poli P, Borgwardt S. 2015. BDNF Val66Met polymorphism and hippocampal volume in neuropsychiatric disorders: a systematic review and meta-analysis. Neurosci Biobehav Rev. 55:107–118. doi: 10.1016/j.neubiorev.2015.04.017.

Höflich A, Hahn A, Küblböck M, Kranz GS, Vanicek T, Windischberger C, Saria A, Kasper S, Winkler D, Lanzenberger R. 2015. Ketamine-induced modulation of the thalamo-cortical network in healthy volunteers as a model for schizophrenia. Int J Neuropsychopharmacol. 18(9):pyv040. doi: 10.1093/ijnp/pyv040.

Höflich A, Kraus C, Pfeiffer RM, Seiger R, Rujescu D, Zarate CAJr., Kasper S, Winkler D, Lanzenberger R. 2021. Translating the immediate effects of S-ketamine using hippocampal subfield analysis in healthy subjects-results of a randomized controlled trial. Transl Psychiatry. 11(1):200. doi: 10.1038/s41398-021-01318-6.

Hu Y, Moore M, Bertels Z, Phan KL, Dolcos F, Dolcos S. 2020. Smaller amygdala volume and increased neuroticism predict anxiety symptoms in healthy subjects: a volumetric approach using manual tracing. Neuropsychologia. 145:106564. doi: 10.1016/j.neuropsychologia.2017.11.008.

Iglesias JE, Augustinack JC, Nguyen K, Player CM, Player A, Wright M, Roy N, Frosch MP, McKee AC, Wald LL, et al. 2015. A computational atlas of the hippocampal formation using *ex vivo*, ultra-high resolution MRI: application to adaptive segmentation of *in vivo* MRI. Neuroimage. 115:117–137. doi: 10.1016/j.neuroimage.2015.04.042.

Johnston JN, Kadriu B, Kraus C, Henter ID, Zarate J, Carlos A. 2024. Ketamine in neuropsychiatric disorders: an update. Neuropsychopharmacology. 49(1):23–40. doi: 10.1038/s41386-023-01632-1.

Kaiser RH, Andrews-Hanna JR, Wager TD, Pizzagalli DA. 2015. Large-scale network dysfunction in major depressive disorder: a meta-analysis of resting-state functional connectivity. JAMA Psychiatry. 72(6):603–611. doi: 10.1001/jamapsychiatry.2015.0071.

Khaled G, Noriaki O, Chi Chung Alan F, Hirotaka A, Yoshito S, Takashi T, Reiko O, Shingo S, Hirofumi N, Mina M, et al. 2019. Orchestrated ensemble activities constitute a hippocampal memory engram. Nat Commun. 10(1):2637–2614.

Klug M, Enneking V, Borgers T, Jacobs CM, Dohm K, Kraus A, Grotegerd D, Opel N, Repple J, Suslow T, et al. 2024. Persistence of amygdala hyperactivity to subliminal negative emotion processing in the long-term course of depression. Mol Psychiatry. 29(5):1501–1509. doi: 10.1038/s41380-024-02429-4.

Kraus C, Rabl U, Vanicek T, Carlberg L, Popovic A, Spies M, Bartova L, Gryglewski G, Papageorgiou K, Lanzenberger R, et al. 2017. Administration of ketamine for unipolar and bipolar depression. Int J Psychiatry Clin Pract. 21(1):2–12. doi: 10.1080/13651501.2016.1254802.

Lacagnina AF, Brockway ET, Crovetti CR, Shue F, McCarty MJ, Sattler KP, Lim SC, Santos SL, Denny CA, Drew MR. 2019. Distinct hippocampal engrams control extinction and relapse of fear memory. Nat Neurosci. 22(5):753–761. doi: 10.1038/s41593-019-0361-z.

Lipschutz R, Powers A, Minton ST, Stenson AF, Ely TD, Stevens JS, Jovanovic T, van Rooij SJH. 2024. Smaller hippocampal volume is associated with anxiety symptoms in high-risk black youth. J Mood Anxiety Disord. 7:100065. doi: 10.1016/j.xjmad.2024.100065.

Liu X, Ramirez S, Pang PT, Puryear CB, Govindarajan A, Deisseroth K, Tonegawa S. 2012. Optogenetic stimulation of a hippocampal engram activates fear memory recall. Nature. 484(7394):381–385. doi: 10.1038/nature11028.

Lobbestael J, Leurgans M, Arntz A. 2011. Inter-rater reliability of the structured clinical interview for DSM-IV axis I disorders (SCID I) and axis II disorders (SCID II). Clin Psychol Psychother. 18(1):75–79. doi: 10.1002/cpp.693.

Moore K, Measham F. 2008. "It's the most fun you can have for twenty quid": motivations, consequences and meanings of British ketamine use. Addict Res Theory. 16(3):231–244. doi: 10.1080/16066350801983681.

Mueller SC, Aouidad A, Gorodetsky E, Goldman D, Pine DS, Ernst M. 2013. Gray matter volume in adolescent anxiety: an impact of the brain-derived neurotrophic factor Val66Met polymorphism? J Am Acad Child Adolesc Psychiatry. 52(2):184–195. doi: 10.1016/j.jaac.2012.11.016.

Naughton M, Clarke G, O'Leary OF, Cryan JF, Dinan TG. 2014. A review of ketamine in affective disorders: current evidence of clinical efficacy, limitations of use and pre-clinical evidence on proposed mechanisms of action. J Affect Disord. 156:24–35. doi: 10.1016/j.jad.2013.11.014.

Nogovitsyn N, Muller M, Souza R, Hassel S, Arnott SR, Davis AD, Hall GB, Harris JK, Zamyadi M, Metzak PD, et al. 2020. Hippocampal tail volume as a predictive biomarker of antidepressant treatment outcomes in patients with major depressive disorder: a CAN-BIND report. Neuropsychopharmacology. 45(2):283–291. doi: 10.1038/s41386-019-0542-1.

Phan KL, Wager T, Taylor SF, Liberzon I. 2002. Functional neuroanatomy of emotion: a meta-analysis of emotion activation studies in PET and fMRI. Neuroimage. 16(2):331–348. doi: 10.1006/nimg.2002.1087.

Pohlack ST, Nees F, Liebscher C, Cacciaglia R, Diener SJ, Ridder S, Woermann FG, Flor H. 2012. Hippocampal but not amygdalar volume affects contextual fear conditioning in humans. Hum Brain Mapp. 33(2):478–488. doi: 10.1002/hbm.21224.

Radford KD, Park TY, Jaiswal S, Pan H, Knutsen A, Zhang M, Driscoll M, Osborne-Smith LA, Dardzinski BJ, Choi KH. 2018. Enhanced fear memories and brain glucose metabolism (18F-FDG-PET) following sub-anesthetic intravenous ketamine infusion in Sprague-Dawley rats. Transl Psychiatry. 8(1):263–212. doi: 10.1038/s41398-018-0310-8.

Ressler KJ. 2010. Amygdala activity, fear, and anxiety: modulation by stress. Biol Psychiatry. 67(12):1117–1119. doi: 10.1016/j.biopsych.2010.04.027.

Roddy DW, Farrell C, Doolin K, Roman E, Tozzi L, Frodl T, O'Keane V, O'Hanlon E. 2019. The hippocampus in depression: more than the sum of its parts? Advanced hippocampal substructure segmentation in depression. Biol Psychiatry. 85(6):487–497. doi: 10.1016/j.biopsych.2018.08.021.

Satpute AB, Mumford JA, Naliboff BD, Poldrack RA. 2012. Human anterior and posterior hippocampus respond distinctly to state and trait anxiety. Emotion. 12(1):58–68. doi: 10.1037/a0026517.

Saygin ZM, Kliemann D, Iglesias JE, van der Kouwe AJW, Boyd E, Reuter M, Stevens A, Van Leemput K, McKee A, Frosch MP, et al. 2017. High-resolution magnetic resonance imaging reveals nuclei of the human amygdala: manual segmentation to automatic atlas. Neuroimage. 155:370–382. doi: 10.1016/j.neuroimage.2017.04.046.

Scheidegger M, Henning A, Walter M, Lehmann M, Kraehenmann R, Boeker H, Seifritz E, Grimm S. 2016. Ketamine administration reduces amygdalo-hippocampal reactivity to emotional stimulation. Hum Brain Mapp. 37(5):1941–1952. doi: 10.1002/hbm.23148.

Schmaal L, Veltman DJ, van Erp TGM, Sämann PG, Frodl T, Jahanshad N, Loehrer E, Tiemeier H, Hofman A, Niessen WJ, et al. 2016. Subcortical brain alterations in major depressive disorder: findings from the ENIGMA major depressive disorder working group. Mol Psychiatry. 21(6):806–812. doi: 10.1038/mp.2015.69.

Seiger R, Hammerle FP, Godbersen GM, Reed MB, Spurny-Dworak B, Handschuh P, Klöbl M, Unterholzner J, Gryglewski G, Vanicek T, et al. 2021. Comparison and reliability of hippocampal subfield segmentations within FreeSurfer utilizing T1- and T2-weighted multispectral MRI data. Front Neurosci. 15:666000. doi: 10.3389/fnins.2021.666000.

Silberbauer LR, Spurny B, Handschuh P, Klöbl M, Bednarik P, Reiter B, Ritter V, Trost P, Konadu ME, Windpassinger M, et al. 2020. Effect of ketamine on limbic GABA and glutamate: a human *in vivo* multivoxel magnetic resonance spectroscopy study. Front Psychiatry. 11:549903. doi: 10.3389/fpsyt.2020.549903.

Strange BA, Witter MP, Lein ES, Moser EI. 2014. Functional organization of the hippocampal longitudinal axis. Nat Rev Neurosci. 15(10):655–669. doi: 10.1038/nrn3785.

Studerus E, Gamma A, Vollenweider FX. 2010. Psychometric evaluation of the altered states of consciousness rating scale (OAV). PLOS One. 5(8):e12412. doi: 10.1371/journal.pone.0012412.

Sumner RL, Chacko E, McMillan R, Spriggs MJ, Anderson C, Chen J, French A, Jung S, Rajan A, Malpas G, et al. 2021. A qualitative and quantitative account of patient's experiences of ketamine and its antidepressant properties. J Psychopharmacol. 35(8):946–961. doi: 10.1177/0269881121998321.

Tang S, Lu L, Zhang L, Hu X, Bu X, Li H, Hu X, Gao Y, Zeng Z, Gong Q, et al. 2018. Abnormal amygdala resting-state

functional connectivity in adults and adolescents with major depressive disorder: a comparative meta-analysis. EBioMedicine. 36:436–445. doi: 10.1016/j.ebiom.2018.09.010.

Teicher MH, Anderson CM, Polcari A. 2012. Childhood maltreatment is associated with reduced volume in the hippocampal subfields CA3, dentate gyrus, and subiculum. Proceedings of the National Academy of Sciences. 109(9):E563–72.

van Eijndhoven P, van Wingen G, van Oijen K, Rijpkema M, Goraj B, Jan Verkes R, Oude Voshaar R, Fernández G, Buitelaar J, Tendolkar I. 2009. Amygdala volume marks the acute state in the early course of depression. Biol Psychiatry. 65(9):812–818. doi: 10.1016/j.biopsych.2008.10.027.

Vogel JW, La Joie R, Grothe MJ, Diaz-Papkovich A, Doyle A, Vachon-Presseau E, Lepage C, Vos de Wael R, Thomas RA, Iturria-Medina Y, et al. 2020. A molecular gradient along the longitudinal axis of the human hippocampus informs large-scale behavioral systems. Nat Commun. 11(1):960. doi: 10.1038/s41467-020-14518-3.

Witt K, Potts J, Hubers A, Grunebaum MF, Murrough JW, Loo C, Cipriani A, Hawton K. 2020. Ketamine for suicidal ideation in adults with psychiatric disorders: a systematic review and meta-analysis of treatment trials. Aust N Z J Psychiatry. 54(1):29–45. doi: 10.1177/0004867419883341.

Wolff K, Winstock AR. 2006. Ketamine: from medicine to misuse. CNS Drugs. 20(3):199–218. doi: 10.2165/00023210-200620030-00003.

Yang X, Wan R, Liu Z, Feng S, Yang J, Jing N, Tang K. 2023. The differentiation and integration of the hippocampal dorsoventral axis are controlled by two nuclear receptor genes. eLife. 12:RP86940. doi: 10.7554/eLife.86940.

Zaki Y, Mau W, Cincotta C, Monasterio A, Odom E, Doucette E, Grella SL, Merfeld E, Shpokayte M, Ramirez S. 2022. Hippocampus and amygdala fear memory engrams re-emerge after contextual fear relapse. Neuropsychopharmacology. 47(11):1992–2001. doi: 10.1038/s41386-022-01407-0.

Zanos P, Gould T. 2018. Mechanisms of ketamine action as an antidepressant. Mol Psychiatry. 23(4):801–811. doi: 10.1038/mp.2017.255.

Zarate CA, Singh JB, Carlson PJ, Brutsche NE, Ameli R, Luckenbaugh DA, Charney DS, Manji HK. 2006. A randomized trial of an N-methyl-D-aspartate antagonist in treatment-resistant major depression. Arch Gen Psychiatry. 63(8):856–864. doi: 10.1001/archpsyc.63.8.856.

Zhang F, Wang C, Lan X, Li W, Ye Y, Liu H, Hu Z, You Z, Zhou Y, Ning Y. 2023. Ketamine-induced hippocampal functional connectivity alterations associated with clinical remission in major depression. J Affect Disord. 325:534–541. doi: 10.1016/j.jad.2023.01.003.

Supplement

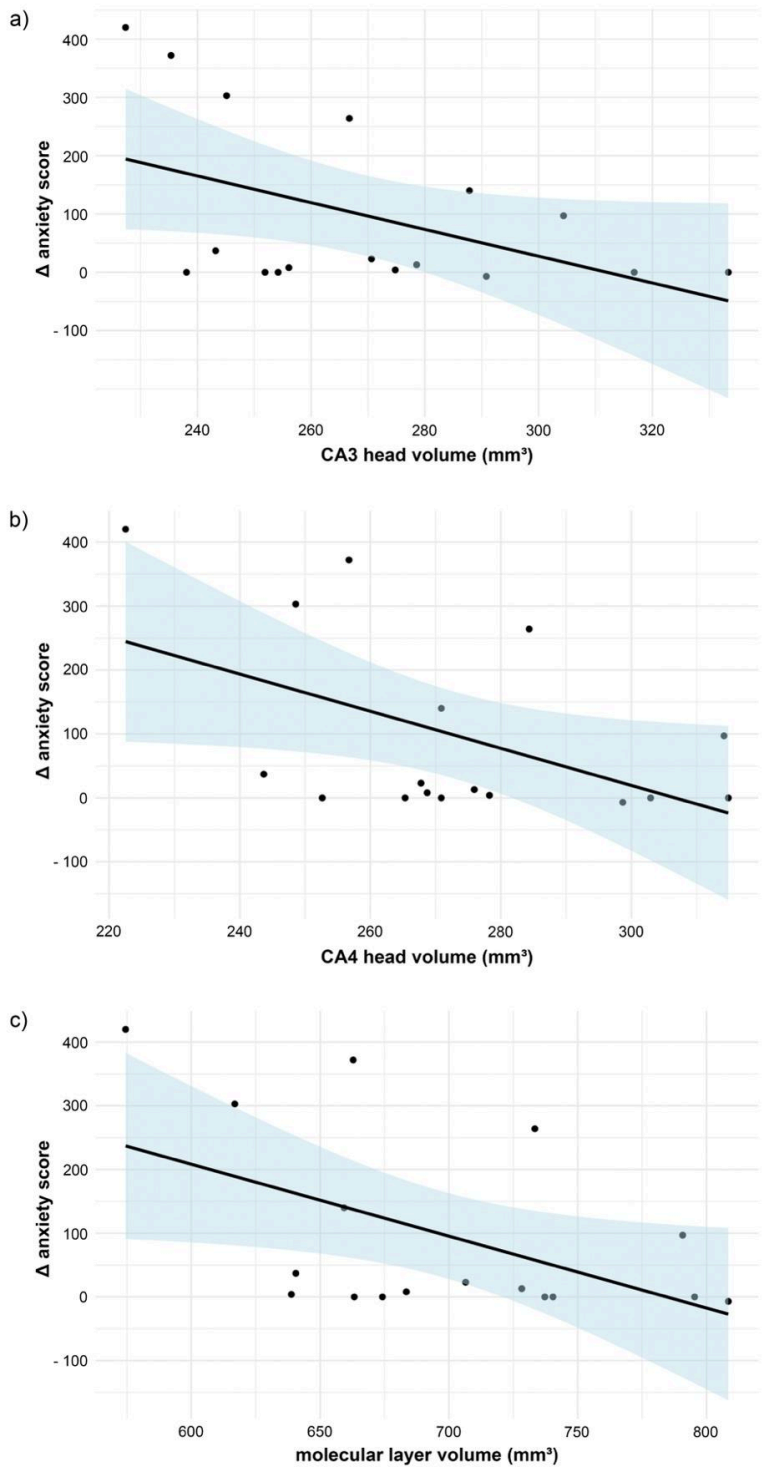

Suppl. Figure 1: Scatter plot of the trend wise relationship of the bilateral CA3 head (A), CA4 head (B) and molecular layer (C) volume and the anxiety score difference. The

anxiety score difference was obtained by subtraction of the measures derived at each scanning session.

Ketamine's Prohedonic Effects Across Reward Processing Stages

Study 3: Briem, E., Stöhrmann, P., Dörl, G., Milz, C., Schlosser, G., Klöbl, M., Reed, M., Atger, M., Schmidt, C., **Kathofer, M.**, Godbersen, G.M., Crone, J.S., Lanzenberger, R., Spies, M. (2025). Subacute Effects of Ketamine on Neural Correlates of Reward Processing. bioRxiv, DOI: https://doi.org/10.1101/2025.09.10.675318

Second stage of review since 16.12.2025

My contribution

As with the previous study, I contributed across multiple stages of this project, including study design and protocol development, participant recruitment and data collection, methodological adjustments, and refining the manuscript.

Subacute Effects of Ketamine on Neural Correlates of Reward Processing

Briem E[1,2], Stöhrmann P[1,2], Dörl G[1,2], Milz C[1,2], Schlosser G[1,2], Klöbl M[1,2], Reed M[1,2], Atger M[1,2], Schmidt C[1,2], Kathofer M[3,4], Godbersen GM[1,2], Crone JS[3,4], Lanzenberger R[1,2]*, Spies M[1,2]

[1]Department of Psychiatry and Psychotherapy, Medical University of Vienna, Vienna, Austria; [2]Comprehensive Center for Clinical Neurosciences and Mental Health (C3NMH), Medical University of Vienna, Vienna, Austria; [3]Vienna Cognitive Science Hub, University of Vienna, Vienna, Austria; [4]Faculty of Psychology, University of Vienna, Vienna, Austria.

*Correspondance to:
Prof. Rupert Lanzenberger, MD PhD
Department of Psychiatry and Psychotherapy, Medical University of Vienna
Waehringer Guertel 18-20, Vienna, 1090, Austria
rupert.lanzenberger@meduniwien.ac.at

For submission to bioRxiv

Abstract

Objectives: Ketamine's prohedonic properties have been linked to enhanced reward-related brain activation during the early post-infusion phase. Its effects during the subacute period (~2-24 h post-infusion), when psychotomimetic symptoms fade and neuroplastic adaptations emerge, are less well characterised. This study assessed ketamine's subacute effects on reward processing using the Monetary Incentive Delay (MID) task.

Methods: In a randomised, placebo-controlled, crossover study, 28 healthy participants received 0.5 mg/kg racemic ketamine or placebo via 40-minute intravenous infusion. Functional magnetic resonance imaging (fMRI) was acquired ~5 h post-infusion. Plasma concentrations of ketamine and norketamine were obtained for individual area under the curve (AUC) estimation. Analyses focused on the contrast between expected and actual trial outcomes.

Results: At five hours post-infusion, ketamine did not significantly modulate MID task-related brain activation, despite pronounced subjective drug effects. Pharmacokinetic modelling confirmed expected ketamine and norketamine profiles, but neither drug exposure (AUC) nor subjective measures correlated with neural activation.

Conclusions: Prohedonic effects of ketamine may not sufficiently manifest in MID task-related activation in healthy individuals ~5 hours after infusion. The lack of significant effects provides valuable extension of the existing literature, as ketamine's effects might be confined to a more acute time window or differ in clinical populations.

Keywords: ketamine; norketamine; fMRI; MID task; reward processing

Introduction

Ketamine's rapid-acting antidepressant effects have led to a major shift in psychiatric research and the treatment of Major Depressive Disorder (MDD) in recent years. Unlike traditional monoaminergic antidepressants, ketamine elicits rapid antidepressant effects within 2 h and sustained effects lasting up to 7 days following a single subanaesthetic dose (Zarate et al. 2006; Coyle and Laws 2015). One of ketamine's most promising properties is its potential to alleviate anhedonia (Lally et al. 2014; Nogo et al. 2022; Kwaśny, Kwaśna, et al. 2024; Kwaśny, Cubała, et al. 2024), a core symptom of MDD characterised by the reduced ability to experience pleasure (Gorwood 2008; Höflich et al. 2018). Anhedonia is of particular clinical interest as it correlates with poorer treatment outcomes (Spijker et al. 2001) and heightened risk of suicidality (Winer et al. 2014). Prior findings suggest that ketamine's prohedonic effects are associated with increased glucose metabolism in reward-related brain regions, specifically the ventral striatum (Nugent et al. 2014; Lally et al. 2015).

At a neurobiological and network level, anhedonia is hypothesised to reflect deficits in reward circuitry (Gorwood 2008; Argyropoulos and Nutt 2013; Höflich et al. 2018; Pulcu et al. 2022). Reward processing relies on coordinated activity across the striatum, insula, amygdala, thalamus, and dopaminergic mesocorticolimbic regions (Oldham et al. 2018), enabling adaptive decision-making and goal-directed behaviour (Balleine and O'Doherty 2010). The Monetary Incentive Delay (MID) task is a well-established paradigm for investigating reward processing, predominantly combined with functional magnetic resonance imaging (fMRI) (Knutson et al. 2000; Lutz and Widmer 2014; Oldham et al. 2018; Wilson et al. 2018) and has been previously applied in our laboratory (Hahn et al. 2021; Hahn et al. 2025). The MID task consists of two phases: anticipation, when a cue signals potential reward or loss, and outcome, when the reward or loss is obtained or

omitted. Anticipation activates regions such as the striatum, insula, thalamus, and amygdala (Knutson et al. 2000; Oldham et al. 2018; Wilson et al. 2018). Similar regions are also active during the outcome phase, suggesting overlapping neural circuits in different stages of reward processing (Knutson et al. 2000; Oldham et al. 2018; Wilson et al. 2018).

Ketamine, originally developed as an anaesthetic (Domino et al. 1965), elicits rapid antidepressant effects after a 40-minute subanaesthetic infusion (0.5 mg/kg), with improvement of depressive symptoms emerging within hours (Berman et al. 2000; Zarate et al. 2006; Nikolin et al. 2023). While its anaesthetic and psychotomimetic properties are mediated by NMDA receptor antagonism, antidepressant actions likely involve downstream mechanisms such as AMPA receptor activation and synaptic plasticity (Zanos et al. 2016; Zanos et al. 2018; Lumsden et al. 2019; Casarotto et al. 2021). Ketamine's pharmacokinetic profile is characterised by rapid distribution, extensive hepatic metabolism, and an elimination half-life of 2 to 4 h (Mion and Villevieille 2013; Peltoniemi et al. 2016). Norketamine, the primary active metabolite, peaks around 100 min post-infusion (Zanos et al. 2016) and also exhibits NMDA receptor antagonism, although with lower affinity than ketamine itself (Ebert et al. 1997; Sałat et al. 2015).

While acute modulatory effects of ketamine on reward processing have been observed 40 min post-infusion in healthy subjects (Francois et al. 2016) and 2 h post-infusion in remitted MDD patients (Kotoula et al. 2022), subacute effects remain underexplored. In this study, we aim to assess the subacute effects of ketamine (~5 h post-infusion) on reward circuitry using task-based fMRI during the MID task. Investigating the intermediate phase may provide unique insights into ketamine's neuromodulatory effects following the resolution of acute psychotomimetic symptoms and during the early stages of synaptic and circuit-level reorganization. Studying healthy participants allows

investigation of ketamine's effects on reward processing without the confounds of clinical symptoms. Based on previous fMRI findings (Francois et al. 2016; Mkrtchian et al. 2021; Kotoula et al. 2022), we hypothesise that ketamine will increase neural activation in the striatum during reward anticipation, potentially reflecting its prohedonic properties (Lally et al. 2014; Nugent et al. 2014; Lally et al. 2015; Mkrtchian et al. 2021; Nogo et al. 2022; Pulcu et al. 2022).

Methods

Participants

Participants were required to be 18-55 years old, right-handed, in good general and psychiatric health (based on medical history, physical exam, and structured DSM-5 interview), and able to provide informed consent. Participants were excluded in case of current or past psychiatric diagnosis, relevant medical illness, pregnancy or breastfeeding, MRI contraindications, substance abuse, or prior ketamine use. Urine drug screening and pregnancy testing (in females) were performed at each visit.

Study Design

This study was approved by the ethics committee of the Medical University of Vienna, Austria (EK 1572/2021) and performed in accordance with the declaration of Helsinki.

The study followed a single-blind, placebo-controlled, crossover design consisting of four sessions: a screening visit, two experimental sessions (ketamine and placebo in a randomised order, both including MRI scanning; Figure 1), and an end-of-study visit. At both MRI sessions, subjects received either placebo (0.9% saline solution) or an infusion of 0.5 mg/kg racemic ketamine diluted in 0.9% saline solution via a venous catheter using a continuous infusion pump over 40 min. The study medication (50 mg/mL ampoules; Hameln Pharma Plus GmbH) was prepared by a medical doctor before each session.

Participants were observed in a clinical setting for at least 90 min post-infusion until full recovery from ketamine-induced sedative and dissociative effects.

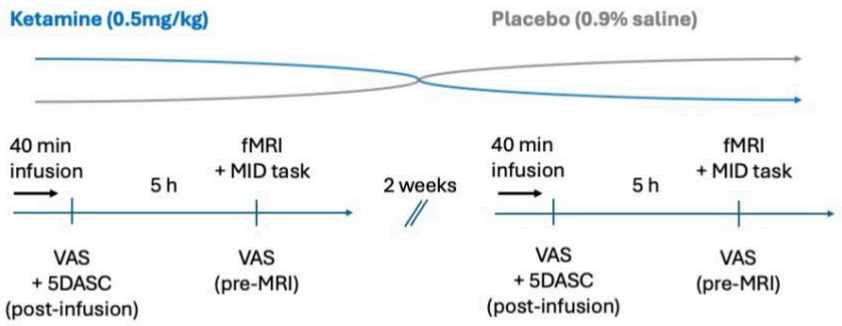

Figure 1. Single-blind, placebo-controlled, crossover design study design. Participants received either ketamine (0.5 mg/kg, 40-min i.v. infusion) or placebo (0.9% saline) in two separate sessions, spaced 2 weeks apart. Following each infusion, subjective drug effects were assessed using a visual analogue scale (VAS) to assess common ketamine-related adverse effects and a 5D-ASC questionnaire immediately post-infusion. Approximately 5 h later, participants underwent fMRI scanning while performing the Monetary Incentive Delay (MID) task, with VAS ratings collected immediately before scanning.

Psychometric Measures

Subjective drug effects as experienced during ketamine application were assessed using the 5-dimensional altered states of consciousness rating scale (5D-ASC), a validated questionnaire designed to assess altered states of consciousness induced by psychoactive substances such as ketamine (Dittrich 1998; Studerus et al. 2010). Participants completed the questionnaire on a tablet in a quiet room under supervision. The 94 items of the 5D-ASC were scored on a scale ranging from 0 (no experience) to 100 (strongest possible experience). A total 5D-ASC score was computed by summing the scores of all 94 items. In addition to the 5D-ASC, participants completed two brief visual analogue scale (VAS) assessments to evaluate the duration and intensity of common ketamine-associated adverse effects, including dizziness, blurred vision, headache, nausea, dry mouth, poor

coordination, and restlessness. (Murrough et al. 2013). Each of the seven symptoms was rated individually from 0 ("no symptom") to 100 ("most severe"), and a total VAS score was obtained by summing the ratings across all symptoms. VAS assessments were conducted shortly after infusion stop as well as immediately before MRI scanning.

fMRI Scanning

Task-based BOLD fMRI scanning was conducted approximately 5 h (mean: 5 h 19 min ± 6.5 min) after the start of the ketamine infusion. MRI scanning was performed on a 3 Tesla MR Scanner (MAGNETOM Prisma, Siemens Medical, Erlangen, Germany). Task-based fMRI data was acquired using a single-shot gradient-recalled echo-planar imaging (EPI) sequence with the following parameters: echo time (TE) / repetition time (TR) = 30 ms / 1600 ms, matrix size of 70 × 70 voxels, a field of view (FOV) of 210 × 210 mm, and a multiband factor of 2. The resulting voxel dimensions were 3 x 3 x 3 mm, with a total of 48 slices (slice thickness = 3 mm). Preprocessing included conversion of data to NIfTI-format, physiological noise correction (PESTICA; Shin et al. 2022), motion correction (SLOMOCO; Beall and Lowe 2014)), slice time correction (SPM12), wavelet despiking (Patel et al. 2014; Patel and Bullmore 2016), distortion correction (TOPUP; Andersson et al. 2003), spatial normalisation to MNI space via the mean T1 image across sessions (SPM12), and spatial smoothing using a 9 mm FWHM Gaussian kernel.

MID Task

During the MID task, participants were instructed to maximise gains and avoid losses during win, lose, and neutral trials. Each trial began with the presentation of a cue (anticipation phase) indicating a potential gain or loss (e.g., –1€, +3€). After a variable delay of 3–5 seconds, a target stimulus appeared ("!"), prompting participants to press a button as quickly as possible. If the reaction time was within a predefined time window

based on their individual average response time determined prior to the scan, the amount was gained or the loss was avoided; otherwise, the amount was not gained, or the loss was incurred. Each response was immediately followed by feedback displaying the outcome and the updated cumulative balance (outcome phase). Unknown to the participants, odds were manipulated during "win" and "loss" trials by increasing or decreasing the valid time window for reaction, respectively. The task lasted 10 min and 5 s and consisted of nine blocks presented in randomised order (three gain, three loss, three neutral e.g., 0 € gambled), comprising a total of 57 trials (3 × 7 gain, 3 × 7 loss, 3 × 5 neutral). Trials were separated by a fixation cross presented for a variable interval of 3–7 seconds. To maintain attention and enable modelling of reward sensitivity, six different monetary amounts were used (0.5€, 1€, and 3€ for both gain and loss trials; initial balance: 10€). Monetary amounts were selected to reflect a range of low to high incentives, in line with previous studies on motivational salience (Knutson et al. 2000; Kotoula et al. 2022). The final balance (if positive) was paid out to participants at the end of the study.

Pharmacokinetic Analysis

Racemic ketamine (0.5 mg/kg) was administered intravenously over 40 min, and blood samples were collected at predefined time points (0, 5, 10, 20, 40, 100, and 360 min). After centrifugation and plasma separation, plasma samples were stored at ≤−20°C until analysis. Ketamine plasma concentrations were determined by gas chromatography–tandem mass spectrometry with multiple reaction monitoring at the Department of Laboratory Medicine, Medical University of Vienna, Austria. The analytical procedure was validated in accordance with EMA guidelines (Bioanalytical method validation - Scientific guideline | European Medicines Agency (EMA) 2011 Aug 1).

Area under the curve (AUC) values for ketamine and its primary metabolite, norketamine, were calculated from model-fitted concentration-time profiles. MATLAB's SimBiology

toolbox was used to estimate individual concentration trajectories based on subject-specific pharmacokinetic (PK) parameters, enabling quantification of systemic drug exposure by accounting for inter-individual variability in drug distribution and clearance. The PK analysis was performed using a two-compartment model (central and peripheral) with two metabolic delay compartments to simulate the conversion of ketamine to norketamine. The model structure was based on the PK framework described by Kamp et al. (Kamp et al. 2020), which applied a compartmental approach to account for the distribution and metabolism of ketamine and its metabolites. Parameter estimation was carried out using nonlinear mixed-effects modelling (NLME) in SimBiology (MATLAB). Individual pharmacokinetic parameters such as clearance (CL), volume of distribution ($V_{central}$, $V_{peripheral}$), and inter-compartmental transfer rates (Q) were estimated from the model based on the observed concentration-time data. Model validation involved visual comparison of simulated and observed plasma concentrations of both ketamine and norketamine.

fMRI Analysis and Statistical Modelling

First Level Analysis

At the first level, each participant's data was modelled using a general linear model (GLM). Pretrial cues (win/loss/neutral), targets, and feedback (gain/no gain/loss/no loss/neutral) were modelled separately - with and without parametric modulation by reward magnitude (absolute value, log- or rank-transformed to test for different neural response profiles). To control for residual physiological and other sources of noise, principal components of the white matter and CSF signal time courses were included as nuisance regressors (CompCor; Behzadi et al. 2007).

In order to capture neural processes associated with the alignment or mismatch between

anticipated and actual outcomes (Knutson and Greer 2008; Schultz 2016), we additionally implemented an Expectation–Outcome Congruency contrast as a measure of reward prediction error. This contrast compared trials in which the actual feedback matched the expected outcome (congruent: potential win/loss was signalized and coincided with feedback "win" or "loss") versus trials where the outcome violated expectations (incongruent: no gains/no losses), thereby extending the traditional MID analysis beyond separate anticipation and outcome. We speculated that psychopathologies (e.g. MDD), their symptoms (anhedonia), and substances affecting reward circuitry (ketamine) might influence not only specific aspects of win and loss processing (e.g. the time window in which positive or negative feedback is received) but also the evaluation of outcomes relative to expectations — that is, how "best" or "worst" anticipated outcomes are perceived compared with the actual experience.

Second Level Analysis

Region of Interest (ROI)-based Analysis

We conducted a literature-driven, a priori ROI-based analysis, focusing on key brain structures implicated in reward and salience processing, including the striatum, nucleus accumbens (NAc), insula, amygdala, and thalamus (Knutson and Greer 2008; Dugré et al. 2018; Oldham et al. 2018; Jauhar et al. 2021; Chen et al. 2022). ROIs were anatomically defined using the Automated Anatomical Labeling 3 (AAL3) atlas (Rolls et al. 2020). For each ROI, contrast estimates (beta values of the first level analysis) were extracted and analysed using linear mixed-effects models in MATLAB to examine the influence of ketamine exposure, subjective drug experience, and covariates on ROI activation.

The primary model specification was:

$$\beta_{ROI} \sim drug_{ketamine,placebo} + ketLvl_{AUC\ to\ MID/2} + sex_{m,f} + age + measurement_{1,2} + drugOrder_{1,2} + fiveDASC + (1 \mid subject)$$

Here, ketLvl represents the area under a piecewise linear approximation of individual ketamine exposure up to half the task duration (z-scored within the ketamine condition, otherwise zero, to avoid collinearity with the drug conditions). fiveDASC reflects subjective drug experience (5D-ASC, z-scored within each condition). A random intercept for subject was included to account for repeated measures.

Whole-Brain Analysis

In addition to the ROI-based approach, on an exploratory basis, the same first-level contrasts were entered into second-level whole-brain analyses using a flexible factorial design in SPM12. The model accounted for drug (placebo/ketamine), measurement, order of drugs (to account for potential carry-over and/or habituation effects), and enabled the testing of main and interaction effects using F- and t-tests. Findings were considered significant if $p_{uncorr} < 0.001$ and $p_{FWE,\ cluster} < 0.05$.

Results

A total of 36 healthy subjects completed the study. After excluding subjects with either excessive head motion during MRI scanning, missing plasma concentration values or irregular ketamine plasma concentration curves (e.g. peak plasma concentration 20 minutes prior to end of infusion), 28 participants (15 females, mean age 23.6 ± 3.8 years) remained eligible for analysis.

Pharmakokinetic Data

Ketamine plasma levels increased rapidly after infusion, peaking at approximately 40 min, i.e., end of infusion (Figure 2A, Table 1,), while norketamine concentrations

increased more slowly, consistent with the expected metabolic conversion over time (Figure 2B, Table 2). AUC values for ketamine and norketamine plasma concentration curves were calculated up to half the task duration (5 h 14 min ± 6 min) using a two-compartment PK model (SimBiology, MATLAB) and model-fitted concentration-time profiles (Figure 3).

Time (min)	Ketamine_Mean (ng/ml)	Ketamine_SD (ng/ml)	Ketamine_Min (ng/ml)	Ketamine_Max (ng/ml)
0	0.0	0.0	0.0	0.0
5	39.08	31.01	8.08	166.7
10	73.05	40.62	32.43	186.44
20	115.01	52.48	58.55	285.85
40	165.19	41.81	111.26	297.0
100	67.18	12.09	46.21	91.27
360	17.19	4.61	8.2	26.05

Table 1. Plasma concentrations of ketamine (n = 28). Mean, standard deviation, minimum, and maximum plasma levels of ketamine at each time point following a 40-minute intravenous ketamine infusion (0.5 mg/kg, infusion start = 0min).

Time (min)	Norketamine_Mean (ng/ml)	Norketamine_SD (ng/ml)	Norketamine_Min (ng/ml)	Norketamine_Max (ng/ml)
0	0.0	0.0	0.0	0.0
5	0.0	0.0	0.0	0.0
10	1.93	2.49	0.0	6.58
20	15.4	9.89	6.84	49.35
40	45.63	18.68	24.04	101.88
100	70.85	17.43	41.79	102.78
360	44.4	13.06	26.83	75.12

Table 2. Plasma concentrations of norketamine (n = 28). Mean, standard deviation, minimum, and maximum plasma levels of norketamine at each time point following a 40-minute intravenous ketamine infusion (0.5 mg/kg, infusion start = 0min).

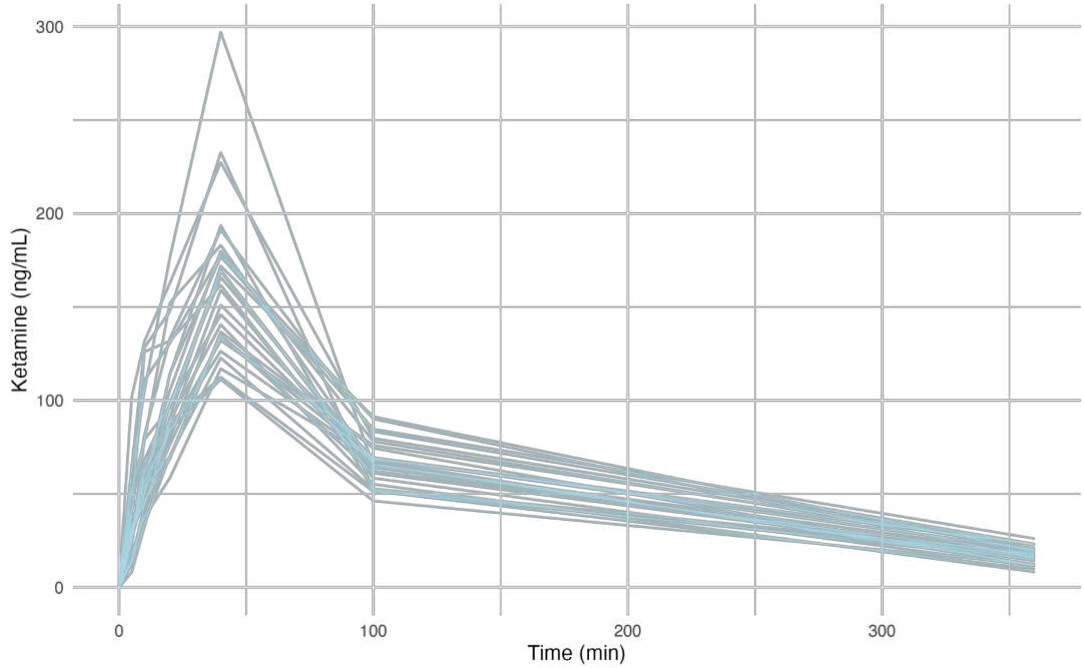

A

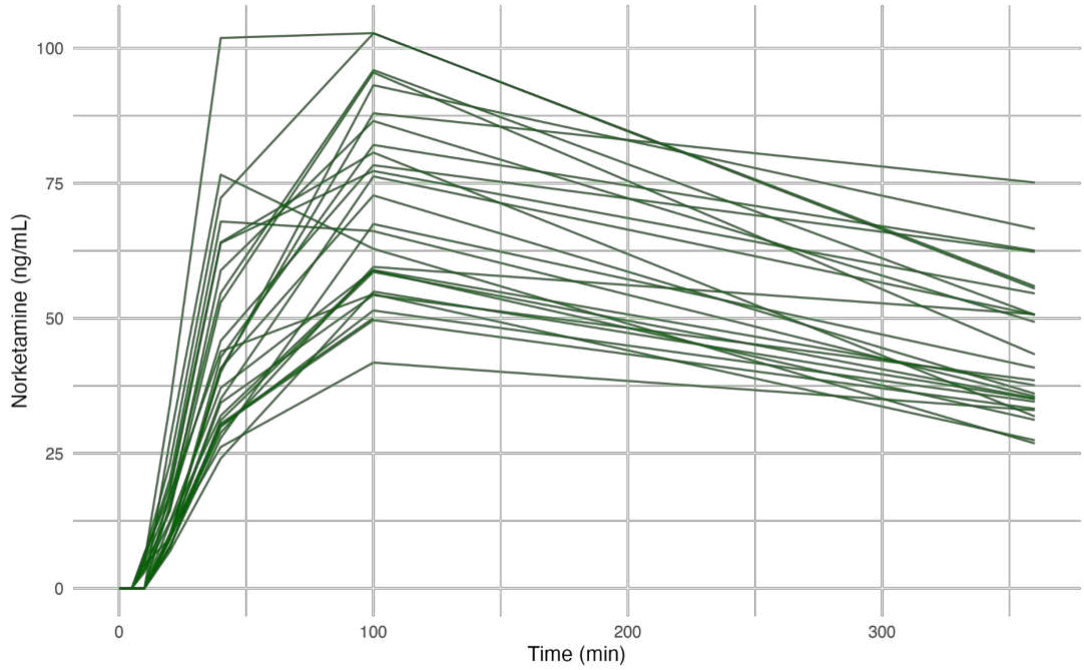

B

Figure 2. Plasma concentration–time curves of ketamine (A, blue) and norketamine (B, green) following a 40-min intravenous infusion of racemic ketamine (0.5 mg/kg). Each line represents an individual subject (n = 28). Ketamine concentrations peak at infusion stop, while norketamine shows a delayed peak due to metabolic conversion.

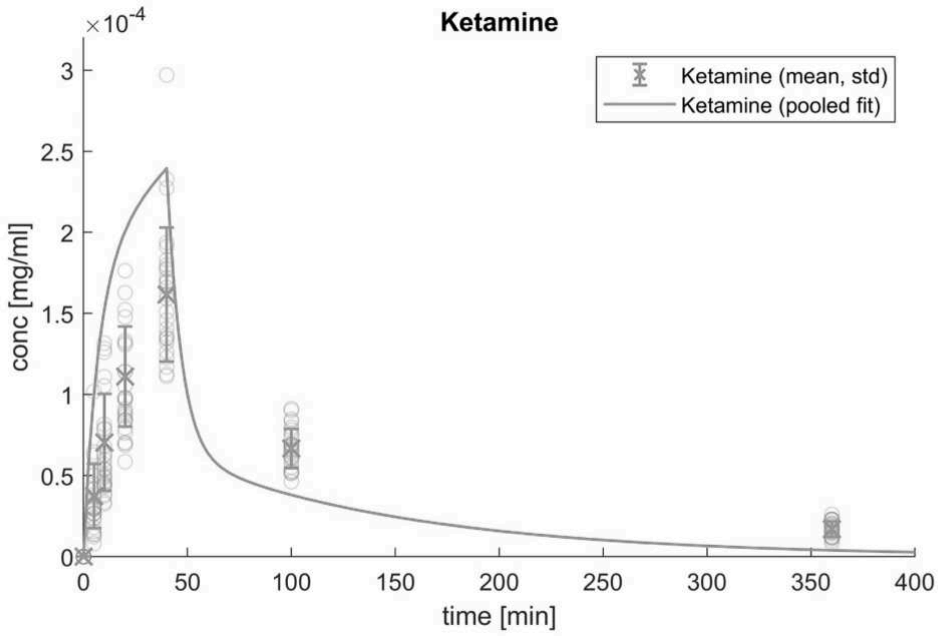

A

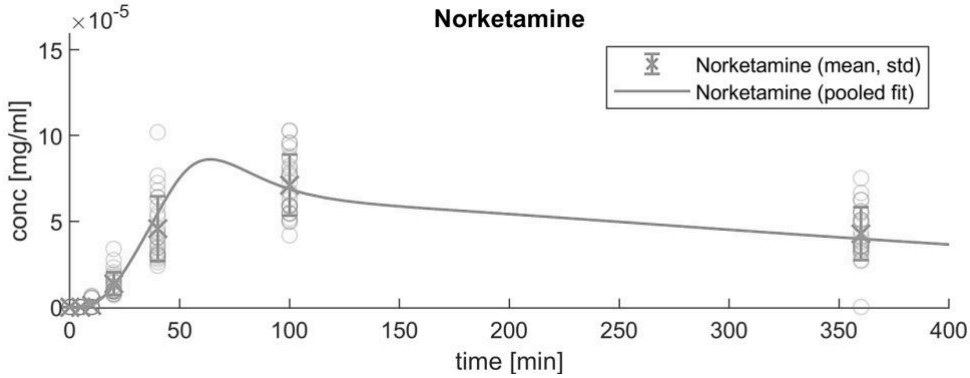

B

Figure 3. Piece-wise, linearly fitted plasma concentration–time curves for ketamine (A) and norketamine (B) following a 40-min intravenous infusion of racemic ketamine (0.5 mg/kg). Symbols (open circles) represent individual data points and mean ± SD (crosses with error bars), while solid lines depict the pooled pharmacokinetic model fit.

Subjective Effects

5D-ASC and VAS scores were available for 27 of the 28 subjects. Total 5D-ASC scores were significantly elevated during ketamine visits (2969.8 ± 1363.3) compared to placebo visits (251.6 ± 406.1; paired $t(26) = 10.09$, $p < .0001$, Cohen's $d = 2.67$; Figure 4),

indicating pronounced subjective drug effects during ketamine sessions. VAS scores immediately post-infusion were also significantly higher (281.5 ± 72.2) compared to placebo (32.8 ± 51.5; paired $t(26) = 16.49$, $p < .0001$, Cohen's $d = 3.93$). During ketamine sessions, VAS scores decreased substantially from immediately post-infusion (281.5 ± 72.2) to just before MRI scanning (35.3 ± 43; paired $t(26) = 18.5$, $p < .0001$, Cohen's $d = 4$). Nevertheless, compared to placebo sessions (9.3 ± 19.1), VAS scores just before MRI remained significantly higher during ketamine sessions (median difference = 26; Wilcoxon signed-rank test: $V = 189$, $p = 0.0018$; Figure 5). Distributional checks confirmed use of paired t-tests for 5D-ASC and VAS post-infusion, while non-normal pre-MRI VAS differences were analysed with the Wilcoxon signed-rank test.

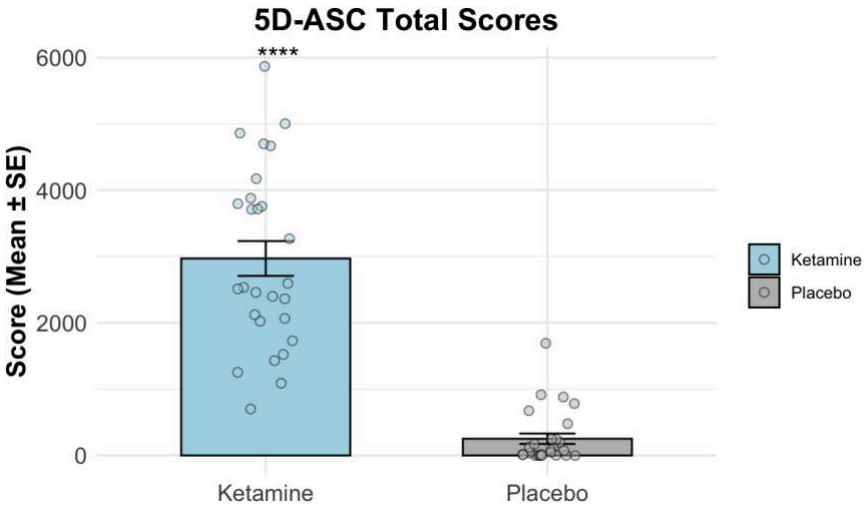

Figure 4. Subjective drug effects measured via the 5-dimensional altered states of consciousness rating scale (5D-ASC) questionnaire (n = 27). Total 5D-ASC scores post-infusion for the ketamine and placebo conditions. Bars represent mean ± standard deviation. Asterisks indicate significant differences (**p < .01, ****p < .0001).

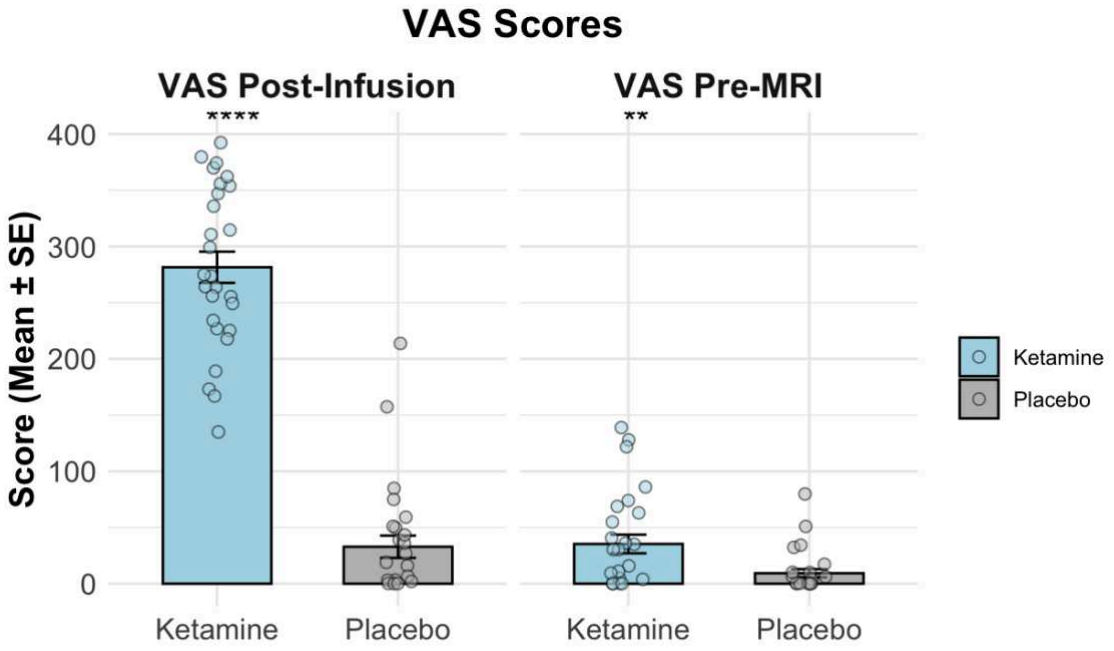

Figure 5. Visual analogue scale (VAS) ratings of common ketamine-associated adverse effects for the ketamine and placebo conditions (n = 27). Ratings were obtained shortly after infusion stop (post-infusion) and immediately before MRI scanning (pre-MRI). The assessed symptoms included dizziness, blurred vision, headache, nausea, dry mouth, poor coordination, and restlessness (Murrough et al. 2013). Bars represent mean ± standard deviation. Asterisks indicate significant differences between conditions (**p < .01, ****p < .0001). Group differences were tested with paired t-tests (VAS Post-Infusion) or Wilcoxon signed-rank tests (VAS Pre-MRI).

MID Task Performance

Reaction times during the MID task did not significantly differ (α = 0.05) between ketamine and placebo condition ($\overline{t_{placebo}} \approx 338\,ms$, $\overline{t_{ketamine}} \approx 352\,ms$, p = 0.07, paired t-test; $\overline{balance_{placebo}} \approx 15.82$ €, $\overline{balance_{ketamine}} \approx 15.51$ €, p = 0.78, paired t-test) (Figure 6). Normality tests confirmed that assumptions for the paired t-test were met (all p > .05).

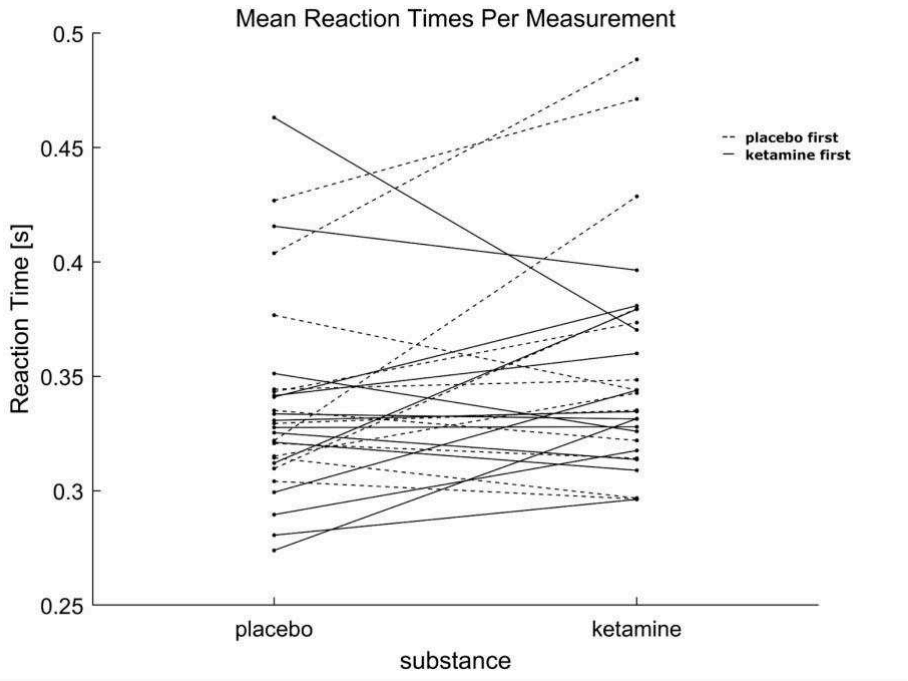

Figure 6. Mean reaction times during the MID task did not significantly differ between ketamine and placebo sessions, irrespective of session order.

fMRI Analysis

First Level Analysis

At the single-subject level, contrasts for anticipation, feedback (win, no-win, loss, no-loss), and Expectation–Outcome Congruency elicited robust activation patterns. Representative first-level statistical maps (Figure 7) illustrate engagement of reward- and salience-related regions.

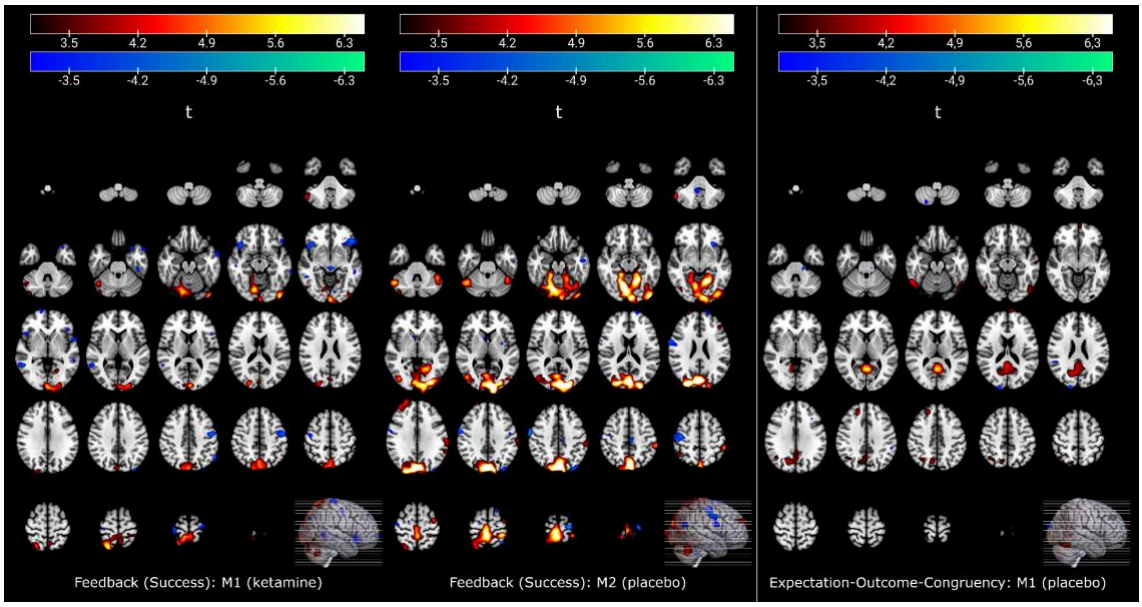

Figure 7. Exemplary first level whole-brain activation maps ($p_{uncorr} < 0.001$ shown) for feedback "success" (win or loss prevented) during the MID task under ketamine (left) and placebo (center) and expectation-outcome-congruency (right, placebo condition).

Second Level Analysis

ROI-based Analysis

ROI analyses focused on the amygdala, insula, NAc, striatum, and thalamus, based on their well-established role in reward and salience processing (Knutson and Greer 2008; Dugré et al. 2018; Oldham et al. 2018; Jauhar et al. 2021; Chen et al. 2022). For each ROI, first level contrast estimates (beta values) were extracted and analysed using linear mixed-effects modelling in MATLAB to assess the influence of drug condition (ketamine vs. placebo), individual ketamine exposure (modelled as AUC until task onset), and subjective drug experience (5D-ASC scores). No significant main effect of drug condition was observed for any ROI. In the thalamus, a significant positive association between 5D-ASC scores and BOLD activation was found ($p = 0.013$). However, given the absence of drug effects and multiplicity adjustments this association may represent a false positive.

Whole-Brain Analysis

Since the ROI-based analysis did not yield any significant results, we conducted an exploratory whole-brain analysis. Group-level statistical analysis was performed using a flexible factorial design in SPM12, which accounted for within-subject variability in the crossover design. Neither the main effect of drug condition (difference between ketamine and placebo measurement) nor exploratory F-contrasts for other factors revealed significant differences in BOLD activation. Additional exploratory models testing alternative parametrizations of monetary reward (reward magnitude, rank, or log magnitude) and feedback- or anticipation-only phases also yielded no detectable substance effects. However, exploring each substance individually, spatially coherent, significant activation patterns were found (Figure 8).

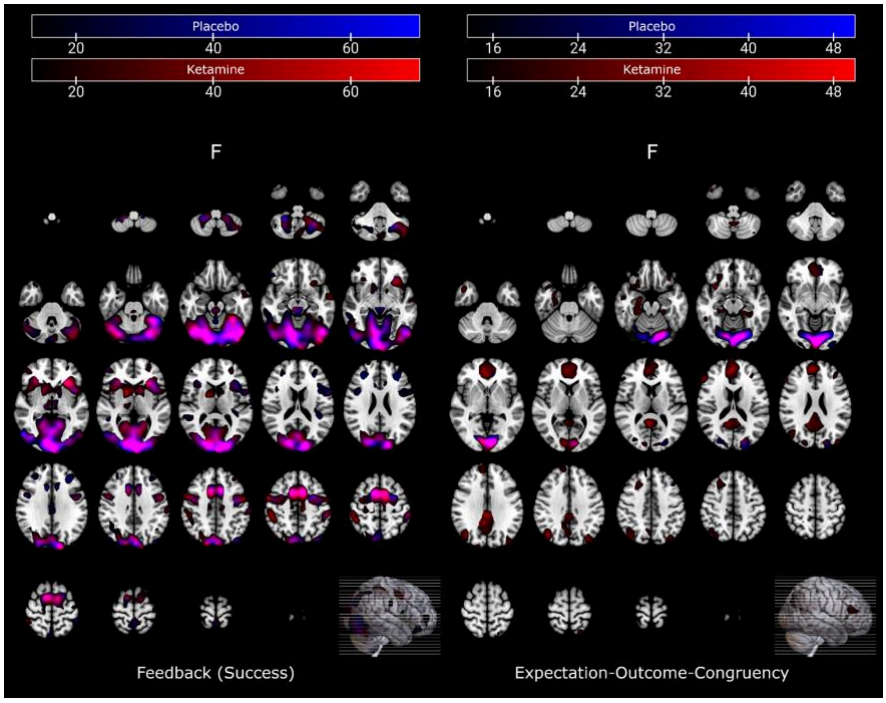

Figure 8. Group-level whole-brain activation maps ($p_{uncorr} < 0.001$ shown) for feedback "success" (win or loss prevented) during the MID task (left) and expectation-outcome-congruency (right). Activation shown was modelled without parametrization of amount gambled. Placebo condition statistics are displayed in blue, ketamine's in red. Additive overlay blending was used for emphasis of spatial overlap between conditions.

Discussion

Ketamine administration 5 h prior to scanning did not significantly alter reward-related brain activation during the MID task at either the ROI or whole-brain level. Pharmacokinetic modelling confirmed expected ketamine and norketamine concentration profiles, but neither individual drug exposure (AUC) nor subjective experience correlated with neural activation.

Our ROI-based analysis focused on the striatum, NAc, thalamus, insula, and amygdala. These regions were selected based on meta-analytic evidence identifying them as core neural substrates of reward and loss anticipation (Knutson and Greer 2008; Dugré et al. 2018; Oldham et al. 2018; Jauhar et al. 2021; Chen et al. 2022). While the insula, amygdala and thalamus are widely associated with motivational salience (Seeley et al. 2007; Menon and Uddin 2010; Oldham et al. 2018), the striatum, particularly the NAc, has been linked to reward magnitude (Knutson et al. 2001; Costumero et al. 2013), reward sensitivity (Carter et al. 2009; Hahn et al. 2009; Costumero et al. 2013) and the subjective experience of motivation (Knutson et al. 2001). Striatal hypoactivation, particularly within the NAc, is consistently observed in depression during reward anticipation and feedback (Pizzagalli et al. 2009; Smoski et al. 2009; Zhang et al. 2013; Admon and Pizzagalli 2015) and is considered a neural correlate of anhedonia (Szczepanik et al. 2019; Borsini et al. 2020). Given ketamine's proposed prohedonic effects (Lally et al. 2014; Nogo et al. 2022; Pulcu et al. 2022), we hypothesised that it might modulate activity within these ROIs during the MID task. Our Expectation-Outcome Congruency contrast was designed to capture neural activity related to outcome monitoring and reward prediction errors, processes essential for adaptive learning and frequently impaired in MDD (Schultz et al. 1997; Pizzagalli et al. 2009; Smoski et al. 2009).

Our findings provide further information on the temporal effects of ketamine on reward

processing when combined with previous studies. Kotoula et al. reported increased activation of the NAc, putamen, insula, and caudate in remitted MDD patients approximately 2 h post-infusion during the feedback phase of the MID task, though only in ROI analyses (Kotoula et al. 2022). François et al. reported attenuated ventral striatal response during reward anticipation in both humans and rodents within 40 min post-infusion (Francois et al. 2016). While these findings may initially appear divergent, they likely reflect differences in timing. Both studies assessed participants in the acute post-infusion phase (40min and 2h post-administration), when plasma concentrations of ketamine and norketamine were near their peak levels and NMDA receptor antagonism ongoing (Zanos et al. 2018; Kamp et al. 2020). François et al. captured the acute phase near peak NMDA receptor blockade, whereas Kotoula et al. examined a slightly later window when acute psychotomimetic effects had subsided but receptor-level modulation was likely ongoing (Duman et al. 2016; Zanos et al. 2016; Zanos et al. 2018; Kamp et al. 2020).

Our scanning time point (~5 h post-infusion) corresponds to a subacute pharmacodynamic phase. This period occurs after the resolution of acute psychotomimetic symptoms (Ballard and Zarate 2020; Tashakkori et al. 2021) and coincides with the onset of antidepressant effects in MDD (Berman et al. 2000; Zarate et al. 2006). Mechanistically, this window is thought to involve glutamate-driven synaptic strengthening and circuit-level reorganisation, mediated by AMPA receptor activation, BDNF release, and mTOR signalling (Li et al. 2010; Duman et al. 2016; Zanos et al. 2016; Zanos et al. 2018; Duman et al. 2021).

Pharmacokinetic and pharmacodynamic data indicate that ketamine's NMDA receptor antagonism peaks rapidly after administration and declines over several hours, consistent with a plasma elimination half-life of approximately 2 to 4 h (Mion and Villevieille 2013;

Peltoniemi et al. 2016). Preclinical evidence suggests that ketamine may continue to block NMDA receptors for up to 24 h due to trapping mechanisms (Ma et al. 2023). Norketamine is eliminated more slowly and maintains high plasma concentrations more than 5 h after infusion (Quibell et al. 2011; Mion and Villevieille 2013). By the time of our scan (~5 h post-infusion), NMDA receptor blockade has likely subsided (Zanos et al. 2018; Kamp et al. 2020), and secondary metabolites such as hydroxynorketamine predominate (Zanos et al. 2018). Although these metabolites are implicated in the sustained antidepressant effects of ketamine (Zanos et al. 2016), their immediate impact on task-evoked BOLD responses during reward processing remains unclear (Lally et al. 2014; Zanos et al. 2016).

The temporal mismatch between the peak of receptor-level effects and our task window may account for the absence of robust effects in our dataset. Ketamine's effects on reward circuitry in healthy subjects may be time-specific, with fMRI alterations most reliably detected during the acute post-infusion window (<2 h) when NMDA receptor antagonism and dissociative effects are most pronounced (Lally et al. 2014; Francois et al. 2016; Kotoula et al. 2022). By approximately 5 h, when pharmacokinetics shift toward downstream metabolites and behavioral normalisation occurs, ketamine's influence on reward processing may become more subtle, potentially manifesting through longer-term plasticity mechanisms rather than immediate modulation of task-related neural activity (Li et al. 2010; Duman et al. 2016; Zanos et al. 2016; Zanos et al. 2018; Duman et al. 2021). This intermediate state may therefore represent a transitional pharmacodynamic window between acute receptor-level effects and sustained synaptic changes. Future studies using denser temporal sampling across acute (≤2 h), intermediate (3–6 h), and later phases (24–72 h) could map evolving neural effects of ketamine more precisely.

It is also conceivable that the absence of ketamine-induced neural effects in our healthy

cohort may result from baseline differences from MDD patients (Kotoula et al. 2022). MDD is associated with deficits in reward processing, including attenuated striatal and prefrontal responses (Zhang et al. 2013; Ng et al. 2019) and ketamine may differently modulate reward processing in individuals with pre-existing reward dysfunction. Indeed, ketamine-induced striatal activation has been reported in depressed individuals (Lally et al. 2014; Kotoula et al. 2022), though some studies have also reported ketamine-induced effects in healthy subjects (Francois et al. 2016; Mkrtchian et al. 2021). Mkrtchian et al. further demonstrated diagnosis-specific connectivity changes 48 h post-infusion, with ketamine normalising fronto-striatal connectivity in MDD but shifting it in healthy controls toward patterns typical of unmedicated MDD (Mkrtchian et al. 2021). These divergent effects suggest that ketamine may restore dysfunctional circuits in depression but disrupt the same networks in healthy individuals, consistent with state-dependent modulation (Reed et al. 2019; Mkrtchian et al. 2021). Evidence indicates that ketamine transiently induces symptoms related to impaired motivation in healthy participants (Driesen et al. 2013; Pollak et al. 2015), further implicating that the direction of ketamine's effects on reward circuitry may be state-dependent.

Limitations

Several limitations should be considered when interpreting these findings. First, our study included healthy subjects only. The lack of a substance effect on contrasts tested may not translate to clinical populations with pre-existing reward dysfunction, such as MDD patients. Second, the timing of the fMRI task (~5 h post-infusion) could have missed the window in which ketamine exerts its most pronounced effects on reward processing. Although this time point was chosen to investigate subacute changes relevant to sustained antidepressant mechanisms, it may have fallen into a transitional pharmacodynamic state in which neither acute pharmacological effects nor long-term synaptic changes were

sufficiently pronounced to produce detectable BOLD signal differences. Denser temporal sampling across acute, intermediate, and later phases would be necessary to fully capture the evolving neural effects of ketamine. Third, while we modelled individual ketamine exposure using AUC values up to task onset, we did not directly assess plasma concentrations of downstream metabolites such as (2R,6R)-hydroxynorketamine at the time of scanning. AUCs may further not sufficiently characterise the complex pharmacokinetics and -dynamics, especially, to model individual (perceived) response.

Finally, limitations in effect size sensitivity should be acknowledged. Whole-brain models estimated 322 to 366 resolution elements for the calculated contrasts, which are equivalent to adjusted type-I error probabilities ranging from 1.6e-4 to 1.4e-4 on voxel level. With 28 participants, six covariates, a power of 0.80, and a reliability of r = 0.21 (Demidenko et al. 2024 July 9) this would require detectable effect sizes of around f = 0.69 / d = 1.38 under repeated-measures ANOVA assumptions. Under the same assumptions, testing a single ROI would require a detectable effect size of f = 0.37 / d = 0.74. Since many different models and contrasts were calculated in the current work, these figures should be interpreted as rough estimates. Effect size calculations were performed in G*Power 3.1.9.7 (ANOVA: Repeated measures, within factors). While these estimates made it unlikely that effects would be detected at the voxel level, the usually more liberal cluster-level or ROI analyses might have detected sufficiently strong neural effects of ketamine.

Conclusion

We observed no significant drug-related effects on reward processing during the MID task in healthy participants five hours after ketamine infusion. These findings combined with previous literature suggest that ketamine's effects on reward circuitry are time-sensitive and potentially most prominent during the acute post-infusion phase (<2 h)

(Lally et al. 2014; Francois et al. 2016; Kotoula et al. 2022). The 5 h post-infusion time point may reflect a transitional pharmacodynamic window, in which receptor-level effects have diminished but sustained synaptic changes have not yet fully developed. In this state, ketamine's influence on anticipation- and feedback-related activation, as well as the Expectation–Outcome Congruency contrast, may be too subtle to detect. Moreover, ketamine's neural effects may be state-dependent, with more robust modulation emerging in individuals with pre-existing reward system dysfunction, such as MDD patients (Lally et al. 2014; Kotoula et al. 2022; Nogo et al. 2022). Future studies should integrate longitudinal designs with denser temporal sampling across acute, intermediate, and later phases, and explicitly compare healthy and clinical cohorts to further characterise temporal dynamics and state-dependence of ketamine's effects on reward processing.

Acknowledgements

The authors would like to thank all staff involved in successful study implementation, including medical doctors and technical colleagues, and diploma students of the Advanced Neuroimaging Labs (aNIL, head: R. Lanzenberger), Department for Psychiatry and Psychotherapy (chair: D. Rujescu). They also express their gratitude to their collaboration partners at the Vienna Science Hub of the University of Vienna.

Statement of Interest

R. Lanzenberger received investigator-initiated research funding from Siemens Healthcare regarding clinical research using PET/MR and travel grants and/or conference speaker honoraria from Janssen-Cilag Pharma GmbH in 2023, and Bruker BioSpin, Shire, AstraZeneca, Lundbeck A/S, Dr. Willmar Schwabe GmbH, Orphan Pharmaceuticals AG, Janssen-Cilag Pharma GmbH, Heel and Roche Austria GmbH., and Janssen-Cilag Pharma GmbH in the years before 2020. He is a shareholder of the company BM Health GmbH, Austria since 2019.

D. Rujescu served as consultant for Janssen, received honoraria from Boehringer-Ingelheim, Gerot Lannacher, Janssen, and Pharmagenetix, received travel support from Angelini, Janssen, and Schwabe, and served on advisory boards of AC Immune, Boehringer-Ingelheim, Roche and Rovi.

M. Spies has received travel grants from AOP Orphan Pharmaceuticals, Janssen and Austroplant, speaker honoraria from Janssen and Austroplant, and workshop participation from Eli Lilly.

C. Schmidt has received a travel grant from Eli Lilly to attend a scientific exchange meeting.

All other authors declare no potential conflicts of interest with respect to the research, authorship, and/or publication of this article.

Consent Declaration

All participants signed an informed consent at the time of enrolment and agreed to participate in the study.

Ethics Statement

This study was approved by the ethics committee of the Medical University of Vienna, Austria (EK 1572/2021) and performed in accordance with the declaration of Helsinki.

Data Availability Statement

Datasets of participants presented in this article are not readily available due to ethical reasons and data sharing regulations. Please contact rupert.lanzenberger@meduniwien.ac.at for questions.

Funding

This study was partly funded by the Research Cluster 'Unraveling the aesthetic mind in anhedonia: Insights from pharmacological imaging of the human brain' between the Medical University of Vienna (PI: Rupert Lanzenberger) and the University of Vienna [Grant number: SO68900012]. G. Dörl, and C. Milz are recipients of a DOC Fellowship of the Austrian Academy of Sciences at the Department of Psychiatry and Psychotherapy, Medical University of Vienna. E. Briem and G. Schlosser have been supported by the MD, PhD Excellence Program of the Medical University of Vienna.

References

Admon R, Pizzagalli DA. 2015. Dysfunctional Reward Processing in Depression. Curr Opin Psychol. 4:114–118. doi:10.1016/j.copsyc.2014.12.011.

Andersson JLR, Skare S, Ashburner J. 2003. How to correct susceptibility distortions in spin-echo echo-planar images: application to diffusion tensor imaging. Neuroimage. 20(2):870–888. doi:10.1016/S1053-8119(03)00336-7.

Argyropoulos SV, Nutt DJ. 2013. Anhedonia revisited: is there a role for dopamine-targeting drugs for depression? J Psychopharmacol. 27(10):869–877. doi:10.1177/0269881113494104.

Ballard ED, Zarate CA. 2020. The role of dissociation in ketamine's antidepressant effects. Nat Commun. 11(1):6431. doi:10.1038/s41467-020-20190-4.

Balleine BW, O'Doherty JP. 2010. Human and Rodent Homologies in Action Control: Corticostriatal Determinants of Goal-Directed and Habitual Action. Neuropsychopharmacol. 35(1):48–69. doi:10.1038/npp.2009.131.

Beall EB, Lowe MJ. 2014. SimPACE: generating simulated motion corrupted BOLD data with synthetic-navigated acquisition for the development and evaluation of SLOMOCO: a new, highly effective slicewise motion correction. Neuroimage. 101:21–34. doi:10.1016/j.neuroimage.2014.06.038.

Behzadi Y, Restom K, Liau J, Liu TT. 2007. A component based noise correction method (CompCor) for BOLD and perfusion based fMRI. Neuroimage. 37(1):90–101. doi:10.1016/j.neuroimage.2007.04.042.

Berman RM, Cappiello A, Anand A, Oren DA, Heninger GR, Charney DS, Krystal JH. 2000. Antidepressant effects of ketamine in depressed patients. Biol Psychiatry. 47(4):351–354. doi:10.1016/s0006-3223(99)00230-9.

Bioanalytical method validation - Scientific guideline | European Medicines Agency (EMA). 2011 Aug 1. [accessed 2025 June 18]. https://www.ema.europa.eu/en/bioanalytical-method-validation-scientific-guideline.

Borsini A, Wallis ASJ, Zunszain P, Pariante CM, Kempton MJ. 2020. Characterizing anhedonia: A systematic review of neuroimaging across the subtypes of reward processing deficits in depression. Cogn Affect Behav Neurosci. 20(4):816–841. doi:10.3758/s13415-020-00804-6.

Carter RM, MacInnes JJ, Huettel SA, Adcock RA. 2009. Activation in the VTA and Nucleus Accumbens Increases in Anticipation of Both Gains and Losses. Front Behav Neurosci. 3:21. doi:10.3389/neuro.08.021.2009.

Casarotto PC, Girych M, Fred SM, Kovaleva V, Moliner R, Enkavi G, Biojone C, Cannarozzo C, Sahu MP, Kaurinkoski K, et al. 2021. Antidepressant drugs act by directly binding to TRKB neurotrophin receptors. Cell. 184(5):1299-1313.e19. doi:10.1016/j.cell.2021.01.034.

Chen Y, Chaudhary S, Li C-SR. 2022. Shared and distinct neural activity during anticipation and outcome of win and loss: A meta-analysis of the monetary incentive delay task. NeuroImage. 264:119764. doi:10.1016/j.neuroimage.2022.119764.

Costumero V, Barrós-Loscertales A, Bustamante JC, Ventura-Campos N, Fuentes P, Ávila C. 2013. Reward sensitivity modulates connectivity among reward brain areas during processing of anticipatory reward cues. European Journal of Neuroscience. 38(3):2399–2407. doi:10.1111/ejn.12234.

Coyle CM, Laws KR. 2015. The use of ketamine as an antidepressant: a systematic review and meta-analysis. Hum Psychopharmacol. 30(3):152–163. doi:10.1002/hup.2475.

Demidenko MI, Mumford JA, Poldrack RA. 2024 July 9. Impact of analytic decisions on test-retest reliability of individual and group estimates in functional magnetic resonance imaging: a multiverse analysis using the monetary incentive delay task. bioRxiv.:2024.03.19.585755. doi:10.1101/2024.03.19.585755.

Dittrich A. 1998. The standardized psychometric assessment of altered states of consciousness (ASCs) in humans. Pharmacopsychiatry. 31 Suppl 2:80–84. doi:10.1055/s-2007-979351.

Domino EF, Chodoff P, Corssen G. 1965. Pharmacologic effects of CI-581, a new dissociative anesthetic, in man. Clinical Pharmacology & Therapeutics. 6(3):279–291. doi:10.1002/cpt196563279.

Driesen NR, McCarthy G, Bhagwagar Z, Bloch M, Calhoun V, D'Souza DC, Gueorguieva R, He G, Ramachandran R, Suckow RF, et al. 2013. Relationship of resting brain hyperconnectivity and schizophrenia-like symptoms produced by the NMDA receptor antagonist ketamine in humans. Mol Psychiatry. 18(11):1199–1204. doi:10.1038/mp.2012.194.

Dugré JR, Dumais A, Bitar N, Potvin S. 2018. Loss anticipation and outcome during the Monetary Incentive Delay Task: a neuroimaging systematic review and meta-analysis. PeerJ. 6:e4749. doi:10.7717/peerj.4749.

Duman RS, Aghajanian GK, Sanacora G, Krystal JH. 2016. Synaptic plasticity and depression: New insights from stress and rapid-acting antidepressants. Nat Med. 22(3):238–249. doi:10.1038/nm.4050.

Duman RS, Deyama S, Fogaça MV. 2021. Role of BDNF in the pathophysiology and treatment of depression: Activity-dependent effects distinguish rapid-acting antidepressants. Eur J Neurosci. 53(1):126–139. doi:10.1111/ejn.14630.

Ebert B, Mikkelsen S, Thorkildsen C, Borgbjerg FM. 1997. Norketamine, the main metabolite of ketamine, is a non-competitive NMDA receptor antagonist in the rat cortex and spinal cord. Eur J Pharmacol. 333(1):99–104. doi:10.1016/s0014-2999(97)01116-3.

Francois J, Grimm O, Schwarz AJ, Schweiger J, Haller L, Risterucci C, Böhringer A, Zang Z, Tost H, Gilmour G, et al. 2016. Ketamine Suppresses the Ventral Striatal Response to Reward Anticipation: A Cross-Species Translational Neuroimaging Study. Neuropsychopharmacol. 41(5):1386–1394. doi:10.1038/npp.2015.291.

Gorwood P. 2008. Neurobiological mechanisms of anhedonia. Dialogues Clin Neurosci. 10(3):291–299. doi:10.31887/DCNS.2008.10.3/pgorwood.

Hahn A, Reed MB, Murgaš M, Vraka C, Klug S, Schmidt C, Godbersen GM, Eggerstorfer B, Gomola D, Silberbauer LR, et al. 2025. Dynamics of human serotonin synthesis differentially link to reward anticipation and feedback. Mol Psychiatry. 30(2):600–607. doi:10.1038/s41380-024-02696-1.

Hahn A, Reed MB, Pichler V, Michenthaler P, Rischka L, Godbersen GM, Wadsak W, Hacker M, Lanzenberger R. 2021. Functional dynamics of dopamine synthesis during monetary reward and punishment processing. J Cereb Blood Flow Metab. 41(11):2973–2985. doi:10.1177/0271678X211019827.

Hahn T, Dresler T, Ehlis A-C, Plichta MM, Heinzel S, Polak T, Lesch K-P, Breuer F, Jakob PM, Fallgatter AJ. 2009. Neural response to reward anticipation is modulated by Gray's impulsivity. Neuroimage. 46(4):1148–1153. doi:10.1016/j.neuroimage.2009.03.038.

Höflich A, Michenthaler P, Kasper S, Lanzenberger R. 2018. Circuit Mechanisms of Reward, Anhedonia, and Depression. Int J Neuropsychopharmacol. 22(2):105–118. doi:10.1093/ijnp/pyy081.

Jauhar S, Fortea L, Solanes A, Albajes-Eizagirre A, McKenna PJ, Radua J. 2021. Brain activations associated with anticipation and delivery of monetary reward: A systematic review and meta-analysis of fMRI studies. PLOS ONE. 16(8):e0255292. doi:10.1371/journal.pone.0255292.

Kamp J, Jonkman K, van Velzen M, Aarts L, Niesters M, Dahan A, Olofsen E. 2020. Pharmacokinetics of ketamine and its major metabolites norketamine,

hydroxynorketamine, and dehydronorketamine: a model-based analysis. Br J Anaesth. 125(5):750–761. doi:10.1016/j.bja.2020.06.067.

Knutson B, Adams CM, Fong GW, Hommer D. 2001. Anticipation of increasing monetary reward selectively recruits nucleus accumbens. J Neurosci. 21(16):RC159. doi:10.1523/JNEUROSCI.21-16-j0002.2001.

Knutson B, Greer SM. 2008. Anticipatory affect: neural correlates and consequences for choice. Philosophical Transactions of the Royal Society B: Biological Sciences. 363(1511):3771–3786. doi:10.1098/rstb.2008.0155.

Knutson B, Westdorp A, Kaiser E, Hommer D. 2000. FMRI Visualization of Brain Activity during a Monetary Incentive Delay Task. NeuroImage. 12(1):20–27. doi:10.1006/nimg.2000.0593.

Kotoula V, Stringaris A, Mackes N, Mazibuko N, Hawkins PCT, Furey M, Curran HV, Mehta MA. 2022. Ketamine Modulates the Neural Correlates of Reward Processing in Unmedicated Patients in Remission From Depression. Biological Psychiatry: Cognitive Neuroscience and Neuroimaging. 7(3):285–292. doi:10.1016/j.bpsc.2021.05.009.

Kwaśny A, Cubała WJ, Włodarczyk A. 2024. Anhedonia and depression severity measures during ketamine administration in treatment-resistant depression. Front Psychiatry. 15:1334293. doi:10.3389/fpsyt.2024.1334293.

Kwaśny A, Kwaśna J, Wilkowska A, Szarmach J, Słupski J, Włodarczyk A, Cubała WJ. 2024. Ketamine treatment for anhedonia in unipolar and bipolar depression: a systematic review. European Neuropsychopharmacology. 86:20–34. doi:10.1016/j.euroneuro.2024.04.014.

Lally N, Nugent AC, Luckenbaugh DA, Ameli R, Roiser JP, Zarate CA. 2014. Anti-anhedonic effect of ketamine and its neural correlates in treatment-resistant bipolar depression. Translational Psychiatry. 4(10):e469. doi:10.1038/tp.2014.105.

Lally N, Nugent AC, Luckenbaugh DA, Niciu MJ, Roiser JP, Zarate CA. 2015. Neural correlates of change in major depressive disorder anhedonia following open-label ketamine. J Psychopharmacol. 29(5):596–607. doi:10.1177/0269881114568041.

Li N, Lee B, Liu R-J, Banasr M, Dwyer JM, Iwata M, Li X-Y, Aghajanian G, Duman RS. 2010. mTOR-Dependent Synapse Formation Underlies the Rapid Antidepressant Effects of NMDA Antagonists. Science. 329(5994):959–964. doi:10.1126/science.1190287.

Lumsden EW, Troppoli TA, Myers SJ, Zanos P, Aracava Y, Kehr J, Lovett J, Kim S, Wang F-H, Schmidt S, et al. 2019. Antidepressant-relevant concentrations of the ketamine metabolite (2R,6R)-hydroxynorketamine do not block NMDA receptor function. Proceedings of the National Academy of Sciences. 116(11):5160–5169. doi:10.1073/pnas.1816071116.

Lutz K, Widmer M. 2014. What can the monetary incentive delay task tell us about the neural processing of reward and punishment? NAN. 3:33–45. doi:10.2147/NAN.S38864.

Ma S, Chen M, Jiang Y, Xiang X, Wang S, Wu Z, Li S, Cui Y, Wang J, Zhu Y, et al. 2023. Sustained antidepressant effect of ketamine through NMDAR trapping in the LHb. Nature. 622(7984):802–809. doi:10.1038/s41586-023-06624-1.

Menon V, Uddin LQ. 2010. Saliency, switching, attention and control: a network model of insula function. Brain Struct Funct. 214(5–6):655–667. doi:10.1007/s00429-010-0262-0.

Mion G, Villevieille T. 2013. Ketamine pharmacology: an update (pharmacodynamics and molecular aspects, recent findings). CNS Neurosci Ther. 19(6):370–380. doi:10.1111/cns.12099.

Mkrtchian A, Evans JW, Kraus C, Yuan P, Kadriu B, Nugent AC, Roiser JP, Zarate CA. 2021. Ketamine modulates fronto-striatal circuitry in depressed and healthy individuals. Mol Psychiatry. 26(7):3292–3301. doi:10.1038/s41380-020-00878-1.

Murrough JW, Iosifescu DV, Chang LC, Al Jurdi RK, Green CE, Perez AM, Iqbal S, Pillemer S, Foulkes A, Shah A, et al. 2013. Antidepressant efficacy of ketamine in treatment-resistant major depression: a two-site randomized controlled trial. Am J Psychiatry. 170(10):1134–1142. doi:10.1176/appi.ajp.2013.13030392.

Ng TH, Alloy LB, Smith DV. 2019. Meta-analysis of reward processing in major depressive disorder reveals distinct abnormalities within the reward circuit. Transl Psychiatry. 9(1):293. doi:10.1038/s41398-019-0644-x.

Nikolin S, Rodgers A, Schwaab A, Bahji A, Zarate C, Vazquez G, Loo C. 2023. Ketamine for the treatment of major depression: a systematic review and meta-analysis. EClinicalMedicine. 62:102127. doi:10.1016/j.eclinm.2023.102127.

Nogo D, Jasrai AK, Kim H, Nasri F, Ceban F, Lui LMW, Rosenblat JD, Vinberg M, Ho R, McIntyre RS. 2022. The effect of ketamine on anhedonia: improvements in dimensions of anticipatory, consummatory, and motivation-related reward

deficits. Psychopharmacology (Berl). 239(7):2011–2039. doi:10.1007/s00213-022-06105-9.

Nugent AC, Diazgranados N, Carlson PJ, Ibrahim L, Luckenbaugh DA, Brutsche N, Herscovitch P, Drevets WC, Zarate CA. 2014. Neural correlates of rapid antidepressant response to ketamine in bipolar disorder. Bipolar Disord. 16(2):119–128. doi:10.1111/bdi.12118.

Oldham S, Murawski C, Fornito A, Youssef G, Yücel M, Lorenzetti V. 2018. The anticipation and outcome phases of reward and loss processing: A neuroimaging meta-analysis of the monetary incentive delay task. Human Brain Mapping. 39(8):3398–3418. doi:10.1002/hbm.24184.

Patel AX, Bullmore ET. 2016. A wavelet-based estimator of the degrees of freedom in denoised fMRI time series for probabilistic testing of functional connectivity and brain graphs. NeuroImage. 142:14–26. doi:10.1016/j.neuroimage.2015.04.052.

Patel AX, Kundu P, Rubinov M, Jones PS, Vértes PE, Ersche KD, Suckling J, Bullmore ET. 2014. A wavelet method for modeling and despiking motion artifacts from resting-state fMRI time series. Neuroimage. 95(100):287–304. doi:10.1016/j.neuroimage.2014.03.012.

Peltoniemi MA, Hagelberg NM, Olkkola KT, Saari TI. 2016. Ketamine: A Review of Clinical Pharmacokinetics and Pharmacodynamics in Anesthesia and Pain Therapy. Clin Pharmacokinet. 55(9):1059–1077. doi:10.1007/s40262-016-0383-6.

Pizzagalli DA, Holmes AJ, Dillon DG, Goetz EL, Birk JL, Bogdan R, Dougherty DD, Iosifescu DV, Rauch SL, Fava M. 2009. Reduced caudate and nucleus accumbens response to rewards in unmedicated individuals with major depressive disorder. Am J Psychiatry. 166(6):702–710. doi:10.1176/appi.ajp.2008.08081201.

Pollak TA, De Simoni S, Barimani B, Zelaya FO, Stone JM, Mehta MA. 2015. Phenomenologically distinct psychotomimetic effects of ketamine are associated with cerebral blood flow changes in functionally relevant cerebral foci: a continuous arterial spin labelling study. Psychopharmacology (Berl). 232(24):4515–4524. doi:10.1007/s00213-015-4078-8.

Pulcu E, Guinea C, Cowen PJ, Murphy SE, Harmer CJ. 2022. A translational perspective on the anti-anhedonic effect of ketamine and its neural underpinnings. Mol Psychiatry. 27(1):81–87. doi:10.1038/s41380-021-01183-1.

Quibell R, Prommer EE, Mihalyo M, Twycross R, Wilcock A. 2011. Ketamine*. Journal of Pain and Symptom Management. 41(3):640–649. doi:10.1016/j.jpainsymman.2011.01.001.

Reed JL, Nugent AC, Furey ML, Szczepanik JE, Evans JW, Zarate CA. 2019. Effects of Ketamine on Brain Activity During Emotional Processing: Differential Findings in Depressed Versus Healthy Control Participants. Biological Psychiatry: Cognitive Neuroscience and Neuroimaging. 4(7):610–618. doi:10.1016/j.bpsc.2019.01.005.

Rolls ET, Huang C-C, Lin C-P, Feng J, Joliot M. 2020. Automated anatomical labelling atlas 3. NeuroImage. 206:116189. doi:10.1016/j.neuroimage.2019.116189.

Sałat K, Siwek A, Starowicz G, Librowski T, Nowak G, Drabik U, Gajdosz R, Popik P. 2015. Antidepressant-like effects of ketamine, norketamine and dehydronorketamine in forced swim test: Role of activity at NMDA receptor. Neuropharmacology. 99:301–307. doi:10.1016/j.neuropharm.2015.07.037.

Schultz W. 2016. Dopamine reward prediction-error signalling: a two-component response. Nat Rev Neurosci. 17(3):183–195. doi:10.1038/nrn.2015.26.

Schultz W, Dayan P, Montague PR. 1997. A neural substrate of prediction and reward. Science. 275(5306):1593–1599. doi:10.1126/science.275.5306.1593.

Seeley WW, Menon V, Schatzberg AF, Keller J, Glover GH, Kenna H, Reiss AL, Greicius MD. 2007. Dissociable Intrinsic Connectivity Networks for Salience Processing and Executive Control. J Neurosci. 27(9):2349–2356. doi:10.1523/JNEUROSCI.5587-06.2007.

Shin W, Koenig KA, Lowe MJ. 2022. A comprehensive investigation of physiologic noise modeling in resting state fMRI; time shifted cardiac noise in EPI and its removal without external physiologic signal measures. Neuroimage. 254:119136. doi:10.1016/j.neuroimage.2022.119136.

Smoski MJ, Felder J, Bizzell J, Green SR, Ernst M, Lynch TR, Dichter GS. 2009. fMRI of alterations in reward selection, anticipation, and feedback in major depressive disorder. J Affect Disord. 118(1–3):69–78. doi:10.1016/j.jad.2009.01.034.

Spijker J, Bijl RV, de Graaf R, Nolen WA. 2001. Determinants of poor 1-year outcome of DSM-III-R major depression in the general population: results of the Netherlands Mental Health Survey and Incidence Study (NEMESIS). Acta Psychiatr Scand. 103(2):122–130. doi:10.1034/j.1600-0447.2001.103002122.x.

Studerus E, Gamma A, Vollenweider FX. 2010. Psychometric Evaluation of the Altered States of Consciousness Rating Scale (OAV). PLoS One. 5(8):e12412. doi:10.1371/journal.pone.0012412.

Szczepanik JE, Reed JL, Nugent AC, Ballard ED, Evans JW, Lejuez CW, Zarate CA. 2019. Mapping anticipatory anhedonia: an fMRI study. Brain Imaging Behav. 13(6):1624–1634. doi:10.1007/s11682-019-00084-w.

Tashakkori M, Ford A, Dragovic M, Gabriel L, Waters F. 2021. The time course of psychotic symptom side effects of ketamine in the treatment of depressive disorders: a systematic review and meta-analysis. Australas Psychiatry. 29(1):80–87. doi:10.1177/1039856220961642.

Wilson RP, Colizzi M, Bossong MG, Allen P, Kempton M, Abe N, Barros-Loscertales AR, Bayer J, Beck A, Bjork J, et al. 2018. The Neural Substrate of Reward Anticipation in Health: A Meta-Analysis of fMRI Findings in the Monetary Incentive Delay Task. Neuropsychol Rev. 28(4):496–506. doi:10.1007/s11065-018-9385-5.

Winer ES, Nadorff MR, Ellis TE, Allen JG, Herrera S, Salem T. 2014. Anhedonia predicts suicidal ideation in a large psychiatric inpatient sample. Psychiatry Res. 218(1–2):124–128. doi:10.1016/j.psychres.2014.04.016.

Zanos P, Moaddel R, Morris PJ, Georgiou P, Fischell J, Elmer GI, Alkondon M, Yuan P, Pribut HJ, Singh NS, et al. 2016. NMDAR inhibition-independent antidepressant actions of ketamine metabolites. Nature. 533(7604):481–486. doi:10.1038/nature17998.

Zanos P, Thompson SM, Duman RS, Zarate CA, Gould TD. 2018. Convergent Mechanisms Underlying Rapid Antidepressant Action. CNS Drugs. 32(3):197–227. doi:10.1007/s40263-018-0492-x.

Zarate CA, Singh JB, Carlson PJ, Brutsche NE, Ameli R, Luckenbaugh DA, Charney DS, Manji HK. 2006. A randomized trial of an N-methyl-D-aspartate antagonist in treatment-resistant major depression. Arch Gen Psychiatry. 63(8):856–864. doi:10.1001/archpsyc.63.8.856.

Zhang W-N, Chang S-H, Guo L-Y, Zhang K-L, Wang J. 2013. The neural correlates of reward-related processing in major depressive disorder: a meta-analysis of functional magnetic resonance imaging studies. J Affect Disord. 151(2):531–539. doi:10.1016/j.jad.2013.06.039.

Hedonic Experiences and Multivariate Neural Information Processing

Study 4: **Kathofer, M.**, Mediano, P.A.M., Spies, M., Liardi, A., Dörl, G., Stöhrmann, P., Schmidt, C., Briem, E., Schlosser, G., Eggerstorfer, B., Klöbl, M., Leder, H., Lanzenberger, R., Crone, J.S. (2025). Hedonic experiences emerge from an orchestrated balance of synergistic and redundant information processing. bioRxiv, DOI: https://doi.org/10.1101/2025.10.05.680521

Submitted for publication: 18.12.2025

My contribution

As the main project of my PhD, I was deeply involved in every stage of this study. I designed the hedonic task used in this publication, coordinated participant recruitment, and served as the primary liaison with the clinic. My aim was to examine how multivariate neural information integration gives rise to subjective hedonic experience and how ketamine modulates these dynamics to facilitate its prohedonic effects. To acquire the necessary methodological expertise in advanced information theory, I spent one year at the Computational Department of Imperial College London as a Marietta Blau Fellow. There, I analyzed the data, and upon returning to Vienna, I drafted the manuscript.

Hedonic experiences emerge from an orchestrated balance of synergistic and redundant information processing

Kathofer M.[1,2], Mediano P.A.M.[3,4], Spies M.[5,6], Liardi A.[3], Dörl G.[5,6], Stöhrmann P.[5,6], Schmidt C.[5,6], Briem E.[5,6], Schlosser G.[5,6], Eggerstorfer B.[5,6], Klöbl M.[5,6], Leder H.[1,2], Lanzenberger R.[5,6], Crone J.S.[1]

[1]Vienna Cognitive Science Hub, University of Vienna, AUT
[2]Department of Cognition, Emotion, and Methods in Psychology, University of Vienna, AUT
[3]Department of Computing, Imperial College London, UK
[4]Division of Psychology and Language Sciences, University College London, UK
[5]Department of Psychiatry and Psychotherapy, Medical University of Vienna, AUT
[6]Comprehensive Center for Clinical Neurosciences and Mental Health (C3NMH), Medical University of Vienna, AUT

Abstract

Ketamine exerts rapid-acting, pro-hedonic effects, yet its precise mechanism remains elusive. Here, we present behavioral and fMRI data from a randomized, placebo-controlled crossover study in 38 healthy participants investigating ketamine's sub-acute effects on multivariate information-processing during music-evoked peak hedonic experiences. Leveraging information-theoretical measures, our findings indicate that hedonic experiences depend on a distinct global (as measured by O-Information) and local (as measured by integrated information) balance between redundant – information shared across nodes – and synergistic – information emerging from joint interactions – processes. As hedonic intensity rises, neural dynamics shift toward greater synergy; with the one exception of a deliberate increase in redundancy particularly for key sensory information to ensure reliable transmission of and access to critical external information for subsequent hedonic processing. In contrast, ketamine's sub-acute pro-hedonic effects arise potentially from enhancing redundant dynamics at rest, boosting the brain's capability to robustly represent and access critical internal information, and thus, fostering an environment optimized to amplify the phenomenological hedonic experience, while simultaneously allowing for more efficient information integration.

Introduction

The hedonic experience is a fundamental aspect of mental health, and its disruption, called anhedonia, is a core symptom of many psychiatric disorders, including depression, schizophrenia, and substance use disorder[1–3]. Addressing anhedonic symptoms specifically is critical for improving treatment outcomes[4–7] and offers the potential for more effective therapies, as emphasized by the National Institute of Mental Health (NIMH), which declares anhedonia as a key focus of its research domain criteria framework[8]. One particularly promising intervention for anhedonia is ketamine, which garnered significant attention for its rapid-acting pro-hedonic effects over the past decade[9]. Administered at a subanesthetic dose, ketamine alleviates depressive[10–12] and anhedonic[13,14] symptoms within hours. However, the neural

mechanisms underlying these effects remain elusive, as much of the existing research relies on post-hoc self-report questionnaires that fail to capture real-time changes in hedonic processing. Since the hedonic experience is thought to emerge from the orchestrated interplay of various cortical and subcortical regions[15–17,see 18 for a review], information theory, a framework that conceptualizes the brain as a multivariate information processing system, serves as a particularly powerful tool for studying these interactions. Thus, combining real-time assessments of hedonic processing with insights from information theory offers a promising avenue to deepen our understanding of the hedonic experience itself and illuminate how ketamine shapes neural dynamics to enhance hedonic experiences.

Higher-order information integration, arising from interactions that span more than two brain regions, is a key feature of brain function. Two complementary forms of integration – synergy and redundancy – offer valuable insights into these multivariate dynamics[19]. Synergy refers to information that emerges solely from the joint activity of multiple regions and cannot be found in any single region alone, thus facilitating more efficient information processing[20]. However, since it depends on the coordinated contribution of these regions, synergistic information is fragile and can be easily lost if even one contributing region is disrupted. In contrast, redundancy indicates information that is duplicated across regions, ensuring robust representation of critical information. Both synergy and redundancy play crucial roles in behavioral and cognitive task performance[21,22], with evidence suggesting that an optimal balance between the two is necessary for effective functioning. Together, they reflect a fundamental trade-off in the brain's integration strategies, balancing the adaptability of emergent information processing with the reliability of robust information representation.

Recent methodological advances have begun to make these higher-order interactions accessible to empirical investigation, each with their own distinct strengths and limitations[23–25]. One such approach, known as *information about organizational structure* (O-Information)[23], provides a simple way to assess whether the information within a large set of brain regions is dominated by redundancy (positive O-Information) or synergy (negative O-Information). While O-information does not explicitly separate these components, it summarizes their balance, providing insights into the dominant mode of multivariate interdependence in a system. On the other hand, *whole-minus-sum integrated information* (Φ^{WMS})[26] can be utilized to investigate how integrative hedonic processes evolve over time. More specifically, Φ^{WMS} examines how brain regions coevolve over time by assessing whether the joint activity of the regions (the "whole") is better at predicting their combined future than the individual regions (the "parts") are at predicting their own. While Φ^{WMS} provides crucial insights into integration dynamics, the recently developed integrated information decomposition (ΦID) framework[27] offers a more intuitive interpretation by allowing Φ^{WMS} to be decomposed into its two key components: Φ^{R} and redundancy (rtr) ($\Phi^{WMS} = \Phi^{R} - rtr$). Thereby, Φ^{R} represents a revised measure of integrated information[28], capturing all synergistic temporal processes as well as information that is transferred from one region to another. In contrast, rtr quantifies whether shared information between regions persists over time, reflecting redundant information storage across brain areas. Thus, positive Φ^{WMS} values indicate that synergistic and transfer processes dominate the temporal dynamics, while negative values suggest that redundant processes outweigh synergistic ones. By disentangling these components, ΦID offers a deeper understanding of the mechanisms driving temporal information integration during neural processing. Leveraging these complementary measures (O-Information, Φ^{WMS}, and its constituents, Φ^{R} and rtr) provides a unique opportunity to overcome the limitations of each measure individually, shedding light

on how distributed brain areas coordinate to give rise to the hedonic experience and how these processes may be modulated by interventions such as ketamine.

To do so, the present study recorded fMRI data during a hedonic task involving self-selected music, a potent and personalized stimulus capable of reliably inducing peak hedonic experiences[29–32]. While ketamine's effects are typically studied in clinical populations suffering from anhedonia, this study focused on a healthy population to minimize confounds such as comorbidities and prior treatment effects. This allowed us to probe the following 4 hypotheses regarding information dynamics underlying the emergence of a hedonic experience in general:

H1: We hypothesized that ketamine would exert measurable pro-hedonic effects in the healthy population.

H2: Given the inherently emergent nature of hedonic experiences – which rely on the integration of both external (e.g., sensory perception) and internal (e.g., cognitive and affective) information[32] – we hypothesized that hedonia arises from enhanced synergistic information integration. Specifically, we expected to observe shifts in both O-Information and Φ^{WMS} measures toward greater synergy during hedonic states.

H3: Furthermore, we hypothesized that ketamine would generally shift neural information dynamics toward greater synergistic integration, promoting a neural state more conducive to the emergence of intense hedonic experiences.

H4: Finally, because hedonic experiences depend on the sustained integration of internal and external inputs over time, we hypothesized that hedonic states would be characterized by a tendency to maintain a highly synergetic state over time.

Results

Ketamine increases hedonic response across multiple dimensions

To reliably induce a range of hedonic experiences in a more ecologically valid setting, we designed an individualized hedonic task (Figure 1A) using self-selected music – a dynamic, real-time stimulation known to elicit strong affective responses[29–32]. During this task, each participant (n = 38) rated their hedonic responses to 70-second excerpts of 10 songs they found highly pleasurable and 10 songs they deemed neutral (initial judgment) on three dimensions: valence (emotional value), moving (being emotionally moved), and chills (perceived chills). The task was performed during fMRI in two sessions: four hours after ketamine (0.5 mg/kg) and four hours after placebo (0.9% saline) administration (Figure 1B). Each session included eight interleaved 30-second baseline segments to evaluate ketamine's sub-acute effects on intrinsic neural dynamics at rest throughout the task.

Behavioral results confirmed successful hedonic manipulation across all tested dimensions: positive songs were considerably more likely than neutral songs to evoke strong responses in valence (Odds Ratio [OR] = 116.08, $p < 0.01$, Bonferroni-adjusted $\alpha = 0.016$), moving (OR = 219.68, $p < 0.01$), and chills (OR = 114.05, $p < 0.01$) (see Tables S1-S3). As hypothesized (H1), ketamine further enhanced hedonic responses across all three tested dimensions, increasing valence (OR = 1.36, $p < 0.01$), amplifying moving

(OR = 1.31, p < 0.01), and markedly enhancing chills (OR = 1.60, p < 0.01). Based on prior model comparisons, no interaction term between treatment (ketamine vs. placebo) and initial judgment (positive vs. neutral) was included in the mixed ordinal regression, suggesting that ketamine promotes a richer and more complex affective and physiological response regardless of the stimulus' initial emotional connotation.

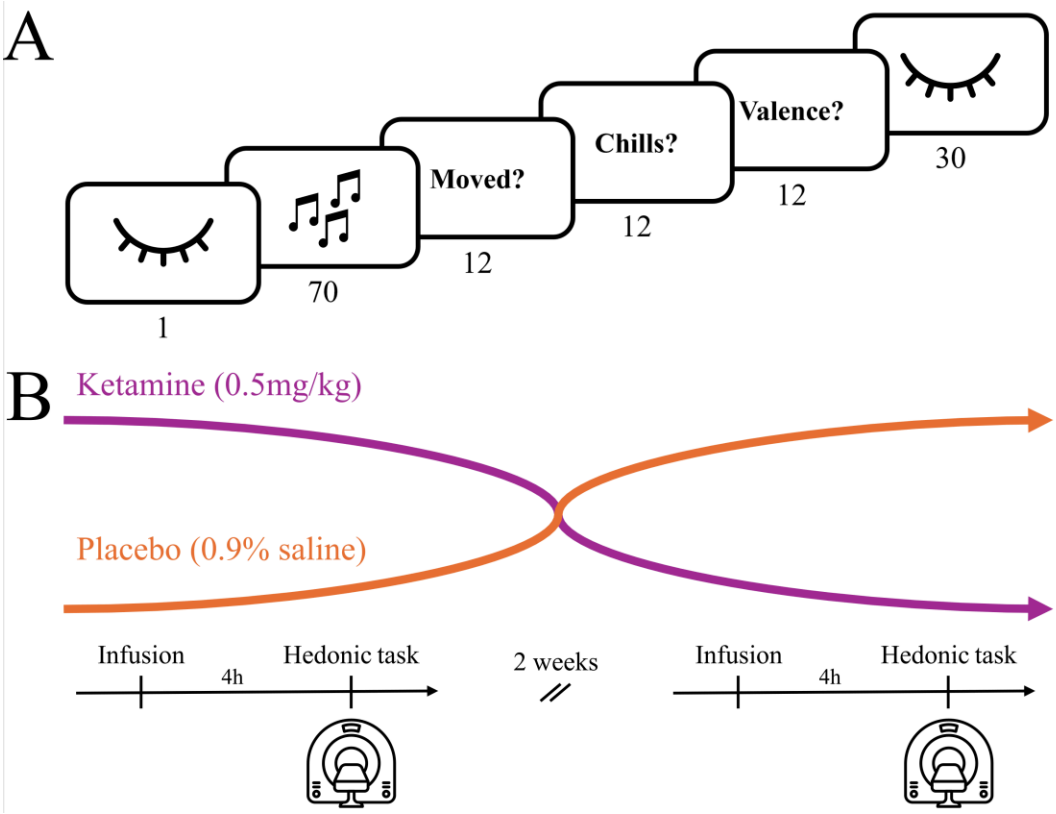

Figure 1. Hedonic task and study design.
(A) Example of one music trial during the hedonic task. With eyes closed, participants listened to a 70-second excerpt from either one of their self-selected 10 most pleasurable songs or 10 neutral songs. After each excerpt, they rated the quality of the evoked hedonic experience along three dimensions: moving, chills, and valence. The task was divided into two runs, each consisting of 9-12 music trials and four interleaved 30-second eyes-closed baseline (resting) segments. Numbers beneath pictograms indicate the duration of each section in seconds. (B) 38 healthy participants (18–55 years) completed a randomized, single-blind, placebo-controlled, cross-over study. Each underwent two fMRI sessions, separated by at least two weeks. Four hours before scanning, participants received either a placebo or 0.5 mg/kg racemic ketamine (40-min infusion), with arm allocation randomized. During each session, they performed the hedonic task.

Music perception and intense hedonic experiences shift global information processing toward synergy

Having established that ketamine does indeed increase all dimensions of the hedonic experience in healthy individuals, we turned to the question of whether hedonic experiences shift the global balance

in information integration toward synergy. To do so, preprocessed BOLD data (n = 32) was parcellated into 116 cortical[33] and subcortical[34] regions, and averaged O-Information values for each music trial and baseline segment were calculated, yielding one value per music trial and baseline segment per subject.

Importantly, our hypothesis (H2) is based on an implicit assumption: when engaging with a dynamical, sensory-rich stimulus such as music, the brain should already naturally shift toward more synergistic dynamics compared to rest, as it requires continuous integration across time. To test this, we fitted a linear mixed-effects model with the O-Information values of the music trial and baseline segments as dependent variables, including fixed-effects regressors for music perception (music vs. baseline), treatment (ketamine vs. placebo), and a random intercept for each participant. Three key findings emerged. First, the brain in its natural state exhibited a highly redundant organization during rest (O-Information = 32.26 nats; see Table S4). Second, during music processing, O-Information shifted significantly toward synergy compared to baseline (standardized beta (β_{stand}) = -0.11, SE = 0.04, t(1748) = -2.46, p = 0.01, Bonferroni-adjusted α = 0.025). Third, ketamine did not affect global information dynamics (β_{stand} = 0.02, SE = 0.04, t(1748) = 0.49, p = 0.62), which was further validated using exclusively the baseline segments (see Table S5).

To examine whether the intensity of subjective hedonic experiences during music stimulation was associated with changes in global neural dynamics, we fitted another linear mixed-effects model, including treatment (ketamine vs placebo) and hedonic intensity (moving rating) as predictors, with a random intercept for participants. Consistent with our hypothesis (H2), we found that more intense hedonic experiences were associated with a greater shift toward global synergistic processing (β_{stand} = -0.07, SE = 0.02, t(1230.9) = -3.02, p < 0.01) (see Table S6). Again, ketamine did not significantly alter global information dynamics during music perception (β_{stand} = 0.05, SE = 0.05, t(1222.2) = 1.10, p = 0.27), suggesting that despite global dynamics shifting in response to the phenomenological experience, the global dynamics during music processing remained unaffected by the neuromodulatory effects of ketamine.

Ketamine, at rest, induces widespread shifts toward redundancy, whereas the hedonic experience induces local shifts toward both synergy and redundancy.

While O-Information provides valuable insights into higher-order information dynamics of large-scale systems, it does not explicitly capture how past neural activity shapes future dynamics – a critical aspect of music-evoked hedonic processing[32]. To address this, we used Φ^{WMS}, a measure of dynamic information integration, to track changes in neural integration over time and identify central hubs involved in hedonic processing. Time-delayed mutual information terms were calculated for each run and then averaged within each trial window to produce mean Φ^{WMS} matrices[35], reflecting time-averaged information dynamics across all pairs of brain regions. To identify changes in neural processing associated with the subjective intensity of the hedonic experience, we analyzed shifts in Φ^{WMS} using a modified version of the network-based statistic (NBS) algorithm[36,37], capable of detecting clusters with both positive (synergy-increasing) and negative (redundancy-increasing) edges simultaneously.

A highly localized cluster (p_{fwer} < 0.01) associated with the main effect of the subjective hedonic experience was identified, comprising 109 positive (Φ^{WMS+}) and 68 negative (Φ^{WMS-}) edges (see hedonic cluster in Figure 2A). More specifically, interactions shifting toward greater synergy increased markedly

within and between the parietal lobe, frontal, and temporal regions, as the intensity of the hedonic experience grew. Strikingly, over one-third (38 of 109) of the synergy-increasing edges involved the insula, pointing to its central role as a hub of interoceptive integrative processing[38,39]. In contrast, a majority of the redundancy-increasing edges emerged between subcortical and frontal structures. The most prominent hub in this subnetwork was the globus pallidus, appearing in 19% of all redundancy-increasing edges. This subcortical region increased redundant, that is, stable interactions with a broad range of areas, including the nucleus accumbens, putamen, insula, and orbitofrontal cortex. Notably, as the hedonic experience intensified, joint information dynamics between the auditory cortex and regions such as the insula, prefrontal cortex, and thalamus, became increasingly redundant, suggesting a more stable relay of auditory content during stronger subjective experiences.

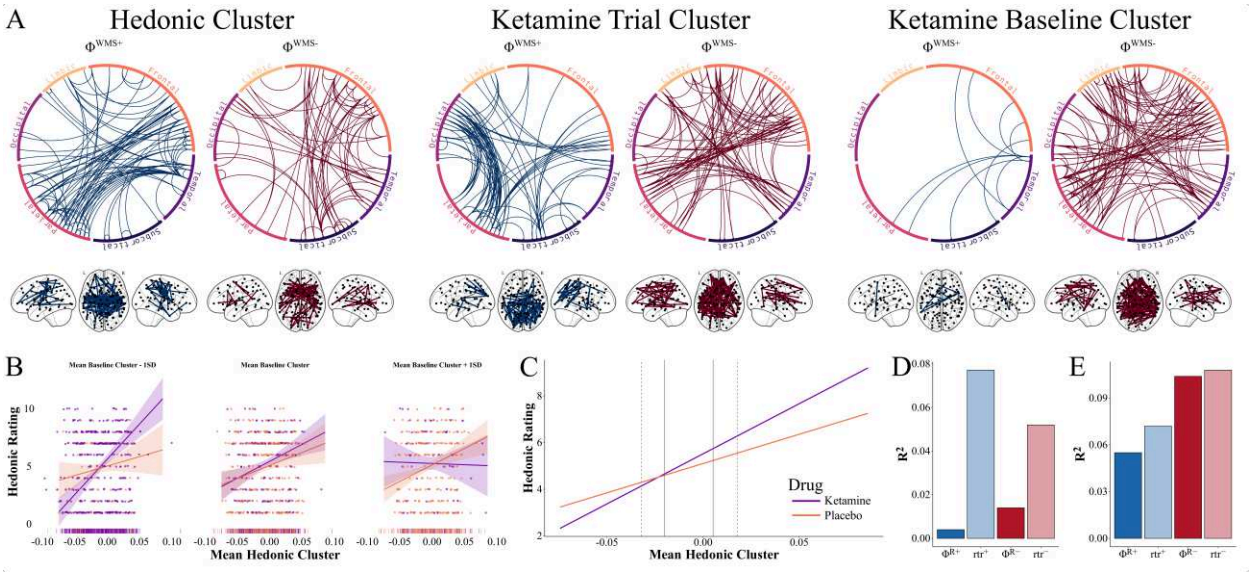

Figure 2: Hedonic experiences induce local shifts toward both synergy and redundancy

(A) Significant NBS clusters are displayed with increasing edges (Φ^{WMS+}) and decreasing edges (Φ^{WMS-}) for all pairs of regions separately. Edges are visualized both using a chord diagram (upper panel) and in a glass brain (lower panel) for each of the cluster solutions: the hedonic cluster, the ketamine trial cluster, and the ketamine baseline cluster. (B) The three panels illustrate the identified three-way interaction between treatment (ketamine vs placebo), the average activity of the hedonic cluster, and the average activity of the baseline ketamine cluster (both measured in nats) in predicting moving experiences. The interaction is visualized across ±1 standard deviation (SD) of the baseline ketamine cluster average. Below, carpet plots display the distribution of observations across baseline ketamine cluster values for each treatment. Due to sparse data at the extreme ends (i.e., low baseline values under placebo and high baseline values under ketamine), the confidence intervals of the inference lines are wider, complicating visual inference. (C) To address this, this panel presents a clearer visualization of the interaction: predicted values of moving experience are plotted across the full range of the hedonic cluster average, separately for two extracted levels of the baseline ketamine cluster (−1 SD under ketamine, +1 SD under placebo). Vertical solid grey lines indicate the ±1 SD range of the hedonic cluster values; dashed grey lines indicate the ±2 SD boundaries. (D) Dominance analysis for the hedonic cluster. Bars represent the average explained variance of each predictor. (E) Dominance analysis for the drug logistic model.

No significant interaction was observed between ketamine administration and moving ratings on neural integration. However, NBS recovered one significant cluster reflecting changes in information dynamics specifically attributed to the main effect of ketamine during music perception (79 positive edges; 92 negative edges; $p_{fwer} < 0.01$). This cluster was characterized by a marked shift toward greater redundancy (Φ^{WMS-}) between frontal and parietal regions, alongside a shift toward greater synergy (Φ^{WMS+}) between parietal and occipital areas (see ketamine trial cluster in Figure 2A). The most prominent hub for Φ^{WMS+} was the primary sensory cortex, involved in 34% of the synergy-increasing edges. In contrast, the most frequent hub associated with a shift toward greater redundancy (Φ^{WMS-}) was the right paracingulate cortex (14%).

Given that ketamine's pro-hedonic effects often persist for up to a week after administration and appear largely independent of the initial valence of the stimulus, enhancing a broad range of experiences, as supported by both prior literature[40–42] and our behavioral findings, we hypothesized that ketamine induces sustained changes in intrinsic neural dynamics that support its therapeutic action. Thus, testing ketamine's effects during music stimulation may be suboptimal for uncovering these mechanisms. Instead, we conjectured that alterations in the absence of stimulation, that is, during rest, should show a shift toward greater synergistic processing, and that these fundamental functional alterations may prime the brain to process subsequent stimuli in a way that enhances the hedonic experience (H3). To test this, we examined ketamine's effects on resting dynamics by applying the same NBS analysis to the mean Φ^{WMS} matrices from the interleaved baseline segments, thereby isolating information integration patterns independent of stimulation (music input). A single significant cluster with a prominent pattern emerged ($p_{fwer} < 0.01$); 93% of the edges following ketamine administration shifted toward greater redundancy (Φ^{WMS-}) with 122 negative and only 9 positive edges. This shift toward greater redundancy was most pronounced between frontal, parietal, and subcortical regions (see ketamine baseline cluster in Figure 2A).

Ketamine fundamentally reshapes associations between neural integration and subjective experience

Given these findings, we explored the idea that ketamine's pro-hedonic effects may stem from its ability to shift resting dynamics toward greater redundancy, enhancing the brain's ability to reliably access critical internal representations. Generally, hedonic experiences are shaped by the interplay of external sensory information, which becomes more robustly represented as the intensity of the experience increases, and internal cognitive processes, which provide the context and meaning for these experiences[43]. Ketamine's effects on resting dynamics may therefore enhance access to critical internal information, fostering a neural state that supports more intense hedonic experiences, even when identical integrative processes are triggered by identical incoming inputs. This, however, suggests a complex three-way interaction: while greater information integration within the hedonic cluster is generally linked to stronger subjective experiences, the strength of this relationship may depend on ketamine's effects on baseline neural dynamics.

To test this, we extracted averaged Φ^{WMS} values for each music trial (hedonic cluster) and baseline segment (baseline cluster) using edge masks derived from their respective NBS cluster results. A linear mixed model revealed the predicted significant three-way interaction between acute hedonic

integration, shifts in baseline integration, and treatment (β_{stand} = 0.17, SE = 0.05, t(1251.29) = 3.14, p < 0.01; Table S7), supporting the idea that ketamine's effects on baseline dynamics modulate the relationship between integration and subjective experience. In the placebo condition, the relationship between greater synergistic integration within the hedonic cluster and stronger hedonic experiences was unaffected by changes in the baseline cluster (Figure 2B). However, under ketamine, this relationship was significantly modulated: the ketamine-induced shift toward redundancy enhanced subjective experiences compared to placebo, even with similar levels of integration within the hedonic cluster. Figure 2C illustrates this effect more clearly, further showing that as subjective experiences intensify, the hedonic cluster shifts from redundancy-dominated to synergy-dominated activity.

Opposite patterns of synergy and redundancy shape ketamine-induced effects on the hedonic experience

In general, changes in Φ^{WMS} (e.g., shifts toward synergy) can arise through three mechanisms: (i) increased synergistic processing (higher Φ^{R}), (ii) reduced redundant processing (lower rtr), or (iii) a combination of both. To better understand the elementary dynamics driving these observed cluster effects, we used Integrated Information Decomposition[44] (ΦID) to decompose Φ^{WMS} into its two components: Φ^{R} (synergistic and transfer processes) and rtr (redundant processes).

Using the hedonic NBS cluster edge masks, we extracted and averaged edge values for each trial, separating Φ^{WMS}-increasing and Φ^{WMS}-decreasing edges. This resulted in four metrics per trial: Φ^{R+} and rtr^{+} (the decomposition of the Φ^{WMS}-increasing edges), Φ^{R-} and rtr^{-} (the decomposition of the Φ^{WMS}-decreasing edges). We then fitted a linear mixed-effects model with all four decomposed dynamics per trial (Φ^{R+}, rtr^{+}, Φ^{R-}, and rtr^{-}) predicting the intensity of the hedonic experience and conducted a dominance analysis (DA) to assess the relative importance of these metrics in predicting changes in hedonic intensity[45]. The linear model shows that all four predictors significantly influence the intensity of the phenomenological experience, highlighting that hedonic experiences arise from a dynamic interplay between redundancy and synergy, rather than being driven solely by synergy (see Table S8). Focusing on the results of the DA reveals that changes in redundancy (rtr) were far more predictive of the subjective intensity of the hedonic experience than changes in synergy (Φ^{R}) (see Table S9 and Figure 2D). This was particularly evident in the Φ^{R+} and rtr^{+} dynamics, for which decreases in redundancy were more strongly associated with changes in subjective hedonic experiences than increases in synergy. Thus, while both synergy and redundancy contribute to the emergence of hedonic experiences, the DA underscores that changes in redundancy play a considerably greater role in shaping these experiences.

Using a similar method, we investigated the dynamics underlying the nearly uniform decrease in Φ^{WMS} observed at rest after ketamine administration, which amplified the subjective hedonic experience. In this case, we fitted a logistic regression model with the four metrics (Φ^{R+}, rtr^{+}, Φ^{R-}, and rtr^{-}) to predict treatment. The model revealed that all four dynamics significantly predicted treatment (see Table S10). The DA highlighted that the Φ^{R-} and rtr^{-} metrics – associated with the majority of all significantly shifting edges after ketamine administration – jointly contributed to the overall shift toward redundancy (see Table S11 and Figure 2E). Both decreases in synergy and increases in redundancy were consistently highly predictive of treatment condition across all model subsets. A similar but weaker pattern was observed for the decomposed dynamics associated with increased Φ^{WMS} edges after ketamine.

The dynamic neural processing signature underlying peak hedonic experiences

Next, we investigated the temporal evolution of information dynamics underlying hedonic experiences, hypothesizing a universal structure (across treatment) driven by one of two patterns: (i) remaining in or frequently transitioning to Φ^{WMS+} states, or (ii) alternating between Φ^{WMS+} and Φ^{WMS-} states, allowing the brain to flexibly integrate (Φ^{WMS+}) and share redundant (Φ^{WMS-}) information to support hedonic experiences. To test this, we concatenated run-wise Φ^{WMS} parcel-by-parcel time courses across participants and clustered them using a Gaussian mixture model. The optimal model identified 9 clusters: 3 integrative states (exclusively Φ^{WMS+}), 3 redundant states (exclusively Φ^{WMS-}), and 3 intermixed states (a mix of Φ^{WMS+} and Φ^{WMS-}) (Figure 3A). From these brain state time series, we derived trial-wise transition matrices to quantify how often the brain transitioned between states. Finally, to explore the relationship between dynamic state switching and subjective experiences (that is, the moving experience, chills, and perceived valence), we utilized sparse canonical correlation analysis (CCA).

The analysis revealed a meaningful shared structure between the two data sets ($r = 0.21$, $p < 0.01$, see Figure 3B). On the behavioral side, all three measures (moving, chills, and valence) loaded positively onto the latent dimension, reflecting a unified positive hedonic experience (Figure 3C). On the neural side, the regularized CCA reduced 81 transition features to 19 non-zero loadings (Figure 3C). The strongest negative loading corresponded to remaining in state 9, a globally redundant state, while all other self-transitions were zeroed out, suggesting that sustained occupancy of any single state – especially a redundant one – is not conducive to the emergence of peak hedonic experiences. Instead, dynamic switching appears critical. The strongest positive loading reflected transitions from state 6 (integrative) to state 5 (redundant), highlighting a sequence where integration is followed by stabilization through redundancy. Other key transitions, such as between state 3 (redundant) and state 6 (integrative), further emphasize the importance of the dynamic interplay between integration and redundancy in shaping hedonic experiences.

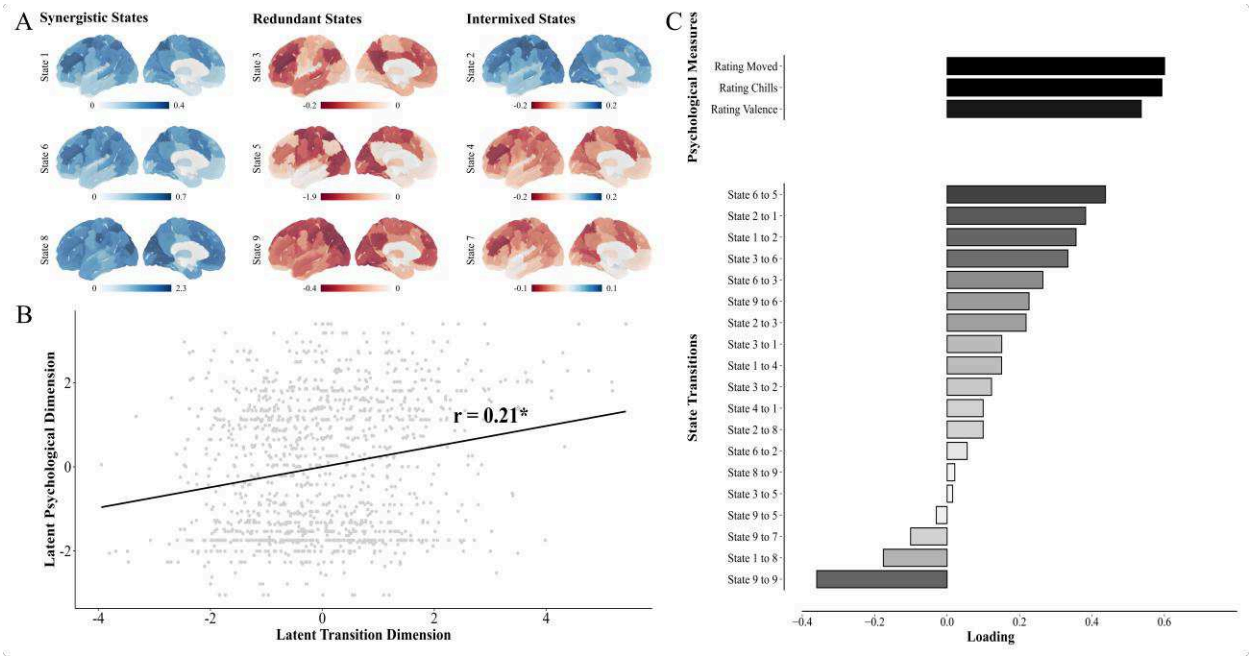

Figure 3. Hedonic experiences emerge from dynamic shifts between synergy and redundancy
(A) shows the clustering solution derived from the Gaussian Mixture Model applied to the recorded neural information dynamics across all participants (n = 32). Among the tested models (7 to 15 clusters), the optimal solution, based on the lowest BIC, was a 9-cluster model, revealing three distinct types of states: states characterized exclusively by increased synergy (left), those with increased redundancy (middle), and intermixed states (right). (B) presents the correlation between hedonic measures and state transitions within the recovered CCA latent space. (C) displays the canonical loadings from the Canonical Correlation Analysis (CCA) linking hedonic (psychological) measures and neural state transitions observed during the music trials. * indicates significance at $p < 0.01$.

The neurobiological mechanisms underlying changes in information integration

To elucidate the neurobiological mechanisms underlying the main interaction between ketamine-induced reductions in information integration at rest and the modulation of information integration during hedonic experiences, we examined the brain's neurotransmitter systems. Specifically, we assessed whether spatial patterns of neurotransmitter systems align with the dominant integration changes identified in the NBS analysis. As distinct neurotransmitter systems might differently contribute to both decreases and increases in information integration, we only focused on the dominant shift of information integration in each identified NBS cluster. For the hedonic cluster, where Φ^{WMS+} edges dominated, we averaged the positive NBS edge weights for each node to create region-wise maps reflecting shifts toward synergy (see Figure 4). Conversely, for the baseline cluster, which was primarily driven by Φ^{WMS-} edges, we averaged the negative edge weights for each node to capture region-wise shifts toward redundancy. These node-level maps, representing the dominant integration changes within each cluster, were compared to neurotransmitter and transporter density maps[46], including serotonin (5-HT1a, 5-HT1b, 5-HT2a, 5-HT4, 5-HT6, and 5-HTT), dopamine (D1, D2, and DAT), acetylcholine (M1, VAChT, and α4β2), glutamate (mGluR5 and NMDA), GABA (GABA), histamine (H3),

cannabinoid (CB1), opioid (MOR), and norepinephrine transporter (NET). In addition, we also conducted an exploratory analysis to identify neurotransmitter systems that might underlie the ketamine-induced effects during music perception which is reported in the supplementary material.

Our analysis revealed a significant association between NET density and Φ^{WMS} increases in the hedonic cluster ($r = 0.53$, $p < 0.01$), which survived Bonferroni correction for multiple comparisons ($p_{corrected} = 0.02$; see Figure 4). While for the ketamine-induced Φ^{WMS} reductions in the baseline cluster, we found no significant correlations with any receptor map.

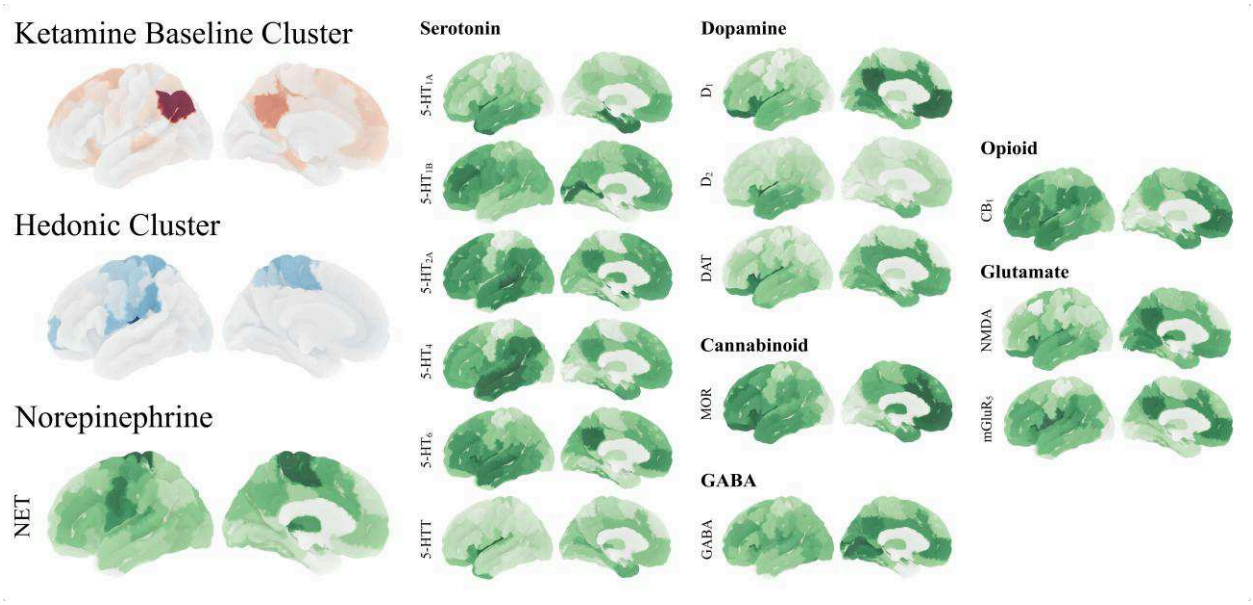

Figure 4. Synergistic hedonic integration is associated with norepinephrine transporter receptor density

Ketamine baseline cluster activity (in red) is shown by summing only the edges that increase in redundancy (Φ^{WMS-}). Hedonic cluster activity (in blue) is shown by summing only the edges that present a significant increase in synergistic interactions (Φ^{WMS+}). Neurotransmitter receptor and transporter density maps are depicted in green. For visual purposes, the significantly associated norepinephrine transporter density map is displayed alongside the hedonic cluster.

Discussion

While ketamine's therapeutic effects are well-documented, the mechanisms underlying its pro-hedonic effects remain poorly understood. To address this gap, we developed a novel paradigm using self-selected music as a dynamic and emotionally rich stimulus to elicit a range of hedonic responses and applied information theory to characterize the resulting shifts in multivariate neural information integration. This approach allowed us to track how hedonic experiences unfold over time and how they

are modulated by ketamine, providing a more nuanced understanding of both the hedonic experience and ketamine's role in shaping it.

Our behavioral findings in healthy participants extend previous clinical research by showing that ketamine enhances all facets of the hedonic experience – ranging from deep emotional engagement to strong physiological responses – regardless of the initial valence of the stimulus. This universal amplification, even in response to mundane stimuli (e.g., neutral music), may help explain ketamine's effectiveness in alleviating severe anhedonia in clinical populations that usually struggle to experience pleasure in their daily lives.

In the absence of external engagement, the brain's global organization (as measured by O-information) is predominantly characterized by redundancy confirming findings from previous studies[47,48]. Yet, engagement with a complex stimulus shifts this organization toward greater synergy, reducing redundancy. This shift becomes even more pronounced during intense music-evoked hedonic experiences, suggesting that hedonic processing relies on the synergistic interaction of many widely distributed cortical and subcortical areas. Reminiscent of the brain's underlying architecture for hedonic processes, these interactions are potent enough to reshape global information dynamics while preserving an overall redundant structure, reflecting a nuanced reconfiguration rather than a complete transformation of global neural dynamics.

So, are hedonic experiences the sole product of increases in synergistic processing, as initially hypothesized? Our findings suggest otherwise. Implementing Φ^{WMS} to analyze the temporal and spatial coevolution of more fine-grained information dynamics, we found that, in general, the pleasure response emerges from a localized balance between synergy and redundancy within a distinct hedonic cluster. Yet, as the hedonic experience intensifies, the overall balance does shift toward a synergy-dominated state, with the insular cortex emerging as a central hub, consistent with its established role in sensory integration[49]. However, primary auditory areas exhibit a different pattern, showing increased redundant coevolution with the insula, the thalamus, and the fusiform gyrus, a multisensory integration region involved in auditory emotion evaluation[50–52]. The observed redundancy ensures that auditory signals – the critical incoming information for the subsequently emerging hedonic experiences – are robustly transmitted to key relay and integration hubs. This pattern suggests that the brain prioritizes redundancy to safeguard the transmission of behaviorally critical information, making the information less error-prone and less susceptible to disruption for reliable and stable downstream processing. This interpretation aligns with neurobiological evidence in humans and animals, which underscores the role of redundancy in stabilizing essential sensory information[48,53–55] and enhancing subsequent behavioral responses[21,22,56,57]. For instance, studies in animals have shown that more redundant encoding of crucial sensory information improves subsequent performance in decision-making tasks[56], despite the higher energy cost of maintaining redundant neural representations. Our decomposition analysis further supports this notion, revealing that peak hedonic experiences are most robustly predicted by changes in redundant information processing (as measured by rtr). Considering the substantial energetic costs of sustaining a highly redundant system, minimizing unnecessary redundancy in large parts of the network is a logical means of reallocating resources more efficiently toward retaining crucial information that is indispensable for subsequent processing. This strategy is most evident in the synergy-increasing edges, which prominently reflect reductions in redundancy between the insula and primary sensory and motor cortices, with the notable exception of the auditory cortex. In addition, the topology of these changes in higher-order dynamics was associated with the distribution of norepinephrine transporter receptors, offering a neurobiologically plausible link between the emergence of a hedonic experience and

norepinephrine[58], a well-known neurotransmitter involved in modulating arousal, motivation, and euphoria, and dopamine[59], an important neurotransmitter of the reward system

While changes in redundancy are clearly crucial for the emergence of hedonic experiences, the interplay with synergy is equally important[54,60], as demonstrated by our computational model. Peak hedonic experiences do not arise from prolonged occupancy of either redundancy or synergy-dominated states, but from dynamic transitions between the two. Synergy-dominated states enable efficient higher-order processing of complex information, while redundancy-dominated states stabilize and maintain these representations over time. This continuous alternation between synergistic integration and redundant stability may represent a general neural mechanism for balancing flexibility and reliability in ongoing experiences: redundancy ensures stable and reliable information access, while synergy allows the system to encode more information than the sum of its individual parts.

How does ketamine now facilitate its pro-hedonic effects? Various theories propose mechanisms such as changes in neurotransmitter systems[61], relaxation of top-down control[62], or neuroplasticity through synaptogenesis[63], but they all converge on a common principle: ketamine must fundamentally alter neural information dynamics to create a state more conducive to the emergence of hedonic experiences. The key question, then, is how these effects are facilitated over the therapeutic timeframe. Are they driven by radical, global shifts in neural dynamics, or by more targeted, localized changes in information processing? While previous studies have shown that ketamine can indeed induce powerful global changes in information dynamics[64], our results indicate that these effects are limited to the acute phase, and thus, are unlikely to underlie its long-term pro-hedonic effects. Although ketamine showed lingering sub-acute effects on localized information dynamics, it did not enhance local information integration directly linked to the strength of the subjective experience during stimulus processing, as no interaction effect between intensity of the experience and treatment was found. Instead, our findings point to a more foundational mechanism: ketamine induces subtle, subacute shifts in resting dynamics, (almost) uniformly shifting information dynamics toward greater redundancy across its network. Interestingly, the greater this shift toward redundancy, the stronger hedonic experiences became in response to the same level of hedonic integration. This shift appeared to result from both increases in redundancy but also decreases in synergy, with both equally predictive of the intensity of the phenomenological experience. Just as encoding critical *external* information more redundantly benefits subsequent (hedonic) processes, ketamine-induced redundant dynamics at rest may similarly enhance the brain's ability to reliably relay and represent critical *internal* information, which in turn supports the emergence of stronger hedonic experiences. This aligns with the idea that hedonic experiences are shaped by both the properties of external stimulation and internal cognitive processes. As basic research has shown, the intensity of a hedonic experience significantly increases when the stimulus is embedded in a rich context with a wide range of knowledge-related or personal associations[65,66]. Robust and widespread access to this internal information is therefore crucial. Ketamine's long-term pro-hedonic effects likely stem from its ability to enhance the reliable representation of (critical) internal information, creating a neural environment optimized for subsequent hedonic processing.

As it is the case for all studies, our work is not without limitations. First, instead of using a classical resting-state scan that is recorded for multiple minutes and detached from the task, we employed interleaved resting periods throughout the task. Although unconventional, these interwoven periods, with eyes closed and no task instructions, were necessary to better link changes in default information dynamics to increased subjective experiences during task engagement. Notably, there is already some prior evidence showing that ketamine increases redundancy in resting-state dynamics[67,68], providing additional support for our hypothesis. Second, while the use of self-selected music may have introduced variability across participants, it was crucial for eliciting strong hedonic experiences tailored to the

individual. Nonetheless, our within-subject design, combined with linear mixed models, ensured robust and reliable results despite this variability. Finally, our conjecture that ketamine's pro-hedonic effects arise from its impact on intrinsic dynamics at rest, enhancing access to internal information, can be easily tested in future studies by examining whether these effects diminish as redundancy returns to baseline and whether this improved access to internal information enhances performance in other tasks as well for which widespread information access is equally essential.

Collectively, our data reveals that hedonic experiences arise from a nuanced interplay between synergistic and redundant information processes. By increasing a redundancy-dominated organization at rest, ketamine facilitates an optimized infrastructure by inducing stable and widespread communication of information. Once external information enters the system, resources can be flexibly reallocated to process critical information from anywhere in the brain, stabilizing higher-order integrative dynamics[69] essential for the hedonic experience, and thus, maximizing the behavioral readout. As a result, even modest increases in information integration during music perception produce disproportionately strong hedonic experiences. Thus, ketamine's pro-hedonic effects likely stem from its ability to boost the brain's capacity to reliably represent critical internal information, fostering a neural environment more conducive to the emergence of hedonic experiences.

Acknowledgements

The authors extend their heartfelt gratitude to the students, medical professionals, and technicians whose contributions were essential to the successful implementation of this study. This work would not have been possible without the collaborative efforts of the Vienna Cognitive Science Hub and the Advanced Neuroimaging Lab.

Funding

This study was partly funded by the Research Cluster 'Unraveling the aesthetic mind in anhedonia: Insights from pharmacological imaging of the human brain' between the Medical University of Vienna and the University of Vienna [grant number: SO68900012]. This research was also funded in whole or in part by the Austrian Science Fund (FWF) 10.55776/CM11 as well as the BMBWF and OeAD-GmbH [grant number: MMC-2023-06988]. G. Dörl is a recipient of a DOC Fellowship of the Austrian Academy of Sciences at the Department of Psychiatry and Psychotherapy, Medical University of Vienna. E. Briem and G. Schlosser have been supported by the MD, PhD Excellence Program of the Medical University of Vienna.

Declaration of interests

R. Lanzenberger received investigator-initiated research funding from Siemens Healthcare regarding clinical research using PET/MR and travel grants and/or conference speaker honoraria from Janssen-Cilag Pharma GmbH in 2023, and Bruker BioSpin, Shire, AstraZeneca, Lundbeck A/S, Dr. Willmar Schwabe GmbH, Orphan Pharmaceuticals AG, Janssen-Cilag Pharma GmbH, Heel and Roche Austria GmbH., and Janssen-Cilag Pharma GmbH in the years before 2020. He is a shareholder of the company BM Health GmbH, Austria since 2019. M. Spies has received travel grants from AOP Orphan Pharmaceuticals, Janssen, and Austroplant, speaker honoraria from Janssen and Austroplant, and

workshop participation from Eli Lilly. C. Schmidt has received a travel grant from Eli Lilly to attend a scientific exchange meeting. All other authors declare no potential conflicts of interest with respect to the research, authorship, and/or publication of this article.

Methods:

Study design

This randomized, single-blind, cross-over, placebo-controlled study enrolled 40 healthy participants between the age of 18 and 55. Physical health was assessed through medical examinations including electrocardiogram, blood, urine, pregnancy, and drug tests, while mental health was evaluated using the Structured Clinical Interview[70]. Exclusion criteria included history of neurological and psychiatric disorders, any current pharmacological treatment, pregnancy, breastfeeding, current or former substance abuse and prior experience with ketamine (in context of recreational or therapeutic use). Participants underwent two functional magnetic resonance imaging (fMRI) sessions, separated by at least two weeks to avoid cross-over effects (see Figure 1B). Four hours prior to each scanning session, participants received either a saline solution (0.9% NaCl) or 0.5mg/kg of racemic ketamine diluted in 0.9% NaCl, administered over 40 minutes. Participants performed a hedonic music task during each scan session (see Hedonic Task). Two scanner malfunctions occurred after drug administration was finished, preventing data collection of two participants. These participants were excluded from the study, resulting in a dataset of N = 38 participants. The study was approved by the ethics committee of the Medical University of Vienna (EK 1572/2021).

Hedonic task

Prior to study inclusion, participants provided 10 self-selected highly positive (moving) songs and 10 self-selected neutral songs, indicating the exact moment in which the hedonic experience peaked during each positive song. Self-selection was used to account for individual variability in emotional responses to music[71], as the focus was on eliciting robust hedonic experiences rather than controlling for music type. Note, neutral songs were included to determine whether ketamine broadly amplifies hedonic responses, regardless of their initial valence, or whether it enhances the hedonic experience only for stimuli already perceived as enjoyable. Participants were given detailed definitions of the concept of moving and chills to minimize semantic misunderstandings. Using ffmpeg[72], 70-second excerpts were created around the individually defined peak moment for positive songs, while random intervals were selected for neutral songs. All excerpts were sampled at 44,100 Hz, volume-normalized, and edited with 2-second fade-ins and fade-outs to ensure smooth transitions.

Before scanning, participants reviewed task instructions, passed comprehension checks, and completed a sound test using Mozart's "Eine kleine Nachtmusik" to optimize music volume in relation to scanner noise. The hedonic task was divided into two runs, each consisting of three blocks alternating between neutral and positive songs, with the starting condition and block size sequence randomized across participants. Positive and neutral songs were randomly assigned to two blocks of three songs and one block of four songs each. Each music trial began with a one-second pictogram of a closed eye, signaling participants to close their eyes for the upcoming trial (see Figure 1A). After listening to each excerpt,

participants had 12 seconds to rate their hedonic experience on three different dimensions: a) moving—how moving the experience was on a scale of 1 to 10; b) chills—whether a chill was induced and how intense the chill was on a scale of 1 (no chill at all) to 10 (utmost chilling experience); and valence—how unpleasurable/pleasurable the experience was on a scale of -5 to 5. To mitigate ceiling effects, they were instructed to compare their experiences to past events that were most moving, chill-inducing, or pleasurable/unpleasurable. While valence reflects the general positivity or negativity of the experience, the neuroaesthetic concept of moving captures deep emotional engagement, which may or may not lead to strong physiological responses such as chills[73,74]. Thirty-second baseline (resting) segments with eyes closed were included before and after each block.

MRI data acquisition

Scan sessions were performed roughly 4 hours after drug administration on a 3 Tesla Siemens MAGNETOM Prisma scanner at the Department of Biomedical Imaging and Image-guided Therapy at the Medical University of Vienna. Structural T1-weighted MRI scans were acquired with a multi-echo MPRAGE sequence (TR = 2400ms, TE = 2.22ms, voxel size 0.8×0.8×0.8mm, anterior-posterior face encoding, field of view read: 256mm). Functional data acquisition used a 64-channel head coil with a multiband 4 sequence for the hedonic task (TR = 800ms, TE = 30ms, voxel size 3×3×3mm, posterior-anterior phase-encoding direction, field of view read: 210mm). To aid distortion correction, short sequences in reversed encoding directions were recorded before each task run.

Behavioral analyses

To assess whether ketamine merely affects the hedonic tone (valence) or also influences deeper affective (moving) and physiological experiences (chills), three independent hierarchical ordinal regressions with a logit link function were conducted using the ordinal package[75] in R (n = 38). Consistent with Bürkner & Vuorre's[76] recommendations, we evaluated potential models based on different combinations of regressors (treatment, initial judgement, order of administration, and sex) and hierarchical effects. Comparisons were made based on the Bayesian Information Criteria (BIC) calculated with the performance package[77]. The winning model included a regressor for treatment (ketamine vs placebo), a regressor for the initial judgement (indicating whether the song was originally selected as neutral or positive), and a random effect for each participant (subject), accounting for the nestedness of the data. Notably, the winning model did not contain an interaction term between treatment and initial judgement. We fit a separate model for each of the three hedonic dimensions: moving, chills, and valence (see Hedonic Task). All model assumptions were visually inspected using the performance package[77]. To account for multiple comparisons, a Bonferroni correction was applied, adjusting the alpha significance level to 0.016.

$$hedonic\_experience\ (moving, chills, or\ valence) \sim treatment + initial\_judgement + (1|subject)$$

MRI data preprocessing

Structural and functional imaging data were preprocessed using fMRIprep[78,79] with default parameters. The structural preprocessing pipeline included intensity non-uniformity correction using N4BiasFieldCorrection[80], brain tissue segmentation, and non-linear spatial normalization to MNI 2mm standard space using ANTS[81]. The MNI template was obtained through TemplateFlow[82].

The functional preprocessing pipeline consisted of slice-timing correction, motion correction using MCFLIRT[83], and B0 inhomogeneity correction using fieldmaps derived from runs with reversed encoding directions processed via TOPUP[84]. Functional data was co-registered to the T1-weighted image using bbregister[85] and high-pass filtered with discrete cosine filters (128-second cut-off). Additional noise reduction was performed using aCompCor[86]. After high-pass filtering, principal components were calculated separately for white matter (WM) and cerebrospinal fluid (CSF) masks. The top five components from each mask, along with 24 motion parameters (six motion parameters, their quadratic terms, their first and second order derivatives), were regressed out using Nipype[87].

Quality control criteria excluded datasets with a mean framewise displacement (FD) exceeding 0.2 mm, more than 20% outlier volumes, or a maximum FD greater than 5 mm[88]. Based on these thresholds, six participants were excluded resulting in a final sample size for the fMRI data analyses of 32 participants. Functional data was parcellated into 116 regions using an atlas combining both the cortical Schaefer100[33] and the subcortical Tian16[34] parcellations.

O-Information analysis

The O-Information (also denoted as Ω) is a scalable measure to assess the interactions of a set of random variables[23]. Although it cannot disentangle separate contributions of synergy and redundancy, the O-Information captures the balance between the two: a system with $\Omega > 0$ is characterized by information being shared across the system and is redundancy-dominated, and a system with $\Omega < 0$ contains irreducible higher-order interactions and is synergy-dominated. Formally, Ω is derived from two generalized measures of mutual information: the total correlation (TC)[89], which quantifies the collective constraints among a set of variables, and the dual total correlation (DTC)[90], which assesses shared randomness across these variables. For a system of *n* random variables $X^n = \{X_1, \ldots, X_n\}$, these measures are defined as:

$$TC(X^n) = \sum_{j=1}^{n} H(X_j) - H(X^n)$$

$$DTC(X^n) = H(X^n) - \sum_{j=1}^{n} H(X_j | X^n_{-j})$$

$$\Omega(X^n) = TC(X^n) - DTC(X^n)$$

Here, $H(X^n)$ is the joint Shannon entropy of the *n*-plet, $H(X_j)$ is the entropy of the *j*-th variable, and $H(X_j | X^n_{-j})$ is the conditional entropy of the *j*-th variable given the rest of the system.

To assess whether peak hedonic experiences modulate global neural information dynamics, we calculated O-Information for the 116-plet containing all brain regions simultaneously. Cleaned, parcellated BOLD data were concatenated across runs and participants and analyzed using the Gaussian copula solver from the JIDT toolbox[91]. This method provided localized O-Information values over time, capturing the balance between redundancy and synergy in neural activity. To account for the hemodynamic lag, O-Information values were extracted for each music trial and baseline segment by shifting the extraction window by 4 TRs. These values were then averaged within each extracted period to yield a single mean O-Information value for each music trial and baseline segment.

To explore the impact of music perception and subjective experiences on global neural processing, we fitted two linear mixed-effects models (n = 32) using the lme4 package[92]. The first model tested the effects of the regressors music perception (music vs baseline) and treatment (ketamine vs placebo) on O-Information, with participants included as a random effect. This model tested the implicit assumption that the engagement with a complex stimulus such as music would shift global neural dynamics toward greater synergy compared to rest.To account for multiple comparisons, a Bonferroni correction was applied, adjusting the alpha significance level to 0.025.

$$\Omega \sim \text{music\_perception} + \text{treatment} + (1|\text{subject})$$

The second model examined how the strength of the hedonic experience – using the moving rating as our main measure, given its role as a deep positive emotional response – and treatment (ketamine vs placebo) influenced O-Information, with participants again included as a random effect to account for the nestedness of the data.

$$\Omega \sim \text{hedonic\_experience} + \text{treatment} + (1|\text{subject})$$

All model assumptions were visually inspected using the performance package[77].

Calculation and decomposition of Φ^{WMS} time courses

At its core, mutual information quantifies the interdependence of two variables X and Y. Specifically, mutual information I(X;Y) quantifies the amount of information that the knowledge of node X provides about node Y. Recently, mutual information was extended to systems of three or more variables using Partial Information Decomposition[93]. In this higher order case, PID decomposes the mutual information I(X,Y;Z) which the two source nodes X and Y provide in respect to a third target node Z into three distinct types of information. Information is considered *unique* (uni) if it is only provided by one of the sources but not the other, whereas *redundant* (red) information denotes information shared by both sources. Lastly, *synergistic* (syn) information arises from the joint interaction of both nodes and cannot be reduced to any node individually.

$$I(X,Y;Z) = red(X,Y;Z) + uni(X;Z|Y) + uni(Y;Z|X) + syn(X,Y;Z)$$

ΦID[27] further extends PID by decomposing time-delayed mutual information (TDMI), both in the past (t_{-1}) and in the future (t). For a pair of nodes, ΦID thus captures how information dynamics evolve over time, considering both the past and present state of the nodes $I(X_{t-1},Y_{t-1};X_t,Y_t)$. In practice, this requires constructing a linear system of 15 equations with 16 unknowns, linking the standard Shannon mutual information to the redundant, unique, and synergistic components of TDMI. To be able to solve this set

of equations, we utilized the widely used minimum mutual information[94] (MMI) definition of redundancy:

$$rtr(X,Y) = \min\{I(X_{t-1};X_t); I(X_{t-1};Y_t); I(Y_{t-1};X_t); I(Y_{t-1};Y_t)\}$$

This temporal decomposition produces 16 distinct information atom time courses, capturing how information is transferred between nodes over time. For example, the atom rtr represents information that was shared by two sources in the past and remains shared in the future. Recent work[95] has shown that *whole-minus-sum integrated information* (Φ^{WMS}) can be expressed as the difference between a specific set of atoms

$$\Phi^{WMS} = \Phi^{R} - rtr$$

Where:

$$\Phi^{R} = rts + xts + yts + sts + stx + sty + str + xty + yts$$

Here, we use the standard shorthand notation for the atoms introduced in prior work[95], e.g. xts represents the atom describing how unique information from the source node X becomes synergistic over time.

For each run, preprocessed and parcellated BOLD data from all pairwise combinations of brain regions was fully decomposed using ΦID, yielding the time courses of all 16 atoms for each pair of regions. We then constructed Φ^{R} and Φ^{WMS} time courses by summing the relevant atoms. Notably, while Φ^{R} requires defining a redundancy function (here, MMI), Φ^{WMS} does not, as it is fully determined by the TDMI. However, we calculated it through the atoms for convenience. The analysis was performed using scripts provided by Luppi et al.[44] and the Gaussian estimator from the JIDT toolbox[91].

Network-Based Statistic (NBS) analysis

To explore how the intensity of the hedonic experience and ketamine influence local neural information integration, we analyzed Φ^{WMS} time courses from music trial and baseline segments, adjusting for the hemodynamic lag by shifting the time series by three time points. Note, the time series was shifted by only 3 TRs because the Φ^{WMS} calculation inherently accounts for how information flows from one time step to the next, resulting in a time series that is already effectively shifted by 1 TR compared to the underlying BOLD signal. These time courses were averaged within each segment to create node-by-node Φ^{WMS} matrices for each condition.

We used a modified version of the Network-Based Statistic (NBS) algorithm[96], based on linear mixed-effects models, which accounts for subject variability, unbalanced designs, and allows the simultaneous inclusion of both positive and negative edges within a single cluster. Briefly, NBS fits a linear model to each connection (edge) and identifies those exceeding a predefined statistical threshold. It then checks whether these significant edges form connected networks through shared nodes. The significance of each network cluster is determined using permutation testing, which corrects for multiple comparisons at the network level.

To examine how hedonic intensity and ketamine influence local information integration during music perception, we fitted a linear mixed-effects model to each connection with the Φ^{WMS} values of the music

trial as the dependent variable, including regressors for treatment (ketamine vs placebo), the hedonic experience (the intensity of the moving experience), their interaction, and a random effect for each participant. Note, the cluster linked to the main effect of hedonic experience is termed the *hedonic cluster*, and the one linked to the main effect of treatment during music perception is referred to as the *ketamine trial cluster*.

$$\Phi^{WMS} \sim \text{treatment} * \text{hedonic\_experience} + (1|\text{subject})$$

To investigate the effects of ketamine independent of music stimulation, we applied a separate linear mixed-effects model to the baseline (resting) segments. This model included a fixed effect for treatment (ketamine vs placebo) and a random effect for participants. The cluster associated with the main effect of treatment during the baseline segments is referred to as the *ketamine baseline cluster* or just *baseline cluster*.

$$\Phi^{WMS} \sim \text{treatment} + (1|\text{subject})$$

In our analysis (n = 32), we used 5,000 permutations and set the threshold to reflect a medium effect size (Cohen's d = 0.5), corresponding to a t-value of 2.8. We used the intensity of each cluster, that is, the sum of t-statistics across connected edges, as the primary statistic for significance testing. Importantly, the results remained consistent when using extent, that is, the number of edges in the cluster, supporting the robustness of our findings regardless of the specific NBS metric.

Linking baseline and hedonic cluster activity to the intensity of the hedonic experience

We next considered whether ketamine's pro-hedonic effects could arise from its ability to shift intrinsic dynamics at rest greater redundancy, thereby enhancing the brain's capacity to reliably access key internal representations. Specifically, we examined whether persistent, ketamine-induced changes in baseline neural integration (ketamine baseline cluster) modulate the relationship between experience-evoked changes in information integration (hedonic cluster) and the phenomenological experience.

For each music trial, we extracted and averaged Φ^{WMS} edge values associated with the hedonic cluster, resulting in a single integration score per trial (avg_hedonic_cluster). Likewise, for each interleaved baseline segment, we extracted edge values from the ketamine baseline cluster and aggregated them into a single baseline integration score per run (avg_ketamine_baseline_cluster). This baseline score reflects persistent drug-induced changes in information integration at rest, independent of music stimulation.

To test whether the activity of these two clusters jointly predicts hedonic responses, we fitted a linear mixed-effects model with the reported hedonic experience (here, the intensity of the moving experience) as the dependent variable. The model (n = 32) included the average hedonic cluster activity per trial, the average change in baseline cluster activity, treatment (ketamine vs placebo), and their three-way interaction as fixed effects, with a random intercept per participant.

$$hedonic\_experience \sim avg\_hedonic\_cluster * avg\_ketamine\_baseline\_cluster * treatment + (1|subejct)$$

To assess statistical significance, we conducted 10,000 wild bootstrap iterations using the lmersampler[97] package in R, which accounts for the hierarchical structure in our data.

Dominance analysis (DA)

To investigate the underlying dynamics driving changes in Φ^{WMS}, we performed a dominance analysis. First, we created separate edge masks for the increasing and decreasing Φ^{WMS} edges identified in the NBS analysis for both the hedonic cluster and the ketamine baseline cluster. We then extracted and averaged the edge values for each trial and baseline segment from the decomposed time series (Φ^{R} and rtr), resulting in four metrics per trial/segment: Φ^{R+} and rtr^{+} (representing the decomposition of Φ^{WMS}-increasing edges) and Φ^{R-} and rtr^{-} (representing the decomposition of Φ^{WMS}-decreasing edges).

Next, we fitted a linear mixed-effects model to predict the intensity of hedonic experiences (here, moving ratings) using these four trial-averaged dynamics, with a random intercept for each participant:

$$hedonic\_experience = \Phi^{R+} + rtr^{+} + \Phi^{R-} + rtr^{-} + (1|subject)$$

The model results were corrected using cluster-robust covariance matrices (CR1) via the sjPlot package[98]. To further assess the relative importance of each dynamic, we conducted a bootstrap dominance analysis with 1,000 iterations of the model parameters using the dominanceanalysis package in R[99].

Similarly, we fitted a generalized linear model (GLM) with a logit link function to predict treatment assignment based on the four dynamics from the baseline segments and conducted a dominance analysis of the model parameters. An earlier version of this model included a random intercept for participants, but it was removed after determining that the random intercept was singular (close to zero) and unnecessary.

$$treatment = \Phi^{R+} + rtr^{+} + \Phi^{R-} + rtr^{-}$$

Association with neurotransmitter density maps

To investigate whether spatial patterns of neurotransmitter receptor and transporter densities align with the ketamine-induced reductions in information integration at rest and the modulation of information integration during hedonic experiences, we conducted a spatial correlation analysis. Since different neurotransmitter systems may uniquely affect increases and decreases in information integration, we concentrated on the dominant shift in each identified NBS cluster. As both NBS-identified clusters contained a mix of positively and negatively weighted edges, we first computed the net effect within each cluster by subtracting the average weight of negative edges from that of positive edges. This allowed us to determine the dominant direction of change in the cluster. The hedonic cluster during music perception was dominated by Φ^{WMS+} edges, whereas the ketamine cluster during the baseline segments was almost exclusively comprised of Φ^{WMS-} edges. As expected, in both cases, the number of edges in the dominant direction also exceeded those in the opposite direction. We did this based on the reasoning that different neurotransmitter systems may underlie increases versus decreases in Φ^{WMS}, thus focusing our analysis on the dominant direction of each cluster. To create node-

level effects for these two observed changes in information dynamics, we collapsed the observed edge dynamics from the NBS analyses by averaging the weights (t-values) of each significantly identified edge per node. These integration maps were compared against PET-derived neurotransmitter and transporter density maps taken from Hansen et al.[100], which were parcellated using the combined Schaefer100[33] and Tian16[34] parcellation scheme, consistent with the rest of our analysis. Tested density distributions included maps for serotonin (5-HT1a[101], 5-HT1b[101,102], 5-HT2a[103], 5-HT4[103], 5-HT6[104], and 5-HTT[101,103]), dopamine (D1[105] , D2[106,107], and DAT[108]), acetylcholine (M1[109], VAChT[110,111], and α4β2[112]), glutamate (mGluR5[100,113] and NMDA[100]), gamma-aminobutyric acid (GABAa[114]), histamine (H3[102]), cannabinoid (CB1[115]), opioid (MOR[116,117]), and norepinephrine transporter (NET[118,119]).

To test the significance of the similarity between neural integration maps and receptor maps, while accounting for the innate spatial autocorrelation of receptors, we created receptor surrogate maps using a variogram-based approach[120]. Compared to traditional spin tests, this method is suitable for whole-brain and particularly parcellated data and has been shown to better preserve the intrinsic spatial autocorrelation of brain maps. Briefly, for each receptor or transporter map, a variogram was computed to quantify the relationship between pairwise variance in parcel density values as a function of their spatial distance, capturing the map's inherent spatial autocorrelation structure. The original map is then randomly shuffled, destroying this structure, and subsequently smoothed using a kernel, which reintroduces a new spatial autocorrelation structure. An iterative optimization process is then used to identify the smoothing kernel that minimizes the deviation between the smoothed surrogate's variogram and the original map's variogram (quantified as the sum of squared errors). The best-fitting kernel is then used to create one surrogate map with shuffled values, yet the same spatial autocorrelation as the original map. We generated 10,000 surrogate maps per receptor/transporter and computed their Spearman's rank correlations with the integration maps derived from the ketamine baseline cluster and the hedonic cluster. Results were corrected for multiple comparisons using the Bonferroni correction method. Additionally, an exploratory analysis was performed by separately examining the node-averaged edge weights of the positively and negatively weighted connections within the NBS cluster linked to the ketamine effect during music perception (see Supplemental Material).

Canonical correlation analysis (CCA)

To investigate whether dynamic changes between brain state-like integration patterns are linked to the emergence of hedonic experiences, we first concatenated run-wise Φ^{WMS} time courses across participants and clustered the resulting data using a Gaussian Mixture Model[121]. We evaluated models with 7 to 15 clusters and selected the optimal number based on BIC. The best-fitting solution consisted of 9 clusters, each representing a recurring pattern of neural information dynamics.

Next, we computed state transition probabilities for each music trial, that is, the likelihood of transitioning from one brain state to another (or remaining in the same state), resulting in 81 transition probabilities per trial. To explore whether these transition dynamics were meaningfully related to participants' reported hedonic experiences, we employed Canonical Correlation Analysis (CCA). CCA is a multivariate statistical technique used to identify shared variance between two sets of variables – in this case, brain-derived state transition probabilities and hedonic experiences (all three behavioral ratings). It does so by finding linear combinations (called canonical variates) within each dataset that are

maximally correlated with one another. Formally, CCA identifies weight vectors that maximize the correlation between these linear combinations, i.e., between the projections of the brain data and behavioral data into a shared latent space. In essence, it reveals a latent dimension that best explains the covariation between the neural and behavioral data.

To determine the appropriate number of canonical dimensions to retain, we first applied Principal Component Analysis and used the elbow method as a visual heuristic. This analysis revealed a single meaningful dimension, explaining 10% of the neural variance and 85% of the behavioral variance. Based on this, we limited our CCA to a single latent canonical dimension. Given the high dimensionality of the neural dataset and the potential for multicollinearity, we implemented a regularized CCA using the PMA package in R[122]. Regularization was applied exclusively to the standardized neural data to improve model interpretability. We iteratively tuned the L1 sparsity parameter from 0.1 to 1.0 in increments of 0.05, using the internal permutation-based tuning function in PMA. Briefly, this procedure permutes the neural dataset 25 times, runs sparse CCA for each permutation and the original data, and then calculates the correlation between the resulting latent variables. These correlations are Fisher-Z-transformed to approximate a normal distribution, and a Z-statistic is computed by comparing the observed correlation against the distribution of permuted results. The tuning parameter with the highest Z-statistic was selected as the optimal level of sparsity. Since we were interested in identifying whether a unique pattern of state transitions is linked to hedonic experiences independently of treatment, we assessed the significance of the CCA results by randomly shuffling behavioral ratings within participants 10,000 times. Specifically, we reassigned complete trial-level ratings to different neural transition matrices. This approach preserved the internal structure of the data while disrupting the correspondence between neural and behavioral variables (as well as their alignment across treatment), thereby generating a null distribution of canonical correlations against which the observed correlation could be compared.

References

1. Trøstheim, M., Eikemo, M., Meir, R., Hansen, I., Paul, E., Kroll, S.L., Garland, E.L., and Leknes, S. (2020). Assessment of Anhedonia in Adults With and Without Mental Illness: A Systematic Review and Meta-analysis. JAMA Netw Open *3*, e2013233. https://doi.org/10.1001/jamanetworkopen.2020.13233.

2. American Psychiatric Association (2013). Diagnostic and Statistical Manual of Mental Disorders (DSM-5®) (American Psychiatric Publishing).

3. Rømer Thomsen, K., Whybrow, P.C., and Kringelbach, M.L. (2015). Reconceptualizing anhedonia: novel perspectives on balancing the pleasure networks in the human brain. Frontiers in Behavioral Neuroscience *9*.

4. Garfield, J.B.B., Lubman, D.I., and Yücel, M. (2013). Anhedonia in substance use disorders: A systematic review of its nature, course and clinical correlates. Australian & New Zealand Journal of Psychiatry. https://doi.org/10.1177/0004867413508455.

5. Destoop, M., Morrens, M., Coppens, V., and Dom, G. (2019). Addiction, Anhedonia, and Comorbid Mood Disorder. A Narrative Review. Frontiers in Psychiatry *10*.

6. Crits-Christoph, P., Wadden, S., Gaines, A., Rieger, A., Gallop, R., McKay, J.R., and Gibbons, M.B.C. (2018). Symptoms of anhedonia, not depression, predict the outcome of treatment of cocaine dependence. Journal of Substance Abuse Treatment *92*, 46–50. https://doi.org/10.1016/j.jsat.2018.06.010.

7. Wong, S., Le, G.H., Phan, L., Rhee, T.G., Ho, R., Meshkat, S., Teopiz, K.M., Kwan, A.T.H., Mansur, R.B., Rosenblat, J.D., et al. (2024). Effects of anhedonia on health-related quality of life and functional outcomes in major depressive disorder: A systematic review and meta-analysis. Journal of Affective Disorders *356*, 684–698. https://doi.org/10.1016/j.jad.2024.04.086.

8. Morris, S.E., Sanislow, C.A., Pacheco, J., Vaidyanathan, U., Gordon, J.A., and Cuthbert, B.N. (2022). Revisiting the seven pillars of RDoC. BMC Medicine *20*, 220. https://doi.org/10.1186/s12916-022-02414-0.

9. Patarroyo-Rodriguez, L., Cavalcanti, S., Vande Voort, J.L., and Singh, B. (2024). The Use of Ketamine for the Treatment of Anhedonia in Depression. CNS Drugs *38*, 583–596. https://doi.org/10.1007/s40263-024-01099-8.

10. Berman, R.M., Cappiello, A., Anand, A., Oren, D.A., Heninger, G.R., Charney, D.S., and Krystal, J.H. (2000). Antidepressant effects of ketamine in depressed patients. Biol Psychiatry *47*, 351–354. https://doi.org/10.1016/s0006-3223(99)00230-9.

11. Kraus, C., Rabl, U., Vanicek, T., Carlberg, L., Popovic, A., Spies, M., Bartova, L., Gryglewski, G., Papageorgiou, K., Lanzenberger, R., et al. (2017). Administration of ketamine for unipolar and bipolar depression. Int J Psychiatry Clin Pract *21*, 2–12. https://doi.org/10.1080/13651501.2016.1254802.

12. Newport, D.J., Carpenter, L.L., McDonald, W.M., Potash, J.B., Tohen, M., Nemeroff, C.B., and APA Council of Research Task Force on Novel Biomarkers and Treatments (2015). Ketamine and Other NMDA Antagonists: Early Clinical Trials and Possible Mechanisms in Depression. Am J Psychiatry *172*, 950–966. https://doi.org/10.1176/appi.ajp.2015.15040465.

13. Lally, N., Nugent, A.C., Luckenbaugh, D.A., Ameli, R., Roiser, J.P., and Zarate, C.A. (2014). Anti-anhedonic effect of ketamine and its neural correlates in treatment-resistant bipolar depression. Transl Psychiatry *4*, e469. https://doi.org/10.1038/tp.2014.105.

14. Saland, S.K., Schoepfer, K.J., and Kabbaj, M. (2016). Hedonic sensitivity to low-dose ketamine is modulated by gonadal hormones in a sex-dependent manner. Sci Rep *6*, 21322. https://doi.org/10.1038/srep21322.

15. Koob, G.F. (1996). Hedonic valence, dopamine and motivation. Mol Psychiatry *1*, 186–189.

16. Nestler, E.J., and Carlezon, W.A. (2006). The mesolimbic dopamine reward circuit in depression. Biol Psychiatry *59*, 1151–1159. https://doi.org/10.1016/j.biopsych.2005.09.018.

17. Willner, P., Muscat, R., Papp, M., Stamford, J., and Kruk, Z. (1991). Dopaminergic mechanisms in an animal model of anhedonia. European Neuropsychopharmacology *1*, 295–296.

18. Höflich, A., Michenthaler, P., Kasper, S., and Lanzenberger, R. (2019). Circuit Mechanisms of Reward, Anhedonia, and Depression. International Journal of Neuropsychopharmacology *22*, 105–118. https://doi.org/10.1093/ijnp/pyy081.

19. Luppi, A.I., Rosas, F.E., Mediano, P.A.M., Menon, D.K., and Stamatakis, E.A. (2024). Information decomposition and the informational architecture of the brain. Trends in Cognitive Sciences *28*, 352–368. https://doi.org/10.1016/j.tics.2023.11.005.

20. Rassouli, B., Rosas, F.E., and Gündüz, D. (2020). Data Disclosure Under Perfect Sample Privacy. IEEE Transactions on Information Forensics and Security *15*, 2012–2025. https://doi.org/10.1109/TIFS.2019.2954652.

21. Varley, T.F., Sporns, O., Schaffelhofer, S., Scherberger, H., and Dann, B. (2023). Information-processing dynamics in neural networks of macaque cerebral cortex reflect cognitive state and behavior. Proceedings of the National Academy of Sciences *120*, e2207677120. https://doi.org/10.1073/pnas.2207677120.

22. Koçillari, L., Celotto, M., Francis, N.A., Mukherjee, S., Babadi, B., Kanold, P.O., and Panzeri, S. (2023). Behavioural relevance of redundant and synergistic stimulus information between functionally connected neurons in mouse auditory cortex. Brain Inform *10*, 34. https://doi.org/10.1186/s40708-023-00212-9.

23. Rosas, F.E., Mediano, P.A.M., Gastpar, M., and Jensen, H.J. (2019). Quantifying high-order interdependencies via multivariate extensions of the mutual information. Phys. Rev. E *100*, 032305. https://doi.org/10.1103/PhysRevE.100.032305.

24. Rosas, F.E., Gutknecht, A., Mediano, P.A.M., and Gastpar, M. (2024). Characterising high-order interdependence via entropic conjugation. Preprint at arXiv, https://doi.org/10.48550/arXiv.2410.10485 https://doi.org/10.48550/arXiv.2410.10485.

25. Varley, T.F., Pope, M., Maria Grazia, Joshua, and Sporns, O. (2023). Partial entropy decomposition reveals higher-order information structures in human brain activity. Proceedings of the National Academy of Sciences *120*, e2300888120. https://doi.org/10.1073/pnas.2300888120.

26. Barrett, A.B., and Seth, A.K. (2011). Practical Measures of Integrated Information for Time-Series Data. PLOS Computational Biology *7*, e1001052. https://doi.org/10.1371/journal.pcbi.1001052.

27. Mediano, P.A.M., Rosas, F.E., Luppi, A.I., Carhart-Harris, R.L., Bor, D., Seth, A.K., and Barrett, A.B. (2021). Towards an extended taxonomy of information dynamics via Integrated Information Decomposition. Preprint at arXiv, https://doi.org/10.48550/arXiv.2109.13186 https://doi.org/10.48550/arXiv.2109.13186.

28. Luppi, A.I., Mediano, P.A.M., Rosas, F.E., Harrison, D.J., Carhart-Harris, R.L., Bor, D., and Stamatakis, E.A. (2021). What it is like to be a bit: an integrated information decomposition account of emergent mental phenomena. Neuroscience of Consciousness *2021*, niab027. https://doi.org/10.1093/nc/niab027.

29. Salimpoor, V.N., Benovoy, M., Longo, G., Cooperstock, J.R., and Zatorre, R.J. (2009). The Rewarding Aspects of Music Listening Are Related to Degree of Emotional Arousal. PLOS ONE *4*, e7487. https://doi.org/10.1371/journal.pone.0007487.

30. Vuust, P., and Kringelbach, M.L. (2010). The Pleasure of Making Sense of Music. Interdisciplinary Science Reviews. https://doi.org/10.1179/030801810X12723585301192.

31. Lingham, J., and Theorell, T. (2009). Self-selected "favourite" stimulative and sedative music listening – how does familiar and preferred music listening affect the body? Nordic Journal of Music Therapy. https://doi.org/10.1080/08098130903062363.

32. Zatorre, R.J., and Salimpoor, V.N. (2013). From perception to pleasure: Music and its neural substrates. Proceedings of the National Academy of Sciences *110*, 10430–10437. https://doi.org/10.1073/pnas.1301228110.

33. Schaefer, A., Kong, R., Gordon, E.M., Laumann, T.O., Zuo, X.-N., Holmes, A.J., Eickhoff, S.B., and Yeo, B.T.T. (2018). Local-Global Parcellation of the Human Cerebral Cortex from Intrinsic Functional Connectivity MRI. Cerebral Cortex *28*, 3095–3114. https://doi.org/10.1093/cercor/bhx179.

34. Tian, Y., Margulies, D.S., Breakspear, M., and Zalesky, A. (2020). Topographic organization of the human subcortex unveiled with functional connectivity gradients. Nat Neurosci *23*, 1421–1432. https://doi.org/10.1038/s41593-020-00711-6.

35. Mediano, P.A.M., Rosas, F.E., Farah, J.C., Shanahan, M., Bor, D., and Barrett, A.B. (2022). Integrated information as a common signature of dynamical and information-processing complexity. Chaos *32*, 013115. https://doi.org/10.1063/5.0063384.

36. Gracia-Tabuenca, Z., and Alcauter, S. (2020). NBR: Network-based R-statistics for (unbalanced) longitudinal samples. Preprint at bioRxiv, https://doi.org/10.1101/2020.11.07.373019 https://doi.org/10.1101/2020.11.07.373019.

37. Zalesky, A., Fornito, A., and Bullmore, E.T. (2010). Network-based statistic: Identifying differences in brain networks. NeuroImage *53*, 1197–1207. https://doi.org/10.1016/j.neuroimage.2010.06.041.

38. Zhang, R., Deng, H., and Xiao, X. (2024). The Insular Cortex: An Interface Between Sensation, Emotion and Cognition. Neurosci. Bull. *40*, 1763–1773. https://doi.org/10.1007/s12264-024-01211-4.

39. Gu, X., Liu, X., Van Dam, N.T., Hof, P.R., and Fan, J. (2013). Cognition–Emotion Integration in the Anterior Insular Cortex. Cereb Cortex *23*, 20–27. https://doi.org/10.1093/cercor/bhr367.

40. Alnefeesi, Y., Chen-Li, D., Krane, E., Jawad, M.Y., Rodrigues, N.B., Ceban, F., Di Vincenzo, J.D., Meshkat, S., Ho, R.C.M., Gill, H., et al. (2022). Real-world effectiveness of ketamine in treatment-resistant depression: A systematic review & meta-analysis. Journal of Psychiatric Research *151*, 693–709. https://doi.org/10.1016/j.jpsychires.2022.04.037.

41. Nikolin, S., Rodgers, A., Schwaab, A., Bahji, A., Zarate, C., Vazquez, G., and Loo, C. (2023). Ketamine for the treatment of major depression: a systematic review and meta-analysis. eClinicalMedicine *62*. https://doi.org/10.1016/j.eclinm.2023.102127.

42. Nogo, D., Jasrai, A.K., Kim, H., Nasri, F., Ceban, F., Lui, L.M.W., Rosenblat, J.D., Vinberg, M., Ho, R., and McIntyre, R.S. (2022). The effect of ketamine on anhedonia: improvements in dimensions of anticipatory, consummatory, and motivation-related reward deficits. Psychopharmacology *239*, 2011–2039. https://doi.org/10.1007/s00213-022-06105-9.

43. Becker, S., Bräscher, A.-K., Bannister, S., Bensafi, M., Calma-Birling, D., Chan, R.C.K., Eerola, T., Ellingsen, D.-M., Ferdenzi, C., Hanson, J.L., et al. (2019). The role of hedonics in the Human Affectome. Neurosci Biobehav Rev *102*, 221–241. https://doi.org/10.1016/j.neubiorev.2019.05.003.

44. Luppi, A.I., Mediano, P.A.M., Rosas, F.E., Allanson, J., Pickard, J.D., Carhart-Harris, R.L., Williams, G.B., Craig, M.M., Finoia, P., Owen, A.M., et al. (2020). A Synergistic Workspace for Human Consciousness Revealed by Integrated Information Decomposition. Preprint at bioRxiv, https://doi.org/10.1101/2020.11.25.398081 https://doi.org/10.1101/2020.11.25.398081.

45. Azen, R., and Budescu, D.V. (2003). The dominance analysis approach for comparing predictors in multiple regression. Psychol Methods *8*, 129–148. https://doi.org/10.1037/1082-989x.8.2.129.

46. Hansen, J.Y., Shafiei, G., Markello, R.D., Smart, K., Cox, S.M.L., Nørgaard, M., Beliveau, V., Wu, Y., Gallezot, J.-D., Aumont, É., et al. (2022). Mapping neurotransmitter systems to the structural and functional organization of the human neocortex. Nat Neurosci *25*, 1569–1581. https://doi.org/10.1038/s41593-022-01186-3.

47. Varley, T.F., Pope, M., Faskowitz, J., and Sporns, O. (2023). Multivariate information theory uncovers synergistic subsystems of the human cerebral cortex. Commun Biol *6*, 1–12. https://doi.org/10.1038/s42003-023-04843-w.

48. Pope, M., Varley, T.F., Grazia Puxeddu, M., Faskowitz, J., and Sporns, O. (2025). Time-varying synergy/redundancy dominance in the human cerebral cortex. J. Phys. Complex. *6*, 015015. https://doi.org/10.1088/2632-072X/adbaa9.

49. Gogolla, N. (2017). The insular cortex. Current Biology *27*, R580–R586. https://doi.org/10.1016/j.cub.2017.05.010.

50. Pehrs, C., Deserno, L., Bakels, J.-H., Schlochtermeier, L.H., Kappelhoff, H., Jacobs, A.M., Fritz, T.H., Koelsch, S., and Kuchinke, L. (2014). How music alters a kiss: superior temporal gyrus controls fusiform-amygdalar effective connectivity. Soc Cogn Affect Neurosci *9*, 1770–1778. https://doi.org/10.1093/scan/nst169.

51. Satoh, M., Nagata, K., and Tomimoto, H. (2015). Sound Richness of Music Might Be Mediated by Color Perception: A PET Study. Behav Neurol *2015*, 241804. https://doi.org/10.1155/2015/241804.

52. Scharinger, M., Knoop, C.A., Wagner, V., and Menninghaus, W. (2022). Neural processing of poems and songs is based on melodic properties. NeuroImage *257*, 119310. https://doi.org/10.1016/j.neuroimage.2022.119310.

53. Newman, E.L., Varley, T.F., Parakkattu, V.K., Sherrill, S.P., and Beggs, J.M. (2022). Revealing the Dynamics of Neural Information Processing with Multivariate Information Decomposition. Entropy *24*, 930. https://doi.org/10.3390/e24070930.

54. Panzeri, S., Moroni, M., Safaai, H., and Harvey, C.D. (2022). The structures and functions of correlations in neural population codes. Nat Rev Neurosci *23*, 551–567. https://doi.org/10.1038/s41583-022-00606-4.

55. So, K., Ganguly, K., Jimenez, J., Gastpar, M.C., and Carmena, J.M. (2012). Redundant information encoding in primary motor cortex during natural and prosthetic motor control. J Comput Neurosci *32*, 555–561. https://doi.org/10.1007/s10827-011-0369-1.

56. Francis, N.A., Mukherjee, S., Koçillari, L., Panzeri, S., Babadi, B., and Kanold, P.O. (2022). Sequential transmission of task-relevant information in cortical neuronal networks. Cell Reports *39*. https://doi.org/10.1016/j.celrep.2022.110878.

57. Koçillari, L., Celotto, M., Francis, N.A., Mukherjee, S., Babadi, B., Kanold, P.O., and Panzeri, S. (2023). Measuring Stimulus-Related Redundant and Synergistic Functional Connectivity with Single Cell Resolution in Auditory Cortex. In Brain Informatics, F. Liu, Y. Zhang, H. Kuai, E. P. Stephen, and H. Wang, eds. (Springer Nature Switzerland), pp. 45–56. https://doi.org/10.1007/978-3-031-43075-6_5.

58. España, R.A., Schmeichel, B.E., and Berridge, C.W. (2016). Norepinephrine at the nexus of arousal, motivation and relapse. Brain Res *1641*, 207–216. https://doi.org/10.1016/j.brainres.2016.01.002.

59. Sofuoglu, M., and Sewell, R.A. (2009). Norepinephrine and Stimulant Addiction. Addict Biol *14*, 119–129. https://doi.org/10.1111/j.1369-1600.2008.00138.x.

60. Nigam, S., Pojoga, S., and Dragoi, V. (2019). Synergistic Coding of Visual Information in Columnar Networks. Neuron *104*, 402-411.e4. https://doi.org/10.1016/j.neuron.2019.07.006.

61. Zanos, P., and Gould, T.D. (2018). Mechanisms of Ketamine Action as an Antidepressant. Mol Psychiatry *23*, 801–811. https://doi.org/10.1038/mp.2017.255.

62. Carhart-Harris, R.L., and Friston, K.J. (2019). REBUS and the Anarchic Brain: Toward a Unified Model of the Brain Action of Psychedelics. Pharmacol Rev *71*, 316–344. https://doi.org/10.1124/pr.118.017160.

63. Aleksandrova, L.R., and Phillips, A.G. (2021). Neuroplasticity as a convergent mechanism of ketamine and classical psychedelics. Trends in Pharmacological Sciences *42*, 929–942. https://doi.org/10.1016/j.tips.2021.08.003.

64. Herzog, R., Barbey, F.M., Islam, M.N., Rueda-Delgado, L., Nolan, H., Prado, P., Krylova, M., Izyurov, I., Javaheripour, N., Danyeli, L.V., et al. (2024). High-order brain interactions in ketamine during rest and task: a double-blinded cross-over design using portable EEG on male participants. Transl Psychiatry *14*, 1–9. https://doi.org/10.1038/s41398-024-03029-0.

65. Szubielska, M., Imbir, K., and Szymańska, A. (2021). The influence of the physical context and knowledge of artworks on the aesthetic experience of interactive installations. Curr Psychol *40*, 3702–3715. https://doi.org/10.1007/s12144-019-00322-w.

66. Millis, K. (2001). Making meaning brings pleasure: the influence of titles on aesthetic experiences. Emotion *1*, 320–329.

67. Herzog, R., Barbey, F.M., Islam, M.N., Rueda-Delgado, L., Nolan, H., Prado, P., Krylova, M., Izyurov, I., Javaheripour, N., Danyeli, L.V., et al. (2024). High-order brain interactions in ketamine during rest and task: a double-blinded cross-over design using portable EEG on male participants. Transl Psychiatry *14*, 1–9. https://doi.org/10.1038/s41398-024-03029-0.

68. Kotoula, V., Webster, T., Stone, J., and Mehta, M.A. (2021). Resting-state connectivity studies as a marker of the acute and delayed effects of subanaesthetic ketamine administration in healthy and depressed individuals: A systematic review. Brain and Neuroscience Advances *5*, 23982128211055426. https://doi.org/10.1177/23982128211055426.

69. Varley, T.F., and Bongard, J. (2024). Evolving higher-order synergies reveals a trade-off between stability and information integration capacity in complex systems. Preprint at arXiv, https://doi.org/10.48550/arXiv.2401.14347 https://doi.org/10.48550/arXiv.2401.14347.

70. Lobbestael, J., Leurgans, M., and Arntz, A. (2011). Inter-rater reliability of the Structured Clinical Interview for DSM-IV Axis I Disorders (SCID I) and Axis II Disorders (SCID II). Clin Psychol Psychother *18*, 75–79. https://doi.org/10.1002/cpp.693.

71. Rentfrow, P.J., Goldberg, L.R., and Levitin, D.J. (2011). The Structure of Musical Preferences: A Five-Factor Model. J Pers Soc Psychol *100*, 1139–1157. https://doi.org/10.1037/a0022406.

72. Tomar, S. (2006). Converting video formats with FFmpeg. Linux J. *2006*, 10.

73. Menninghaus, W., Wagner, V., Wassiliwizky, E., Schindler, I., Hanich, J., Jacobsen, T., and Koelsch, S. (2019). What are aesthetic emotions? Psychological Review *126*, 171–195. https://doi.org/10.1037/rev0000135.

74. Menninghaus, W., Wagner, V., Hanich, J., Wassiliwizky, E., Kuehnast, M., and Jacobsen, T. (2015). Towards a Psychological Construct of Being Moved. PLOS ONE *10*, e0128451. https://doi.org/10.1371/journal.pone.0128451.

75. Christensen, R.H.B. (2023). ordinal—regression models for ordinal data.

76. Bürkner, P.-C., and Vuorre, M. (2019). Ordinal Regression Models in Psychology: A Tutorial. Advances in Methods and Practices in Psychological Science *2*, 77–101. https://doi.org/10.1177/2515245918823199.

77. Lüdecke, D., Ben-Shachar, M.S., Patil, I., Waggoner, P., and Makowski, D. (2021). performance: An R Package for Assessment, Comparison and Testing of Statistical Models. Journal of Open Source Software *6*, 3139. https://doi.org/10.21105/joss.03139.

78. Esteban, O., Markiewicz, C.J., Blair, R.W., Moodie, C.A., Isik, A.I., Erramuzpe, A., Kent, J.D., Goncalves, M., DuPre, E., Snyder, M., et al. (2019). fMRIPrep: a robust preprocessing pipeline for functional MRI. Nat Methods *16*, 111–116. https://doi.org/10.1038/s41592-018-0235-4.

79. Esteban, O., Ciric, R., Finc, K., Blair, R.W., Markiewicz, C.J., Moodie, C.A., Kent, J.D., Goncalves, M., DuPre, E., Gomez, D.E.P., et al. (2020). Analysis of task-based functional MRI data preprocessed with fMRIPrep. Nat Protoc *15*, 2186–2202. https://doi.org/10.1038/s41596-020-0327-3.

80. Tustison, N.J., Avants, B.B., Cook, P.A., Zheng, Y., Egan, A., Yushkevich, P.A., and Gee, J.C. (2010). N4ITK: improved N3 bias correction. IEEE Trans Med Imaging *29*, 1310–1320. https://doi.org/10.1109/TMI.2010.2046908.

81. Zhang, Y., Brady, M., and Smith, S. (2001). Segmentation of brain MR images through a hidden Markov random field model and the expectation-maximization algorithm. IEEE Transactions on Medical Imaging *20*, 45–57. https://doi.org/10.1109/42.906424.

82. Ciric, R., Thompson, W.H., Lorenz, R., Goncalves, M., MacNicol, E.E., Markiewicz, C.J., Halchenko, Y.O., Ghosh, S.S., Gorgolewski, K.J., Poldrack, R.A., et al. (2022). TemplateFlow: FAIR-sharing of multi-scale, multi-species brain models. Nat Methods *19*, 1568–1571. https://doi.org/10.1038/s41592-022-01681-2.

83. Jenkinson, M., Bannister, P., Brady, M., and Smith, S. (2002). Improved Optimization for the Robust and Accurate Linear Registration and Motion Correction of Brain Images. NeuroImage *17*, 825–841. https://doi.org/10.1006/nimg.2002.1132.

84. Andersson, J.L.R., Skare, S., and Ashburner, J. (2003). How to correct susceptibility distortions in spin-echo echo-planar images: application to diffusion tensor imaging. Neuroimage *20*, 870–888. https://doi.org/10.1016/S1053-8119(03)00336-7.

85. Greve, D.N., and Fischl, B. (2009). Accurate and Robust Brain Image Alignment using Boundary-based Registration. Neuroimage *48*, 63–72. https://doi.org/10.1016/j.neuroimage.2009.06.060.

86. Behzadi, Y., Restom, K., Liau, J., and Liu, T.T. (2007). A component based noise correction method (CompCor) for BOLD and perfusion based fMRI. Neuroimage *37*, 90–101. https://doi.org/10.1016/j.neuroimage.2007.04.042.

87. Gorgolewski, K., Burns, C.D., Madison, C., Clark, D., Halchenko, Y.O., Waskom, M.L., and Ghosh, S.S. (2011). Nipype: A Flexible, Lightweight and Extensible Neuroimaging Data Processing Framework in Python. Front. Neuroinform. *5*. https://doi.org/10.3389/fninf.2011.00013.

88. Parkes, L., Fulcher, B., Yücel, M., and Fornito, A. (2018). An evaluation of the efficacy, reliability, and sensitivity of motion correction strategies for resting-state functional MRI. NeuroImage *171*, 415–436. https://doi.org/10.1016/j.neuroimage.2017.12.073.

89. Watanabe, S. (1960). Information Theoretical Analysis of Multivariate Correlation. IBM Journal of Research and Development *4*, 66–82. https://doi.org/10.1147/rd.41.0066.

90. Han, T.S. (1975). Linear dependence structure of the entropy space. Information and Control *29*, 337–368. https://doi.org/10.1016/S0019-9958(75)80004-0.

91. Lizier, J.T. (2014). JIDT: An Information-Theoretic Toolkit for Studying the Dynamics of Complex Systems. Front. Robot. AI *1*. https://doi.org/10.3389/frobt.2014.00011.

92. Bates, D., Mächler, M., Bolker, B., and Walker, S. (2015). Fitting Linear Mixed-Effects Models Using lme4. Journal of Statistical Software *67*, 1–48. https://doi.org/10.18637/jss.v067.i01.

93. Williams, P.L., and Beer, R.D. (2010). Nonnegative Decomposition of Multivariate Information. Preprint at arXiv, https://doi.org/10.48550/arXiv.1004.2515 https://doi.org/10.48550/arXiv.1004.2515.

94. Luppi, A.I., Mediano, P.A.M., Rosas, F.E., Holland, N., Fryer, T.D., O'Brien, J.T., Rowe, J.B., Menon, D.K., Bor, D., and Stamatakis, E.A. (2022). A synergistic core for human brain evolution and cognition. Nat Neurosci *25*, 771–782. https://doi.org/10.1038/s41593-022-01070-0.

95. Mediano, P.A.M., Rosas, F.E., Luppi, A.I., Carhart-Harris, R.L., Bor, D., Seth, A.K., and Barrett, A.B. (2021). Towards an extended taxonomy of information dynamics via Integrated Information Decomposition. Preprint at arXiv, https://doi.org/10.48550/arXiv.2109.13186 https://doi.org/10.48550/arXiv.2109.13186.

96. Gracia-Tabuenca, Z., and Alcauter, S. (2020). NBR: Network-based R-statistics for (unbalanced) longitudinal samples. Preprint at bioRxiv, https://doi.org/10.1101/2020.11.07.373019 https://doi.org/10.1101/2020.11.07.373019.

97. Loy, A., and Korobova, J. (2021). Bootstrapping Clustered Data in R using lmeresampler. Preprint at arXiv, https://doi.org/10.48550/arXiv.2106.06568 https://doi.org/10.48550/arXiv.2106.06568.

98. Lüdecke, D., Bartel, A., Schwemmer, C., Powell, C., Djalovski, A., and Titz, J. (2025). sjPlot: Data Visualization for Statistics in Social Science. Version 2.9.0.

99. Navarrete, C.B., and Soares, F.C. (2024). dominanceanalysis: Dominance Analysis. Version 2.1.0.

100. Hansen, J.Y., Shafiei, G., Markello, R.D., Smart, K., Cox, S.M.L., Nørgaard, M., Beliveau, V., Wu, Y., Gallezot, J.-D., Aumont, É., et al. (2022). Mapping neurotransmitter systems to the structural and functional organization of the human neocortex. Nat Neurosci *25*, 1569–1581. https://doi.org/10.1038/s41593-022-01186-3.

101. Savli, M., Bauer, A., Mitterhauser, M., Ding, Y.-S., Hahn, A., Kroll, T., Neumeister, A., Haeusler, D., Ungersboeck, J., Henry, S., et al. (2012). Normative database of the serotonergic system in healthy subjects using multi-tracer PET. NeuroImage *63*, 447–459. https://doi.org/10.1016/j.neuroimage.2012.07.001.

102. Gallezot, J.-D., Nabulsi, N., Neumeister, A., Planeta-Wilson, B., Williams, W.A., Singhal, T., Kim, S., Maguire, R.P., McCarthy, T., Frost, J.J., et al. (2010). Kinetic Modeling of the Serotonin 5-HT1B Receptor Radioligand [11C]P943 in Humans. J Cereb Blood Flow Metab *30*, 196–210. https://doi.org/10.1038/jcbfm.2009.195.

103. Beliveau, V., Ganz, M., Feng, L., Ozenne, B., Højgaard, L., Fisher, P.M., Svarer, C., Greve, D.N., and Knudsen, G.M. (2017). A High-Resolution In Vivo Atlas of the Human Brain's Serotonin System. J. Neurosci. *37*, 120–128. https://doi.org/10.1523/JNEUROSCI.2830-16.2016.

104. Radhakrishnan, R., Nabulsi, N., Gaiser, E., Gallezot, J.-D., Henry, S., Planeta, B., Lin, S., Ropchan, J., Williams, W., Morris, E., et al. (2018). Age-Related Change in 5-HT6 Receptor Availability in Healthy Male Volunteers Measured with 11C-GSK215083 PET. Journal of Nuclear Medicine *59*, 1445–1450. https://doi.org/10.2967/jnumed.117.206516.

105. Kaller, S., Rullmann, M., Patt, M., Becker, G.-A., Luthardt, J., Girbardt, J., Meyer, P.M., Werner, P., Barthel, H., Bresch, A., et al. (2017). Test–retest measurements of dopamine D1-type receptors using simultaneous PET/MRI imaging. Eur J Nucl Med Mol Imaging *44*, 1025–1032. https://doi.org/10.1007/s00259-017-3645-0.

106. Sandiego, C.M., Gallezot, J.-D., Lim, K., Ropchan, J., Lin, S., Gao, H., Morris, E.D., and Cosgrove, K.P. (2015). Reference region modeling approaches for amphetamine challenge studies with [11C]FLB 457 and PET. J Cereb Blood Flow Metab *35*, 623–629. https://doi.org/10.1038/jcbfm.2014.237.

107. Smith, C.T., Crawford, J.L., Dang, L.C., Seaman, K.L., San Juan, M.D., Vijay, A., Katz, D.T., Matuskey, D., Cowan, R.L., Morris, E.D., et al. (2019). Partial-volume correction increases estimated dopamine D2-like receptor binding potential and reduces adult age differences. J Cereb Blood Flow Metab *39*, 822–833. https://doi.org/10.1177/0271678X17737693.

108. Dukart, J., Holiga, Š., Chatham, C., Hawkins, P., Forsyth, A., McMillan, R., Myers, J., Lingford-Hughes, A.R., Nutt, D.J., Merlo-Pich, E., et al. (2018). Cerebral blood flow predicts differential neurotransmitter activity. Sci Rep *8*, 4074. https://doi.org/10.1038/s41598-018-22444-0.

109. Naganawa, M., Nabulsi, N., Henry, S., Matuskey, D., Lin, S.-F., Slieker, L., Schwarz, A.J., Kant, N., Jesudason, C., Ruley, K., et al. (2021). First-in-Human Assessment of 11C-LSN3172176, an M1 Muscarinic Acetylcholine Receptor PET Radiotracer. Journal of Nuclear Medicine *62*, 553–560. https://doi.org/10.2967/jnumed.120.246967.

110. Aghourian, M., Legault-Denis, C., Soucy, J.-P., Rosa-Neto, P., Gauthier, S., Kostikov, A., Gravel, P., and Bédard, M.-A. (2017). Quantification of brain cholinergic denervation in Alzheimer's disease using PET imaging with [18F]-FEOBV. Mol Psychiatry *22*, 1531–1538. https://doi.org/10.1038/mp.2017.183.

111. Bedard, M.-A., Aghourian, M., Legault-Denis, C., Postuma, R.B., Soucy, J.-P., Gagnon, J.-F., Pelletier, A., and Montplaisir, J. (2019). Brain cholinergic alterations in idiopathic REM sleep behaviour disorder: a PET imaging study with 18F-FEOBV. Sleep Med *58*, 35–41. https://doi.org/10.1016/j.sleep.2018.12.020.

112. Hillmer, A.T., Esterlis, I., Gallezot, J.D., Bois, F., Zheng, M.Q., Nabulsi, N., Lin, S.F., Papke, R.L., Huang, Y., Sabri, O., et al. (2016). Imaging of cerebral α4β2* nicotinic acetylcholine receptors with (−)-[18F]Flubatine PET: Implementation of bolus plus constant infusion and sensitivity to acetylcholine in human brain. NeuroImage *141*, 71–80. https://doi.org/10.1016/j.neuroimage.2016.07.026.

113. Smart, K., Cox, S.M.L., Scala, S.G., Tippler, M., Jaworska, N., Boivin, M., Séguin, J.R., Benkelfat, C., and Leyton, M. (2019). Sex differences in [11C]ABP688 binding: a positron emission tomography study of mGlu5 receptors. Eur J Nucl Med Mol Imaging *46*, 1179–1183. https://doi.org/10.1007/s00259-018-4252-4.

114. Nørgaard, M., Beliveau, V., Ganz, M., Svarer, C., Pinborg, L.H., Keller, S.H., Jensen, P.S., Greve, D.N., and Knudsen, G.M. (2021). A high-resolution in vivo atlas of the human brain's benzodiazepine binding site of GABAA receptors. NeuroImage *232*, 117878. https://doi.org/10.1016/j.neuroimage.2021.117878.

115. Normandin, M.D., Zheng, M.-Q., Lin, K.-S., Mason, N.S., Lin, S.-F., Ropchan, J., Labaree, D., Henry, S., Williams, W.A., Carson, R.E., et al. (2015). Imaging the Cannabinoid CB1 Receptor in Humans with [11C] OMAR: Assessment of Kinetic Analysis Methods, Test–Retest Reproducibility, and Gender Differences. J Cereb Blood Flow Metab *35*, 1313–1322. https://doi.org/10.1038/jcbfm.2015.46.

116. Kantonen, T., Karjalainen, T., Isojärvi, J., Nuutila, P., Tuisku, J., Rinne, J., Hietala, J., Kaasinen, V., Kalliokoski, K., Scheinin, H., et al. (2020). Interindividual variability and lateralization of μ-opioid receptors in the human brain. NeuroImage *217*, 116922. https://doi.org/10.1016/j.neuroimage.2020.116922.

117. Turtonen, O., Saarinen, A., Nummenmaa, L., Tuominen, L., Tikka, M., Armio, R.-L., Hautamäki, A., Laurikainen, H., Raitakari, O., Keltikangas-Järvinen, L., et al. (2021). Adult Attachment System Links With Brain Mu Opioid Receptor Availability In Vivo. Biological Psychiatry: Cognitive Neuroscience and Neuroimaging *6*, 360–369. https://doi.org/10.1016/j.bpsc.2020.10.013.

118. Ding, Y.-S., Singhal, T., Planeta-Wilson, B., Gallezot, J.-D., Nabulsi, N., Labaree, D., Ropchan, J., Henry, S., Williams, W., Carson, R.E., et al. (2010). PET imaging of the effects of age and cocaine on the norepinephrine transporter in the human brain using (S,S)-[11C]O-methylreboxetine and HRRT. Synapse *64*, 30–38. https://doi.org/10.1002/syn.20696.

119. Hesse, S., Becker, G.-A., Rullmann, M., Bresch, A., Luthardt, J., Hankir, M.K., Zientek, F., Reißig, G., Patt, M., Arelin, K., et al. (2017). Central noradrenaline transporter availability in highly obese, non-depressed individuals. Eur J Nucl Med Mol Imaging *44*, 1056–1064. https://doi.org/10.1007/s00259-016-3590-3.

120. Burt, J.B., Helmer, M., Shinn, M., Anticevic, A., and Murray, J.D. (2020). Generative modeling of brain maps with spatial autocorrelation. NeuroImage *220*, 117038. https://doi.org/10.1016/j.neuroimage.2020.117038.

121. Pedregosa, F., Varoquaux, G., Gramfort, A., Michel, V., Thirion, B., Grisel, O., Blondel, M., Prettenhofer, P., Weiss, R., Dubourg, V., et al. (2011). Scikit-learn: Machine Learning in Python. Journal of Machine Learning Research *12*, 2825–2830.

122. Witten, D., Tibshirani, R., Gross, S., and Narasimhan, B. (2009). PMA: Penalized Multivariate Analysis. https://doi.org/10.32614/CRAN.package.PMA https://doi.org/10.32614/CRAN.package.PMA.

Table S1: Ordinal regression results for valence ratings
This table presents the results of the cumulative ordinal regression analysis on valence ratings using a logit link function. The model includes drug condition (placebo, ketamine) and initial judgment (neutral, positive) as predictors, with a random intercept for each participant to account for repeated measures. Exponentiated parameter estimates (Odds Ratios) along with their 95% confidence intervals (CI) and standard error (SE) are reported. For the random effects, the within-group (σ^2) and between-group (τ_{00}) variances, as well as the intraclass correlation coefficient (ICC), are reported.

		Valence			
Predictors	*Odds Ratios*	*SE*	*CI (95%)*	*z-statistic*	*p-Value*
-5|-4	0.01	0.00	0.01 – 0.02	-12.77	**<0.001**
-4|-3	0.03	0.01	0.01 – 0.04	-13.49	**<0.001**
-3|-2	0.05	0.01	0.03 – 0.08	-12.75	**<0.001**
-2|-1	0.14	0.03	0.10 – 0.21	-9.57	**<0.001**
-1|0	0.41	0.08	0.28 – 0.60	-4.63	**<0.001**
0|1	3.56	0.69	2.44 – 5.20	6.59	**<0.001**
1|2	18.16	3.88	11.94 – 27.62	13.56	**<0.001**
2|3	92.99	21.72	58.84 – 146.98	19.41	**<0.001**
3|4	368.66	91.14	227.09 – 598.50	23.91	**<0.001**
4|5	1547.13	416.24	913.11 – 2621.39	27.30	**<0.001**
Drug condition [Ketamine]	1.36	0.13	1.13 – 1.63	3.24	**0.001**
Initial Judgment [Positive]	116.08	18.61	84.77 – 158.94	29.65	**<0.001**
Random Effects					
σ^2	3.29				
$\tau_{00\ ID}$	1.03				
ICC	0.24				
$N_{\ ID}$	38				
Observations	1501				

Table S2: Ordinal regression results for moving ratings
This table presents the results of the cumulative ordinal regression analysis on moving ratings using a logit link function. The model includes drug condition (placebo, ketamine) and initial judgment (neutral, positive) as predictors, with a random intercept for each participant to account for repeated measures. Exponentiated parameter estimates (Odds Ratios) along with their 95% confidence intervals (CI) and standard error (SE) are reported. For the random effects, the within-group (σ^2) and between-group (τ_{00}) variances, as well as the intraclass correlation coefficient (ICC), are reported.

		Moving			
Predictors	*Odds Ratios*	*SE*	*CI (95%)*	*z-statistic*	*p-Value*
1|2	0.45	0.08	0.32 – 0.64	-4.48	**<0.001**
2|3	1.14	0.20	0.80 – 1.60	0.72	0.472
3|4	2.78	0.50	1.95 – 3.95	5.69	**<0.001**
4|5	5.45	1.01	3.79 – 7.84	9.14	**<0.001**

5|6	10.29	2.00	7.03 – 15.05	12.00	**<0.001**
6|7	44.21	9.75	28.69 – 68.13	17.18	**<0.001**
7|8	333.51	81.47	206.62 – 538.32	23.78	**<0.001**
8|9	1548.58	404.37	928.25 – 2583.46	28.13	**<0.001**
9|10	7022.94	2115.09	3891.91 – 12672.85	29.41	**<0.001**
Drug condition [Ketamine]	1.31	0.12	1.09 – 1.58	2.88	**0.004**
Initial Judgment [Positive]	219.68	39.28	154.74 – 311.87	30.16	**<0.001**

Random Effects

σ^2	3.29
$\tau_{00\ ID}$	0.87
ICC	0.21
$N_{\ ID}$	38
Observations	1488

Table S3: Ordinal regression results for chills ratings

This table presents the results of the cumulative ordinal regression analysis on chills ratings using a logit link function. The model includes drug condition (placebo, ketamine) and initial judgment (neutral, positive) as predictors, with a random intercept for each participant to account for repeated measures. Exponentiated parameter estimates (Odds Ratios) along with their 95% confidence intervals (CI) and standard error (SE) are reported. For the random effects, the within-group (σ^2) and between-group (τ_{00}) variances, as well as the intraclass correlation coefficient (ICC), are reported.

	Chills				
Predictors	*Odds Ratios*	*SE*	*CI (95%)*	*z-statistic*	*p-Value*
1|2	4.09	1.13	2.37 – 7.03	5.08	**<0.001**
2|3	8.69	2.44	5.01 – 15.08	7.69	**<0.001**
3|4	17.51	5.03	9.97 – 30.75	9.96	**<0.001**
4|5	34.76	10.26	19.48 – 62.00	12.01	**<0.001**
5|6	66.47	20.17	36.67 – 120.49	13.83	**<0.001**
6|7	274.02	87.45	146.60 – 512.17	17.59	**<0.001**
7|8	1123.91	374.64	584.78 – 2160.06	21.07	**<0.001**
8|9	3452.90	1213.63	1733.81 – 6876.46	23.18	**<0.001**
9|10	13886.20	5725.81	6188.72 – 31157.74	23.13	**<0.001**
Drug condition [Ketamine]	1.60	0.17	1.31 – 1.96	4.52	**<0.001**
Initial Judgment [Positive]	114.32	18.62	83.07 – 157.33	29.09	**<0.001**

Random Effects

σ^2	3.29
$\tau_{00\ ID}$	2.46

ICC	0.43
N_{ID}	38
Observations	1499

Table S4: Linear mixed-effects model for O-Information across rest and music perception
The model includes current state (rest, music perception) and drug condition (placebo, ketamine) as predictors, with a random intercept for each participant to account for repeated measures. Standardized beta estimates (std. Beta), along with their 95% confidence intervals (std. CI) and standard error (std. SE), are reported. For the random effects, the within-group (σ^2) and between-group (τ_{00}) variances, as well as the intraclass correlation coefficient (ICC), are reported.

O-Information Music vs Rest

Predictors	*std. Beta*	*std. SE*	*std. CI (95%)*	*t-statistic*	*p-Value*
Intercept	0.09	0.10	-0.11 – 0.29	0.87	0.39
Music or Rest [Music]	-0.11	0.04	-0.20 – -0.02	-2.46	**0.014**
Drug Condition [Placebo]	-0.02	0.04	-0.10 – 0.06	-0.49	0.623
Random Effects					
σ2	0.73				
τ00 subject	0.27				
ICC	0.27				
N subject	32				
Observations	1782				

Table S5: Linear mixed-effects model for O-Information across rest segments
The model includes drug condition (placebo, ketamine) as a predictor, with a random intercept for each participant to account for repeated measures. Standardized beta estimates (std. Beta), along with their 95% confidence intervals (std. CI) and standard error (std. SE), are reported. For the random effects, the within-group (σ^2) and between-group (τ_{00}) variances, as well as the intraclass correlation coefficient (ICC), are reported.

O-Information Rest Segments

Predictors	*std. Beta*	*std. SE*	*std. CI (95%)*	*t-statistic*	*p-Value*
Intercept	0.07	0.12	-0.17 – 0.30	0.55	0.583
Drug Condition [Placebo]	0.02	0.10	-0.18 – 0.22	0.20	0.843
Random Effects					
σ2	1.30				
τ00 subject	0.30				
ICC	0.19				
N subject	32				
Observations	508				

Table S6: Linear mixed-effects model for O-Information across moving experiences
The model includes the strength of the moving experience (ranging from 1-10) and drug condition (placebo, ketamine) as predictors, with a random intercept for each participant to account for repeated measures. Standardized beta estimates (std. Beta), along with their 95% confidence intervals (std. CI) and standard error (std. SE), are reported. For the random effects, the within-group (σ^2) and between-group (τ_{00}) variances, as well as the intraclass correlation coefficient (ICC), are reported.

	O-Information Moving Experience				
Predictors	*std. Beta*	*std. SE*	*std. CI (95%)*	*t-statistic*	*p-Value*
Intercept	0.03	0.11	-0.18 – 0.24	0.30	0.770
Moving	-0.07	0.02	-0.12 – -0.03	-3.02	**0.003**
Drug Condition [Placebo]	-0.05	0.05	-0.14 – 0.04	-1.10	0.271
Random Effects					
σ2	0.67				
τ00 subject	0.34				
ICC	0.34				
N subject	32				
Observations	1256				

Table S7: Linear mixed-effects model predicting hedonic experiences from hedonic and baseline NBS cluster activity
The model includes the trial-averaged activity of the hedonic cluster, the run-wise averaged activity of the ketamine baseline cluster, and the drug condition (placebo vs. ketamine) as fixed effects. A random intercept for each participant accounts for repeated measures. Data was z-scored prior to calculations. Shown values are based on 10000 wild bootstrap (boot.) iterations. Beta estimates (boot. Beta), along with their 95% confidence intervals (boot. CI) and standard error (boot. SE), are reported. For the random effects, the within-group (σ^2) and between-group (τ_{00}) variances, as well as the intraclass correlation coefficient (ICC), are reported.

			3-way Interaction		
Predictors	*boot. Beta*	*boot. SE*	*boot. CI (95%)*	*t-statistic*	*boot. p-Value*
Intercept	0.08	0.06	-0.05 – 0.20	1.14	0.259
Baseline Cluster	0.04	0.07	-0.10 – 0.17	0.503	0.587
Hedonic Cluster	0.13	0.04	0.05 – 0.21	2.81	**0.012**
Drug [Placebo]	-0.12	0.05	-0.22 – -0.01	-1.75	**0.038**
Baseline Cluster x Hedonic Cluster	-0.14	0.04	-0.23 – -0.05	-2.91	**0.002**
Baseline Cluster x Drug [Placebo]	-0.03	0.07	-0.16 – 0.10	-0.41	0.659
Hedonic Cluster x Drug [Placebo]	-0.03	0.04	-0.11 – 0.05	-0.47	0.493
Baseline Cluster x Hedonic Cluster x Drug [Placebo]	0.17	0.04	0.08 – 0.25	3.22	**0.002**

Random Effects	
σ^2	0.92
$\tau_{00\ subject}$	0.06
ICC	0.06
$N_{\ subject}$	32
Observations	1260

Table S8: Linear mixed-effects model predicting the intensity of the hedonic experience from decomposed NBS hedonic cluster activity

The model predicts the strength of the hedonic experience using the four decomposed dynamics per trial (ΦR^+, rtr^+, ΦR^-, and rtr^-). A random intercept for each participant accounts for repeated measures. Data was z-scored prior to calculations. Parameter estimates are reported along with their 95% confidence intervals (std. CI) and standard errors (std. SE). Reported results are based on cluster-robust covariance matrices (CR1). For the random effects, the within-group (σ^2) and between-group (τ_{00}) variances, as well as the intraclass correlation coefficient (ICC), are reported.

Hedonic experience predicted by Φ^R and rtr

Predictors	*std. Beta*	*std. SE*	*std. CI (95%)*	*t-statistic*	*p-Value*
Intercept	-0.00	0.05	-0.11 – 0.10	-0.01	0.992
Φ^{R+}	0.12	0.04	0.03 – 0.20	2.64	**0.008**
Φ^{R-}	-0.17	0.06	-0.28 – -0.06	-3.07	**0.002**
rtr^+	-0.31	0.04	-0.40 – -0.23	-7.16	**<0.001**
rtr^-	0.26	0.04	0.18 – 0.35	6.19	**<0.001**
Random Effects					
σ^2	0.81				
$\tau_{00\ subject}$	0.07				
ICC	0.08				
$N_{\ subject}$	32				
Observations	1260				

Table S9: Dominance analysis of the linear mixed-effects model predicting the intensity of the hedonic experience from decomposed NBS hedonic cluster activity

Reported results are based on 1000 bootstrap iterations. Changes in marginal R2 and standard errors (SE) are reported.

Dominance analysis of the effects of Φ^R and rtr on hedonic experiences

Predictors	*R2 estimate*	*SE*
Φ^{R+}	0.004	0.003
Φ^{R-}	0.014	0.007
rtr^+	0.077	0.013
rtr^-	0.052	0.012

Table S10: General linear model predicting treatment from decomposed NBS baseline cluster activity

The model predicts drug treatment using the four decomposed dynamics per trial (ΦR^+, rtr^+, ΦR^-, and rtr^-) and a logit-link function. Odds Ratios are reported along with their 95% confidence intervals (CI) and standard errors (SE).

Treatment predicted by Φ^R and rtr

Predictors	*Odds Ratios*	*SE*	*CI*	*Statistic*	*p*
Intercept	0.94	0.10	0.76 – 1.16	-0.57	0.570
Φ^{R+}	2.10	0.27	1.64 – 2.73	5.69	**<0.001**
Φ^{R-}	0.31	0.06	0.21 – 0.43	-6.56	**<0.001**

rtr^-	2.50	0.35	1.92 – 3.34	6.48	**<0.001**
rtr^+	0.45	0.06	0.34 – 0.58	-6.07	**<0.001**

Table S11: Dominance analysis of the generalized linear model predicting drug treatment from decomposed NBS baseline cluster activity
Reported results are based on 1000 bootstrap iterations. Changes in marginal R2 and standard errors (SE) are reported.

	Dominance analysis of the generalized linear model predicting treatment using Φ^R and rtr dynamics	
Predictors	*R2 estimate*	*SE*
Φ^{R+}	0.055	0.020
Φ^{R-}	0.104	0.025
rtr^+	0.072	0.024
rtr^-	0.108	0.029

Table S12: Exploratory analysis of information shifts in the ketamine trial cluster and receptor densities
The ketamine trial cluster, associated with ketamine's effect on neural information dynamics during music perception, exhibited an almost perfectly balanced distribution of increasing and decreasing Φ^{WMS} edges. Thus, we conducted a separate exploratory analysis for both dynamics. Node-level effects were summarized by averaging the weights of significant edges per node for each direction of information shift. These averaged dynamics were then correlated with 19 receptor maps using Spearman rank correlation, with significance determined via 10000 surrogate maps per receptor. Both raw and Bonferroni-corrected p-values are reported.

	Φ^{WMS+}			**Φ^{WMS-}**		
Receptor Name	$r_{spearman}$	*p-value*	*Bonf. p-value*	$r_{spearman}$	*p-value*	*Bonf. p-value*
5HT1a	-0,112	0,682	1	-0,062	0,672	1
5HT1b	0,053	0,784	1	-0,153	0,275	1
5HT2a	0,118	0,670	1	-0,179	0,219	1
5HT4	-0,188	0,324	1	-0,113	0,419	1
5HT6	-0,298	0,113	1	-0,206	0,132	1
5HTT	-0,390	0,126	1	0,217	0,136	1
A4B2	-0,420	0,077	1	-0,110	0,459	1
CB1	-0,179	0,309	1	-0,074	0,593	1
D1	-0,351	0,096	1	0,007	0,957	1
D2	-0,432	**0,046**	0,870	0,073	0,621	1
DAT	-0,463	**0,026**	0,488	0,225	0,120	1
GABAa	0,073	0,816	1	-0,192	0,189	1
H3	-0,381	**0,033**	0,635	-0,214	0,118	1
M1	-0,047	0,821	1	-0,070	0,625	1
mGluR5	-0,280	0,134	1	-0,179	0,202	1
MOR	-0,402	**0,026**	0,488	-0,124	0,387	1
NET	0,064	0,794	1	0,031	0,826	1
NMDA	-0,443	0,050	0,958	0,158	0,291	1
VAChT	-0,422	0,028	0,534	0,132	0,351	1

Table S13: Association between Φ^{WMS+} edges of the hedonic cluster and receptor densities
To examine the relationship between the predominant shift in information integration during hedonic experiences and receptor densities, we averaged the NBS Φ^{WMS+} edge weights for each node to generate node-level representations of the cluster activity. These node-level activities were then correlated with 19 receptor maps using Spearman rank correlation, with significance assessed via 10000 surrogate maps for each receptor. Both raw and Bonferroni-corrected p-values are reported.

Receptor Name	$r_{spearman}$	*p-value*	*Bonf. p-value*
5HT1a	-0,080	0,721	1
5HT1b	-0,139	0,408	1
5HT2a	-0,191	0,380	1
5HT4	-0,083	0,600	1
5HT6	-0,057	0,725	1
5HTT	-0,076	0,732	1
A4B2	0,165	0,466	1
CB1	-0,109	0,513	1
D1	-0,214	0,244	1
D2	-0,089	0,667	1
DAT	-0,173	0,409	1
GABAa	-0,136	0,535	1
H3	0,050	0,757	1
M1	-0,124	0,469	1
mGluR5	0,013	0,933	1
MOR	0,015	0,932	1
NET	0,527	**> 0,001**	**0,017**
NMDA	-0,135	0,538	1
VAChT	0,187	0,274	1

Table S14: Association between Φ^{WMS-} edges of the baseline cluster and receptor densities
To examine the relationship between the predominant shift in information integration associated with ketamine administration and receptor densities, we averaged the NBS Φ^{WMS-} edge weights for each node to generate node-level representations of the cluster activity. These node-level activities were then correlated with 19 receptor maps using Spearman rank correlation, with significance assessed via 10000 surrogate maps for each receptor. Both raw and Bonferroni-corrected p-values are reported.

Receptor Name	$r_{spearman}$	*p-value*	*Bonf. p-value*
5HT1a	0,1	0,5	1
5HT1b	0,014	0,911	1
5HT2a	-0,063	0,674	1
5HT4	-0,01	0,935	1
5HT6	0	0,998	1
5HTT	0,232	0,089	1
A4B2	0,057	0,713	1
CB1	0,079	0,529	1
D1	0,075	0,563	1
D2	0,193	0,153	1
DAT	0,204	0,137	1
GABAa	0,043	0,775	1
H3	-0,03	0,814	1
M1	-0,027	0,832	1

mGluR5	-0,066	0,598	1
MOR	0,127	0,319	1
NET	0,048	0,728	1
NMDA	0,114	0,445	1
VAChT	0,192	0,131	1

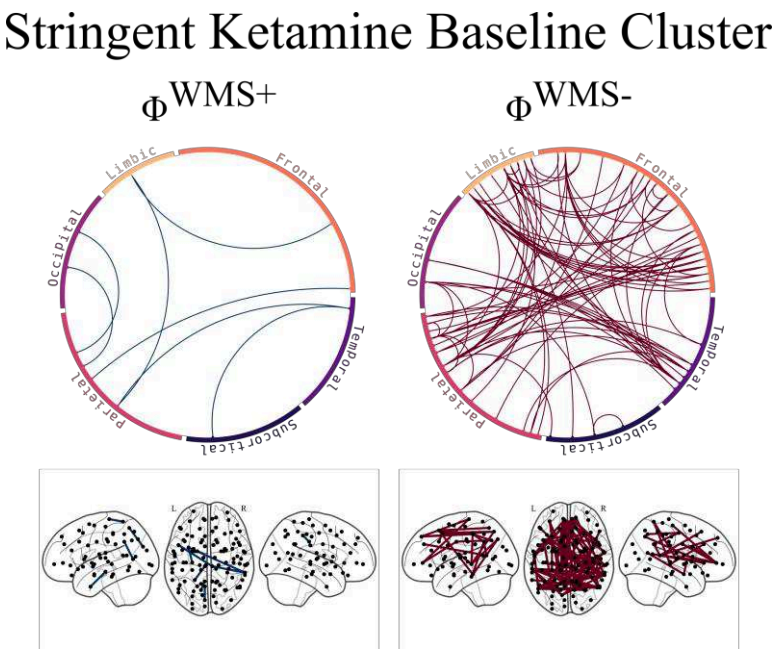

Figure S1: Replication of ketamine's shift of baseline neural dynamics toward redundancy using a conservative window size
To further validate our findings that ketamine predominantly shifts neural dynamics at rest toward redundancy, we analyzed the baseline data using a highly conservative window size. Specifically, the first 14.4 seconds of each baseline segment were excluded to eliminate potential contamination from residual task-related activity. The figure displays the significant Network-Based Statistics cluster for baseline neural activity with increasing edges (Φ^{WMS+}) and decreasing edges (Φ^{WMS-}) for all pairs of regions separately. Edges are visualized both using a chord diagram (upper panel) and in a glass brain (lower panel).

Table S15: Replication of the interaction effect using data of the stringent baseline cluster
The model includes the trial-averaged activity of the hedonic cluster, the run-wise averaged activity of the stringent ketamine baseline cluster, and the drug condition (placebo vs. ketamine) as fixed effects. A random intercept for each participant accounts for repeated measures. Data was z-scored prior to calculations. Shown values are based on 10000 wild bootstrap (boot.) iterations. Beta estimates (boot. Beta), along with their 95% confidence intervals (boot. CI) and standard error (boot. SE), are reported. For the random effects, the within-group (σ^2) and between-group (τ_{00}) variances, as well as the intraclass correlation coefficient (ICC), are reported.

	3-way Interaction				
Predictors	*boot. Beta*	*boot. SE*	*boot. CI (95%)*	*t-statistic*	*boot. p-Value*
Intercept	0.06	0.06	-0.05 – 0.17	0.94	0.347
Baseline Cluster	0.02	0.07	-0.12 – 0.16	0.29	0.786

Hedonic Cluster	0.20	0.04	0.10 – 0.29	4.61	**0.004**
Drug [Placebo]	-0.10	0.06	-0.18 – -0.02	-1.61	**0.026**
Baseline Cluster x Hedonic Cluster	-0.07	0.04	-0.13 – 0.00	-1.70	0.060
Baseline Cluster x Drug [Placebo]	-0.08	0.08	-0.25 – 0.09	-1.05	0.379
Hedonic Cluster x Drug [Placebo]	-0.08	0.06	-0.16 – 0.00	-1.28	0.052
Baseline Cluster x Hedonic Cluster x Drug [Placebo]	0.10	0.05	0.02 – 0.18	2.28	**0.010**

Random Effects

σ^2	0.92
$\tau_{00\ subject}$	0.07
ICC	0.07
$N_{\ subject}$	32
Observations	1260

General Discussion

The aim of this thesis is to advance our understanding of the hedonic experience as a whole by illuminating its inception, tracing its neural emergence, and examining its modulation by the prohedonic agent ketamine. Thereby, the presented work addresses four interrelated questions: (1) Can a hedonic experience arise without external (visual) input purely through mental processes? (2) Is the hedonic experience neurally encoded in a similar way across different stimulus modalities? (3) What are the multivariate information dynamics that underpin peak hedonic states? (4) And how are these processes, behaviorally and neurally, modulated by ketamine across the acute and subacute phase to facilitate its prohedonic effects? To answer these questions, I[1] deployed a diverse set of stimuli, ranging from faces and artworks to monetary rewards and music, and integrated traditional reward paradigms with neuroaesthetic and information-theoretic tools, thereby selecting each methodological approach tailored to each specific question.

To reiterate, Study 1 (Kathofer, Lamm, et al., 2025) examined whether hedonic experiences necessitate direct sensory input or can similarly arise through mental imagery. It further used RSA to systematically test theory-derived encoding models to examine whether behaviorally indistinguishable hedonic experiences across visual perception and visual imagery share the same neural encoding or retain modality-specific signatures. Extending insights into the neural signature of pleasure, Study 4 (Kathofer, Mediano, et al., 2025) characterized the multivariate information processing underlying hedonic experience by applying global and local measures of information integration to determine whether higher-order dynamics, specifically synergy or redundancy, primarily underlie its emergence. Additionally, the study investigated how global integrative brain states dynamically reconfigure over time to facilitate peak hedonic experiences. Lastly, to deepen understanding of ketamine's prohedonic and neuromodulatory effects across the acute and subacute phases, Studies 2 (Graf et al., 2024), 3 (Briem et al., 2025), and 4 (Kathofer, Lamm, et al., 2025) examined ketamine's impact on reward processing by: (i) identifying morphological predictors of adverse psychological responses during administration; (ii) quantifying its effects on neural signatures of reward anticipation and consumption; and (iii) characterizing how ketamine reshapes multivariate neural information integration to enable prohedonic effects.

Taken together, the present thesis contributes both basic and practical insights: it provides insights into a mechanistic account of the hedonic experience grounded in multivariate neural information integration; it highlights morphological markers that may inform personalized treatment and risk mitigation in future clinical studies; and sheds

[1] "I" should be understood to acknowledge the collaborative nature of scientific research and the contributions of coauthors, colleagues, and supervisors whose ideas, feedback, and efforts helped shape, conduct, and refine the studies presented within this thesis.

light on the elusive mechanisms by which ketamine may exert its prohedonic effects. The remainder of this chapter synthesizes these empirical findings, discusses their implications in more detail, and delineates promising avenues for future research.

Do hedonic experiences require direct sensory input? And are they similarly encoded across different modalities? – No, they do not, and given sufficient vivid imagery, hedonic experiences are behaviorally indistinguishable across perception and imagery, yet their neural encodings retain modality-specific signatures.

While the field of neuroaesthetics has substantially advanced our understanding of how cognition (Brielmann & Pelli, 2017), context (Darda & Chatterjee, 2023), and meaning (Trupp et al., 2023) shape the intensity of hedonic experiences evoked by aesthetic stimuli, it has never explicitly tested whether mental processes can themselves generate hedonic responses, rather than merely shape the experience itself. Thus, although intuitively trivial, prior to this thesis it had never been experimentally confirmed whether hedonic experiences require direct input to the sensory system. Additionally motivated by work from Dijkstra and colleagues (2021), who reported that individuals with high imagery abilities can occasionally mistake vivid visual imagery for reality and drive real-world behavior, I expanded this line of inquiry to reward processing by asking whether visual imagery itself can evoke hedonic experiences. Utilizing both biologically and culturally significant stimuli, faces and artworks respectively, Study 1 (Kathofer, Lamm, et al., 2025), found robust evidence that mental imagery is sufficient to elicit pleasurable experiences, as well as related positive affective aesthetic responses, such as being moved or experiences of beauty, alongside physiological markers like chills, indicating that imagery can engage affective and autonomic systems similarly to direct perception. Beyond establishing that direct sensory input is not necessary, the results also highlight that the similarity of hedonic experiences across stimulation modalities converges with increasing vividness of the mental image. This dependency is rather intuitive as a low-fidelity coarse mental image fails to provide a sufficiently detailed representational substrate from which a (similar) hedonic experience could arise. The key finding, however, is that their neural representations remain strongly modality-driven: even when imagined and perceived stimuli receive virtually identical behavioral ratings in high-vividness trials, the brain's encoding patterns still differ markedly and primarily encode the modality in which the stimulus was originally perceived, even in highly specialized regions such as the NAc. In short, behavioral convergence does not imply neural equivalence as modality-specific encoding remains a dominant driving factor for (dis)similarity patterns even when subjective experiences appear the same.

Looking beyond neuroaesthetics, Study 1 (Kathofer, Lamm, et al., 2025) is not the first to show that mental imagery can elicit measurable effects. Rather, it situates itself within an emerging field examining how mental imagery can shape behavior and mental health. Within this diverse field, research has demonstrated that mental images can induce

both positive and negative valence (Görgen et al., 2015; Koivisto & Grassini, 2023), modulate stress-related physiology, i.e., skin conductance (Agren, 2023; Koivisto & Grassini, 2024), and that evoked neural responses tend to converge across stimulation modalities as imagery vividness increases (Dijkstra et al., 2017, 2019). However, Study 1 (Kathofer, Lamm, et al., 2025) extends this literature in three key ways. First, it shows that mental imagery can elicit not only shifts in valence but also other strong positive hedonic emotions, such as feelings of being moved and experiences of beauty, opening avenues to test whether imagery can likewise induce other aesthetic responses, including awe or the sublime. Second, it demonstrates that mental imagery can also evoke potent physiological responses such as piloerection, showing that imagery can be sufficiently evocative to trigger rare, intense autonomic reactions that usually serve as objective indices of the experienced intensity of currently processed representations (Schoeller et al., 2024). Third, while earlier work has reported that responses in visual areas become more similar across modalities during high-vividness trials (Dijkstra et al., 2019), the presented data, targeting higher-level reward processing, paints a more nuanced picture. Although increasing vividness is associated with greater cross-modal neural similarity, this effect is relative rather than absolute. Even when analyses were restricted to strictly high-vividness trials, where neural patterns should, in principle, be most similar across imagery and perception, the winning RSA encoding models consistently showed that neural activity primarily encodes the modality of origin within the reward network and its constituents – regions typically associated with affective processing – underscoring that the brain reliably tracks the source of a stimulus even in highly specialized areas and that mental imagery, while potent, does not fully converge with perception at the neural level.

Study 1 (Kathofer, Lamm, et al., 2025) also opens up several directions for future work. Generally, as imagery ability increases, hedonic responses elicited by visual mental imagery appear to converge toward those elicited by visual perception; future studies should test whether this convergence generalizes to other senses (smell, taste, touch, audition) as a function of sense-specific imagery ability as well. Although the association between higher imagery abilities and more similar ratings across stimulation modalities was evident in the study above, the effect was only modest, likely because the sample was preselected for medium to high imagery ability, thereby reducing variance. Yet, it would be valuable to examine the full spectrum of vividness, from absent imagery as in aphantasia (Blomkvist & Marks, 2023) to exceptionally vivid imagery, to test for a continuous gradient, explaining the full variance in evoked experiences across stimulation modalities, from no detectable hedonic experience in individuals with aphantasia, making imagery maximally dissimilar to perception, to near-equivalence across modalities in those with unusually high vivid imagery.

Are hedonic experiences reliant on a single higher-order information-integration dynamic? No, hedonic experiences appear to arise from complex information dynamics that draw on both synergistic and redundant integration over time.

From its inception to its final moments, the brain continuously integrates signals from internal states and from outside inputs across its large, distributed network. Yet the mechanisms by which these integration dynamics give rise to subjective experience, and specifically to hedonic experience, remain poorly understood. Study 4 (Kathofer, Mediano, et al., 2025) addresses this gap by applying multivariate information-theoretic tools to quantify how neural integration changes over time as subjective hedonic intensity rises. Using various measures to capture the balance between synergistic and redundant interactions, and complementary brain-state analyses to track global shifts in integration dynamics, Study 4 (Kathofer, Mediano, et al., 2025) offers, to my knowledge, the first systematic characterization of information dynamics underlying subjective hedonic experiences.

Together, the results highlight that neural integration associated with the hedonic experience is not confined to canonical reward regions. Instead, increases in hedonic intensity are reflected in information shifts distributed across the entire cortex. Thus, converging with, but extending beyond, prior MVPA analyses (Kahnt, 2018), O-information results show that hedonic experiences alter large-scale integrative dynamics across the entire brain, indicating that hedonia is not a highly localized phenomenon but actually demands the reconfiguration of global information dynamics. This notion is further corroborated by the time-resolved brain-state analysis, revealing that the system alternates between globally expressed synergistic and redundant states, and that the balance and sequencing of these states track the intensity of the hedonic experience. Put differently, hedonia emerges from coordinated whole-brain shifts in both synergy, where signals are integrated to convey more than their individual parts, and redundancy, where signals are shared collaboratively across regions, rather than from a single region-bound information dynamic alone.

Interestingly, while the WMS analysis replicated the broad finding that hedonic experiences emerge from shifts in both synergy and redundancy, a finer decomposition of these dynamics showed that most of these higher-order integration changes are driven by shifts in redundancy. This insight is possible as WMS reflects, in essence, the balance of synergistic and transfer processes relative to redundancy (Mediano et al., 2021). Consequently, an increase in WMS, often interpreted as a net increase of synergistic processing, can arise from (i) an actual increase in synergy, (ii) a reduction in redundancy, or (iii) a combination of both. In this regard, the results indicate that particularly shifts in redundancy account for the observed changes of WMS, even as both dynamics remain relevant to the hedonic experience. Yet, given the extensive fMRI literature on reward processing utilizing (pairwise) correlation of brain activity over time (Dugré et al., 2023; Ng et al., 2019; Tolomeo & Yu, 2022), it is unsurprising that hedonic

experiences appear heavily reliant on redundant information sharing. By construction, these pairwise correlations can only capture the shared variance between two time series and are thus sensitive only to redundant information processing, unable to detect emergent synergistic interactions (Luppi, Rosas, et al., 2024). Extending this literature, our analysis indicates that although emergent synergistic dynamics contribute to reward processing, their role is modest, underscoring the predominance of redundancy. Furthermore, a plausible neurobiological substrate facilitating these changes in neural information integration underlying hedonia was identified, as the topology of the observed WMS cluster activity closely aligns with the spatial distribution of norepinephrine transporter receptors, a system often implicated in arousal, motivation, and euphoria (Sofuoglu & Sewell, 2009).

Lastly, neural information originating in primary auditory areas, which encodes the music input underlying all subsequently elicited hedonic responses, exhibits a distinct reliance on redundant information sharing with its connected cluster nodes. In particular, auditory areas exhibited increased sharing of redundant information with key relay and integration hubs, including the thalamus (Hwang et al., 2017) and insula (Zhang et al., 2024). Storing vital incoming signals redundantly across multiple nodes, especially canonical gateways and information synthesis regions, serves two main functions. First, it ensures rapid availability of information across critical areas for further integration and downstream processing. Secondly, maintaining multiple redundant neural representations makes the information less susceptible to disruption, thereby supporting reliable and stable processing. Though speculative, this interpretation aligns with human and animal evidence that redundancy stabilizes essential sensory information (Newman et al., 2022; Panzeri et al., 2022; Pope et al., 2025; So et al., 2012) and enhances subsequent behavioral performance (Francis et al., 2022; Koçillari et al., 2023c, 2023b; Varley, Sporns, et al., 2023b).

Although demonstrated here in the context of hedonic processing, I suspect that this general pattern, i.e., shifts in synergistic and redundant information dynamics, underlies cognitive function more broadly. While speculative, it is reasonable to assume that the brain leverages both forms of higher-order information processing, each with distinct advantages and trade-offs. As noted in the introduction, synergy, though fragile, enables the system to encode and compute information that is emerging from the coordinated activity of multiple streams, vastly expanding neural computational power. By contrast, redundancy, especially for vital inputs that must be accessed across multiple relay hubs and multimodal integration centers, promotes rapid availability and robustness, albeit at the cost of allocating resources to maintain duplicated representations. Recent advances in multivariate information theory have spurred efforts to map specific information dynamics to specific cognitive functions (Luppi, Rosas, et al., 2024; Varley, Sporns, et al., 2023a). Prior work has suggested that synergy may be central to the emergence of consciousness (Luppi, Mediano, et al., 2024), whereas redundancy may be critical for stabilizing sensory representations (Varley, Pope, et al., 2023). However, it

is unlikely that neural information dynamics can be cleanly partitioned into one-to-one mappings onto particular functions, partly because most studies a priori focus on a single dynamic and do not jointly examine others. A more plausible trajectory of this field mirrors the evolution of our understanding of distinct neurotransmitter contributions to reward: from an initial emphasis on a single neurotransmitter system, to multiple systems, to a consensus that coordinated interactions among many systems are necessary for a hedonic experience to successfully emerge. Likewise, the study of multivariate information dynamics will likely progress from isolating specific components to recognizing that synergy, redundancy, and related processes jointly and flexibly support cognition. Going forward, research should prioritize comprehensive assessments of higher-order information dynamics, examining how synergy, redundancy, and related processes interact to support reward and other cognitive functions. However, progress is currently limited by the combinatorial complexity of observable dynamics and by the fact that different estimator implementations, reflecting distinct mathematical conceptualizations of higher-order interactions, often yield divergent results. To advance, the field needs stronger theoretical unification, novel statistical frameworks to better evaluate shifts in multivariate information flows, and coordinated benchmarking to guarantee comparability and robustness across existing metrics.

Are morphological predispositions linked to the acute aversive anxiety-inducing effects of ketamine during administration? Yes, hippocampal, not amygdalar, volume is negatively correlated with acute anxiety during ketamine administration.

Beyond a more thorough understanding of the multivariate information dynamics that give rise to hedonic experiences, it is equally important to determine how they can be more effectively modulated. This is especially important given that anhedonia, the inability to experience pleasure, is common across many psychiatric disorders (Destoop et al., 2019; Rømer Thomsen et al., 2015; Trøstheim et al., 2020) and associated with poorer prognosis (Crits-Christoph et al., 2018; Garfield et al., 2013; Luca et al., 2024; Vrieze et al., 2014; Wong et al., 2024). Limited efficacy of conventional medication (Cao et al., 2019; Craske et al., 2016) and rising rates of anhedonic symptoms in the general population (Abbott, 2021) further underscore the dire need for more effective treatments. Consequently, the present thesis aimed to contribute to a more detailed understanding of the mechanisms underlying ketamine's unique, rapid-acting prohedonic effects, which, unlike those of common antidepressants (Boku et al., 2018), emerge within hours of administration (Krystal et al., 2019). While Study 2 (Graf et al., 2024) focused on the acute phase, examining psychotomimetic effects and their relationship to morphological neural correlates, Studies 3 (Briem et al., 2025) and 4 (Kathofer, Mediano, et al., 2025) characterized ketamine's neuromodulatory effects in the subacute phase, when psychotomimetic effects have typically subsided and

prohedonic effects begin to emerge (Zarate et al., 2006), thereby advancing insight across these two critical phases.

Although it remains contentious whether the acute psychomimetic effects of ketamine and other psychoplastogens, e.g., psilocybin, during administration are causally responsible for, merely modulatory of, or entirely unrelated to their therapeutic effects (Ballard & Zarate, 2020; Grabski et al., 2020; Hesselgrave et al., 2021; Yaden & Griffiths, 2020), multiple studies highlight that the acute experiences during ketamine administration, both positive and negative (Aepfelbacher et al., 2024; Aust et al., 2019; Luckenbaugh et al., 2014), are associated with subsequent clinical outcomes. In general, the most common acute side effect of subanesthetic ketamine is anxiety (Short et al., 2018). Given that infusion-related anxiety has been linked to significantly poorer clinical outcomes (Aust et al., 2019) and can even lead to treatment discontinuation (Feifel et al., 2020), Study 2 (Graf et al., 2024) sought to test whether individual differences in neural morphology are associated with this common adverse response. The goal was to provide insight relevant to precision medicine by identifying morphological predictors of experienced anxiety during administration, thereby improving risk stratification and individualized care. To do so, the study assessed hippocampal and amygdalar volumes, two regions strongly implicated in anxiety (Espinoza Oyarce et al., 2020; Ghasemi et al., 2022; Hayano et al., 2009; Kim et al., 2011; Shi et al., 2023), and tested whether these measures are associated with the intensity of subjective anxiety during infusion. The analysis indicates an inverse relationship between hippocampal head volume and the intensity of acute anxiety during ketamine administration. Yet, it should be noted that these findings were derived from a single study in healthy individuals and replication, particularly in the clinical populations for whom ketamine is indicated, is essential to determine whether hippocampal head morphology is exclusively predictive of infusion-related anxiety, without any contributions of the amygdalar volume. Nevertheless, the observed pattern aligns with prior work (Satpute et al., 2012), suggesting distinct functional specialization of hippocampal subfields. More specifically, the anterior hippocampus is more closely linked to state anxiety, the transient experience of fear, while posterior regions are more associated with trait anxiety. In this context, the present morphological results are consistent with reduced anterior hippocampal volume being associated with acute state-like anxiogenic responses during ketamine administration.

So, should individuals, especially focusing here on the generalization of these findings to patients with major depressive disorder, be excluded from ketamine treatment on the basis of a smaller hippocampal head volume due to a potentially higher likelihood of acute averse anxiogenic responses and treatment discontinuation? No. These findings should be interpreted primarily as a potential moderator, linking phenomenology to a biological marker, which is useful for modeling treatment outcomes and informing risk mitigation. This recommendation is based on several observations in the broader depression literature. First, the very patients for whom ketamine treatment is usually

intended, patients with (treatment-resistant) major depressive disorder, typically exhibit significantly reduced hippocampal volume (Espinoza Oyarce et al., 2020). Second, some evidence suggests that ketamine exerts a more pronounced antidepressant effect in patients with smaller hippocampal volume (Abdallah et al., 2015; however also see Dutton et al., 2024). Third, although evidence is scarce in humans, findings suggest that ketamine increases hippocampal volume through its neuroplastic properties, providing a plausible pathway for its antidepressant and prohedonic effects (Höflich et al., 2021). Thus, while the presented results highlight that smaller hippocampal volume is associated with a greater likelihood of acute anxiety-provoking experiences during ketamine administration, the very patients for whom ketamine treatment is typically intended exhibit this particular morphology. Hence, rather than concluding that a smaller hippocampal volume might be predictive of worse overall treatment outcomes and warranting the exclusion of such individuals from treatment a priori, it merely highlights an important trade-off: heightened acute anxiety-inducing responses during administration versus the potential for meaningful improvement afterward. Clinically, the question should thus not be whether these patients are suitable for ketamine treatment, but how best to anticipate, support, and manage acute anxiety during administration.

Does ketamine exert measurable behavioral effects on reward processing in healthy participants in the subacute phase? Yes, it increases the hedonic experience, both affective and physiological markers; however, residual adverse effects are still present.

As alluded to above, subanesthetic doses of ketamine can induce a range of common adverse side effects, including anxiety, blurred vision, headache, nausea, dry mouth, poor coordination, restlessness, and dizziness (Murrough et al., 2013; Short et al., 2018). Although these responses are typically assumed to abate shortly after infusion and thus be confined to the acute phase, data from Study 2 (Graf et al., 2024) indicate that they persist into the subacute phase. Despite a marked reduction in symptom intensity from the acute to the subacute phase following ketamine administration, participants still reported significantly more adverse effects four hours post-infusion under ketamine than under placebo. Since residual side effects, such as nausea or general malaise (Becker et al., 2019), can dampen hedonic experience and reduce task-based pleasure ratings, monitoring of psychotomimetic and adverse effects should extend way beyond the infusion into the subacute and early post-acute windows. More specifically, researchers should track these symptoms and include them as time-varying covariates even when tasks occur several hours after dosing, as lingering symptoms may attenuate ketamine's therapeutic effects. This is especially important to consider for studies of ketamine's prohedonic effects in healthy participants, where expected effects are likely small in the absence of aberrant reward processing.

Nonetheless, Study 4 (Kathofer, Mediano, et al., 2025) provides clear evidence that ketamine exerts prohedonic effects in healthy participants during the subacute phase. Data from the specifically designed hedonic music task highlights that ketamine increased all tested dimensions of the hedonic experience, from basic judgments of stimulus valence to the more emotionally connoted positive experience of being moved (Menninghaus et al., 2015). It likewise enhanced the subjective intensity of experienced chills, a physiological marker of peak hedonic experience (Schoeller et al., 2024). Together, these findings support the conclusion that ketamine increases the hedonic experience, the consummatory component of reward processing, even in people who do not present with reward dysfunction or anhedonia, indicating that ketamine can exert its prohedonic effects also in individuals without clinical deficits. This is especially noteworthy as, unlike other studies typically relying on self-report questionnaires, our paradigm provides experimental evidence of ketamine's prohedonic effects at an understudied time point within its therapeutic window, addressing a notable gap in the literature. However, compared with the robust, large therapeutic effects often reported in patients with major depressive disorder (Almeida et al., 2024; Nikolin et al., 2023), the effects observed in this study were only small. A fact largely anticipated, as healthy individuals, by definition, should not exhibit pronounced anhedonic symptoms, leaving limited room for improvement. Despite this potential ceiling effect, the data demonstrates that ketamine's prohedonic effects also manifest in healthy individuals during the subacute phase, roughly four hours after drug administration.

A key implication of these results for prevention research is that if ketamine can enhance hedonic experience even in individuals without clinical deficits, it may help buffer against emerging anhedonia and depressive symptoms in those with subclinical depression. This group typically exhibits mild anhedonic and depressive symptoms without meeting diagnostic criteria, yet faces a substantially elevated risk of progressing to major depressive disorder (Lee et al., 2019). Prevention studies should therefore examine whether transient reductions in depressive symptoms using ketamine can serve as strategic interventions to stabilize affective functioning before a full depressive episode consolidates.

What are ketamine's effects on neural activity in the sub-acute phase? In the MID, ketamine showed no effects on any stages of reward processing, whereas during the hedonic music task, multivariate analyses revealed a distinct shift toward redundancy-dominated information processing in the resting-state, potentially underlying its pro-hedonic effects.

Despite clear behavioral evidence that ketamine robustly enhances hedonic experiences in the subacute phase, its corresponding neuromodulatory effects were rather elusive. Especially, the analysis of the MID task did not reveal any ketamine-related changes in neural activity associated with either the anticipatory or the

consummatory phase of pleasure. This is surprising given that we specifically examined canonical reward regions, including the amygdala, insula, NAc, striatum, and thalamus, which are typically implicated in general reward processing (Yarkoni et al., 2011). Although evidence is scarce, prior studies using the MID have reported ketamine-induced alterations in similar regions, though at different post-infusion time points and across different cohorts. For instance, in remitted patients with depression, ketamine-related neuromodulatory effects have been observed around 2 hours post-administration during both anticipation and consumption (feedback), across mesolimbic structures including the amygdala, ventral and dorsal striatum, VTA, and insula (Kotoula et al., 2021). By contrast, when focusing on healthy participants, the neuromodulatory effects of ketamine appear to be less distinct. François and colleagues (2016) reported attenuated ventral striatal responses confined to the anticipatory phase at 40 minutes post-infusion, with no corresponding change during the feedback phase. In comparison, our study, which detected no ketamine-related neuromodulation, examined a later subacute window, when ketamine and its metabolite norketamine are well past peak concentrations (Kamp et al., 2020). As ketamine's effects appear to depend on both cohort, with clinical samples showing more robust findings, and timing, our null result might reflect a transitional period in which acute psychotomimetic and acute wide-spread receptor blocking effects have already subsided and neuroplastic processes are beginning, but are not yet detectable as robust task-evoked BOLD changes in canonical reward regions.

An alternative complementary explanation is analytic sensitivity. The analysis of the MID task relied on mass-univariate contrasts, which may have been unable to detect more subtle distributed neural shifts associated with ketamine's neuromodulatory effects. An interpretation corroborated by a power analysis, highlighting that the study was only sufficiently powered to detect large effects, rendering smaller ketamine-related changes effectively invisible. In general, this approach stands in sharp contrast to the analysis used for the hedonic music task, which employed multivariate methods to characterize ketamine's effects on neural dynamics. Thereby, the study fundamentally shifted its focus from detecting localized activation differences to examining how ketamine modulates neural information exchange across the brain's network.

While the emergence of the hedonic experience itself appears to reshape global neural information dynamics (Kathofer, Mediano, et al., 2025), the same O-information analysis indicates that ketamine does not significantly alter global information processing in the subacute phase. Although prior work has reported that ketamine can indeed induce powerful global changes in information dynamics using the same measure (Herzog et al., 2024), our results suggest these effects are confined to the tested acute window and are therefore unlikely to underwrite its prohedonic effects during the subacute phase. In contrast, finer-grained examinations of pairwise information dynamics using WMS revealed ketamine-related modulation of neural information flow during both rest and music listening (task performance). At rest, ketamine shifted dynamics almost

unanimously toward greater redundancy across a broad network spanning frontal, parietal, and subcortical regions, whereas during task performance, effects were more heterogeneous, with distinct increases and decreases across regions. Together, these findings provide the first evidence of ketamine's neuromodulatory impact on neural information flow in the subacute phase and highlight a fundamental dissociation: ketamine promotes redundant dynamics at rest but exerts mixed region-dependent effects during active music listening.

Nevertheless, the WMS analysis did not clearly reveal how ketamine specifically exerts its prohedonic effect during the task, as no interaction effect emerged between the intensity of evoked hedonic experiences and ketamine on neural information dynamics during task performance. Given the observed importance of redundancy for the emergence of the hedonic experience in the hedonic music task and the distinct redundant shift of resting dynamics following ketamine administration, I hypothesized that ketamine might facilitate its therapeutic effects through precisely this shift of resting information dynamics toward greater redundancy, and that the magnitude of this shift would be predicative of ketamine's prohedonic effects during the task. The rationale being that increased redundancy enhances the brain's baseline access to critical internal representations distributed across its network, and since hedonic experiences are shaped by both internal and external processes (Leder et al., 2004), ketamine basically fosters a neural state that supports more intense hedonic experiences, even when identical integrative processes within the observed hedonic cluster are triggered from the same identical incoming (musical) inputs. An additional analysis supported this conjecture, showing that the greater ketamine shifted neural information dynamics toward redundancy at rest, the more intense the subjective hedonic experience during music listening, despite identical stimulus-driven integrative demands. To my knowledge, this provides the first experimental evidence that ketamine's prohedonic effects may be mediated by a widespread shift of resting neural dynamics toward redundancy, potentially enabling more reliable access to internal representations through increased information sharing across regions.

However, the association links ketamine-induced changes in resting-state information dynamics to subsequent hedonic responses during task performance, rather than demonstrating a direct ketamine-by-hedonic-intensity interaction in task-evoked dynamics. This is a valid limitation. That said, numerous studies show that resting-state dynamics are closely linked to task-evoked neural activity and can predict subsequent task performance (Biernacki et al., 2026; Cole et al., 2016; Sala-Llonch et al., 2012; Stevens & Spreng, 2014), supporting the view that baseline activity can be indicative of downstream behavior. In this context, it seems reasonable to posit that ketamine alters intrinsic (resting) dynamics in particular ways that are predictive of its prohedonic effect during later task performance. Indeed, emerging evidence suggests that ketamine can increase redundancy in resting-state dynamics (Herzog et al., 2024; Kotoula et al.,

2021), aligning with our observed association. Our proposed mechanism that ketamine's prohedonic effects arise from its impact on intrinsic resting-state dynamics that enhance access to (critical) internal information, though plausible, requires further validation, ideally in clinical populations in which baseline reward processing is atypical. Studies with dense sampling across ketamine's therapeutic window are necessary to further corroborate the idea that ketamine's therapeutic effects diminish as redundancy returns toward baseline. Lastly, our tentative interpretation that ketamine's shift toward more redundant resting-state information dynamics facilitates a brain state with improved access to internal representations, unconscious thought, and other intrinsic processes requires targeted tests. Specifically, future work needs to examine whether this putative enhancement of access to internal information improves performance on tasks that rely heavily on intrinsic processing and similarly diminish as ketamine's effects on resting-state dynamics wane. Still, the presented work outlines a theoretically plausible and easily testable mechanism for how ketamine might facilitate its prohedonic effects.

Conclusion

Reward processing is vital to all living organisms, as it underlies motivation, learning, decision-making, and, more generally, goal-directed behavior (Dayan & Balleine, 2002; Grace et al., 2007; Rushworth et al., 2011). Consequently, enormous interdisciplinary efforts have been dedicated to understanding its normal and aberrant forms (Ng et al., 2019), the neural mechanisms that support it (Watabe-Uchida et al., 2017), and its effective pharmacological modulation (Cao et al., 2019). To do so, researchers have employed a myriad of different paradigms across a multitude of species (Berridge & Kringelbach, 2008). The work presented in this thesis aimed to meaningfully contribute to this collaborative endeavor by expanding our knowledge of the hedonic experience in particular, from its inception and acute phenomenological experience to its modulation by the prohedonic agent ketamine. Acknowledging the many ways hedonic experiences can be elicited, the studies deliberately used a diverse set of stimuli, including money, music, and art, and leveraged task-appropriate analytic methods to address open questions in these domains.

Collectively, the results of this thesis expand our understanding of the necessary conditions under which hedonic experiences emerge and refine our view of their neural substrate, the reward network, by showing that these populations encode more than pleasure per se, challenging the common, overly narrow view that activity in these regions is purely valence-related. By integrating the study of neural encoding with an account of the dynamic, multivariate information processes that underlie hedonic experience, the thesis provides valuable insights into the neural basis of hedonia from two complementary angles. Although the brain continuously integrates information across its vast network of neurons, this process is not directly measurable with current

methods. Nonetheless, as technological and mathematical tools have advanced over the decades, neuroscience has progressed from simple activation studies to network neuroscience and causal modeling, seeking ever more faithful descriptions of brain function. Building on these advances, the present thesis provides evidence that intense hedonic experiences arise from a distinct temporal evolution of both synergistic and redundant brain states and emphasizes the important role of redundancy in information sharing about an incoming stimulation, on which subsequent hedonic processes rely. Together, these insights provide, for the first time, a glimpse into the multivariate information dynamics underpinning hedonic experience and lay the groundwork for future investigations into the specific role that early redundancy in stimulus-information propagation plays in shaping subsequent behavior.

Yet, this thesis aimed not only to deepen our understanding of how hedonic experiences emerge from neural activity, but also to provide a clearer account of ketamine's therapeutic and neuromodulatory effects across the acute and subacute phases. Importantly, the presented work highlights a link between individual morphological predispositions and acute adverse side effects. Extrapolating these findings to MDD patients, clinicians are advised to proactively anticipate intense anxiety-related symptoms in MDD patients during ketamine administration and implement targeted mitigation strategies to improve well-being and thus potentially preserve ketamine's therapeutic efficacy. Furthermore, the findings of this thesis also advance our understanding of ketamine's neuromodulatory effects in the subacute phase. While a traditional activation-contrast paradigm did not detect any ketamine-related neural modulation during either the anticipation or consumption phases, the analysis of multivariate neural information dynamics revealed that ketamine does indeed markedly shift dynamics at rest. This, in combination with the observed increase in hedonic responses, clearly demonstrates that ketamine already exerted its prohedonic neuromodulatory effects at the time of testing and thus should have been detectable by the MID task, which was conducted immediately after the hedonic music task. One explanation is that traditional contrast paradigms may lack the necessary sensitivity to detect ketamine's impact on neural activity in the subacute phase, whereas multivariate information-theoretic approaches may be better suited to study its (subtler) neuromodulatory effects. This multivariate approach further identified a potential neural correlate, a uniform shift toward redundancy in resting-state information dynamics, that may underpin ketamine's rapid-acting prohedonic effects and thus provides a tangible starting point for more focused mechanistic studies.

In conclusion, this thesis advances our understanding of the hedonic experience, from its static encoding in the reward network and the dynamic information processes underlying its emergence, to its effective modulation by the prohedonic agent ketamine.

Literature

Abbott, A. (2021). COVID's mental-health toll: How scientists are tracking a surge in depression. *Nature*, *590*(7845), 194–195. https://doi.org/10.1038/d41586-021-00175-z

Abdallah, C. G., Salas, R., Jackowski, A., Baldwin, P., Sato, J. R., & Mathew, S. J. (2015). Hippocampal Volume And The Rapid Antidepressant Effect Of Ketamine. *Journal of Psychopharmacology (Oxford, England)*, *29*(5), 591–595. https://doi.org/10.1177/0269881114544776

Aepfelbacher, J., Panny, B., & Price, R. B. (2024). Experiences of Awe Mediate Ketamine's Antidepressant Effects: Findings From a Randomized Controlled Trial in Treatment-Resistant Depression. *Biological Psychiatry Global Open Science*, *4*(4), 100316. https://doi.org/10.1016/j.bpsgos.2024.100316

Agren, T. (2023). Physiological and subjective arousal to prospective mental imagery: A mechanism for behavioral change? *PLOS ONE*, *18*(12), e0294629. https://doi.org/10.1371/journal.pone.0294629

Alí Diez, I., Fàbrega-Camps, G., Parra-Tíjaro, J., & Marco-Pallarés, J. (2024). Anticipatory and consummatory neural correlates of monetary and music rewarding stimuli. *Brain and Cognition*, *179*, 106186. https://doi.org/10.1016/j.bandc.2024.106186

Almeida, T. M., Generoso, I. P., Rosa, D. A. A., Pinheiro, T. B., Foletto, L. D., Jorge, G. M. T., Grilo, L. B., da Silva, U. R. L., Cordeiro, Q., & Uchida, R. R. (2024). The anti-anhedonic effects of ketamine in the treatment of resistant unipolar and bipolar depression: A systematic review and meta-analysis of current data. *Journal of Affective Disorders Reports*, *17*, 100829. https://doi.org/10.1016/j.jadr.2024.100829

Alnefeesi, Y., Chen-Li, D., Krane, E., Jawad, M. Y., Rodrigues, N. B., Ceban, F., Di Vincenzo, J. D., Meshkat, S., Ho, R. C. M., Gill, H., Teopiz, K. M., Cao, B., Lee, Y., McIntyre, R. S., & Rosenblat, J. D. (2022). Real-world effectiveness of ketamine in treatment-resistant depression: A systematic review & meta-analysis. *Journal of Psychiatric Research*, *151*, 693–709. https://doi.org/10.1016/j.jpsychires.2022.04.037

American Psychiatric Association. (2013). *Diagnostic and Statistical Manual of Mental Disorders (DSM-5®)*. American Psychiatric Publishing.

Arcangeli, M., Sperduti, M., Jacquot, A., Piolino, P., & Dokic, J. (2020). Awe and the Experience of the Sublime: A Complex Relationship. *Frontiers in Psychology*, *11*. https://doi.org/10.3389/fpsyg.2020.01340

Ashok, A. H., Marques, T. R., Jauhar, S., Nour, M. M., Goodwin, G. M., Young, A. H., & Howes, O. D. (2017). The dopamine hypothesis of bipolar affective disorder: The state of the art and implications for treatment. *Molecular Psychiatry*, *22*(5), 666–679. https://doi.org/10.1038/mp.2017.16

Aust, S., Gärtner, M., Basso, L., Otte, C., Wingenfeld, K., Chae, W. R., Heuser-Collier, I., Regen, F., Cosma, N. C., van Hall, F., Grimm, S., & Bajbouj, M. (2019). Anxiety during ketamine infusions is associated with negative treatment responses in

major depressive disorder. *European Neuropsychopharmacology: The Journal of the European College of Neuropsychopharmacology*, *29*(4), 529–538. https://doi.org/10.1016/j.euroneuro.2019.02.005

Bahji, A., Vazquez, G. H., & Zarate, C. A. (2021). Comparative efficacy of racemic ketamine and esketamine for depression: A systematic review and meta-analysis. *Journal of Affective Disorders*, *278*, 542–555. https://doi.org/10.1016/j.jad.2020.09.071

Ballard, E. D., & Zarate, C. A. (2020). The role of dissociation in ketamine's antidepressant effects. *Nature Communications*, *11*(1), 6431. https://doi.org/10.1038/s41467-020-20190-4

Balodis, I. M., & Potenza, M. N. (2015). Anticipatory Reward Processing in Addicted Populations: A Focus on the Monetary Incentive Delay Task. *Biological Psychiatry, Neural Mechanisms in Addiction*, *77*(5), 434–444. https://doi.org/10.1016/j.biopsych.2014.08.020

Barrett, A. B., & Seth, A. K. (2011). Practical Measures of Integrated Information for Time-Series Data. *PLOS Computational Biology*, *7*(1), e1001052. https://doi.org/10.1371/journal.pcbi.1001052

Barron, A. B., Søvik, E., & Cornish, J. L. (2010). The Roles of Dopamine and Related Compounds in Reward-Seeking Behavior Across Animal Phyla. *Frontiers in Behavioral Neuroscience*, *4*. https://doi.org/10.3389/fnbeh.2010.00163

Becker, S., Bräscher, A.-K., Bannister, S., Bensafi, M., Calma-Birling, D., Chan, R. C. K., Eerola, T., Ellingsen, D.-M., Ferdenzi, C., Hanson, J. L., Joffily, M., Lidhar, N. K., Lowe, L. J., Martin, L. J., Musser, E. D., Noll-Hussong, M., Olino, T. M., Pintos Lobo, R., & Wang, Y. (2019). The role of hedonics in the Human Affectome. *Neuroscience & Biobehavioral Reviews*, *102*, 221–241. https://doi.org/10.1016/j.neubiorev.2019.05.003

Belujon, P., & Grace, A. A. (2017). Dopamine System Dysregulation in Major Depressive Disorders. *International Journal of Neuropsychopharmacology*, *20*(12), 1036–1046. https://doi.org/10.1093/ijnp/pyx056

Berridge, K. C., & Kringelbach, M. L. (2008). Affective neuroscience of pleasure: Reward in humans and animals. *Psychopharmacology*, *199*(3), 457–480. https://doi.org/10.1007/s00213-008-1099-6

Berridge, K. C., Robinson, T. E., & Aldridge, J. W. (2009). Dissecting components of reward: 'Liking', 'wanting', and learning. *Current Opinion in Pharmacology*, *9*(1), 65–73. https://doi.org/10.1016/j.coph.2008.12.014

Biernacki, K., Zhai, T., Hill, J., McConnell, E., Salmeron, B.-J., Kaiser, R. H., & Janes, A. C. (2026). From rest to focus: Pharmacological modulation of the relationship between resting state dorsal attention network dynamics and task-based brain activation. *Neuropsychopharmacology*, 1–8. https://doi.org/10.1038/s41386-025-02318-6

Blomkvist, A., & Marks, D. F. (2023). Defining and 'diagnosing' aphantasia: Condition or individual difference? *Cortex*, *169*, 220–234. https://doi.org/10.1016/j.cortex.2023.09.004

Boku, S., Nakagawa, S., Toda, H., & Hishimoto, A. (2018). Neural basis of major depressive disorder: Beyond monoamine hypothesis. *Psychiatry and Clinical Neurosciences*, *72*(1), 3–12. https://doi.org/10.1111/pcn.12604

Brielmann, A. A., & Pelli, D. G. (2017). Beauty Requires Thought. *Current Biology*, *27*(10), 1506-1513.e3. https://doi.org/10.1016/j.cub.2017.04.018

Brielmann, A. A., Vale, L., & Pelli, D. G. (2017). Beauty at a glance: The feeling of beauty and the amplitude of pleasure are independent of stimulus duration. *Journal of Vision*, *17*(14), 9. https://doi.org/10.1167/17.14.9

Briem, E., Stöhrmann, P., Dörl, G., Milz, C., Schlosser, G., Klöbl, M., Reed, M., Atger, M., Schmidt, C., Kathofer, M., Godbersen, G. M., Crone, J. S., Lanzenberger, R., & Spies, M. (2025). *Subacute Effects of Ketamine on Neural Correlates of Reward Processing* (p. 2025.09.10.675318). bioRxiv. https://doi.org/10.1101/2025.09.10.675318

Cao, B., Zhu, J., Zuckerman, H., Rosenblat, J. D., Brietzke, E., Pan, Z., Subramanieapillai, M., Park, C., Lee, Y., & McIntyre, R. S. (2019). Pharmacological interventions targeting anhedonia in patients with major depressive disorder: A systematic review. *Progress in Neuro-Psychopharmacology and Biological Psychiatry*, *92*, 109–117. https://doi.org/10.1016/j.pnpbp.2019.01.002

Castro, D. C., Cole, S. L., & Berridge, K. C. (2015). Lateral hypothalamus, nucleus accumbens, and ventral pallidum roles in eating and hunger: Interactions between homeostatic and reward circuitry. *Frontiers in Systems Neuroscience*, *9*. https://doi.org/10.3389/fnsys.2015.00090

Ceban, F., Rosenblat, J. D., Kratiuk, K., Lee, Y., Rodrigues, N. B., Gill, H., Subramaniapillai, M., Nasri, F., Lui, L. M. W., Lipsitz, O., Kumar, A., Lee, J. G., Chau, E. H., Cao, B., Lin, K., Ho, R. C., Mansur, R. B., Swainson, J., & McIntyre, R. S. (2021). Prevention and Management of Common Adverse Effects of Ketamine and Esketamine in Patients with Mood Disorders. *CNS Drugs*, *35*(9), 925–934. https://doi.org/10.1007/s40263-021-00846-5

Chen, G., Lai, S., Bao, G., Ke, J., Meng, X., Lu, S., Wu, X., Xu, H., Wu, F., Xu, Y., Xu, F., Bi, G.-Q., Peng, G., Zhou, K., & Zhu, Y. (2023). Distinct reward processing by subregions of the nucleus accumbens. *Cell Reports*, *42*(2). https://doi.org/10.1016/j.celrep.2023.112069

Chen, M.-H., Lin, W.-C., Wu, H.-J., Bai, Y.-M., Li, C.-T., Tsai, S.-J., Hong, C.-J., Tu, P.-C., Cheng, C.-M., & Su, T.-P. (2020). Happiness During Low-Dose Ketamine Infusion Predicts Treatment Response: Reexploring the Adjunctive Ketamine Study of Taiwanese Patients With Treatment-Resistant Depression. *The Journal of Clinical Psychiatry*, *81*(6), 20m13232. https://doi.org/10.4088/JCP.20m13232

Cole, M. W., Ito, T., Bassett, D. S., & Schultz, D. H. (2016). Activity flow over resting-state networks shapes cognitive task activations. *Nature Neuroscience*, *19*(12), 1718–1726. https://doi.org/10.1038/nn.4406

Cousins, D. A., Butts, K., & Young, A. H. (2009). The role of dopamine in bipolar disorder. *Bipolar Disorders*, *11*(8), 787–806. https://doi.org/10.1111/j.1399-5618.2009.00760.x

Craske, M. G., Meuret, A. E., Ritz, T., Treanor, M., & Dour, H. J. (2016). Treatment for Anhedonia: A Neuroscience Driven Approach. *Depression and Anxiety*, *33*(10), 927–938. https://doi.org/10.1002/da.22490

Crits-Christoph, P., Wadden, S., Gaines, A., Rieger, A., Gallop, R., McKay, J. R., & Gibbons, M. B. C. (2018). Symptoms of anhedonia, not depression, predict the outcome of treatment of cocaine dependence. *Journal of Substance Abuse Treatment*, *92*, 46–50. https://doi.org/10.1016/j.jsat.2018.06.010

Darda, K. M., & Chatterjee, A. (2023). The impact of contextual information on aesthetic engagement of artworks. *Scientific Reports*, *13*(1), 4273. https://doi.org/10.1038/s41598-023-30768-9

Davis, T., LaRocque, K. F., Mumford, J. A., Norman, K. A., Wagner, A. D., & Poldrack, R. A. (2014). What do differences between multi-voxel and univariate analysis mean? How subject-, voxel-, and trial-level variance impact fMRI analysis. *NeuroImage*, *97*, 271–283. https://doi.org/10.1016/j.neuroimage.2014.04.037

Dayan, P., & Balleine, B. W. (2002). Reward, Motivation, and Reinforcement Learning. *Neuron*, *36*(2), 285–298. https://doi.org/10.1016/S0896-6273(02)00963-7

Destoop, M., Morrens, M., Coppens, V., & Dom, G. (2019). Addiction, Anhedonia, and Comorbid Mood Disorder. A Narrative Review. *Frontiers in Psychiatry*, *10*. https://doi.org/10.3389/fpsyt.2019.00311

Diedrichsen, J., & Kriegeskorte, N. (2017). Representational models: A common framework for understanding encoding, pattern-component, and representational-similarity analysis. *PLOS Computational Biology*, *13*(4), e1005508. https://doi.org/10.1371/journal.pcbi.1005508

Dijkstra, N., Bosch, S. E., & Gerven, M. A. J. van. (2017). Vividness of Visual Imagery Depends on the Neural Overlap with Perception in Visual Areas. *Journal of Neuroscience*, *37*(5), 1367–1373. https://doi.org/10.1523/JNEUROSCI.3022-16.2016

Dijkstra, N., Bosch, S. E., & Gerven, M. A. J. van. (2019). Shared Neural Mechanisms of Visual Perception and Imagery. *Trends in Cognitive Sciences*, *23*(5), 423–434. https://doi.org/10.1016/j.tics.2019.02.004

Dijkstra, N., Mazor, M., Kok, P., & Fleming, S. (2021). Mistaking imagination for reality: Congruent mental imagery leads to more liberal perceptual detection. *Cognition*, *212*, 104719. https://doi.org/10.1016/j.cognition.2021.104719

Drozdz, S. J., Goel, A., McGarr, M. W., Katz, J., Ritvo, P., Mattina, G. F., Bhat, V., Diep, C., & Ladha, K. S. (2022). Ketamine Assisted Psychotherapy: A Systematic Narrative

Review of the Literature. *Journal of Pain Research*, *15*, 1691–1706. https://doi.org/10.2147/JPR.S360733

Dugré, J. R., Orban, P., & Potvin, S. (2023). Disrupted functional connectivity of the brain reward system in substance use problems: A meta-analysis of functional neuroimaging studies. *Addiction Biology*, *28*(1), e13257. https://doi.org/10.1111/adb.13257

Dunlop, B. W., & Nemeroff, C. B. (2007). The Role of Dopamine in the Pathophysiology of Depression. *Archives of General Psychiatry*, *64*(3), 327–337. https://doi.org/10.1001/archpsyc.64.3.327

Dutton, M., Boyes, A., Can, A. T., Mohamed, A. Z., Hajishafiee, M., Shan, Z. Y., Lagopoulos, J., & Hermens, D. F. (2024). Hippocampal subfield volumes predict treatment response to oral ketamine in people with suicidality. *Journal of Psychiatric Research*, *169*, 192–200. https://doi.org/10.1016/j.jpsychires.2023.11.040

Eshel, N., & Roiser, J. P. (2010). Reward and Punishment Processing in Depression. *Biological Psychiatry, Vascular Function in Depression in Older Adults*, *68*(2), 118–124. https://doi.org/10.1016/j.biopsych.2010.01.027

Espinoza Oyarce, D. A., Shaw, M. E., Alateeq, K., & Cherbuin, N. (2020). Volumetric brain differences in clinical depression in association with anxiety: A systematic review with meta-analysis. *Journal of Psychiatry and Neuroscience*, *45*(6), 406–429. https://doi.org/10.1503/jpn.190156

Feifel, D., Dadiomov, D., & C. Lee, K. (2020). Safety of Repeated Administration of Parenteral Ketamine for Depression. *Pharmaceuticals*, *13*(7), 151. https://doi.org/10.3390/ph13070151

Ferenczi, E. A., Zalocusky, K. A., Liston, C., Grosenick, L., Warden, M. R., Amatya, D., Katovich, K., Mehta, H., Patenaude, B., Ramakrishnan, C., Kalanithi, P., Etkin, A., Knutson, B., Glover, G. H., & Deisseroth, K. (2016). Prefrontal cortical regulation of brainwide circuit dynamics and reward-related behavior. *Science*, *351*(6268), aac9698. https://doi.org/10.1126/science.aac9698

Francis, N. A., Mukherjee, S., Koçillari, L., Panzeri, S., Babadi, B., & Kanold, P. O. (2022). Sequential transmission of task-relevant information in cortical neuronal networks. *Cell Reports*, *39*(9). https://doi.org/10.1016/j.celrep.2022.110878

Francois, J., Grimm, O., Schwarz, A. J., Schweiger, J., Haller, L., Risterucci, C., Böhringer, A., Zang, Z., Tost, H., Gilmour, G., & Meyer-Lindenberg, A. (2016). Ketamine Suppresses the Ventral Striatal Response to Reward Anticipation: A Cross-Species Translational Neuroimaging Study. *Neuropsychopharmacology*, *41*(5), 1386–1394. https://doi.org/10.1038/npp.2015.291

Frank, D. W., Dewitt, M., Hudgens-Haney, M., Schaeffer, D. J., Ball, B. H., Schwarz, N. F., Hussein, A. A., Smart, L. M., & Sabatinelli, D. (2014). Emotion regulation: Quantitative meta-analysis of functional activation and deactivation. *Neuroscience & Biobehavioral Reviews*, *45*, 202–211. https://doi.org/10.1016/j.neubiorev.2014.06.010

Gabay, A. S., Radua, J., Kempton, M. J., & Mehta, M. A. (2014). The Ultimatum Game and the brain: A meta-analysis of neuroimaging studies. *Neuroscience & Biobehavioral Reviews*, *47*, 549–558. https://doi.org/10.1016/j.neubiorev.2014.10.014

Garfield, J. B. B., Lubman, D. I., & Yücel, M. (2013). Anhedonia in substance use disorders: A systematic review of its nature, course and clinical correlates. *Australian & New Zealand Journal of Psychiatry*. (Sage UK: London, England). https://doi.org/10.1177/0004867413508455

Ghasemi, M., Navidhamidi, M., Rezaei, F., Azizikia, A., & Mehranfard, N. (2022). Anxiety and hippocampal neuronal activity: Relationship and potential mechanisms. *Cognitive, Affective, & Behavioral Neuroscience*, *22*(3), 431–449. https://doi.org/10.3758/s13415-021-00973-y

Görgen, S. M., Joormann, J., Hiller, W., & Witthöft, M. (2015). The Role of Mental Imagery in Depression: Negative Mental Imagery Induces Strong Implicit and Explicit Affect in Depression. *Frontiers in Psychiatry*, *6*. https://doi.org/10.3389/fpsyt.2015.00094

Grabski, M., Borissova, A., Marsh, B., Morgan, C. J. A., & Curran, H. V. (2020). Ketamine as a mental health treatment: Are acute psychoactive effects associated with outcomes? A systematic review. *Behavioural Brain Research*, *392*, 112629. https://doi.org/10.1016/j.bbr.2020.112629

Grace, A. A., Floresco, S. B., Goto, Y., & Lodge, D. J. (2007). Regulation of firing of dopaminergic neurons and control of goal-directed behaviors. *Trends in Neurosciences, Fifty Years of Dopamine Research*, *30*(5), 220–227. https://doi.org/10.1016/j.tins.2007.03.003

Graf, S., Dörl, G., Milz, C., Kathofer, M., Stöhrmann, P., Gomola, D., Briem, E., Schlosser, G., Mayerweg, A., Semmelweis-Tomits, J., Hoti, A., Eggerstorfer, B., Schmidt, C., Crone, J., Rujescu, D., Spies, M., Lanzenberger, R., & Spurny-Dworak, B. (2024). Morphological correlates of anxiety-related experiences during a ketamine infusion. *The World Journal of Biological Psychiatry*, *25*(9), 537–546. https://doi.org/10.1080/15622975.2024.2402261

Hanewald, B., Lockhofen, D. E. L., Sammer, G., Stingl, M., Gallhofer, B., Mulert, C., & Iffland, J. R. (2023). Functional connectivity in a monetary and social incentive delay task in medicated patients with schizophrenia. *Frontiers in Psychiatry*, *14*. https://doi.org/10.3389/fpsyt.2023.1200860

Haxby, J. V. (2012). Multivariate pattern analysis of fMRI: The early beginnings. *NeuroImage*, *62*(2), 852–855. https://doi.org/10.1016/j.neuroimage.2012.03.016

Haxby, J. V., Gobbini, M. I., Furey, M. L., Ishai, A., Schouten, J. L., & Pietrini, P. (2001). Distributed and Overlapping Representations of Faces and Objects in Ventral Temporal Cortex. *Science*, *293*(5539), 2425–2430. https://doi.org/10.1126/science.1063736

Hayano, F., Nakamura, M., Asami, T., Uehara, K., Yoshida, T., Roppongi, T., Otsuka, T., Inoue, T., & Hirayasu, Y. (2009). Smaller amygdala is associated with anxiety in

patients with panic disorder. *Psychiatry and Clinical Neurosciences*, *63*(3), 266–276. https://doi.org/10.1111/j.1440-1819.2009.01960.x

He, Z., Zhang, D., Muhlert, N., & Elliott, R. (2019). Neural substrates for anticipation and consumption of social and monetary incentives in depression. *Social Cognitive and Affective Neuroscience*, *14*(8), 815–826. https://doi.org/10.1093/scan/nsz061

Heinrich, C. J., & Marschke, G. (2010). Incentives and their dynamics in public sector performance management systems. *Journal of Policy Analysis and Management*, *29*(1), 183–208. https://doi.org/10.1002/pam.20484

Herzog, R., Barbey, F. M., Islam, M. N., Rueda-Delgado, L., Nolan, H., Prado, P., Krylova, M., Izyurov, I., Javaheripour, N., Danyeli, L. V., Sen, Z. D., Walter, M., O'Donnell, P., Buhl, D. L., Murphy, B., & Ibanez, A. (2024). High-order brain interactions in ketamine during rest and task: A double-blinded cross-over design using portable EEG on male participants. *Translational Psychiatry*, *14*(1), 1–9. https://doi.org/10.1038/s41398-024-03029-0

Hesselgrave, N., Troppoli, T. A., Wulff, A. B., Cole, A. B., & Thompson, S. M. (2021). Harnessing psilocybin: Antidepressant-like behavioral and synaptic actions of psilocybin are independent of 5-HT2R activation in mice. *Proceedings of the National Academy of Sciences*, *118*(17), e2022489118. https://doi.org/10.1073/pnas.2022489118

Höflich, A., Kraus, C., Pfeiffer, R. M., Seiger, R., Rujescu, D., Zarate, C. A., Kasper, S., Winkler, D., & Lanzenberger, R. (2021). Translating the immediate effects of S-Ketamine using hippocampal subfield analysis in healthy subjects-results of a randomized controlled trial. *Translational Psychiatry*, *11*(1), 200. https://doi.org/10.1038/s41398-021-01318-6

Höflich, A., Michenthaler, P., Kasper, S., & Lanzenberger, R. (2019). Circuit Mechanisms of Reward, Anhedonia, and Depression. *International Journal of Neuropsychopharmacology*, *22*(2), 105–118. https://doi.org/10.1093/ijnp/pyy081

Hwang, K., Bertolero, M. A., Liu, W. B., & D'Esposito, M. (2017). The Human Thalamus Is an Integrative Hub for Functional Brain Networks. *Journal of Neuroscience*, *37*(23), 5594–5607. https://doi.org/10.1523/JNEUROSCI.0067-17.2017

Ishizu, T., & Zeki, S. (n.d.). *The brain's specialized systems for aesthetic and perceptual judgment*. https://doi.org/10.1111/ejn.12135

Ishizu, T., & Zeki, S. (2011). Toward A Brain-Based Theory of Beauty. *PLOS ONE*, *6*(7), e21852. https://doi.org/10.1371/journal.pone.0021852

Johnson, S. T., & Grabenhorst, F. (2025). The amygdala and the pursuit of future rewards. *Frontiers in Neuroscience*, *18*, 1517231. https://doi.org/10.3389/fnins.2024.1517231

Kahnt, T. (2018). A decade of decoding reward-related fMRI signals and where we go from here. *NeuroImage, New Advances in Encoding and Decoding of Brain Signals*, *180*, 324–333. https://doi.org/10.1016/j.neuroimage.2017.03.067

Kahnt, T., Heinzle, J., Park, S. Q., & Haynes, J.-D. (2010). The neural code of reward anticipation in human orbitofrontal cortex. *Proceedings of the National Academy of Sciences of the United States of America*, *107*(13), 6010–6015. https://doi.org/10.1073/pnas.0912838107

Kamp, J., Olofsen, E., Henthorn, T. K., van Velzen, M., Niesters, M., Dahan, A., & Group, for the K. P. S. (2020). Ketamine Pharmacokinetics: A Systematic Review of the Literature, Meta-analysis, and Population Analysis. *Anesthesiology*, *133*(6), 1192. https://doi.org/10.1097/ALN.0000000000003577

Kathofer, M., Lamm, C., Leder, H., & Crone, J. S. (2025). Aesthetic experiences across visual perception and mental imagery: Behaviorally indistinguishable, neurally distinct. *iScience*, *28*(6). https://doi.org/10.1016/j.isci.2025.112588

Kathofer, M., Mediano, P. a. M., Spies, M., Liardi, A., Dörl, G., Stöhrmann, P., Schmidt, C., Briem, E., Schlosser, G., Eggerstorfer, B., Klöbl, M., Leder, H., Lanzenberger, R., & Crone, J. S. (2025). *Hedonic experiences emerge from an orchestrated balance of synergistic and redundant information processing* (p. 2025.10.05.680521). bioRxiv. https://doi.org/10.1101/2025.10.05.680521

Kelleher, R. T., & Gollub, L. R. (1962). A Review of Positive Conditioned Reinforcement. *Journal of the Experimental Analysis of Behavior*, *5*(S4), 543–597. https://doi.org/10.1901/jeab.1962.5-s543

Kim, M. J., Loucks, R. A., Palmer, A. L., Brown, A. C., Solomon, K. M., Marchante, A. N., & Whalen, P. J. (2011). The structural and functional connectivity of the amygdala: From normal emotion to pathological anxiety. *Behavioural Brain Research*, *223*(2), 403–410. https://doi.org/10.1016/j.bbr.2011.04.025

Knutson, B., Westdorp, A., Kaiser, E., & Hommer, D. (2000). FMRI Visualization of Brain Activity during a Monetary Incentive Delay Task. *NeuroImage*, *12*(1), 20–27. https://doi.org/10.1006/nimg.2000.0593

Koçillari, L., Celotto, M., Francis, N. A., Mukherjee, S., Babadi, B., Kanold, P. O., & Panzeri, S. (2023a). Behavioural relevance of redundant and synergistic stimulus information between functionally connected neurons in mouse auditory cortex. *Brain Informatics*, *10*(1), 34. https://doi.org/10.1186/s40708-023-00212-9

Koçillari, L., Celotto, M., Francis, N. A., Mukherjee, S., Babadi, B., Kanold, P. O., & Panzeri, S. (2023b). Behavioural relevance of redundant and synergistic stimulus information between functionally connected neurons in mouse auditory cortex. *Brain Informatics*, *10*(1), 34. https://doi.org/10.1186/s40708-023-00212-9

Koçillari, L., Celotto, M., Francis, N. A., Mukherjee, S., Babadi, B., Kanold, P. O., & Panzeri, S. (2023c). Measuring Stimulus-Related Redundant and Synergistic Functional Connectivity with Single Cell Resolution in Auditory Cortex. In F. Liu, Y. Zhang, H. Kuai, E. P. Stephen, & H. Wang (Eds.), *Brain Informatics* (pp. 45–56). Springer Nature Switzerland. https://doi.org/10.1007/978-3-031-43075-6_5

Koivisto, M., & Grassini, S. (2023). Mental imagery of nature induces positive psychological effects. *Current Psychology*, *42*(34), 30348–30363. https://doi.org/10.1007/s12144-022-04088-6

Koivisto, M., & Grassini, S. (2024). The restorative effects of mental imagery of nature: A study on subjective and physiological responses. *Journal of Environmental Psychology*, *96*, 102346. https://doi.org/10.1016/j.jenvp.2024.102346

Kotoula, V., Webster, T., Stone, J., & Mehta, M. A. (2021). Resting-state connectivity studies as a marker of the acute and delayed effects of subanaesthetic ketamine administration in healthy and depressed individuals: A systematic review. *Brain and Neuroscience Advances*, *5*, 23982128211055426. https://doi.org/10.1177/23982128211055426

Kriegeskorte, N., & Douglas, P. K. (2019). Interpreting encoding and decoding models. *Current Opinion in Neurobiology*, *55*, 167–179. https://doi.org/10.1016/j.conb.2019.04.002

Kringelbach, M. L. (2005). The human orbitofrontal cortex: Linking reward to hedonic experience. *Nature Reviews Neuroscience*, *6*(9), 691–702. https://doi.org/10.1038/nrn1747

Kringelbach, M. L. (2015). The pleasure of food: Underlying brain mechanisms of eating and other pleasures. *Flavour*, *4*(1), 20. https://doi.org/10.1186/s13411-014-0029-2

Kryst, J., Kawalec, P., Mitoraj, A. M., Pilc, A., Lasoń, W., & Brzostek, T. (2020). Efficacy of single and repeated administration of ketamine in unipolar and bipolar depression: A meta-analysis of randomized clinical trials. *Pharmacological Reports*, *72*(3), 543–562. https://doi.org/10.1007/s43440-020-00097-z

Krystal, J. H., Abdallah, C. G., Sanacora, G., Charney, D. S., & Duman, R. S. (2019). Ketamine: A Paradigm Shift for Depression Research and Treatment. *Neuron*, *101*(5), 774–778. https://doi.org/10.1016/j.neuron.2019.02.005

Lally, N., Nugent, A. C., Luckenbaugh, D. A., Ameli, R., Roiser, J. P., & Zarate, C. A. (2014). Anti-anhedonic effect of ketamine and its neural correlates in treatment-resistant bipolar depression. *Translational Psychiatry*, *4*(10), e469. https://doi.org/10.1038/tp.2014.105

Lambert, G., Johansson, M., Ågren, H., & Friberg, P. (2000). Reduced Brain Norepinephrine and Dopamine Release in Treatment-Refractory Depressive Illness: Evidence in Support of the Catecholamine Hypothesis of Mood Disorders. *Archives of General Psychiatry*, *57*(8), 787–793. https://doi.org/10.1001/archpsyc.57.8.787

Lapidus, K. A. B., Levitch, C. F., Perez, A. M., Brallier, J. W., Parides, M. K., Soleimani, L., Feder, A., Iosifescu, D. V., Charney, D. S., & Murrough, J. W. (2014). A Randomized Controlled Trial of Intranasal Ketamine in Major Depressive Disorder. *Biological Psychiatry, N-Methyl-D-Aspartate Receptors, Synaptic Plasticity, Psychopathology, and Treatment*, *76*(12), 970–976. https://doi.org/10.1016/j.biopsych.2014.03.026

Leder, H., Belke, B., Oeberst, A., & Augustin, D. (2004). A model of aesthetic appreciation and aesthetic judgments. *British Journal of Psychology (London, England: 1953)*, *95*(Pt 4), 489–508. https://doi.org/10.1348/0007126042369811

Lee, Y. Y., Stockings, E. A., Harris, M. G., Doi, S. a. R., Page, I. S., Davidson, S. K., & Barendregt, J. J. (2019). The risk of developing major depression among individuals with subthreshold depression: A systematic review and meta-analysis of longitudinal cohort studies. *Psychological Medicine*, *49*(1), 92–102. https://doi.org/10.1017/S0033291718000557

Luca, A., Luca, M., Kasper, S., Pecorino, B., Zohar, J., Souery, D., Montgomery, S., Ferentinos, P., Rujescu, D., Messina, A., Zanardi, R., Ferri, R., Tripodi, M., Baune, B. T., Fanelli, G., Fabbri, C., Mendlewicz, J., & Serretti, A. (2024). Anhedonia is associated with a specific depression profile and poor antidepressant response. *International Journal of Neuropsychopharmacology*, *27*(12), pyae055. https://doi.org/10.1093/ijnp/pyae055

Luckenbaugh, D. A., Niciu, M. J., Ionescu, D. F., Nolan, N. M., Richards, E. M., Brutsche, N. E., Guevara, S., & Zarate, C. A. (2014). Do the dissociative side effects of ketamine mediate its antidepressant effects? *Journal of Affective Disorders*, *159*, 56–61. https://doi.org/10.1016/j.jad.2014.02.017

Luijten, M., Schellekens, A. F., Kühn, S., Machielse, M. W. J., & Sescousse, G. (2017). Disruption of Reward Processing in Addiction: An Image-Based Meta-analysis of Functional Magnetic Resonance Imaging Studies. *JAMA Psychiatry*, *74*(4), 387–398. https://doi.org/10.1001/jamapsychiatry.2016.3084

Luppi, A. I., Mediano, P. A., Rosas, F. E., Allanson, J., Pickard, J., Carhart-Harris, R. L., Williams, G. B., Craig, M. M., Finoia, P., Owen, A. M., Naci, L., Menon, D. K., Bor, D., & Stamatakis, E. A. (2024). A synergistic workspace for human consciousness revealed by Integrated Information Decomposition. *eLife*, *12*, RP88173. https://doi.org/10.7554/eLife.88173

Luppi, A. I., Rosas, F. E., Mediano, P. A. M., Menon, D. K., & Stamatakis, E. A. (2024). Information decomposition and the informational architecture of the brain. *Trends in Cognitive Sciences*, *28*(4), 352–368. https://doi.org/10.1016/j.tics.2023.11.005

Lutz, K., & Widmer, M. (2014). What can the monetary incentive delay task tell us about the neural processing of reward and punishment? *Neuroscience and Neuroeconomics*, *3*, 33–45. https://doi.org/10.2147/NAN.S38864

Ma, Z. Z., Guzikowski, N. J., Kim, J.-W., Kavalali, E. T., & Monteggia, L. M. (2025). Enhanced ERK activity extends ketamine's antidepressant effects by augmenting synaptic plasticity. *Science*, *388*(6747), 646–655. https://doi.org/10.1126/science.abb6748

MacClancy, J. M., Macbeth, H., & Henry, J. (2007). *Consuming the Inedible: Neglected Dimensions of Food Choice*. 1–258.

Margulis, E. H., Levine, W. H., Simchy-Gross, R., & Kroger, C. (2017). Expressive intent, ambiguity, and aesthetic experiences of music and poetry. *PLOS ONE*, *12*(7), e0179145. https://doi.org/10.1371/journal.pone.0179145

Maslow, A. H. (1971). *The farther reaches of human nature* (pp. xxi, 407). Arkana/Penguin Books.

Medeiros, G. C., Matheson, M., Demo, I., Reid, M. J., Matheson, S., Twose, C., Smith, G. S., Gould, T. D., Zarate, C. A., Barrett, F. S., & Goes, F. S. (2023). Brain-based correlates of antidepressant response to ketamine: A comprehensive systematic review of neuroimaging studies. *The Lancet Psychiatry*, *10*(10), 790–800. https://doi.org/10.1016/S2215-0366(23)00183-9

Mediano, P. A. M., Rosas, F. E., Farah, J. C., Shanahan, M., Bor, D., & Barrett, A. B. (2022). Integrated information as a common signature of dynamical and information-processing complexity. *Chaos: An Interdisciplinary Journal of Nonlinear Science*, *32*(1), 013115. https://doi.org/10.1063/5.0063384

Mediano, P. A. M., Rosas, F. E., Luppi, A. I., Carhart-Harris, R. L., Bor, D., Seth, A. K., & Barrett, A. B. (2021). *Towards an extended taxonomy of information dynamics via Integrated Information Decomposition* (arXiv:2109.13186). arXiv. https://doi.org/10.48550/arXiv.2109.13186

Menninghaus, W., Wagner, V., Hanich, J., Wassiliwizky, E., Kuehnast, M., & Jacobsen, T. (2015). Towards a Psychological Construct of Being Moved. *PLOS ONE*, *10*(6), e0128451. https://doi.org/10.1371/journal.pone.0128451

Moda-Sava, R. N., Murdock, M. H., Parekh, P. K., Fetcho, R. N., Huang, B. S., Huynh, T. N., Witztum, J., Shaver, D. C., Rosenthal, D. L., Alway, E. J., Lopez, K., Meng, Y., Nellissen, L., Grosenick, L., Milner, T. A., Deisseroth, K., Bito, H., Kasai, H., & Liston, C. (2019). Sustained rescue of prefrontal circuit dysfunction by antidepressant-induced spine formation. *Science*, *364*(6436), eaat8078. https://doi.org/10.1126/science.aat8078

Murphy, E. S., McSweeney, F. K., Smith, R. G., & McComas, J. J. (2003). Dynamic Changes in Reinforcer Effectiveness: Theoretical, Methodological, and Practical Implications for Applied Research. *Journal of Applied Behavior Analysis*, *36*(4), 421–438. https://doi.org/10.1901/jaba.2003.36-421

Murrough, J. W., Iosifescu, D. V., Chang, L. C., Jurdi, R. K. A., Green, C. E., Perez, A. M., Iqbal, S., Pillemer, S., Foulkes, A., Shah, A., Charney, D. S., & Mathew, S. J. (2013). Antidepressant Efficacy of Ketamine in Treatment-Resistant Major Depression: A Two-Site Randomized Controlled Trial. *American Journal of Psychiatry*. (Arlington, VA). https://doi.org/10.1176/appi.ajp.2013.13030392

Newman, E. L., Varley, T. F., Parakkattu, V. K., Sherrill, S. P., & Beggs, J. M. (2022). Revealing the Dynamics of Neural Information Processing with Multivariate Information Decomposition. *Entropy*, *24*(7), Article 7. https://doi.org/10.3390/e24070930

Ng, T. H., Alloy, L. B., & Smith, D. V. (2019). Meta-analysis of reward processing in major depressive disorder reveals distinct abnormalities within the reward circuit. *Translational Psychiatry*, *9*(1), 293. https://doi.org/10.1038/s41398-019-0644-x

Nikolin, S., Rodgers, A., Schwaab, A., Bahji, A., Zarate, C., Vazquez, G., & Loo, C. (2023). Ketamine for the treatment of major depression: A systematic review and meta-analysis. *eClinicalMedicine*, *62*. https://doi.org/10.1016/j.eclinm.2023.102127

Oldham, S., Murawski, C., Fornito, A., Youssef, G., Yücel, M., & Lorenzetti, V. (2018). The anticipation and outcome phases of reward and loss processing: A neuroimaging meta-analysis of the monetary incentive delay task. *Human Brain Mapping*, *39*(8), 3398–3418. https://doi.org/10.1002/hbm.24184

Palmer, S. E., Schloss, K. B., & Sammartino, J. (2013). Visual Aesthetics and Human Preference. *Annual Review of Psychology*, *64*(Volume 64, 2013), 77–107. https://doi.org/10.1146/annurev-psych-120710-100504

Panzeri, S., Moroni, M., Safaai, H., & Harvey, C. D. (2022). The structures and functions of correlations in neural population codes. *Nature Reviews Neuroscience*, *23*(9), 551–567. https://doi.org/10.1038/s41583-022-00606-4

Peacocke, A. (2024). Aesthetic Experience. In E. N. Zalta & U. Nodelman (Eds.), *The Stanford Encyclopedia of Philosophy* (Fall 2024). Metaphysics Research Lab, Stanford University. https://plato.stanford.edu/archives/fall2024/entries/aesthetic-experience/

Pelowski, M., Markey, P. S., Forster, M., Gerger, G., & Leder, H. (2017). Move me, astonish me… delight my eyes and brain: The Vienna Integrated Model of top-down and bottom-up processes in Art Perception (VIMAP) and corresponding affective, evaluative, and neurophysiological correlates. *Physics of Life Reviews*, *21*, 80–125. https://doi.org/10.1016/j.plrev.2017.02.003

Pool, E., Sennwald, V., Delplanque, S., Brosch, T., & Sander, D. (2016). Measuring wanting and liking from animals to humans: A systematic review. *Neuroscience & Biobehavioral Reviews*, *63*, 124–142. https://doi.org/10.1016/j.neubiorev.2016.01.006

Popal, H., Wang, Y., & Olson, I. R. (2019). A Guide to Representational Similarity Analysis for Social Neuroscience. *Social Cognitive and Affective Neuroscience*, *14*(11), 1243–1253. https://doi.org/10.1093/scan/nsz099

Pope, M., Varley, T. F., Grazia Puxeddu, M., Faskowitz, J., & Sporns, O. (2025). Time-varying synergy/redundancy dominance in the human cerebral cortex. *Journal of Physics: Complexity*, *6*(1), 015015. https://doi.org/10.1088/2632-072X/adbaa9

Price, J., Cole, V., & Goodwin, G. M. (2009). Emotional side-effects of selective serotonin reuptakeinhibitors: Qualitative study. *The British Journal of Psychiatry*, *195*(3), 211–217. https://doi.org/10.1192/bjp.bp.108.051110

Privette, G. (1983). Peak experience, peak performance, and flow: A comparative analysis of positive human experiences. *Journal of Personality and Social Psychology*, *45*(6), 1361–1368. https://doi.org/10.1037/0022-3514.45.6.1361

Ramayya, A. G., Pedisich, I., & Kahana, M. J. (2015). Expectation modulates neural representations of valence throughout the human brain. *NeuroImage*, *115*, 214–223. https://doi.org/10.1016/j.neuroimage.2015.04.037

Redies, C. (2015). Combining universal beauty and cultural context in a unifying model of visual aesthetic experience. *Frontiers in Human Neuroscience*, *9*. https://doi.org/10.3389/fnhum.2015.00218

Rømer Thomsen, K., Whybrow, P. C., & Kringelbach, M. L. (2015). Reconceptualizing anhedonia: Novel perspectives on balancing the pleasure networks in the human brain. *Frontiers in Behavioral Neuroscience*, *9*. https://www.frontiersin.org/articles/10.3389/fnbeh.2015.00049

Rosas, F. E., Mediano, P. A. M., Gastpar, M., & Jensen, H. J. (2019). Quantifying high-order interdependencies via multivariate extensions of the mutual information. *Physical Review E*, *100*(3), 032305. https://doi.org/10.1103/PhysRevE.100.032305

Rushworth, M. F. S., Noonan, M. P., Boorman, E. D., Walton, M. E., & Behrens, T. E. (2011). Frontal Cortex and Reward-Guided Learning and Decision-Making. *Neuron*, *70*(6), 1054–1069. https://doi.org/10.1016/j.neuron.2011.05.014

Russo, S. J., & Nestler, E. J. (2013). The Brain Reward Circuitry in Mood Disorders. *Nature Reviews. Neuroscience*, *14*(9), 10.1038/nrn3381. https://doi.org/10.1038/nrn3381

Sala-Llonch, R., Peña-Gómez, C., Arenaza-Urquijo, E. M., Vidal-Piñeiro, D., Bargalló, N., Junqué, C., & Bartrés-Faz, D. (2012). Brain connectivity during resting state and subsequent working memory task predicts behavioural performance. *Cortex*, *48*(9), 1187–1196. https://doi.org/10.1016/j.cortex.2011.07.006

Satpute, A. B., Mumford, J. A., Naliboff, B. D., & Poldrack, R. A. (2012). Human anterior and posterior hippocampus respond distinctly to state and trait anxiety. *Emotion*, *12*(1), 58–68. https://doi.org/10.1037/a0026517

Schloss, K. B., & Palmer, S. E. (2011). Aesthetic response to color combinations: Preference, harmony, and similarity. *Attention, Perception, & Psychophysics*, *73*(2), 551–571. https://doi.org/10.3758/s13414-010-0027-0

Schoeller, F., Jain, A., Pizzagalli, D. A., & Reggente, N. (2024). The neurobiology of aesthetic chills: How bodily sensations shape emotional experiences. *Cognitive, Affective, & Behavioral Neuroscience*, *24*(4), 617–630. https://doi.org/10.3758/s13415-024-01168-x

Schultz, W. (2002). Getting Formal with Dopamine and Reward. *Neuron*, *36*(2), 241–263. https://doi.org/10.1016/S0896-6273(02)00967-4

Schultz, W. (2024). A dopamine mechanism for reward maximization. *Proceedings of the National Academy of Sciences*, *121*(20), e2316658121. https://doi.org/10.1073/pnas.2316658121

Sesack, S. R., & Grace, A. A. (2010). Cortico-Basal Ganglia Reward Network: Microcircuitry. *Neuropsychopharmacology*, *35*(1), 27–47. https://doi.org/10.1038/npp.2009.93

Sescousse, G., Caldú, X., Segura, B., & Dreher, J.-C. (2013). Processing of primary and secondary rewards: A quantitative meta-analysis and review of human functional neuroimaging studies. *Neuroscience & Biobehavioral Reviews*, *37*(4), 681–696. https://doi.org/10.1016/j.neubiorev.2013.02.002

Shi, H.-J., Wang, S., Wang, X.-P., Zhang, R.-X., & Zhu, L.-J. (2023). Hippocampus: Molecular, Cellular, and Circuit Features in Anxiety. *Neuroscience Bulletin*, *39*(6), 1009–1026. https://doi.org/10.1007/s12264-023-01020-1

Short, B., Fong, J., Galvez, V., Shelker, W., & Loo, C. K. (2018). Side-effects associated with ketamine use in depression: A systematic review. *The Lancet. Psychiatry*, *5*(1), 65–78. https://doi.org/10.1016/S2215-0366(17)30272-9

Sigmund, K., Hauert, C., & Nowak, M. A. (2001). Reward and punishment. *Proceedings of the National Academy of Sciences*, *98*(19), 10757–10762. https://doi.org/10.1073/pnas.161155698

So, K., Ganguly, K., Jimenez, J., Gastpar, M. C., & Carmena, J. M. (2012). Redundant information encoding in primary motor cortex during natural and prosthetic motor control. *Journal of Computational Neuroscience*, *32*(3), 555–561. https://doi.org/10.1007/s10827-011-0369-1

Sofuoglu, M., & Sewell, R. A. (2009). Norepinephrine and Stimulant Addiction. *Addiction Biology*, *14*(2), 119–129. https://doi.org/10.1111/j.1369-1600.2008.00138.x

Stevens, W. D., & Spreng, R. N. (2014). Resting-state functional connectivity MRI reveals active processes central to cognition. *WIREs Cognitive Science*, *5*(2), 233–245. https://doi.org/10.1002/wcs.1275

Sun, Z., & Firestone, C. (2022). Beautiful on the inside: Aesthetic preferences and the skeletal complexity of shapes. *Perception*, *51*(12), 904–918. https://doi.org/10.1177/03010066221124872

Szubielska, M., Imbir, K., & Szymańska, A. (2021). The influence of the physical context and knowledge of artworks on the aesthetic experience of interactive installations. *Current Psychology*, *40*(8), 3702–3715. https://doi.org/10.1007/s12144-019-00322-w

Tiihonen, M., Brattico, E., Maksimainen, J., Wikgren, J., & Saarikallio, S. (2017). Constituents of Music and Visual-Art Related Pleasure – A Critical Integrative Literature Review. *Frontiers in Psychology*, *8*. https://doi.org/10.3389/fpsyg.2017.01218

Timme, N., Alford, W., Flecker, B., & Beggs, J. M. (2014). Synergy, redundancy, and multivariate information measures: An experimentalist's perspective. *Journal of Computational Neuroscience*, *36*(2), 119–140. https://doi.org/10.1007/s10827-013-0458-4

Tolomeo, S., & Yu, R. (2022). Brain network dysfunctions in addiction: A meta-analysis of resting-state functional connectivity. *Translational Psychiatry*, *12*(1), 41. https://doi.org/10.1038/s41398-022-01792-6

Trøstheim, M., Eikemo, M., Meir, R., Hansen, I., Paul, E., Kroll, S. L., Garland, E. L., & Leknes, S. (2020). Assessment of Anhedonia in Adults With and Without Mental Illness: A Systematic Review and Meta-analysis. *JAMA Network Open*, *3*(8), e2013233. https://doi.org/10.1001/jamanetworkopen.2020.13233

Trupp, M. D., Bignardi, G., Specker, E., Vessel, E. A., & Pelowski, M. (2023). Who benefits from online art viewing, and how: The role of pleasure, meaningfulness, and trait

aesthetic responsiveness in computer-based art interventions for well-being. *Computers in Human Behavior*, *145*, 107764. https://doi.org/10.1016/j.chb.2023.107764

Varley, T. F., Pope, M., Maria Grazia, Joshua, & Sporns, O. (2023). Partial entropy decomposition reveals higher-order information structures in human brain activity. *Proceedings of the National Academy of Sciences*, *120*(30), e2300888120. https://doi.org/10.1073/pnas.2300888120

Varley, T. F., Sporns, O., Schaffelhofer, S., Scherberger, H., & Dann, B. (2023a). Information-processing dynamics in neural networks of macaque cerebral cortex reflect cognitive state and behavior. *Proceedings of the National Academy of Sciences*, *120*(2), e2207677120. https://doi.org/10.1073/pnas.2207677120

Varley, T. F., Sporns, O., Schaffelhofer, S., Scherberger, H., & Dann, B. (2023b). Information-processing dynamics in neural networks of macaque cerebral cortex reflect cognitive state and behavior. *Proceedings of the National Academy of Sciences*, *120*(2), e2207677120. https://doi.org/10.1073/pnas.2207677120

Vel Tromp, M. J. B., Huizenga, H. M., Jansen, B. R. J., van Duijvenvoorde, A. C. K., & Veer, I. M. (2025). Investigating Neural Reward Sensitivity in the School Grade Incentive Delay Task and Its Relation to Academic Buoyancy. *Behavioral Sciences*, *15*(10), 1321. https://doi.org/10.3390/bs15101321

Vickery, T. J., Chun, M. M., & Lee, D. (2011). Ubiquity and Specificity of Reinforcement Signals throughout the Human Brain. *Neuron*, *72*(1), 166–177. https://doi.org/10.1016/j.neuron.2011.08.011

Vrieze, E., Demyttenaere, K., Bruffaerts, R., Hermans, D., Pizzagalli, D. A., Sienaert, P., Hompes, T., de Boer, P., Schmidt, M., & Claes, S. (2014). Dimensions in Major Depressive Disorder and their Relevance for Treatment Outcome. *Journal of Affective Disorders*, *155*, 35–41. https://doi.org/10.1016/j.jad.2013.10.020

Vuust, P., Heggli, O. A., Friston, K. J., & Kringelbach, M. L. (2022). Music in the brain. *Nature Reviews Neuroscience*, *23*(5), 287–305. https://doi.org/10.1038/s41583-022-00578-5

Vuust, P., & Kringelbach, M. L. (2010). The Pleasure of Making Sense of Music. *Interdisciplinary Science Reviews*, *35*(2), 166–182. https://doi.org/10.1179/030801810X12723585301192

Wassum, K. M. (2022). Amygdala-cortical collaboration in reward learning and decision making. *eLife*, *11*, e80926. https://doi.org/10.7554/eLife.80926

Watabe-Uchida, M., Eshel, N., & Uchida, N. (2017). Neural Circuitry of Reward Prediction Error. *Annual Review of Neuroscience*, *40*(Volume 40, 2017), 373–394. https://doi.org/10.1146/annurev-neuro-072116-031109

Williams, P. L., & Beer, R. D. (2010). *Nonnegative Decomposition of Multivariate Information* (arXiv:1004.2515). arXiv. https://doi.org/10.48550/arXiv.1004.2515

Wilson, R. P., Colizzi, M., Bossong, M. G., Allen, P., Kempton, M., Abe, N., Barros-Loscertales, A. R., Bayer, J., Beck, A., Bjork, J., Boecker, R., Bustamante, J. C., Choi, J. S., Delmonte, S., Dillon, D., Figee, M., Garavan, H., Hagele, C., Hermans,

E. J., … MTAC. (2018). The Neural Substrate of Reward Anticipation in Health: A Meta-Analysis of fMRI Findings in the Monetary Incentive Delay Task. *Neuropsychology Review*, *28*(4), 496–506. https://doi.org/10.1007/s11065-018-9385-5

Wong, S., Le, G. H., Phan, L., Rhee, T. G., Ho, R., Meshkat, S., Teopiz, K. M., Kwan, A. T. H., Mansur, R. B., Rosenblat, J. D., & McIntyre, R. S. (2024). Effects of anhedonia on health-related quality of life and functional outcomes in major depressive disorder: A systematic review and meta-analysis. *Journal of Affective Disorders*, *356*, 684–698. https://doi.org/10.1016/j.jad.2024.04.086

Yaden, D. B., & Griffiths, R. R. (2020). The Subjective Effects of Psychedelics Are Necessary for Their Enduring Therapeutic Effects. *ACS Pharmacology & Translational Science*, *4*(2), 568–572. https://doi.org/10.1021/acsptsci.0c00194

Yan, C., Su, L., Wang, Y., Xu, T., Yin, D., Fan, M., Deng, C., Hu, Y., Wang, Z., Cheung, E. F. C., Lim, K. O., & Chan, R. C. K. (2016). Multivariate Neural Representations of Value during Reward Anticipation and Consummation in the Human Orbitofrontal Cortex. *Scientific Reports*, *6*(1), 29079. https://doi.org/10.1038/srep29079

Yarkoni, T., Poldrack, R. A., Nichols, T. E., Van Essen, D. C., & Wager, T. D. (2011). Large-scale automated synthesis of human functional neuroimaging data. *Nature Methods*, *8*(8), 665–670. https://doi.org/10.1038/nmeth.1635

Zanos, P., & Gould, T. D. (2018). Mechanisms of ketamine action as an antidepressant. *Molecular Psychiatry*, *23*(4), 801–811. https://doi.org/10.1038/mp.2017.255

Zarate, C. A., Jr, Singh, J. B., Carlson, P. J., Brutsche, N. E., Ameli, R., Luckenbaugh, D. A., Charney, D. S., & Manji, H. K. (2006). A Randomized Trial of an N-methyl-D-aspartate Antagonist in Treatment-Resistant Major Depression. *Archives of General Psychiatry*, *63*(8), 856–864. https://doi.org/10.1001/archpsyc.63.8.856

Zeng, J., Yan, J., Cao, H., Su, Y., Song, Y., Luo, Y., & Yang, X. (2022). Neural substrates of reward anticipation and outcome in schizophrenia: A meta-analysis of fMRI findings in the monetary incentive delay task. *Translational Psychiatry*, *12*(1), 448. https://doi.org/10.1038/s41398-022-02201-8

Zhang, R., Deng, H., & Xiao, X. (2024). The Insular Cortex: An Interface Between Sensation, Emotion and Cognition. *Neuroscience Bulletin*, *40*(11), 1763–1773. https://doi.org/10.1007/s12264-024-01211-4